

8-22-2018

Development of Self-Healing Mechanisms for Asphalt Pavements

Max Abelardo Aguirre Deras

Louisiana State University and Agricultural and Mechanical College

Follow this and additional works at: https://digitalcommons.lsu.edu/gradschool_dissertations



Part of the [Civil Engineering Commons](#), [Construction Engineering and Management Commons](#), [Other Engineering Science and Materials Commons](#), and the [Transportation Engineering Commons](#)

Recommended Citation

Aguirre Deras, Max Abelardo, "Development of Self-Healing Mechanisms for Asphalt Pavements" (2018).
LSU Doctoral Dissertations. 4696.

https://digitalcommons.lsu.edu/gradschool_dissertations/4696

This Dissertation is brought to you for free and open access by the Graduate School at LSU Digital Commons. It has been accepted for inclusion in LSU Doctoral Dissertations by an authorized graduate school editor of LSU Digital Commons. For more information, please contact gradetd@lsu.edu.

DEVELOPMENT OF SELF-HEALING MECHANISMS FOR ASPHALT PAVEMENTS

A Dissertation

Submitted to the Graduate Faculty of the
Louisiana State University and
Agricultural and Mechanical College
in partial fulfillment of the
requirements for the degree of
Doctor of Philosophy

in

The Interdepartmental Program in Engineering Science

by
Max Abelardo Aguirre Deras
B.S., Louisiana State University, 2013
M.S., Louisiana State University, 2015
December 2018

TABLE OF CONTENTS

LIST OF TABLES	iv
LIST OF FIGURES	vi
NOMENCLATURE, SYMBOLS AND ACRONYMS	x
ABSTRACT.....	xiii
CHAPTER 1. INTRODUCTION	1
1.1 Problem Statement	2
1.2 Objectives	3
1.3 Scope.....	4
1.4 Research Approach	4
1.5 References	14
CHAPTER 2. LITERATURE REVIEW	16
2.1 Introduction.....	16
2.2 Asphalt Binder	18
2.3 Asphalt Mixture Performance Tests	21
2.4 Sustainable Pavement Technology	26
2.5 Asphalt Rejuvenation.....	34
2.6 Self-Healing Technology in Asphalt Pavement.....	37
2.7 Microcapsules Synthesis	51
2.8 Fibers Synthesis	59
2.9 References	64
CHAPTER 3. PERFORMANCE OF ASPHALT REJUVENATORS IN HOT MIX ASPHALT CONTAINING RECYCLED ASPHALT SHINGLES	74
3.1 Introduction.....	74
3.2 Objectives	76
3.3 Background	76
3.4 Experimental Program	78
3.4.4 Experimental Test Matrix	80
3.5 Results and Analysis	84
3.6 Conclusions.....	91
3.7 References	92
CHAPTER 4. LABORATORY TESTING OF SELF-HEALING MICROCAPSULES IN ASPHALT MIXTURES PREPARED WITH RECYCLED ASPHALT SHINGLES	96
4.1 Introduction.....	96
4.2 Objectives	97
4.3 Background	97
4.4 Experimental Program	100
4.5 Results and Analysis	106

4.6 Summary and Conclusions	117
4.7 References	119
CHAPTER 5. EVALUATION OF HOLLOW-FIBERS ENCAPSULATING A	
REJUVENATOR IN ASPHALT BINDERS WITH RECYCLED ASPHALT SHINGLES.....	121
5.1 Introduction.....	121
5.2 Objectives	122
5.3 Background	122
5.4 Experimental Program	124
5.5 Results and Analysis	131
5.6 Summary and Conclusions	153
5.7 References	154
CHAPTER 6. LABORATORY TESTING OF SELF-HEALING FIBERS IN ASPHALT	
MIXTURES PREPARED WITH RECYCLED MATERIALS	158
6.1 Introduction.....	158
6.2 Objectives	159
6.3 Background	159
6.4 Experimental Program	161
6.5 Results and Analysis	166
6.6 Summary and Conclusions	181
6.7 References	182
CHAPTER 7. EVALUATION OF SODIUM-ALGINATE HOLLOW FIBERS AS A	
REJUVENATING MECHANISM FOR ASPHALT BINDERS WITH RECYCLED	
MATERIALS.....	184
7.1 Introduction.....	184
7.2 Objectives	185
7.3 Background	185
7.4 Experimental Program	187
7.5 Results and Analysis	191
7.6 Summary and Conclusions	204
7.7 References	205
CHAPTER 8. SUMMARY AND CONCLUSIONS	
8.1 Evaluation of Asphalt Rejuvenators on HMA Mixtures.....	208
8.2 Development of Self-Healing Mechanisms for Asphalt Pavement	209
8.3 Evaluation of Self-Healing Properties of the Developed Self-Healing Mechanisms	211
8.4 Future Work	215
8.5 General Limitations	215
APPENDIX A. COPYRIGHT	217
VITA.....	219

LIST OF TABLES

Table 1.1. HMA Mixture Description.....	5
Table 1.2. Test Matrix for Fiber’s Optimization.....	9
Table 1.3. Test-Matrix for Tasks 14	10
Table 1.4. Test-Matrix for Tasks 15	11
Table 1.5. HMA Mixtures Description for Self-Healing Mixture Testing	12
Table 2.1. Quality Acceptance Summary of Four Section [52].....	33
Table 2.2. Superpave Mixtures [60]	37
Table 2.3. Biomimetic Self-healing Inspiration in Novel Self-healing Materials [69]	39
Table 2.4. Experimental Test Matrix for Microcapsule Preparation Variable [83].....	45
Table 2.5. Healing Programme for Test 1 and Test 2 [88]	50
Table 2.6. Ranges of Microcapsule’s Size with Different Microencapsulation Procedure [89] ..	54
Table 3.1. HMA Mixture Description.....	79
Table 3.2. Job-Mix Formula	80
Table 3.3. Mixture Performance Tests.....	82
Table 3.4. Statistical Ranking of Mixtures	89
Table 3.5. Rheological Test Results of Extracted Asphalt Binder Blends	90
Table 3.6. HP-GPC Calculations for Extracted Binders.....	91
Table 4.1. Job-Mix Formula	102
Table 4.2. Diameter Measurements and Yield Rates for Double-Walled Microcapsules	106
Table 4.3. Room-Temperature Healing Condition	109
Table 4.4. High-Temperature Healing Condition	109
Table 4.5. Statistical Analysis of Test Results.....	115

Table 5.1. Test Matrix for Fiber’s Optimization.....	127
Table 5.2. Test-Matrix for Optimization of Content of Fibers in Asphalt Binder.....	129
Table 5.3. Optimization Test Results of Sodium-Alginate Fibers.....	132
Table 5.4. Rheological Test Results of Asphalt Binder Blends Prepared with PG 64-22.....	136
Table 5.5. Rheological Test Results of Asphalt Binder Blends Prepared with PG 70-22.....	137
Table 5.6. MSCR Test Results of Asphalt Binder Blends Prepared with PG 64-22	141
Table 5.7. MSCR Test Results of Asphalt Binder Blends Prepared with PG 70-22	142
Table 6.1. Test Matrix for the Study.....	162
Table 6.2. Asphalt Mixture Performance Tests	165
Table 7.1. Test Matrix for Evaluation of the Effects of Adding Sodium-Alginate Fibers in Asphalt Binder Blends	190
Table 7.2. Chemical Composition of Evaluated Binder Blends	194
Table 7.3. Summary of PG Grading Results for: (a) Binder PG 70-22 and (b) Binder PG 64-22	197
Table 7.4. MSCR Test Results for: (a) Binder PG 70-22 and (b) Binder PG 64-22	199

LIST OF FIGURES

Figure 2.1. Effect of Preventive Maintenance at Life Cycle Cost of the Pavement [4]	18
Figure 2.2. Composition of Crude Oil [9].....	19
Figure 2.3. Stress-Strain Relationship under Sinusoidal Load	22
Figure 2.4. Loaded Wheel-Tracking (LWT) Test.....	23
Figure 2.5. Semi-Circular Bending (SCB) Test.....	24
Figure 2.6. Thermal Stress Restrained Specimen Tensile (TSRST) Test.....	26
Figure 2.7. Schematic for Induction Heating in Asphalt Concrete [78]	41
Figure 2.8. SEM Pictures of Microcapsules Containing Sunflower Oil [83]	45
Figure 2.9. SEM Pictures of Single-Walled Microcapsules [84].....	46
Figure 2.10. Self-Healing Process of Microcapsules/Bitumen: (a) Micro-Crack Generation, (b) Microcapsules Broken, (c) Capillarity and the Diffusion Behaviors of Rejuvenator, and (d) Micro-Crack Closure [85].....	46
Figure 2.11. Load-Strain Curves for BOEF Test at (a) 0°C and (b) 25°C; Self-Healing Cycles: ① First Cycle, ② Second Cycle, ③ Third Cycle, ④ Aged Bitumen, and ⑤ Fourth Cycle [85].....	47
Figure 2.12. Compartment Fiber with a Rejuvenator Product by Optical Microscope [88]	48
Figure 2.13. Thermogravimetric Analysis of Sodium-Alginate Fibers Containing a Rejuvenator Product [88]	49
Figure 2.14. Uniaxial Tensile Strength of Sodium-Alginate Fibers Containing a Rejuvenator Product [88]	49
Figure 2.15. 3PB Results: Load vs Deflection Plots for Asphalt Mastic Mixtures at 20°C a) with Fibers, and b) without Fibers [88].....	51
Figure 2.16. 3PB Results: Load vs Deflection Plots for Asphalt Mastic Mixtures at -5°C a) with Fibers, and b) without Fibers [88].....	51
Figure 2.17. Schematic of Microcapsule [89].....	52
Figure 2.18. Morphology of Microcapsules [89].....	53

Figure 2.19. Schematic Representation of a Melamine Resin Microencapsulation Process [101]	56
Figure 2.20. Schematic Representation of Microencapsulation Via Interfacial Polymerization [104]	57
Figure 2.21. Schematic Representation of a Microencapsulation Process by Coacervation [105]	58
Figure 2.22. Schematic Diagram of Wet Spinning Procedure [110]	60
Figure 2.23. Schematic Diagram of Dry Spinning Procedure [107]	63
Figure 2.24. Schematic Diagram of Melt Spinning Procedure [107]	64
Figure 3.1. Schematic of a Typical HWTB Test Data Analysis Showing the Different Regions [21]	83
Figure 3.2. Master Curve of Asphalt Mixtures	85
Figure 3.3. Dynamic Complex Modulus Test Results (a) Rut Factor Ratio, and (b) Fatigue Factor Ratio	86
Figure 3.4. Rutting Depth for Evaluated Superpave Asphalt Mixtures	87
Figure 3.5. Rutting Depth versus Number Of Cycles	87
Figure 3.6. Critical Strain Energy Release Rate	88
Figure 4.1. (a) Rectangular Specimen Obtained by Sawing Cylindrical Samples and (b) Three-Point Bending Test Setup	103
Figure 4.2. Calculation of Undamaged Stiffness (a) Load-Deformation Plot from First Bending Test (b) and Stiffness Calculation	104
Figure 4.3. Double-Walled Microcapsules Containing an Asphalt Rejuvenator: (a) Undamaged Microcapsules; (b) Microcapsules After 2 H at 136°C; (c) Microcapsules After Mixing Experiment; and (d) Thermogravimetric Analysis Results	108
Figure 4.4. Cracks Before and After Healing at Room-temperature	111
Figure 4.5. Cracks Before and After Healing at High-Temperature	112
Figure 4.6. Healing Efficiency at (a) Room-temperature; and (b) High-temperature	113
Figure 4.7. Stiffness Ratio Recovery at (a) Room-temperature; and at (b) High-Temperature	116

Figure 5.1. (a) Tensile Test Setup for Sodium-Alginate Fibers and (b) Broken Sodium-Alginate Fiber	133
Figure 5.2. Fibers with Optimum Parameters (a) SEM Picture with 65x Magnification, (b) UTS Test Results, and (c) TGA Test Results.....	135
Figure 5.3. “A” Parameter of Fatigue Law: (a) Asphalt Blends Prepared with PG 64-22, and (b) Asphalt Blends Prepared with PG 70-22	144
Figure 5.4. Absolute “B” Parameter of Fatigue Law: (a) Asphalt Blends Prepared with PG 64-22, and (b) Asphalt Blends Prepared with PG 70-22.....	145
Figure 5.5. Number of Cycles to Failure (Nf): (a) Asphalt Blends Prepared with PG 64-22, and (b) Asphalt Blends Prepared with PG 70-22.....	146
Figure 5.6. Complex Shear Modulus ($ G^* $) (a) Asphalt Blends Prepared with PG 64-22, and (b) Asphalt Blends Prepared with PG 70-22	148
Figure 5.7. Black Diagrams (a) Asphalt Blends Prepared with PG 64-22, and (b) Asphalt Blends Prepared with PG 70-22.....	150
Figure 5.8. Carbonyl Index (ICO) (a) Asphalt Blends Prepared with PG 64-22, and (b) Asphalt Blends Prepared with PG 70-22.....	152
Figure 6.1. (a) Three-Point Bending Test Setup	164
Figure 6.2. Fibers with Optimum Parameters (a) SEM Picture with 65x Magnification, (b) TGA Test Results, (c) Tensile Test Setup, and (d) UTS Test Results	167
Figure 6.3. Strength Recovery at Room-Temperature for: (a) Mixtures Prepared with Binder PG 70-22 and Containing Fibers, and (b) Mixtures Prepared with Binder PG 64-22 and Containing Fibers.....	168
Figure 6.4. Strength Recovery at Room-Temperature for (a) Mixtures Prepared with Binder PG 70-22 and Containing RAP and (b) Mixtures Prepared with Binder PG 64-22 and Containing RAP.....	170
Figure 6.5. Strength Recovery at Room-Temperature for (a) Mixtures Prepared with Binder PG 70-22 and Containing RAS and (b) Mixtures Prepared with Binder PG 64-22 and Containing RAS.....	171
Figure 6.6. Effect of Curing Conditions in the Strength Recovery of: (a) Mixtures with Binder PG 70-22 and (B) Mixtures with Binder PG 64-22	173
Figure 6.7. Rutting Susceptibility: (a) HMA Mixtures with PG 70-22 and (b) HMA Mixtures with PG 64-22	175

Figure 6.8. Fracture Resistance: (a) HMA Mixtures with PG 70-22 and (b) HMA Mixtures with PG 64-22	177
Figure 6.9. Failure Load: (a) HMA Mixtures with PG 70-22 and (b) HMA Mixtures with PG 64-22.....	178
Figure 6.10. Failure Temperature for: (a) Mixtures with PG 70-22 and (b) Mixtures with PG 64-22.....	180
Figure 7.1. Fibers with Optimum Parameters (a) TGA Test Results of Fiber’s Material Composition, and (b) Broken Fiber after Tensile Test	193
Figure 7.2. ICO Aging Index for (a) Binder PG 70-22 and (b) Binder PG 64-22	195
Figure 7.3. LAS Test Results for Binder PG 70-22: (a) “A” Parameter Fatigue Law and (b) Absolute “B” Parameter Fatigue Law.....	202
Figure 7.4. LAS Test Results for Binder PG 64-22: (a) “A” Parameter Fatigue Law and (b) Absolute “B” Parameter Fatigue Law.....	203

NOMENCLATURE, SYMBOLS AND ACRONYMS

AASHTO	American Association of State Highway and Transportation Officials
ASTM	American Society for Testing Materials
BBR	Bending Beam Rheometer
$\text{CaCl}_2 \cdot 6\text{H}_2\text{O}$	Calcium Chloride Hexahydrate
Cw_0	Initial Crack width (mm)
Cw_t	Crack width at the time of analysis (mm)
DCB	O-Dichlorobenzene
DI	De-Ionized
DSR	Dynamic Shear Rheometer
FHWA	Federal Highway Administration
G_{mm}	Maximum Theoretical Specific Gravity
H_e	Healing efficiency (%);
HMA	Hot-Mix Asphalt
HWTD	Hamburg Wheel-Tracking Device
IDT	Indirect Tensile Test
ITS	Indirect Tensile Strength

Jc-value	Critical Strain Energy Release Rate
LADOTD	Louisiana Department of Transportation and Development
LTRC	Louisiana Transportation Research Center
mm	Millimeters
MSCR	Multiple Stress Creep Recovery
MWS	Manufactured Waste Shingles
NMAS	Nominal Maximum Aggregate Size
PCWS	Post-Consumer Waste Shingles
PEMA	Ethylene-Alt-Maleic-Anhydride
RAP	Recycled Asphalt Pavement
RAS	Recycled Asphalt Shingles
SEM	Scanning Electron Microscope
SBS	Styrene Butadiene Styrene
SCB	Semi-Circular Bending
TGA	Thermal Gravimetric Analysis
Tran-SET	Transportation Consortium of South-Central States
TSRST	Thermal Stress Restrained Specimen Test
UTS	Ultimate Tensile Strength
VDOT	Virginia Department of Transportation

3PB

3 point-bending

ABSTRACT

Self-healing mechanisms, such as microcapsules or hollow-fibers, filled with an asphalt rejuvenator present an emerging technology that would enhance an asphalt mixture's resistance to cracking damage caused by vehicular and environmental loading. The objectives of this study were to: (a) Evaluate the effects of asphalt rejuvenators on hot-mix asphalt mixtures in order to test its effects on the fundamental engineering properties of the mixtures at high and intermediate temperatures; (b) Develop a synthesis procedure for production of microcapsules and hollow-fibers containing an asphalt rejuvenator; (c) Evaluate the self-healing efficiency of double-walled microcapsules and hollow-fibers filled with an asphalt rejuvenator, through crack healing and stiffness recovery of damaged mixture specimens under two different curing conditions.

The core material for the self-healing mechanisms was selected by evaluating four different asphalt rejuvenator products through a set of laboratory tests to characterize the performance of asphalt mixtures against permanent deformation and fatigue cracking. Afterwards, the evaluated self-healing mechanisms were produced by modifying chemical synthesis procedures to develop double-walled microcapsules and hollow-fibers containing the selected rejuvenator product as core material. Furthermore, a self-healing experiment was designed to evaluate the rejuvenating and healing properties of the developed self-healing mechanisms.

The evaluation of HMA mixtures containing recycled materials showed that the rutting and cracking susceptibility increased with the addition of the evaluated asphalt rejuvenators. The activation of more binder from the recycled materials with the addition of asphalt rejuvenators was observed in the GPC test results as an increased in the asphaltenes-to-maltenes ratio was observed. The evaluation of self-healing microcapsules showed that the mixtures containing the produced microcapsules had a lower healing efficiency at both environmental curing conditions

compared to the mixture with Rejuvn8. Also, an opposite relationship between healing recovery and stiffness recovery was observed as the mixture containing microcapsules had a better stiffness recovery at both environmental curing conditions as the mixture with Rejuvn8. The self-healing experiment conducted to evaluate the strength recovery of the produced fibers showed an enhancement at both room and high-temperature of mixtures prepared with unmodified binder containing recycled materials with the addition of fibers.

CHAPTER 1. INTRODUCTION

The United States has more than 2.6 million miles of paved roads, of which 93 percent are surfaced with asphalt pavement. The persistent requests for asphalt binder resulted in a high demand for energy and promoted an increase in the asphalt pavement infrastructure. Demands rose exponentially as the price of asphalt binder increased in recent years. Researchers have emerged with innovative concepts to address such problems by using sustainable pavement technologies. Some examples of sustainable pavement technologies incorporate recycled materials, such as Reclaimed Asphalt Pavement (RAP) and Recycled Asphalt Shingles (RAS) in Hot-Mix Asphalt (HMA) mixtures. Another example of sustainable pavement technologies is to perform a Warm-Mix Asphalt (WMA) mixture. The benefits of using either type of this sustainable pavement technology leads not only to a reduction in the amount of virgin material consumption, but also a decrease in negative environmental effects.

The main problem of incorporating either RAS or RAP into HMA mixtures is that the binder from these recycled materials constitutes an aged binder, which means that an asphalt pavement with recycled materials would have a higher cracking susceptibility. The reduction in the capacity of relaxation is due to the aged binder and the exposure of the pavement to natural elements such as traffic and environmental loads. As a result, this origin of cracking in asphalt pavements with recycled materials strongly affects the serviceability and quality of the pavement [1]. Maintenance is the key to enhancement of pavement performance. According to the World Bank's Pavement Deterioration Model, the maintenance of a deteriorated asphalt pavement can rise up to four times the cost of maintaining a pavement in good condition [2].

Asphalt rejuvenators products have emerged to address the issues related to the aged binder in recycled materials. Asphalt rejuvenators may be defined as cationic emulsions containing maltenes, which are responsible for the elastic properties of the binder [3]. Asphalt rejuvenators are shown to be the only product that can partially restore the properties of aged binder. This remedy is accomplished by softening the oxidized asphalt and restoring the asphalts/maltenes ratio [4]. Furthermore, asphalt rejuvenators can extend the life of the pavement by sealing the pavement and minimizing future oxidation [5]. The effectiveness of restoring asphalt properties relates to the amount of penetration into the asphalt [6]. Previous studies indicate that asphalt rejuvenators do not penetrate more than 2 cm, which is insufficient for a product benefit [6]. Therefore, innovative concepts such as encapsulation methods, used in self-healing mechanisms, were studied to serve as rejuvenators [7].

Self-healing concepts were successful when applied in polymeric materials; hence, the interest in using self-healing mechanisms in asphalt concrete has increased in the last years. A promising self-healing mechanism for asphalt pavement is the encapsulation of asphalt rejuvenator, since that application would allow this particular material to resist the initiation and propagation of cracking caused by vehicular and environmental loading. It would also support a more reliable and resilient design of asphalt mixture, which is intended to provide a service lifetime of 20 years or more without delays to the users. The addition of self-healing mechanisms with asphalt rejuvenator products would also enhance the use of recycled materials such as RAS by restoring the properties of the aged binder.

1.1 Problem Statement

Asphalt pavements are the most common types of roadways in the United States, representing more than 93 percent of the 2.6 million miles of paved roads. A common problem in asphalt

pavement is the oxidation process of the asphalt binder, which yields to the hardening and stiffening of the binder, thus decreasing the functional and structural performance of the pavement. A useful treatment is the application of asphalt rejuvenators, not only to help reconstitute the chemical composition of aged binder, but also to recover the properties of aged binder [8]. A deep penetration of rejuvenator products must be accomplished to have the desired effect. However, studies show that the penetration extends to no more than 2 cm [6]. Therefore, self-healing mechanisms such as microcapsules and hollowed-fibers emerged as an innovative idea to design asphalt rejuvenators and to allow these a greater penetration. However, the evaluation and application of this method have not been considered to date.

1.2 Objectives

To address the aforementioned problem statement, the objectives of this study are as follows:

- a) Evaluate the effects of asphalt rejuvenators on hot-mix asphalt mixtures in order to test its effects in the fundamental engineering properties of the mixtures at high and intermediate temperatures;
- b) Develop a synthesis procedure for production of microcapsules and hollow-fibers containing an asphalt rejuvenator;
- c) Evaluation of the self-healing efficiency of double-walled microcapsules, through crack healing and stiffness recovery of damaged mixture specimens under two different healing conditions;
- d) Evaluation of self-healing efficiency of hollow-fibers, through crack healing and stiffness recovery of damaged mixture specimens under two different healing conditions.

1.3 Scope

This study will evaluate the effects of asphalt rejuvenators in the performance of hot-mix asphalt mixtures at high and intermediate temperatures. Furthermore, a rejuvenator product will be chosen to develop a microencapsulation procedure in which double-walled microcapsules would contain asphalt rejuvenator as a core material. Also, the same asphalt product would be encapsulated in hollow-fibers of sodium-alginate as a second self-healing mechanism alternative for asphalt pavements. Additionally, the study will assess the self-healing efficiency of hot-mix asphalt mixtures with either double-walled microcapsules or sodium-alginate fibers under different healing conditions, using a controlled laboratory set-up.

1.4 Research Approach

Proposed research activities will be organized into five phases and twenty-one tasks, as detailed in the following section.

Phase 1: Laboratory Testing of Asphalt Rejuvenators

Task 1: Hot-Mix Asphalt Mixtures Preparation

In Task 1, Hot-Mix Asphalt (HMA) mixtures will be prepared by using a polymer-modified asphalt binder PG 70-22M and aggregates (5/8" gravel, 1/4" gravel, coarse sand and fine sand), thus satisfying the mix design for a 12.5 Nominal Maximum Aggregate size asphalt mixture. A Recycled Asphalt Shingles (RAS) will be incorporated in selected mixtures at 5% by total weight of the mix. Furthermore, four asphalt rejuvenators will be added in selected asphalt mixtures at 5% of the total weight of RAS. Table 1.1 describes the different HMA mixtures developed for the study.

Task 2: Hot-Mix Asphalt Mixtures Performances at Intermediate Temperature

The evaluation of the prepared HMA mixtures at intermediate temperature will be characterized using the Semi-circular Bending (SCB) test. The SCB test will be conducted in accordance to AASHTO TP 105.

Table 0.1. HMA Mixture Description

Mixture Type	RAS Content (%)	Rejuvenator Content (%)
70CO	-	-
70PG5P	5% PCWS	-
70PG5SUN	5% PCWS	5% Sunflower Oil
70PG5REJ8	5% PCWS	5% Rejuvn8
70PG1252	5% PCWS	5% Cargill1252
70PG1253	5% PCWS	5% Cargill1253

Task 3: Hot-Mix Asphalt Mixtures Performances at High-Temperature

The evaluation of the prepared HMA mixtures at high-temperature will be characterized using a Loaded Wheel Tracking (LWT) test. The LWT test will be conducted in accordance to AASHTO 324.

Task 4: Dynamic Modulus $|E^*|$ Test

The dynamic modulus test will be conducted in the evaluated mixtures in accordance to AASHTO T 342. This test will evaluate the performance of the mixtures against permanent deformation and fatigue cracking resistance.

Phase 2: Evaluation of the Molecular Composition and Rheological Properties of Extracted Binders

Task 5: Extraction of Binder from HMA Mixtures

The procedure to extract the asphalt binder from the evaluated HMA mixtures will be performed in accordance AASHTO T 164, “Standard Method of Test for Quantitative Extraction of Asphalt Binder from Hot Mix Asphalt HMA – Method A.” Afterwards, the solution of solvent (trichloroethylene) and asphalt binder obtained from AASHTO T 164 – Method A will be then distilled to a point where most of the solvent is removed; finally, carbon dioxide gas will be introduced to remove all traces of trichloroethylene. This procedure will be conducted in accordance with AASHTO R 59, “Standard Practice for Recovery of Asphalt Binder from Solution by Abson Method.”

Task 6: High-Pressure Gel Permeation Chromatography

The High-Pressure Gel Permeation Chromatography (HP-GPC) will be conducted to determine the molecular weight distribution of asphalt binder. The molecules will be divided into high-molecular weight (HMW) and low-molecular weight (LMW) to determine the percentage of asphaltene and maltenes in the extracted binders from the different evaluated HMA mixtures.

Task 7: Superpave Performance Grading

The evaluation of rheological properties of extracted binders will be conducted using fundamental rheological tests such as dynamic shear rheometry, rotational viscosity, and bending beam rheometer. The characterization of binders will be conducted using the PG grading systems described in AASHTO M 320-09 (Standard Specification for Performance-Graded Asphalt Binder)

Phase 3: Production of Self-Healing Microcapsules Mechanism

Task 8: Microcapsule Synthesis

A green bio-oil product, Rejuvn8, from Sripath Technologies, was selected as the core material of the microcapsules. Double-walled microcapsules will be synthesized via in-situ polymerization, using polyurethane and urea-formaldehyde. Shirzad et al. presented a microencapsulation procedure and optimization [9].

Task 9: Thermal Stability of Microcapsules

The objective of this task is to evaluate the thermal stability of the microcapsules prepared in task 8 to assess their resistance to HMA production processes. A good thermal stability is required for the microcapsules to resist the high-temperature in an asphalt mix production. The thermal stability will be evaluated by performing a Thermal Gravimetric Analysis (TGA) with a rate of 10.00°C/min from room-temperature (i.e. 25°C) to 600°C for the developed fibers to determine their degradation rate at high-temperatures.

Task 10: Characterization of the Developed Microcapsules

The study will employ a scanning electron microscope (SEM-FEI 186 Quanta 3D FEG dual beam SEM/FIB) to evaluate the morphology of the produced microcapsules.

Microcapsules will be sprinkled on top of a double-sided tape attached to a pin stub specimen mount; then, the microcapsules will be sputter-coated with platinum for 4 min before imaging the specimens under a secondary electron mode at an accelerated voltage of 5 kV.

Phase 4: Production of Self-Healing Fibers Mechanism

Task 11: Polymer Fibers Synthesis

The objective of this task is to successfully develop hollow-fibers containing a rejuvenator product. In order to achieve this, a green bio-oil product will be encapsulated

in sodium-alginate fibers using a wet-spinning line. The procedure to develop the polymer fibers containing a rejuvenator will be modified from a previous study [10]. The encapsulating material was selected to be Sodium-alginate, as an agent for a low cost, organic, and low environmental impact, and as a self-degrading material.

Task 12a: Optimization of production parameters to prepare the fibers

Different fibers samples will be prepared at varying production parameters, which include: percentage of emulsifier, percentage of plasticizer, and amount of rejuvenator used. The different percentages of emulsifier are expected to affect the stability of the solution between the rejuvenator product and the encapsulating material. Furthermore, the study will assess the effects of adding a plasticizer into the healing solution to study its influence on the thermal stability of the developed fibers. Lastly, different ratios of rejuvenator to encapsulating material will be incorporated into the experimental matrix to determine its effects on both thermal stability and tensile strength of the fibers. Table 1.2 summarizes the experimental test factorial for the optimization process.

Task 12b: Test the thermal Stability and Tensile Strength of the produced fibers

The objective of this task is to evaluate the thermal stability and tensile strength of the fibers prepared according to table 1.2 to assess their resistance to HMA production processes. A good thermal stability is required for the fibers to resist the high-temperature in an asphalt mix production. The thermal stability will be evaluated by performing a Thermal Gravimetric Analysis (TGA) with a rate of 10.00°C/min from room-temperature (i.e. 25°C) to 600°C for the developed fibers to determine their degradation rate at high-temperatures.

Tensile strength will be assessed to evaluate the fibers resistance to breakage during the mixing process. Based on the literature, the fibers should have an Ultimate Tensile Strength (UTS) higher than 12 MPa to resist the typical compaction pressure during an asphalt mix production processes [11, 12]. The UTS of the developed fibers will be tested in tension using a tensile machine with 50 N load cell and at a cross-head speed of 0.01mm/s.

Table 0.2. Test Matrix for Fiber's Optimization

Sample ID	Rejuvenator to Polymer Ratio	Emulsifier Content (%)	Plasticizer Content (%)
Fibers1	1:1.5	30	-
Fibers2	1:1.5	40	-
Fibers3	1:1.5	50	-
Fibers4	1:1.5	30	10
Fibers5	1:1.5	30	20
Fibers6	1:1.5	30	30
Fibers7	1:1.5	30	40
Fibers8	2:1	30	10
Fibers9	2:1	30	40
Fibers 10	3:1	30	10
Fibers 11	3:1	30	40

Task 13: Characterization of the produced biodegradable fibers

A scanning electron microscope, a FEI Quanta 3D FEG Dual Beam SEM/FIB, will be used in this study to evaluate the size and morphology of the developed fiber with best thermal stability and tensile strength from Table 1.2. The fibers will be sprinkled on top of a double-sided tape attached to a pin stub specimen mount. The samples will then

sputter-coated with platinum for four minutes before imaging them under a secondary electron mode at an accelerating voltage of 10 kV. Furthermore, an EDX analysis on the surface of the developed fibers will be performed to determine the percentage of each chemical element that is present in the sodium-alginate fibers

Task 14: Determine optimum amount of fibers

The objective of this task will be to determine the optimum amount of fibers (i.e., % by weight of recycled materials) that enhances the performance of asphalt blends with recycled materials. Two different tests will be performed in this optimization process: Multiple Stress Creep Recovery (MSCR) and SCB test. The test-matrix for task 14 is shown in table 1.3.

The MSCR test will apply creep and recovery periods to measure the percentage recovery and non-recoverable creep compliance (J_{nr}). The MSCR will be performed in accordance to AASHTO TP 70, which consists of applying a low stress (0.1 KPa) for 10 creep/recovery cycles then the stress is increased to 3.2 KPa and repeated for an additional 10 cycles.

The SCB test will evaluate the susceptibility of mixtures in table 1.3 against fatigue cracking. The SCB test will be conducted in accordance to AASHTO TP 105.

Table 0.3. Test-Matrix for Tasks 14

Mixture Type	RAS	Fiber Content (%)
70CO	-	-
70PG5P	5% PCWS	-
70PGF1	5% PCWS	1%
70PGF2	5% PCWS	3%
70PGF3	5% PCWS	5%

Task 15: Characterization of asphalt binders containing fibers

The objective of this task is to perform a Superpave Performance Grading (PG grading) to evaluate the rheological properties of the asphalt blends for the test matrix described in Table 1.4. PG grading will be conducted using rheological tests such as dynamic shear rheometry, rotational viscosity, and bending beam rheometer. The characterization of binders will be conducted using the PG grading protocol described in AASHTO M 320-09.

Task 16: Performance testing of asphalt mixtures containing fibers

In addition to test asphalt mixtures against fatigue cracking in task 14, asphalt mixtures shown in table 1.4 will be subject through a controlled laboratory setup to test the low-temperature and high-temperature. High-temperature rutting resistance will be characterized using a Loaded Wheel Tracking (LWT) test in accordance to AASHTO T324. The low-temperature cracking performance of the mixture will be characterized using the Thermal Stress Restrained Specimen Tensile Strength (TSRST) test in accordance to AASHTO TP 10-93.

Table 0.4. Test-Matrix for Tasks 15

Mixture Type	RAS	Fiber Content (%)	RAP
Mix1	-	-	-
Mix2	5% PCWS	-	-
Mix3	5% PCWS	% Determined by task 14	-
Mix4	-	-	15%
Mix5		% Determined by task 14	40%
Mix6	5% PCWS		40%
Mix7	5% PCWS	% Determined by task 14	40%

Phase 5: Self-Healing Mixture Testing

Task 17: Specimen Preparation

Rectangular specimens with the dimensions of 40mm x 40mm x 160mm will be prepared by sawing cylindrical samples produced by a Superpave Gyratory Compactor. Five different mixtures will be evaluated to assess the self-healing efficiency from the different self-healing mechanisms. All specimens will be prepared to an air voids of $7.0 \pm 0.5\%$. Table 1.5 shows the description for each mixture.

Task 18: Environmental Conditions for Self-Healing

Specimens for each of the evaluated asphalt mixtures will be exposed to different dry temperature conditionings. The purpose is to evaluate the variability in the healing efficiency caused by the exposure of different environmental conditions. Six specimens will be prepared for each asphalt mixture type shown in Table 1.3, with three to be exposed to room-temperature healing conditions and three to be exposed to high-temperature healing conditions after cracking.

Table 0.5. HMA Mixtures Description for Self-Healing Mixture Testing

Mixture Type	RAS Content (%)	Rejuvenator Content (%)	Microcapsules Content (%)	Fibers Content (%)
70CO	-	-	-	-
70PG5P	5% PCWS	-	-	-
70PG5REJ8	5% PCWS	5% Rejuvn8	-	-
MCRcj8	5% PCWS	-	5%	-
FIBRej8	5% PCWS	-	-	% Determined by task 14

Task 19: Damaging of the Specimens

A three-point bending setup will be used to induce cracks at room-temperature in the prepared rectangular specimens and without prior conditioning, through a strain-controlled load applied at a rate of 0.25 mm/min, which allows the test to stop before any sudden failure.

Task 20: Quantification of Self-Healing

Utilizing an optical light microscope, the study will quantify the healing process of cracked specimens as a function of time, by adopting a magnification rate of 12x in order to measure the different cracks in the specimens. Immediately after crack characterization, specimens will then be subjected to a 6-day healing period under controlled environmental conditions. Specimens will be placed horizontally over a flat surface during the healing period. Cracks will be monitored at healing periods of 0, 1, 2, 3 and 6 days. The study will also perform a digital image analysis to measure the crack width over time. The healing efficiency of the specimens at the different healing periods will be calculated as follows:

$$H_e = \left(1 - \frac{Cw_t}{Cw_0}\right) * 100 \quad (1)$$

where,

H_e = Healing efficiency (%);

Cw_0 = Initial Crack width, mm; and

Cw_t = Crack width at the time of analysis, mm.

Task 21: Stiffness Recovery

A relationship between undamaged, damaged, and healed stiffness will be evaluated to determine the stiffness recovery at the end of the healing period. The three-point bending test results will be used to calculate the stiffness for three different conditions. The undamaged stiffness will be defined as the slope of the linear equation from the steepest part of the load-deformation plot, established from the first three-point bending test performed to induce the cracks. The same procedure will be repeated for a second three-point bending test before healing, in order to calculate the damaged stiffness and to increase the severity of the cracks before healing. Following healing, a third three-point bending test will be conducted to estimate the healed stiffness.

1.5 References

- [1] Z. Wu, L. Mohammad, L. Wang and M. Mull, "Fracture Resistance Characterization of Superpave Mixtures Using the Semi-Circular Bending Test," *Journal of ASTM International*, vol. 2, no. 3, 2005.
- [2] M. Y. Sahin, "Pavement Management for Airports, Roads and Parking Lots," Springer Science, 2005.
- [3] J. Brownridge, *The Role of an Asphalt Rejuvenator in Pavement Preservation: Use and Need for Asphalt Rejuvenation*, Bakersfield, California: Tricor Refining, LLC.
- [4] R. Karlsson and U. Isacson, "Material-related aspects of asphalt recycling—state of the art," *J. Mater. Civil Eng.* 18, 2006.
- [5] E. R. Brown, "Preventative Maintenance Of Asphalt Concrete Pavements," 1988.
- [6] C. Chiu and M. Lee, "Effectiveness of seal rejuvenators for bituminous pavement surfaces," *J. Test. Eval.*, vol. 34, pp. 390-294, 2006.
- [7] A. Garcia, E. Schlangen, M. van de Ven and G. Sierra-Beltrán, "Preparation of capsules containing rejuvenators for their use in asphalt concrete," *J. Hazard. Mater.*, vol. 184, pp. 603-611, 2010.

- [8] J. Shen, S. Amirkhanian and J. A. Miller , "Effects of Rejuvenating Agents on Superpave Mixtures Containing Reclaimed Asphalt Pavement," *Journal of Materials in Civil Engineering*, vol. 19, no. 5, 1 May 2007.
- [9] S. Shirzad, M. M. Hassan, M. A. Aguirre, L. N. Mohammad and W. H. Daly, "Evaluation of sunflower Oil as a Rejuvenator and Its Microencapsulation as a Healing Agent," *J. Mater. Civil. Eng.*, 2016.
- [10] S. D. Mookhoek, H. R. Fischer and S. van der Zwaag, "Alginate fibres containing discrete liquid filled vacuoles for controlled delivery," *Composites Part A: Applied Science and Manufacturing*, vol. 43, no. 12, pp. 2176-2182, 2012.
- [11] A. M. Hartman, M. D. Gilchrist and G. Walsh, "Effect of mixture compaction on indirect tensile stiffness and fatigue," *J. Transp. Eng.*, vol. 127, no. 5, 2001.
- [12] J. Bonnot, "Selection and use of the procedure for laboratory compaction of bitumen mixtures," *Performance Related Test Procedures for Bitumen Mixtures*, 1997.

CHAPTER 2. LITERATURE REVIEW

2.1 Introduction

Asphalt is the most used material in pavement application in the United States, as evidenced by more than 2.6 million miles of paved roads, of which 93 percent are crafted with asphalt binder.

Asphalt binder is a liquid or semi-solid substance derived from petroleum. The American Society of Testing Materials (ASTM) defines asphalt as a “dark brown to black cementitious material in which the predominant constituents are bitumen’s which occur in nature or are obtained in the petroleum processing” [1].

Asphalt binder is primarily used in pavement applications, where it is used as a glue to put together aggregate particles to create asphalt concrete. In addition, the versatility of the material offers valuable properties to engineers, such as good permeability, as well as a strong bonding with aggregates. Furthermore, asphalt binder is classified as thermoplastic and rheological material. Asphalt bitumen is considered to be a thermoplastic material because its properties change with respect to temperature. At high temperatures, the material may be used as a lubricant; on the other hand, the asphalt behaves on a viscoelastic state at low temperatures, enabling the asphalt to hold aggregates together. Similarly, asphalt binder properties are affected with change of time or frequency of loading. The material presents an elastic behavior during high-speed loading, opposed to a viscous behavior during low-speed loading. The changes in properties of asphalt binder with respect to temperature and frequency loading allow the material to be used not only for paving roads, but also for recreational projects such as a) playgrounds, b) bicycle paths, c) running tracks, d) agriculture projects such as barn floors and greenhouse floors, and e) industrial sectors such as ports and landfill caps.

Characteristics such as smoothness, durability, safety, sustainability, and easy construction make the asphalt a commonly used material for paving applications. The vehicle's fuel economy has a positive impact by the smoothness of the asphalt as it provides a lower wear and tear on the vehicle. Furthermore, the intended serviceability life of asphalt pavement roads may be obtained by performing an adequate design and construction procedure, as well as maintenance and rehabilitation treatments. Another advantage of using asphalt material is that asphalt may be recycled and is reusable to reduce the environmental impact from the manufacturing process. Lastly, there is no delay in opening lanes for travel, since asphalt construction requires no curing time.

Rehabilitation and maintenance techniques are the key toward enhancement of asphalt performance, which serves in providing a better opportunity to achieve the intended design life, accompanied by less premature failures, together with a lower overall cost in the future.

According to the World Bank Pavement Deterioration Model, if an asphalt pavement road is left to deteriorate, the cost of reinstating a new road may be four times more expensive than the cost of maintenance to keep the road in good condition [2]. Further, a Utah Department of Transportation (UDOT) study demonstrated that the cost was found to be less in maintaining roads that were in good condition than those in poor condition (Zavitski). Another study conducted by the National Cooperative Highway Research Program revealed that every dollar spent on maintenance at the correct time saves \$3 - \$4 in future costs [3]. Finally, Figure 2.1 presents the results from a study conducted by Galehouse, Moulthrop, and Hicks, where results show that future rehabilitation cost savings exhibited a strong \$6 - \$10 for every \$1 spent on preventive maintenance [4].

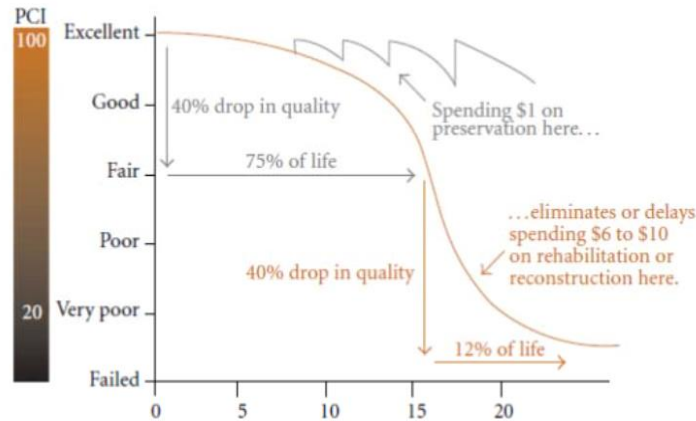


Figure 0.1. Effect of Preventive Maintenance at Life Cycle Cost of the Pavement [4]

2.2 Asphalt Binder

Asphalt cement is one of the oldest materials used for engineering purposes. Early civilization used asphalt binder extensively for its adhesive and waterproofing properties [5]. The commercial types of asphalt cement may be classified as natural and petroleum asphalts. The natural asphalt can be found as a hard, friable, black material in rock formation veins, or infused in limestone and sandstone formations. Some examples of natural asphalts may be found in the Trinidad Lake deposit on the Island of Trinidad, as well as the Bermudez Lake in Venezuela [6]. The petroleum asphalt is obtained by refining petroleum crudes. The composition of the crude petroleum differs from source to source by variances in the amount of bitumen residual and other distillable materials such as gasoline, kerosene, light gas oil and heavy gas oil [7]. Figure 2.2 shows the variation in the volume percentages of refinery materials in three different locations. Crude oils may be classified based on the American Petroleum Institute (API) gravity, which presents a relationship in the specific gravity of a material at 60° F [8]. Equation 2.1 shows the API relationship. For reference, the API gravity value for water is 10, and most of the asphalts products have a value found between 5-10.

$$API = \frac{141.5}{\text{Specific Gravity}} - 131.5 \quad (2.1)$$

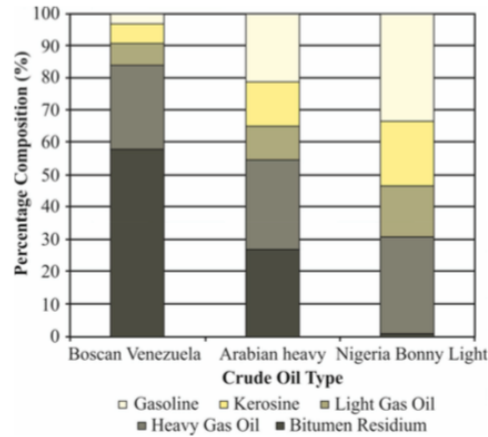


Figure 0.2. Composition of Crude Oil [9]

2.2.1 Types of Asphalt Binder

The asphalt types most commonly used in the paving industry are: asphalt cement, emulsified asphalts, and cutback asphalts. Asphalt cement is obtained by the distillation process of crude petroleum, using different refining techniques. Some of the refining techniques utilized are the Solvent Deasphalthing (SDA), Residuum Oil Supercritical Extraction (ROSE) and Air-blowing. The production of Hot Mix Asphalt (HMA) involves the primary application of asphalt cements. HMA is produced by liquefying the asphalt cement by means of high temperatures and then mixing the cement with both fine and coarse aggregates. Asphalt cement performs as a glue for the aggregate particles. The HMA mixture is then compacted and allowed to cool to ambient temperatures, where the mixture becomes capable to handle heavy traffic loads.

Emulsified asphalt or asphalt emulsion is a mixture of asphalt cement, water, and an emulsifier agent. An emulsifier agent may be defined as a chemical, soluble in both fat and water, which enables the dispersion of fat into water as an emulsion. A colloid mill is required for use in order to produce small droplets of asphalt cement suspended in water. Emulsified asphalts are

commonly used to apply asphalt cement in a lower application temperature. ASTM specifies two types of emulsified asphalts in ASTM D977 and ASTM D2397 for use: anionic and cationic emulsions. An anionic emulsion is an emulsion where the asphalt droplets carry a negative charge; whereas in a cationic emulsion, the asphalt droplets carry a positive charge [10] [11].

Cutback asphalts are liquid asphalts that are produced by adding a petroleum solvent to reduce the viscosity of the asphalt cement. In the same manner as emulsified asphalts, cutback asphalts are used in low application temperature environments. Cutback asphalts are divided in three categories, based on the evaporation rate: rapid curing, medium curing, and slow curing. Rapid curing cutback asphalt is commonly used for tack coat and surface treatments. Prime coat and patching mixtures are usually performed with either medium curing or slow curing cutback asphalts [12].

2.2.2 Chemical Composition

The chemical composition of an asphalt binder is divided in asphaltenes and maltenes.

Asphaltenes may be defined as the chemical component from the asphalt binder that is soluble in toluene and it dissipates in n-alkane solvents [13]. Asphaltenes are considered the “bodying” component of asphalt cements by playing an important role as the viscosity-builder [14]. The fraction part of the binder that is soluble in n-alkane solvents such as pentane and heptane are defined as maltenes. The maltenes component of the asphalt binder is divided in nitrogen bases as follows: first acidifins, second acidifins, and paraffins. The nitrogen bases act as a peptizer for asphaltenes [15]. The first acidifins are components of resinous hydrocarbons, which function as a solvent for the peptized asphaltenes [15]. The second acidifins are unsaturated hydrocarbons that are used as the first acidifins [15]. Lastly, the saturated hydrocarbons or paraffins are used as a jelling agent [15].

2.2.3 Binder Oxidation Process

The oxidation process in the asphalt binder affects its physical and chemical properties by making the binder harder and stiffer [16]. The oxidation process allows carbonyl ($-C=O$) groups to be formed, which in turn, increases the polarity of the compounds and causes these to associate with other polar compounds [17]. As a result, the association of the carbonyl groups with other polar compounds produces less soluble asphaltene materials, which result in asphalt hardening [17].

The reduction in the pavement performance results in the impact of the oxidation process on the binder, as the binder becomes stiffer and more brittle [18]. The viscosity and elastic properties of the binders are affected, due to the changes in the binder composition that occur during the oxidation process [19]. The high elastic stiffness that results from the oxidation process subsequently yields to a material that cannot relieve the stress, which results in a material displaying a high susceptibility of fatigue and thermal cracking.

2.3 Asphalt Mixture Performance Tests

The laboratory mechanistic performance and material characterization tests are conducted to evaluate Hot-Mix Asphalt mixtures against distresses such as fatigue cracking, low-temperature cracking, rutting, and moisture susceptibility.

2.3.1 Dynamic Modulus, $|E^*|$

The Dynamic Modulus test is a triaxial compression test, standardized in 1979 as ASTM D3497, “Standard Test Method for Dynamic Modulus of Asphalt Concrete Mixtures” [20]. A uniaxial sinusoidal (i.e., harmonic) compressive stress is applied to an unconfined or confined HMA cylindrical test specimen, as shown in Figure 2.3. The “complex modulus (E^*)” is defined as the stress to strain relationship under a continuous sinusoidal loading for linear viscoelastic materials

[20]. The absolute value of the complex modulus is defined as the dynamic modulus, $|E^*|$. The dynamic modulus is mathematically defined as the ratio between the peak dynamic stress (σ_0) and the peak recoverable strain (ϵ_0).

$$|E^*| = \frac{\sigma_0}{\epsilon_0} \quad (2.2)$$

A dynamic modulus tests is usually conducted at -10, 4, 20, 38.8 and 54.4°C at loading frequencies of 0.1, 0.5, 1.0, 5, 10, 25 Hz at each temperature [21].

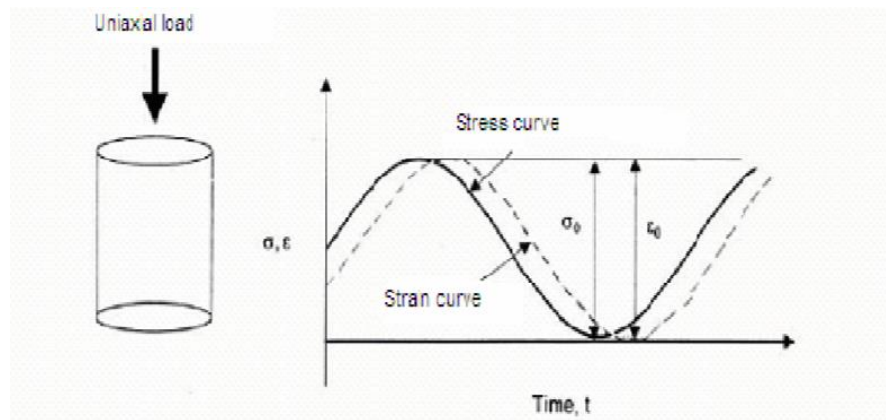


Figure 0.3. Stress-Strain Relationship under Sinusoidal Load

2.3.2 Loaded Wheel Tracking (LWT) Test

The Loaded Wheel Tracking (LWT) test is performed to evaluate HMA mixtures at high-temperature to assess the rutting susceptibility due to traffic loading. The LWT test is performed, based on the standard AASHTO T324-04, “Standard Method of Test for Hamburg Wheel-Tracking Testing of Compacted Hot-Mix asphalt (HMA)” [22]. The test consists of submerging two HMA cylindrical specimens under hot water with a temperature of 50°C. The specimens are subject to a steel wheel weighing 703 N (158 pounds), which repeatedly rolls across its surface. The test is complete when the specimens have been subjected either to a maximum of 20,000

cycles or attained a 20 mm deformation, whichever is first reached. Upon completion of the test, the average rut depth for the tested samples is recorded. Figure 2.4 shows a typical LWT test.



Figure 0.4. Loaded Wheel-Tracking (LWT) Test

2.3.3 Semi-Circular Bending (SCB) Test

The Semi-Circular Bending (SCB) test is performed to evaluate HMA mixtures at an intermediate-temperature to assess the cracking resistance of an asphalt mixture. The fracture resistance of an HMA is evaluated based on the fracture mechanics principles, described by the critical strain energy release rate, also called the critical value of J-integral (J_c) [23]. The mathematically formula to describe the critical strain energy release rate is the following:

$$J_c = - \left(\frac{1}{b} \right) \frac{dU}{da} \quad (2.3)$$

Where:

J_c = critical strain energy release rate (kJ/m²);

b = sample thickness (mm);

a = notch depth (mm);

U = strain energy to failure (N·mm); and

dU/da = change of strain energy with notch depth

Semi-circular specimens with notch depths of 25.4 mm, 31.8 mm, and 38 mm are used to determine the critical value of J-integral, using Equation 2.3 by calculating the change of strain energy with each notch depth (dU/da). A three-point bending load configuration is utilized to apply a monotonical load under a constant cross-head deformation rate of 0.5 mm/min, as shown in Figure 2.5. The load and deformation are continuously recorded and the test is performed at a temperature of 25°C. The strain energy to failure (U) is represented by the area under the loading portion of the load deflection curves, up to the maximum load measured for each notch depth. The average values of U are then plotted versus the different notch depths to compute a regression line slope, which gives the value of (dU/da). Finally, the J_c is computed by dividing dU/da value by the specimen thickness.

The semi-circular specimens are compacted in a Superpave Gyratory Compactor (SGC) to an air void level of $7 \pm 0.5\%$. The compacted samples are aged in accordance with AASHTO PP2 by placing compacted specimens in a forced draft oven for five days at 85°C [24]. Three specimens per notch depth are utilized to control the variation in the critical strain energy release rate values (J_c). High J_c values are desirable for fracture-resistant mixtures.

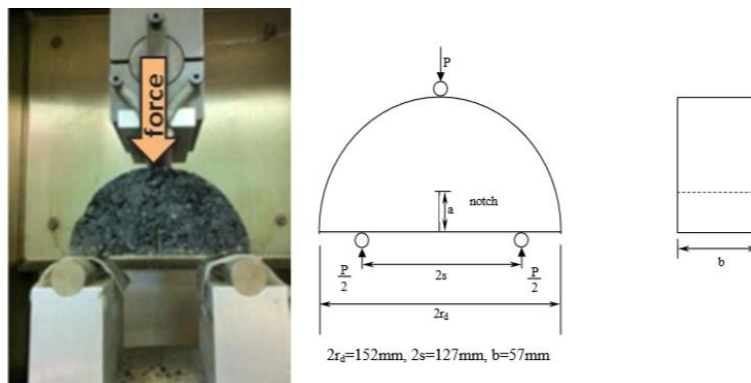


Figure 0.5. Semi-Circular Bending (SCB) Test

2.3.4 Thermal Stress Restrained Specimen Tensile Strength (TSRST) Test

The low-temperature cracking susceptibility of HMA mixtures is evaluated by performing a Thermal Stress Restrained Specimen Tensile Strength (TSRST) Test based on the standard AASHTO TP 10-93 [25]. The test consists in cooling an HMA specimen at a constant rate while being constrained from contraction. The TSRST determines the tensile strength and temperature at fracture, which can be used to evaluate the susceptibility of an HMA mixture against low-temperature cracking.

The TSRST test uses rectangular specimens with dimensions of 50 ± 5 mm (2.0 ± 0.15 in.) square and 250 ± 5 mm (10.0 ± 0.25 in.) in length, which are manufactured by sawing each test specimen from a rectangular HMA slab of dimensions 260.8 mm (10.25 inches) wide, by 320.3 mm (12.5 inches) long, by 50mm (2 inches). The prepared beams are affixed at each end to platens of the test machine, and enclosed in an environmental chamber for conditioning. Afterwards, a tensile load of 50 ± 5 N (10 ± 1 lbs.) is applied to the HMA beam specimen, and the specimen is cooled at the rate of $10.0 \pm 1^\circ\text{C}$ per hour until tensile fracture occurs. The thermal contraction along the long axis of the specimen is monitored electronically. A typical setup for a TSRST test is shown in Figure 2.6.

The fracture stress of the HMA beam specimen is calculated with the following expression:

$$\text{Fracture Stress} = \frac{P_{ult}}{A} \quad (2.4)$$

Where:

P_{ult} = ultimate tensile load at fracture (pounds); and

A = average cross-sectional area of beam specimen (mm²)



Figure 0.6. Thermal Stress Restrained Specimen Tensile (TSRST) Test

2.4 Sustainable Pavement Technology

The demand of asphalt pavement, as the most commonly used pavement surface material globally, increases every year; predictions expect a demand in the United States (US) of 28.6 million tons by 2019 [26]. This expansive call for energy, together with increased resource employment in asphalt paving construction, and in tandem with a continual increased price in asphalt cement, motivates researchers to seek out innovative, tenable approaches.

Researchers have investigated the usage of sustainable pavement technologies into the HMA mixture process to reduce virgin material consumption as well as negative environmental effects, together with the cost of asphalt pavement. Some examples of sustainable pavement technologies adopted by the asphalt pavement industry are the use of Recycled Asphalt Pavement (RAP), Reclaimed Asphalt Shingles (RAS), and Warm-Mix Asphalt (WMA).

The use of RAP in the pavement industry started in the 1970s. By the 1980s, the first field trials evidenced a very high RAP content [27]. RAP, as a processed asphalt pavement, was removed during a resurfacing, rehabilitation, or reconstruction operation. An important characteristic of RAP reflects an amount of asphalt binder and aggregates that are presented in the recycled material, as shown in Figure 2.3. The Federal Highway Association (FHWA) and the U.S.

Environmental Protection Agency estimated that more than 90 million tons of asphalt pavements were reclaimed every year, of which more than 80 percent is processed to produce RAP [28].

The most common role of the RAP is to provide a substitute for aggregate and virgin binder in recycled asphalt paving, yet RAP also may be used as a granular base or sub-base, a stabilized base aggregate, or as an embankment/fill material.

RAS is a material commonly used in the roofing industry, which consists of asphalt binder, mineral filler, organic paper felt, and glass fiber matting [29]. An estimated 11 million tons of waste shingles are produced every year, which leads to 22 million cubic yards of waste material that in the past would be disposed as landfill [30]. Studies have shown that the use of RAS in asphalt pavement not only decreases the negative environmental impact of virgin material extraction and transportation, but also reduces the need for landfill space. A previous estimate predicted that one barrel of asphalt binder could be replaced by one ton of recycled shingles [31]. Despite the several advantages of RAS, the aged binder existing in the RAS remains as a main challenge toward incorporation into the HMA mixture process. In addition, the aged binder in the RAS tends to limit use of the high percentages of RAS in asphalt pavements, which also resonates the limited allowance to use RAS in the US. A threshold level of 5% is used in certain states of the US where allowed. Previous studies indicate that utilizing RAS up to 5% by weight of the asphalt mixture displays a similar behavior with conventional mixtures [32]. Another disadvantage of RAS is the variability and inconsistency of the resources [33].

For asphalt pavements, WMA is another sustainable technique that can lower the mixing and compacting temperature of asphalt mixes. Lowering the mixing and compacting the temperature is achieved either by lowering the viscosity of the binder or by increasing the workability of the mix [34]. Lowering the mixing temperature can lead to a reduction on plant emissions and fuel

cost [35]. Another advantage of lowering the mixing temperature of asphalt mixture is the reduction of fumes. Higher percentages of RAP can be incorporated into WMA mixes rather than into HMA mixes, due to the aging reduction of the virgin binder during the mixture process, thus adding to environmental advantages [36]. An increase in workability is also a benefit of using WMA, which leads to a better density in the field [37]. Lowering the viscosity of the binder in a WMA is accomplished by using organic additives, chemical additives, and foaming. Organic additives lower the viscosity of the binder by incorporating a long chain of hydrocarbons in the mix [38]. Chemical additives such as emulsifier agents are utilized to improve coating, mixture workability, and compaction [38]. Lastly, water may be added to hot asphalt to produce small bubbles in the binder that cause a decrease in viscosity [38].

2.4.1 HMA Performance with Asphalt Pavement Technology

A previous study evaluated the effect of different percentages of RAP in HMA mixtures, based on the complex modulus relationship with the control mixtures [39]. The study concluded that there is an increase in the complex modulus of the mixtures containing up to 15% RAP level from the control mixtures, although the complex modulus curves of the mixtures with 25% and 40% RAP were similar to the control mixture for both tension and compression. Researches concluded that the unexpected similarity between the high RAP content mixtures and the control mixture in the complex modulus was due a combination of gradation, asphalt content, and volumetric properties.

A similar study was conducted by Shah et al., where researchers reported that the complex modulus curve showed no increase in stiffness due to the addition of 15% RAP when compared to the control mixture. However, high percentages of RAP (25% and 40%) resulted in an increase in the complex modulus curve, compared to the control mixture [40].

A study performed by Li et al. evaluated the effect of RAP percentages and sources on the properties of HMA by conducting complex modulus and semi-circular bending (SCB) tests [41]. Results showed a trend at high temperatures, where the HMA mixtures containing 40% RAP had a higher or similar complex modulus compared to mixtures with 20% RAP. However, the HMA mixtures containing 20% RAP showed the highest complex modulus at either low temperatures or high frequencies. The SCB test results indicated that the HMA mixtures containing 20% RAP performed similarly to the control mixtures, which had the highest fracture energies.

Furthermore, the susceptibility to low-temperature fracture increased on HMA with a 40% RAP.

The thermal cracking resistance of recycled hot mixtures (RHM) was evaluated in a previous study [42]. The thermal resistance was evaluated with laboratory and field mixes by using McLeod's limiting stiffness criteria and the pavement fracture temperature (FT) method. The study concluded that the RHM showed a lower resistance to thermal cracking, compared to non-recycled mixes.

The rutting, fatigue and low-temperature cracking susceptibilities were evaluated by Gardiner et al. [43]. The study evaluated two sources of RAP (Georgia and Minnesota) in an HMA mixture containing between 15%-40% RAP. The temperature susceptibility was conducted by determining the resilient modulus of the mixtures according to ASTM D4123. An asphalt pavement analyzer (APA) loaded wheel tester with 685 kPa at a test temperature of 64° C was utilized to evaluate the rutting potential. Lastly, the low-temperature properties were determined by the indirect tensile creep test. The results indicated an increase in tensile strength ratio (TSR) as the RAP percentage increased. Also, the HMA mixtures containing RAP had a positive influence in decreasing the temperature susceptibility, when compared to the control mixture.

Finally, the rutting potential was decreased about 20% in mixtures containing RAP, compared to the control mixture at 8,000 cycles.

Widyatmoko evaluated the containment of different percentages of RAP (i.e., 10%, 30% and 50%) in HMA to determine the varying mechanical resistance properties against fatigue and rutting [44]. The study revealed a lower resistance against rutting in the mixtures containing RAP, compared to the control mixtures. Also, softer mixes (i.e., a decrease in stiffness) were found as the percentage of RAP increased. However, this behavior may be explained, due to the high amounts of rejuvenator oil added in the mixtures as the RAP percentage increased. The addition of rejuvenator oil influenced the performance of mixtures containing RAP, since these performed similarly to the mixtures without RAP. Lastly, the study showed that different mixtures with RAP were not affected by moisture damage.

The fatigue life of mixtures containing RAP was evaluated for NCHRP 9-12, where the study revealed that mixtures containing more than 20% RAP had a lower fatigue life than virgin mixtures [45]. However, the fatigue life of mixtures with RAP was also evaluated by Shu et al.; the results showed an increased fatigue life, based on a failure criterion of 50% reduction in stiffness [46].

The appropriateness of using up to 5% of RAS in asphalt concrete was evaluated by Maupin [47]. The objective of the study was to determine whether the addition of RAS would result in a negative performance in the durability of an asphalt pavement. Maupin determined that the fatigue life of mixtures containing RAS was similar to conventional mixtures. The rutting depths of the mixtures with RAS were determined to be within the guidelines of the Virginia Department of Transportation (VDOT). The binder from the evaluated mixtures was recovered,

and found to have improvements in the high-temperature grading; the low-temperature grading was within state specifications.

Asphalt Pavements containing 5% Manufactured Waste Shingles (MWS) in the state of Georgia were evaluated by Watson et al. [48]. The prepared asphalt mixtures were made with binder AC-20 and AC-30 and were 5% MWS by weight of binder. The study tested the asphalt mixtures for a) gradation, b) AC content, c) maximum specific gravity, d) bulk specific gravity, e) stability and flow, f) LWT test, g) viscosity, h) penetration, and i) moisture susceptibility. The performance against rutting and fatigue of the evaluated mixtures was determined to be similar to the control mixtures. The viscosity of the recovered binder from the mixtures with RAs was found to be higher than the one recovered from the control mixtures; thus, a negative effect on the performance was not found. Researchers deduced that the increase of viscosity due to RAS could be beneficial in reducing rutting susceptibility.

Sengoz et al. evaluated the stability and the resistance against rutting in mixtures containing RAS from 1% to 5% by weight of the binder [49]. Also, the behavior of the variability of the optimum asphalt content was evaluated. The study concluded that the addition of RAS in HMA mixture could positively affect the Marshal Stability and rutting resistance. Furthermore, the study observed that the optimum binder content was reduced by 0.5% in the HMA mixture containing 1% RAS, thereby increasing the stability values of the mixture.

The susceptibility to cracking using Indirect Tensile Testing and the resistance to permanent deformation using the dynamic creep test and the Asphalt Pavement Analyzer (APA) were evaluated in HMA mixtures containing RAS as a possible replacement for a portion of the neat asphalt binder and aggregate [50]. The conclusions of the study were: a) the mechanistic properties of the mixtures with RAS are comparable to conventional HMA mixtures; b) the

binder from RAS causes an increase in the stiffness of the recycled asphalt binder, as well as an increase in the performance grade of the recycled asphalt by one grade, causing 5% RAS to be sufficient; and c) the rutting susceptibility decreases with the application of RAS in HMA mixtures. However, the fatigue resistance and low-temperature cracking resistance can be negatively affected by the RAS.

The State of Missouri has a provision in the standard specifications to allow the addition of RAS in any mixture requiring the use of Performance Grade (PG) 64-22 [51]. Missouri allows up to 7% RAS in HMA mixtures, and the RAS can be either manufactured waste shingles (MWS) or post-consumer waste shingles (PWS). One of the first concerns in the usage of RAS was the reduction in resistance to fatigue and low-temperature cracking, due to the aged binder in RAS. Studies determined that the usage of RAS did not affect negatively the low-temperature grading of the binder when an asphalt mixture composed at least 70% of virgin binder of the required binder. The low-temperature cracking susceptibility became a concern only when the percentage of virgin binder dipped below 70%, based on test results.

Washington State performed a study to investigate the performance of HMA with and without recycled materials, based on the evaluation of field cores from four experimental pavement sections constructed in 2009 [52]. The description of each of the four evaluated experimental sections may be found in Table 2.1. The performance parameters evaluated in the study consisted of the resistance against rutting, fatigue, and thermal cracking.

Table 0.1. Quality Acceptance Summary of Four Section [52]

Section	RAP/RAS	Asphalt content (%)	Baghouse fines content (%)	Air void content (%)
1	15% RAP	5.6	6.5	2.3
2	3% RAS+15% RAP	5.6	7	3.3
3	3% RAS+15% RAP	6.4	7	1
4	15% RAP	5.4	5.9	3.3

The study results show that the PG grading from the recovered binders of the evaluated mixture was not affected by the addition of RAS, based on a statistical analysis. However, the binder tests indicated a better performance against rutting for mixtures with RAS, based on MSCR test results. This behavior was consistent with the HWTD test result. Both binder test and mixture testing showed no statistical difference between mixtures with or without RAS against fatigue susceptibility. Lastly, the thermal cracking susceptibility resulting from binder tests indicated that the addition of RAS adversely affected the performance against thermal cracking, whereas a similar performance was observed between mixtures with and without RAS in the mixture testing.

As mentioned before, an advantage of using WMA technologies is to lower the viscosity of the binder at lower temperatures. However, the rutting capacity of these technologies is a concern, as the binder can show a result of being less stiff than HMA binder. Hurley and Prowell evaluated the performance against rutting of several WMA additives [37]. The rutting capacity of the evaluated mixtures was determined by an Asphalt pavement analyzer (APA). The results show

that the WMA additive Aspha-min had little impact on the rut depth, when compared to the control mixture [34]. Another tested WMA additive, Sasobit, was determined to reduce rut depths compared to the control HMA mixture [53]. Lastly, a similar result from Sasobit was observed with another WMA additive (Evotherm), where rut depth decreased compared to the control mixture [54].

A foaming technology in a WMA was evaluated to determine its effects on rutting resistance [55]. The foaming product utilized was Astec Double Barrel Green; an APA was utilized to evaluate the rutting susceptibility of the WMA mixtures. The study concluded that the WMA mixes were more susceptible to rutting, compared to the control HMA mixture. However, the rut depth of the WMA mixture with the foaming technology was still acceptable according to the APA test. A similar study evaluated the rutting performance of the same foaming technology in a WMA with 15% RAP, where the rut depth was slightly larger than the control HMA; thus it was still acceptable for the APA test [56].

2.5 Asphalt Rejuvenation

Despite advantages such as reducing virgin material consumption and decreasing the negative environmental effects of using recycled materials, the performance of HMA mixtures containing RAP or RAS are affected due to the aged binder existing in those recycled materials. Properties of the binder become highly dependent on the aging process during the service life of shingles. A binder's property, which is affected due to the aging and oxidation process, is shown by an increase of the asphaltene to maltene ratio [57]. Further, the fatigue and thermal cracking resistance of HMA mixtures is negatively affected due to the increase of the asphaltene to maltene ratio as the binder becomes stiffer and more brittle [58]. A recommended solution is to address the issues related to aging of recycled material with the use of a rejuvenator product.

An Asphalt rejuvenator may be defined as a cationic emulsion containing maltenes, purposed to soften the aged binder and its flux in order to end the serviceability life of the pavement, thus recovering the properties of the oxidized asphalt binder [59]. A rejuvenator product recovered the properties of the aged binder by rebuilding the chemical composition of the binder, i.e., restoring the asphaltene to maltene ratio [60]. Also, a rejuvenator can penetrate into an asphalt pavement to fill voids in the pavement, thus decreasing any further oxidation process, since the rate of oxidation depends on the voids in the total mixture (VTM) [61]. Lastly, rejuvenators also may be used in a combination of various recycled materials in order to further increase the blending of the aged and virgin binders and increase deformation capability, thereby ultimately reduce the stiffness of the aged binder.

Rejuvenator products must satisfy some requirements in order to be eligible for use in preservation techniques. First, asphalt rejuvenators should have a minimum ratio between Nitrogen Base and Paraffins of 0.5 to assure compatibility and to prevent syneresis [60]. Furthermore, a rejuvenator product must satisfy requirements for viscosity (60° C), flash point, volatility, compatibility, chemical composition, and specific gravity [62].

Studies on asphalt rejuvenators have shown that these are the most effective treatment to partially restore asphalt properties [63]. However, in order for rejuvenators to restore the aged binder, the rejuvenators must penetrate deeply into the asphalt; other than that, rejuvenators could cause the surface to become slick, especially in wet weather [61].

Flux oil, Reclamite, Dutrex, and dust oil were selected as rejuvenating agents. Each of the oils was evaluated to determine the rejuvenating effect on recycled asphalt mixtures and on-laboratory compacted mixtures with aging [64]. The purpose of the study was to determine whether these rejuvenating agents had the capabilities to restore the aged binder properties. The

study shows that both Dutrex and dust oil were most effective to soften the aged binder, followed by positive results in Reclamite and then flux oil. Also, the study found that both the Marshall stability and resilient modulus of the recycled mixtures were reduced, due to the effects of asphalt rejuvenators.

Shen et al. evaluated HMA mixtures containing RAP with either a rejuvenator or a softening agent to determine the mixture performance in an indirect tensile strength (ITS) and rutting performance with an asphalt pavement analyzer (APA) [60]. A total of 12 Superpave mixtures, including 10 recycled and 2 virgin mixtures, evaluated in the study as shown in Table 2.2. The selected rejuvenator was a commercial oil product in the United States, where the percentage of rejuvenator in the mixtures needed to rejuvenate the RAP binder to PG 64-22 was determined, based on results from Dynamic Shear Rheometer (DSR) and Bending Beam Rheometer (BBR) tests. The results from ITS showed that the mixtures containing RAP and rejuvenator performed similarly with the virgin mixtures: Results were within the requirements. Also, the evaluated mixtures were not susceptible to moisture damages, as observed visually with the ITS test. Finally, all the rut depths from the different mixtures were less than the 8.0 mm criteria based on APA results.

A study evaluated the ability to recover the properties of aged binder with a soft binder containing a low asphaltene content of 2 wt% as a rejuvenator product at various percentages shown at three stages: no aging, rolling thin-film oven (RTFO), and RTFO+ pressure aging vessel (PAV) by performing DSR and BBR tests [65]. Furthermore, the effect of the rejuvenator agent was evaluated in HMA mixture by evaluating the rutting and low-temperature cracking performance. The binder test results showed an increase in performance of the threatened aged binder, using a rejuvenator agent against fatigue and shrinkage. On the other hand, the

performance against rutting decreased. Similar behavior was observed during the mixture testing, where the rutting performance of the mixtures with rejuvenator was not as good as the virgin mixtures, whereas the fracture properties were improved by the addition of the rejuvenator product. Lastly, the thermal stress restrained specimen test (TSRST) showed a decrease in strength on the mixture with a rejuvenator, compared to virgin mixtures. Researchers explained this outcome was due to a repeated cooling and heating of cycles that served to decrease the elasticity of the samples.

Table 0.2. Superpave Mixtures [60]

Mixture Code	Binder	RAP (%)
CV0	PG 64-22	0
CV15	PG 52-28	15
CR15	Rejuvenator, PG 64-22	15
CV38	PG 52-28	38
CR38	Rejuvenator, PG 64-22	38
CR48	Rejuvenator, PG 64-22	48
LV0	PG 64-22	0
LV15	PG 52-28	15
LR15	Rejuvenator, PG 64-22	15
LV30	PG 52-28	30
LR30	Rejuvenator, PG 64-22	30

2.6 Self-Healing Technology in Asphalt Pavement

Asphalt binder can be defined as a self-healing material, which means the asphalt binder has a built-in ability to partially repair damage occurring during service life [66]. The binder's properties, such as stiffness and strength, degrade over time due to an exposure to load and to

micro-cracking. In the 1960s, researchers observed for the first time that the capacity of the asphalt binder demonstrated the ability to recover stiffness and strength under a fatigue test with rest periods [67].

The concept of self-healing systems was incorporated to man-made materials by White, when he introduced the microencapsulation self-healing systems into an epoxy matrix [68]. The principle in testing the healing of a material is to incorporate healing periods between two loadings.

Furthermore, the healing efficiency can be characterized by comparing the response of the material with and without healing periods. The most common types of test methods used to evaluate the healing of a material are:

1. Fatigue related healing test

- Fatigue related healing with intermittent loading: This is when an intermittent load, followed by a rest period, is applied to a specimen.
- Fatigue related healing with storage periods: The specimen is subjected to continuous load repetitions for certain time. Afterwards, the load is suspended, applying a storage period where the specimen is kept under given conditions without loading.

2. Fracture related healing test: Two fracture tests are performed on a specimen with a healing period between them.

The concept of developing self-healing mechanisms mimics the healing capacity of the skin to recover after an injury. Injured skins and tissues may be self-healed, owing to the presence of nutrient supplies in the body that substitute the damaged cells. Hence, researchers have developed novel self-healing mechanisms for composite structures by pursuing this biological principle. A list of innovative self-healing mechanisms can be observed in Table 2.3.

Table 0.3. Biomimetic Self-Healing Inspiration in Novel Self-Healing Materials [69]

Biological attribute	Composite/polymer engineering	Systems	Biomimetic self-healing or repair strategy
Bleeding	Capsules	Liquid based	Action of bleeding from a storage medium housed within the structure, 2-phase polymeric cure process rather than enzyme “waterfall” reaction
Bleeding	Hollow Fibers	Liquid based	Action of bleeding from a storage medium housed within the structure, 2-phase polymeric cure process rather than enzyme “waterfall” reaction
Blood flow	Hollow Fibers	Liquid based	2D or 3D network would permit the healing agent to be replenished and renewed during the life of structure
Blood clotting	Healing resin	Liquid based	Synthetic self-healing resin systems designed to clot locally to the damage site. Remote from the damage site clotting is inhibited and the network remains flowing.
Concept of self-healing	Remendable Polymers	Solid based	Bio-inspired healing requiring external intervention to initiate repair
Blood cells	Nano-particle	Solid based	Artificial cells that deposit nano-particles into regions of damage
Skeleton/bone healing	Reinforcing fibers	Solid based	Deposition, resorption, and remodeling of fractured reinforcing fibers

The self-healing mechanisms currently investigated for asphalt applications are the application of nanoparticles such as nanoclay and nanorubber, induction heating, and asphalt rejuvenation. A discussion for each mechanism may be reviewed in Section 2.6.1-2.6.3.

2.6.1 Nanoparticles in Asphalt Pavement

Nanotechnology may be defined as the creation of new materials, devices, and systems at the molecular level, to induce desirable improvements into macroscopic material properties [70].

The general idea for asphalt pavement application is to enhance the binder properties using

nanotechnology to increase the performance of the pavement against distresses such as rutting or cracking.

The study evaluated the addition in asphalt binder of two types of nanoclay materials, Nanofil-15 and Cloiste-15A [71]. The conclusion from the study was that an addition of both types of nanoclay has the potential to increase the stiffness (better rutting performance), decrease the phase angle, and reduce the aging characteristics of the asphalt binder.

Xiao et al. conducted a study to evaluate the effects of short-term aging on the rheological properties of several asphalt binders containing various percentages of carbon nanoparticles [72]. Different percentages of nanoparticles by weight of the virgin binder (i.e. 0.5%, 1% and 1.5%) were mixed with five asphalt binders. The study concluded that an addition of nanoparticles results in an increase in the failure temperature of all binders and contributed to an improvement in rutting resistance. In addition, the study determined that the viscosity and the elastic modulus values increased as the percentage of nanoparticles increased.

Most of the nanotechnology applications in asphalt pavement are accomplished by adding nanoparticles directly to polymer-modified asphalt. Thus, Wang et al. performed a study to evaluate an overlay for asphalt pavement made of nanoparticles [73]. The overlay was a solar heat reflective coating developed to lower the surface temperature of asphalt pavements. The goal was to lower the asphalt temperature as an effective method to decrease rutting on asphalt pavement. Four different coating layers were prepared by epoxy or acrylic filled with TiO_2 or TiNO_2 nanoparticles. The study concluded that there was a drop in the pavement temperature of 12.9°C in the TiO_2 /acrylic overlay. Also, the good dispersion of TiNO_2 nanoparticles resulted in a efficient alternative to lower the surface temperature. Lastly, the study suggested a TiO_2 /acrylic as a potential reflective coating layer.

2.6.2 Induction Heating in Asphalt Pavement

As previously discussed, asphalt is a self-healing material that can partially restore its strength and stiffness during rest periods. However, the self-healing recovery rate at ambient temperature is very slow; frequently, traffic cannot be blocked to allow rest periods. Therefore, the concept of induction heating emerged as an asphalt application to enhance the self-healing capacity and speed of asphalt concrete by increasing its temperature. Studies have shown that the self-healing efficiency of the asphalt concrete is temperature dependent. The self-healing efficiency increases as the pavement is subjected to high temperatures during the rest period [74]. Furthermore, studies have shown that increasing the healing temperature reduces the total recovery time [75].

Induction heating for asphalt pavement application consists of adding steel wool to the asphalt to make it conductive and suitable for induction heating [76]. Figure 2.7 shows a schematic of induction heating in asphalt concrete. The temperature of the asphalt binder may be increased by induction heating to reduce the viscosity of the binder in order to start and accelerate the healing process when small cracks occur in the pavement [77].

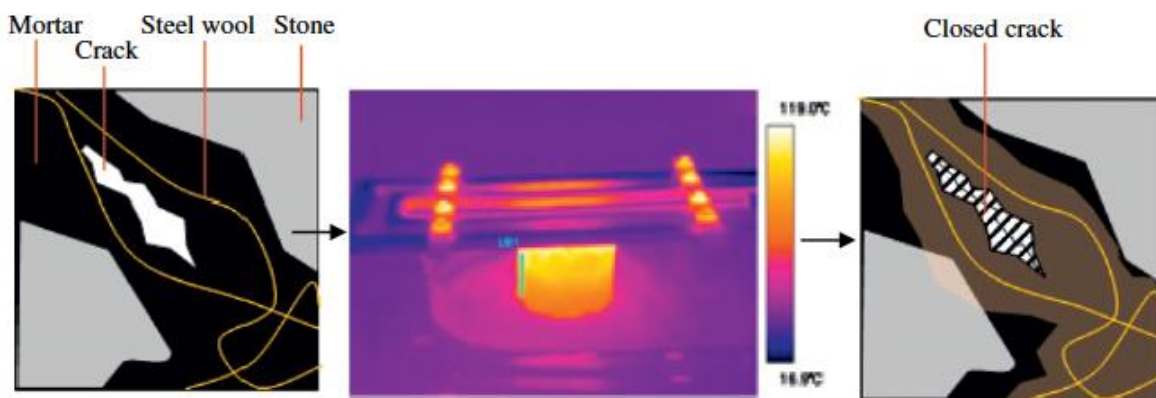


Figure 0.7. Schematic for Induction Heating in Asphalt Concrete [78]

Liu et al. conducted a study to evaluate the induction healing effect of porous asphalt by means of a point bending test and to determine the optimal heating temperature and the starting point of induction heating [78]. The study consisted of damaging rectangular porous asphalt beams by fatigue, then heating the samples via induction energy, followed by a final test in fatigue to quantify the healing. The healing quantification was measured, because the fatigue life extension ratio of fatigue damages beams after induction heating. The stiffness before and after the induction heating was also measured as a numerical measurement of the samples' healing efficiency. The study concluded that an increase in the fatigue life extension ratio was observed as an outcome, due to the induction heating of the samples. Also, the study determined the optimum temperature to be 85°C for the best healing effects, since higher temperatures can cause swelling and binder drainage problems. Furthermore, the stiffness recovery from the samples with induction healing was higher than the control samples. Lastly, researchers concluded that the fatigue life of porous asphalt can be significantly extended by multiple induction heating.

An investigation evaluated the efficiency of different conductive additives in the induction heating speed, healing potential of asphalt mastic samples, and the effect of each conductive additive in the mechanical properties [79]. The evaluated conductive additives consisted of type 00 steel wool, steel fibers, and steel slag. The experimental procedure consisted of fracturing the asphalt mastic samples at -20°C with a three-point bending test, followed by heating the samples to 85°C to induct healing to promote the self-healing ability of the binder. A second, three-point bending test was performed on the healed beams. The healing efficiency was determined, based on the recovered bending strength of the fractured sample and induced by induction heating. A conclusion from the study was that steel wool and steel fibers were successful in promoting the increase of induction heating speed, as opposed to steel slag. Also, the bending strength of

samples with steel wool and steel fibers was increased, in contrast to the results for steel slag samples. Lastly, it was observed that the bending strength of fractured samples with steel wool and steel fibers had recovered to the strength value of the control samples, due to induction heating.

2.6.3 Rejuvenation

As previously discussed in Section 2.5, the efficiency of asphalt rejuvenators to partially restore the asphalt properties of aged binder depends on the depth of penetration into the asphalt [61]. Previous studies have shown that asphalt rejuvenators penetrate no more than 2 cm, which is insufficient for applying the benefits of the product [80]. Therefore, researchers adapted innovative methods to incorporate asphalt rejuvenators into asphalt. Methods such as encapsulation of rejuvenators in microcapsules and fibers are discussed in the following sections.

2.5.3.1 Microencapsulation of Asphalt Rejuvenators. Microencapsulation may be defined as the process to encapsulate a solid, liquid, or gas as a core material, surrounded by a coating layer or shell [81]. The microencapsulation technique has been evaluated in numerous construction materials including mortar, lime, cement, concrete, marble, sealant, and paints [82].

The concept of microencapsulation is to protect the core material from external elements such as environmental conditions, or to control a release of the core material by controlling the permeability of the shell material. For asphalt applications, the use of self-healing microcapsules containing a rejuvenator is promising, as it will allow the material to resist the initiation and propagation of cracking caused by vehicular and environmental loading. When cracking occurs due to the aging process of the binder, the shell of microcapsules containing rejuvenator will

rupture. At that point, the rejuvenator flows through the binder, which consequently results in a reversal of the aging process.

Sharareh et al. conducted a study to evaluate the effect of rejuvenator agents in the binder properties, to develop a microencapsulation process and to characterize the developed microcapsules [83]. The effects of the rejuvenator products were assessed by blending them with virgin binder and with aged binder from RAP. The dosage rate for both rejuvenators was 5% by weight of the binder. The effective performance of the rejuvenators was tested by conducting a PG grading from the different blends. The PG grading showed that sunflower oil was effective in reversing the aging of asphalt binder, together with a positive influence on both high and low temperature grades of the blend.

Researchers conducted a microencapsulation process for sunflower oil, based on the positive results in the PG grading. The microencapsulation process was synthesized via in situ polymerization, using polyurethane and urea-formaldehyde, which resulted in double-walled microcapsules. An optimization process for sunflower oil microcapsules was performed by varying product parameters, such as agitation rate, heating temperature, and reaction time. Table 2.4 shows the experimental test matrix for the optimization process. The developed, double-walled microcapsules containing sunflower oil are shown in Figure 2.8.

A rejuvenator product, PennzSuppress, was successfully encapsulated via in situ polymerization using Methanol-Melamine-Formaldehyde, which results in single-walled microcapsules [84]. The microencapsulation process was synthesized through a double polymerization process to enhance rigidity and toughness of shell. Furthermore, the selected material has been shown to increase the thermal stability and mechanical properties of microcapsules. Figure 2.9 shows the SEM pictures of developed microcapsules of the discussed study.

Table 0.4. Experimental Test Matrix for Microcapsule Preparation Variable [83]

Agitation rate (rpm)	Temperature (°C)	Reaction time (h)
1,000	55	3
1,000	55	4
1,000	55	5
1,000	50	4
1,000	60	4
500	55	4
2,000	55	4

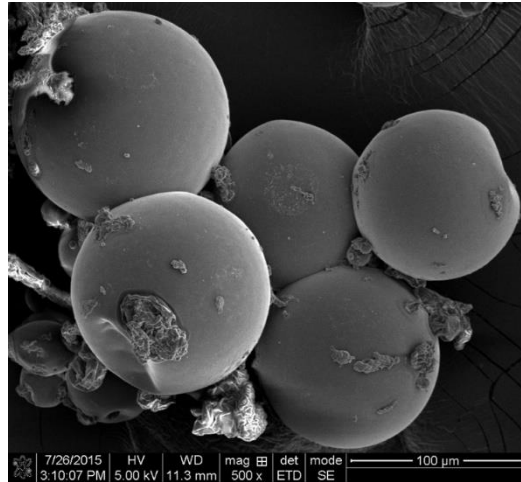


Figure 0.8. SEM Pictures of Microcapsules Containing Sunflower Oil [83]

The multi-self-healing behavior of bitumen using microcapsules containing a rejuvenator was evaluated in a previous study [85]. Figure 2.10 shows the overall self-healing process of microcapsules/bitumen. The study conducted a beam, applying the elastic foundation (BOEF) method to investigate the cracking and healing behaviors of bitumen. The tested samples consisted in bitumen samples containing 2% microcapsules by weight of binder. The BOEF test consists of loading-unloading-loading cycles in order to prove the multi-recovery of the mechanical properties of the binder. A total of four healing cycles were performed under two

different healing temperatures: 0°C and 25°C. Figure 2.11 shows the load-strain curves of the BOEF for both healing temperatures. The study concluded that the multi-self-healing ability of the binder can only repair the damage to the bitumen during service life. In addition, research established that the healing temperature and healing time has a great effect on the healing ability.

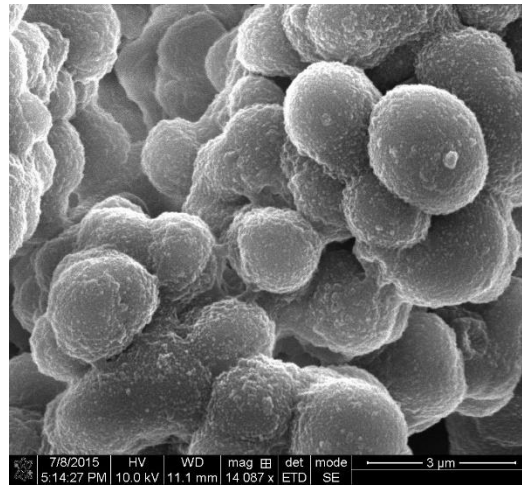


Figure 0.9. SEM Pictures of Single-Walled Microcapsules [84]

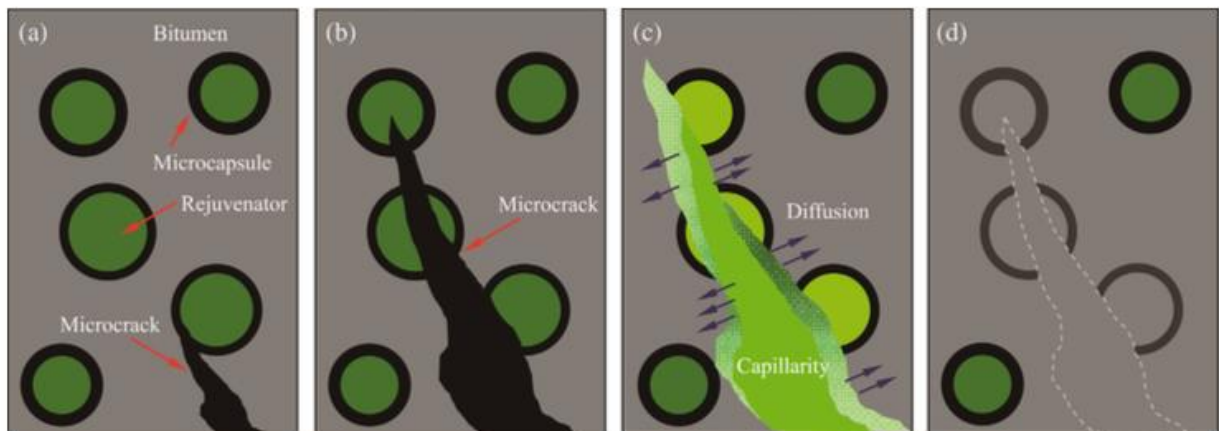


Figure 0.10. Self-Healing Process of Microcapsules/Bitumen: (a) Micro-Crack Generation, (b) Microcapsules Broken, (c) Capillarity and the Diffusion Behaviors of Rejuvenator, and (d) Micro-Crack Closure [85]

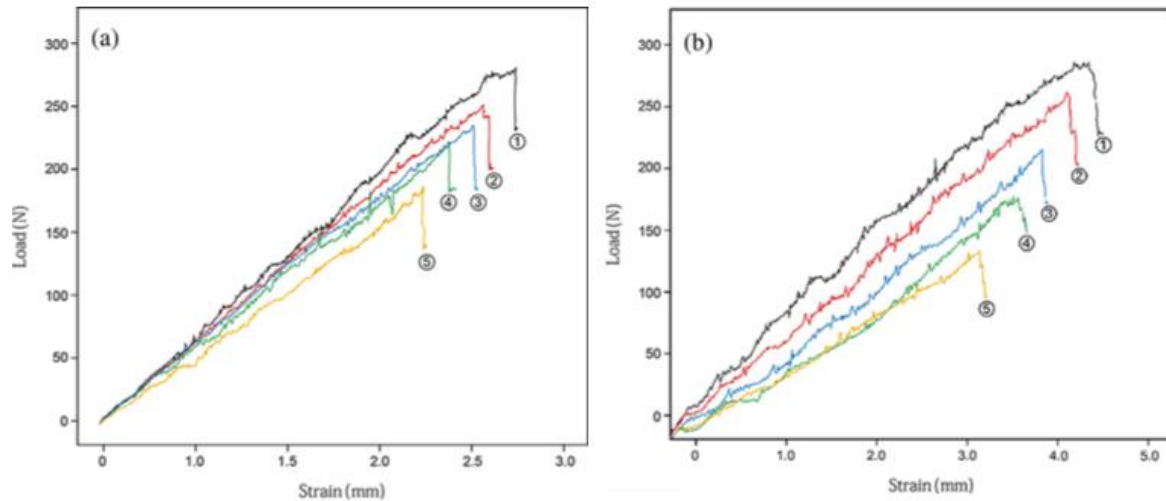


Figure 0.11. Load-Strain Curves for BOEF Test at (a) 0°C and (b) 25°C; Self-Healing Cycles: ① First Cycle, ② Second Cycle, ③ Third Cycle, ④ Aged Bitumen, and ⑤ Fourth Cycle [85]

2.5.3.2 Compartment fibers with asphalt rejuvenators. Another approach to solve the poor penetration of asphalt rejuvenators is to develop hollow fibers containing a rejuvenator and then to embed the fibers throughout the asphalt matrix. The concept emerged to produce fibers instead of microcapsules in order to avoid any non-desirable effects, such as reduction in the stiffness of the binder, which could lead to an increase in rutting susceptibility, as shown in a previous study [86]. The reduction of the stiffness may be due to the addition of sand-like particles (microcapsules). Well documented studies noted that deformation in the asphalt mix is caused by sand granulates [87]. Another motivation for the production of fibers is to avoid some chemical compounds, such as melamine-formaldehyde (i.e., shell material for microcapsules), that could be an environmental threat in large quantities.

The encapsulation of rejuvenator in alginate-based compartmented fibers was explored as a solution to the poor penetration of asphalt rejuvenators and to the environmental threats produced by some chemical compounds in a microencapsulation process [88]. For an objective,

the study investigated the applicability of compartmented alginate fibers containing rejuvenator as a healing agent delivery, as well as a healing triggering mechanism for asphalt pavements. The study prepared samples of asphalt mastic mix with and without fibers, which then were subjected to a multiple three-point-bending (3PB) loading and healing events. Also, the study evaluated the thermal resistance and the tensile strength of the prepared fibers containing a rejuvenator product. Figure 2.12 shows an image of a compartmented alginate fiber encapsulating rejuvenator, captured by optical microscope.



Figure 0.12. Compartment Fiber with a Rejuvenator Product by Optical Microscope [88]

A test of the thermal stability of sodium-alginate fibers containing a rejuvenator used the NETZSCH STA 449 F3 Jupiter TGA system, at a scanning rate of $6.5\text{ }^{\circ}\text{C min}^{-1}$ in argon gas (Ar) at flow of 50 ml min^{-1} . The TGA results are shown in Figure 2.9. Figure 2.13 indicates that in principle, the developed fibers can resist the high-temperature from the asphalt mixing process, due to the fact that only 9% of weight loss was observed at a temperature of 160°C , which researchers explained could be due to residual water evaporation from the calcium alginate.

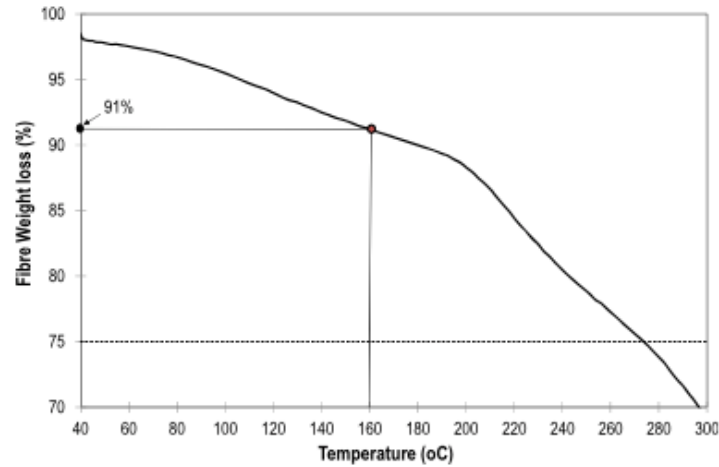


Figure 0.13. Thermogravimetric Analysis of Sodium-Alginate Fibers Containing a Rejuvenator Product [88]

The uniaxial tensile strength (UTS) of the fibers was tested using a micro-tensile testing machine with 50N load cell, at a cross-head speed of 0.01mms⁻¹. The fiber strain was measured from the machine cross-head displacement, taking into account the system compliance. The UTS results can be observed from Figure 2.14. Figure 2.14 shows that the UTS of the fibers is 30MPa and Young's modulus (E) is 0.64GPa.

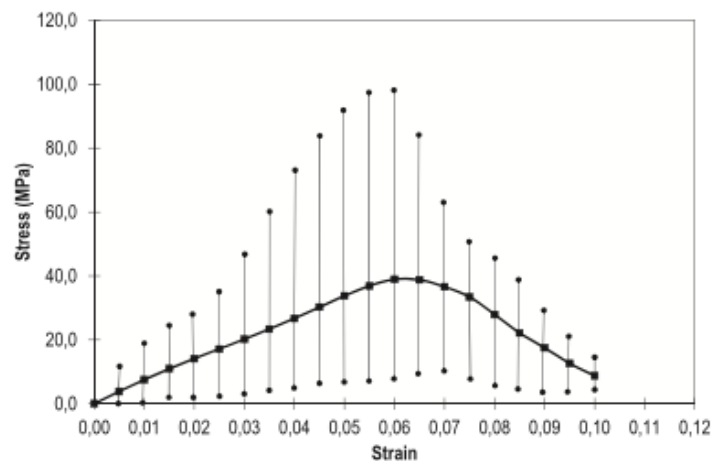


Figure 0.14. Uniaxial Tensile Strength of Sodium-Alginate Fibers Containing a Rejuvenator Product [88]

The study conducted an evaluation of the healing capacity of the fibers by means of a three-point-bending (3PB) test in accordance with ASTM E 1820. The specimens were rectangular asphalt mastic mixes with dimensions of length = 120 mm, width = 25 mm, and thickness = 20 mm. The 3PB tests were conducted on an Instron 8872 10 kN uniaxial testing frame. The tests were conducted at test rate of 0.1 mm s^{-1} . Table 2.5 shows the testing program utilized for the evaluated study. The researchers explained that the different bending temperatures were to allow micro-crack formations at test temperature 1 and a large crack formation for test temperature 2. Furthermore, the rationale for having a longer healing stage for test 2, compared to test 1, was based on the size of the developed cracks.

Table 0.5. Healing Programme for Test 1 and Test 2 [88]

Healing State	Test 1-bending temperature 20°C	Test 2-bending temperature -5°C
1	30 min after first bending	3 h after first bending
2	1 h after second bending	12 h after second bending
3	3 h after third bending	-

The results from the 3PB show that the asphalt mastic mixtures containing fibers outperformed the control mixture at both testing temperatures (i.e., 20°C and -5°C). Figure 2.15a shows the strength recovery of the specimens, containing fibers at 20°C. Thus, the study observed a better strength recovery on specimens without fibers at 20°C, as observed in Figure 2.15b. However, researchers observed that the samples containing fibers showed a better stiffness recovery than control specimens, which means that the specimens with fibers are less prone to rutting. The results for test 2 showed a better healing efficiency for samples containing fibers than the control mixtures, but the healing efficiencies are very low for both specimens, as shown in Figure 2.16.

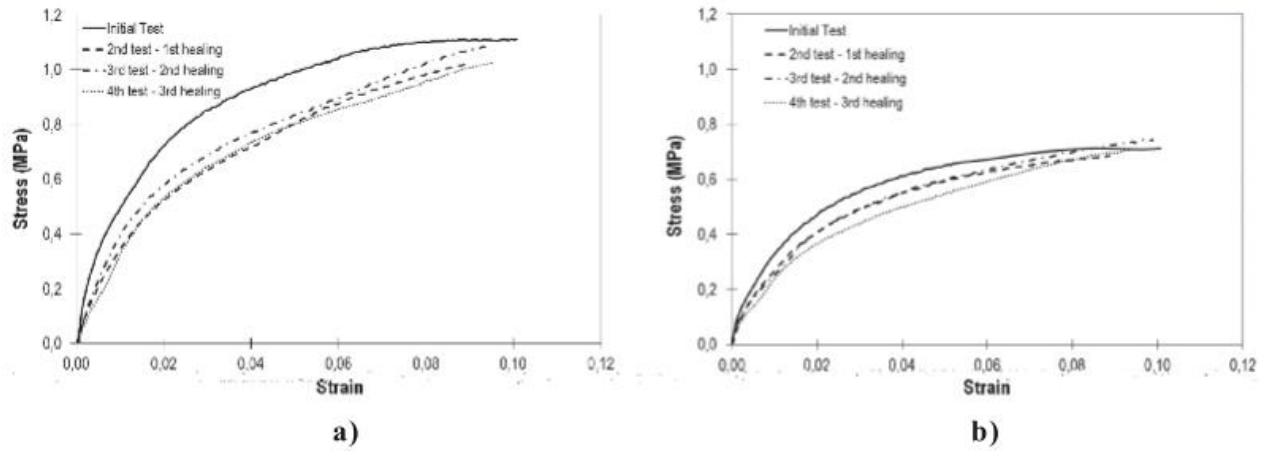


Figure 0.15. 3PB Results: Load vs Deflection Plots for Asphalt Mastic Mixtures at 20°C a) with Fibers, and B) without Fibers [88]

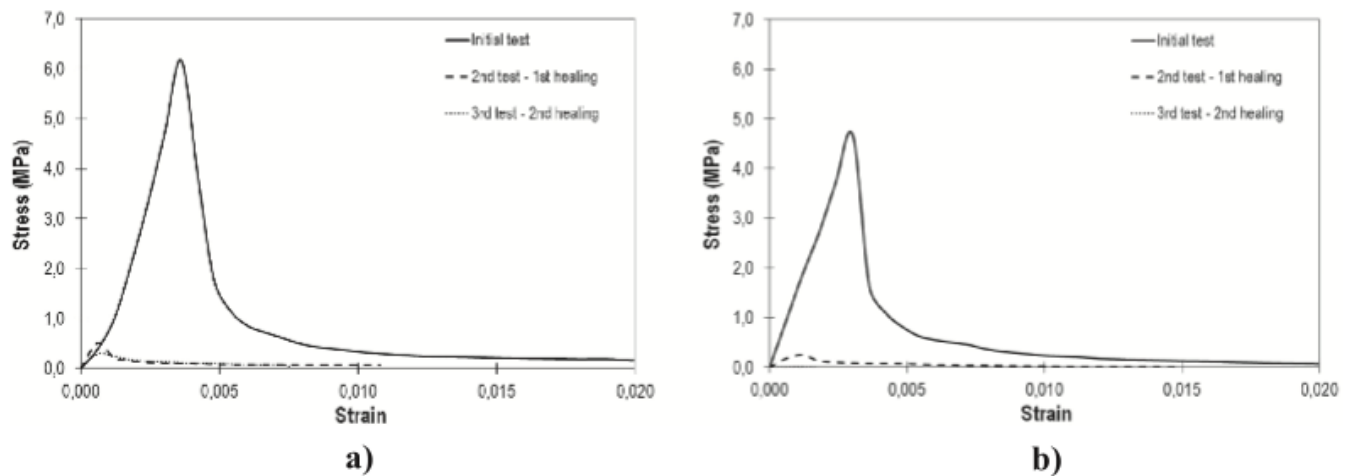


Figure 0.16. 3PB Results: Load vs Deflection Plots for Asphalt Mastic Mixtures at -5°C a) with Fibers, and B) without Fibers [88]

2.7 Microcapsules Synthesis

As previously defined, microencapsulation is the process to encapsulate a solid, liquid, or gas as a core material, surrounded by a coating layer or shell [81]. The microencapsulation concept has been successfully utilized in construction materials such as mortar, lime, cement, concrete,

marble, sealant, and paints [82]. Furthermore, many industries such as food, chemical, textile and pharmaceutical industries have implemented the microencapsulation process.

Microcapsules have a spherical or regular shape, which can be divided into two parts: core and shell. The core material or intrinsic part contains the active ingredient. For asphalt applications, an asphalt rejuvenator will act as core material. The shell or extrinsic part is the responsible to protect the core material permanently or temporarily from external factors [89]. A schematic of a microcapsules is shown in figure 2.17. A solution, dispersion or emulsion is commonly used for the core material, which can be either solid, liquid or gas. An important criterion to enhance the efficiency of microencapsulation is to select a shell material compatible with the core material [89].

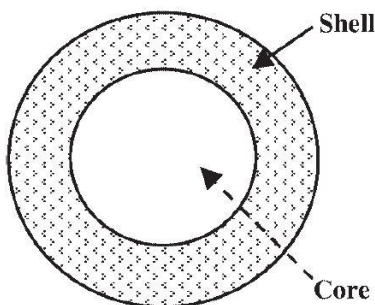


Figure 0.17. Schematic of Microcapsule [89]

Microcapsules can be classified based on their morphologies as mononuclear, polynuclear and matrix as shown in figure 2.18. Mononuclear microcapsules are those capsules containing only one core surrounded by the shell material. Polynuclear microcapsules have many cores enclosed in the same shell. In addition, a matrix microcapsule is formed when the core material is distributed homogeneously into the shell material [89].

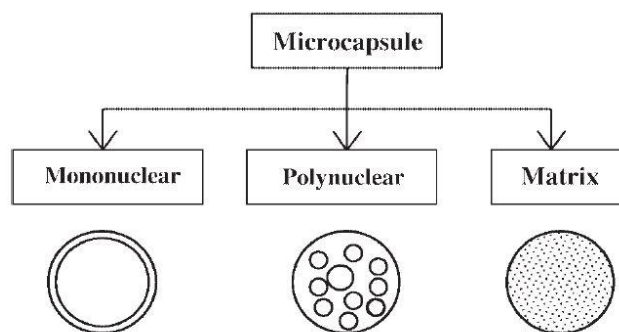


Figure 0.18. Morphology of Microcapsules [89]

The various microencapsulation procedures can be divided into chemical, physiochemical, and physical processes. Some examples of chemical procedures are the interfacial and in-situ polymerization methods. Physiochemical procedures include coacervation and complex coacervation. Lastly, the physical procedures include the co-extrusion and spray-drying. The selection of the of microencapsulation procedure depends in the type of core material and physical properties of the microcapsules. Also, the shell material, the morphology and the particle size will influence the selection of the microencapsulation procedure [89]. Table 2.6 provides an overview of the size of microcapsules developed by the different techniques available.

2.7.1 In-situ Polymerization

In-situ polymerization is a chemical microencapsulation procedure, which is very developed and commercialized in many industries [90]. In this technique the reactants, either monomers or oligomer, are in a single phase. Also, the polymerization process occurs mostly in the continuous phase, but it is possible to have the polymerization in the dispersed phased as occurs in an in-situ water-in-oil microencapsulation [91]. The advantages of this technique are: (1) inexpensive, (2) easy and controllable process, (3) highly cross-linked impermeable wall with high thermal and mechanical properties, (4) high encapsulation efficiency and (5) easy for the industry to scale-up

the production [90, 92, 93]. The typical wall materials for this technique are aminoplast resins such as melamine-formaldehyde, urea-formaldehyde, urea-melamine-formaldehyde and resorcinol-modified-melamine-formaldehyde [90].

Table 0.6. Ranges of Microcapsule's Size with Different Microencapsulation Procedure [89]

Microencapsulation Procedure	Particle size (μm)
Extrusion	250-2500
Spray-drying	5-5000
Fluid bed coating	20-1500
Rotating disk	5-1500
Coacervation	2-1200
Solvent evaporation	0.5-1000
Phase separation	0.5-1000
In-situ polymerization	0.5-1000
Interfacial polymerization	0.5-1000
Mini-emulsion	0.1-0.5
Sol-gel encapsulation	2-20
Layer-by-layer assembly	0.02-20

The microencapsulation procedure may differ from different core and shell materials [93]. But in general, the following procedure is utilized for an oil-in water emulsion microencapsulation procedure:

1. Prepare a stable oil-in-water solution containing the reactants (i.e. melamine-formaldehyde or urea-formaldehyde resin prepolymer)
2. Polymerize from the water phase and deposit monomer/oligomer on the oil phase
3. Build wall thickness and cure

Some of the factors that influence the in-situ polymerization technique are:

1. Type of emulsifier agent: the emulsifier agent can affect the microencapsulation preparation, mean particle size, and particle size distribution [94].
2. pH value: the pH value does not only affect the polycondensation rate, but also the surface activity of the resin prepolymer [95].
3. Salt: the presence of salts such as KCL, Na₂SO₄ and KH₂PO₄ can help to reduce the viscosity of solutions and to achieve a higher solid content microcapsules with increased wall impermeability [96, 97]. Other salts such as NaCl can increase the encapsulation efficiency and have a positive impact in surface's morphology [98].
4. Temperature and stirring: increasing the stirring rates result in a reduce in the diameter size of microcapsules and a narrow size distribution. Also, the amount of core material in the microcapsules decreases as the stirring rate increases since the core weight fraction in the microcapsule reduced for smaller microcapsules [99]. Furthermore, the combination of low temperature and high stirring rates result in a decrease in the encapsulation yield rate [100].
5. Formaldehyde scavenger: the amount of formaldehyde added in the process must not affect negatively the polymerization process. The use of formaldehyde in this particular technique can be considered as a disadvantage as the use of this chemical is regulated for environmental and health considerations [93]. Figure 2.19 shows a schematic of an in-situ polymerization process using melamine resin.

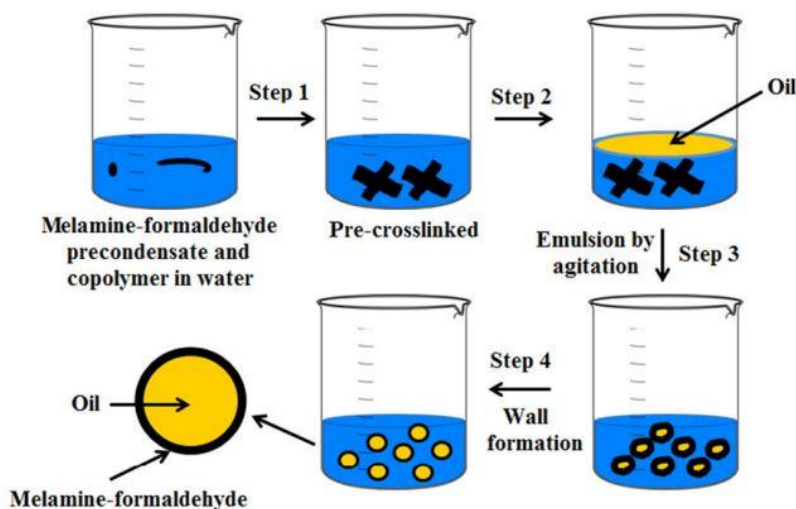


Figure 0.19. Schematic Representation of a Melamine Resin Microencapsulation Process [101]

2.7.2 Interfacial Polymerization

Interfacial polymerization is a technique consisting in the dispersion of one phase containing a reactive monomer, into a second immiscible phase to which is added a second monomer. Both monomers react at the interface forming a polymeric membrane [102]. An example of interfacial polymerization is when a monomer such as diamine is dissolved in water and the aqueous phase is dispersed in the oil phase. Then, a second monomer, for example diacid chloride, is added and reacts with the first monomer at the interface forming the wall material [103]. Some advantages of this technique are the follows: (1) simple and reliable, (2) direct control on microcapsule's size and shell's thickness, (3) high active loading and tunable delivery process, (4) stable mechanical and chemical properties of the shell, (5) impermeable microcapsules, (6) low-cost and (7) easy to scale-up [102]. They shell formed during an interfacial polymerization depends on the material with which isocyanate reacts: a polyuria shell will be formed with a reaction between isocyanate and amine; a polyurethane shell will be formed when isocyanates react with a hydroxyl containing monomer; and lastly, a polynylon or polyamine shell will be formed with

the reaction between acid chloride and amine [104]. Figure 2.20 shows a schematic representation of interfacial polymerization.

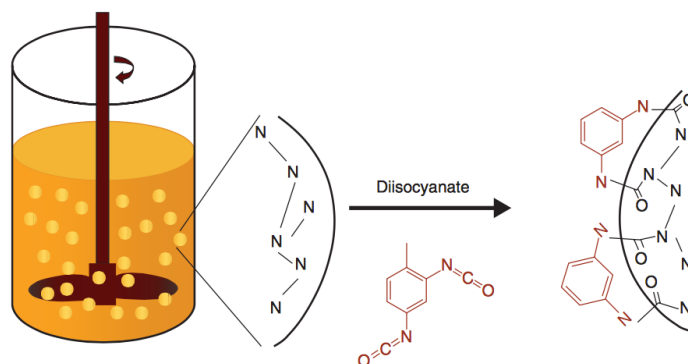


Figure 0.20. Schematic Representation of Microencapsulation Via Interfacial Polymerization [104]

2.7.3 Coacervation

The coacervation procedure, also called phase separation, is the oldest encapsulation technique first developed by the National Cash Register Company for carbonless copy-paper. The technique involves a phase separation of one or more hydrocolloids from an initial solution and the subsequent deposition of a newly formed coacervated phase around the active ingredient (i.e. core material) suspended or emulsified in the same media. After hardening, the microcapsule's wall forms a cross-linked structure, which enhance the thermal and moisture-resistant properties of the microcapsules [105]. Figure 2.21 shows a schematic representation of a microencapsulation process by coacervation. A common procedure to perform a coacervation microencapsulation is the following:

1. Dispersion of the oil phase into a solution of a surface-active hydrocolloid.
2. Precipitation of the hydrocolloid onto the oil phase by lowering the solubility of the hydrocolloid. A non-solvent, change in pH or a change in the temperature will result in the precipitation of the hydrocolloid.

3. A second complex hydrocolloid is added to induce the formation of the polymer-polymer complex.
4. Formation of cross-linked structure to stabilize the microcapsules.
5. Drying of the developed microcapsules.

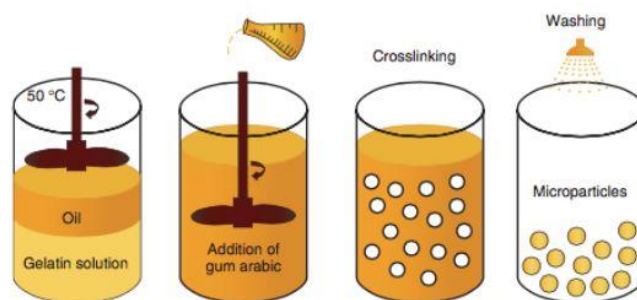


Figure 0.21. Schematic Representation of a Microencapsulation Process by Coacervation [105]

2.7.4 Release Mechanisms

The idea to encapsulate a core material is to provide a controlled, sustained or targeted release of the active ingredient. There are three different mechanisms by which a core material is released from a microcapsule: (1) mechanical rupture of the capsule wall, (2) dissolution or melting of the wall, and (3) diffusion through the wall. A less common release mechanisms are the ablation, slow erosion of the shell, and biodegradation of the capsule [106]. Some examples are the following:

- The dissolution of the wall is commonly used in the detergent industry in order to remove bloodstains from clothing.
- The melting of the shell is utilized in the food industry when the capsule reaches certain temperature to react with food acid in order to produce leaving agents.
- For pesticides applications, the diffusion through time is usually utilized, which allows farmers to apply the pesticides less often rather than using a very high concentration.

- In pharmaceutical products, the release of the active ingredient is either obtained by biodegradation of the shell or by diffusion through the shell.
- For self-healing applications, the release mechanism is usually the mechanical rupture of the shell to release the active ingredient.

For asphalt applications, the use of self-healing microcapsules containing a rejuvenator is promising, as it will allow the material to resist the initiation and propagation of cracking caused by vehicular and environmental loading. When cracking occurs due to the aging process of the binder, the shell of microcapsules containing rejuvenator will rupture, and the rejuvenator will flow through the binder, which consequently results in reversing the aging process.

2.8 Fibers Synthesis

The development of fibers containing a rejuvenator product has emerged as an alternative for self-healing mechanisms in asphalt pavement. The idea is to avoid negative effects in the rutting susceptibility of an HMA mixture by adding sand-like particles (i.e. microcapsules) as previously discovered in a study [86]. Another motivation to produce fibers is to avoid some chemical compounds, such as melamine-formaldehyde (i.e., shell material for microcapsules), that could be an environmental threat in large quantities as previously discussed in section 2.7.1. In this section, the most common techniques for fibers fabrication will be discussed.

Synthetic fibers are mostly derived from by-products of petroleum and natural gas such as nylon, polyethylene terephthalate. Also, synthetic fibers can be made of other compounds such as acrylics, polyurethanes and polypropylene. Synthetic fibers are commonly used in the textile industry for products ranging from clothing and home furnishings [107].

Every fiber synthesis technique has 3 basic steps: (1) production of polymer solution, (2) extrusion of the fibers, and (3) solidification of the fibers. The first step consists in dissolving the polymer into a solvent to form a stable solution. When a thermoplastic polymer is utilized, the polymer is usually melted to form the solution. The extrusion of the polymer solution is usually performed by utilizing a spinneret. A spinneret is an instrument with an appearance similar to a bathroom shower head with many holes ranging from one to several hundreds. Lastly, the solidification of the fibers can be performed by either wet-spinning, dry spinning, melt spinning, and gel spinning. The process of extrusion and solidification of the polymer solution is called spinning process [107].

2.8.1 Wet Spinning

This technique is usually utilized for polymers that are dissolved in a solvent. A wet spinning consists in extruding the polymer solution into a coagulation bath (i.e. non-solvent) to precipitate the polymer. Then, the extruded fibers are washed to remove the excess coagulant and subsequently wound on a bobbin [108, 109]. Figure 2.22 shows a schematic diagram of a wet spinning procedure.

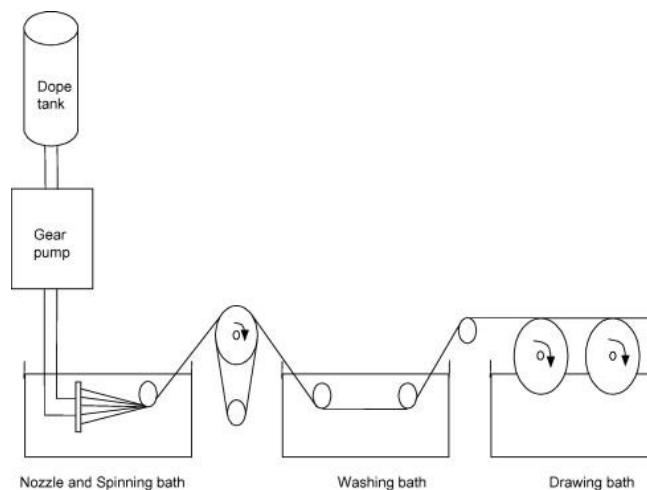


Figure 0.22. Schematic Diagram of Wet Spinning Procedure [110]

Calcium alginate fibers are commonly developed using a wet spinning process. Alginate is a natural polymer commonly used in the textile industry. The application of calcium alginate fibers for asphalt applications emerges with the idea to avoid negative effects of using hazardous materials (i.e. formaldehyde) for the development of self-healing mechanisms. Calcium alginate is not only a non-toxic and safe material for the environment and the user, but also has a low-cost and biodegradability property. Furthermore, alginate is a renewable resource with unlimited supply in nature [111, 112].

The wet spinning process to develop calcium alginate fibers starts by dissolving sodium alginate powder in water. Then, the sodium alginate solution is extruded through a spinneret into a calcium chloride coagulation bath. During the extrusion process, there is an exchange between the calcium and sodium ions resulting in a firm gel structure [113]. Based on previous studies, some factors that affects the production efficiency and the product performance are discussed in the next sections.

2.8.1.1 Molecular weight of the alginate powder. Studies have shown that the strength of the fiber will be enhanced with a higher molecular weight of the alginate powder [113]. However, the viscosity of the alginate solution increases with a higher molecular weight making it difficult to dissolve a high concentration of alginate. A study recommended that a particular 1% alginate solution should have a viscosity ranging from 40-100 mPa in order to have a balance between the production efficiency and the product performance [111].

2.8.1.2 Concentration of the spinning solution. As mentioned in the previous section, the viscosity of the alginate solution increases as the concentration increases. For wet spinning process, a concentration of 5%-6% of sodium alginate for the spinning solution is recommended [113].

2.8.1.3 Temperature of the solution. It is recommended to heat the sodium alginate solution during the dissolution process as the viscosity decreases as temperature increases, at a rate of about 2.5% per degree Celsius. However, a long exposing time to high-temperature such as 50 °C can depolymerize the alginate powder resulting in a loss of viscosity and molecular weight [113].

2.8.1.4 pH of the solution. The viscosity of the alginate solution is not affected over the range pH= 5-11. Below a pH= 5, a higher viscosity occurs as the free -COO^- ions start to protonate into -COOH . Furthermore, hydrogen bonds start to form as the electrostatic repulsion between the -COOH chains is reduced. The result of the formation of hydrogen bonds is the formation of a gel between pH= 3-4. For a wet spinning process, it is recommended to use deionized water with pH around 7 [113].

2.8.2 Dry Spinning

In an analogous way than wet spinning, the polymer is dissolved in a solvent and then is extruded. During the extrusion process, the solution emerges through the spinneret where the solvent is evaporated off with hot air. The solvent can be recollected and reuse it for another spinning process. Some common examples of fibers produced with this technique are acetate fiber, triacetate fiber, acrylic fiber, modacrylic fiber, and vinyon. Figure 2.23 shows a schematic diagram of a dry spinning procedure.

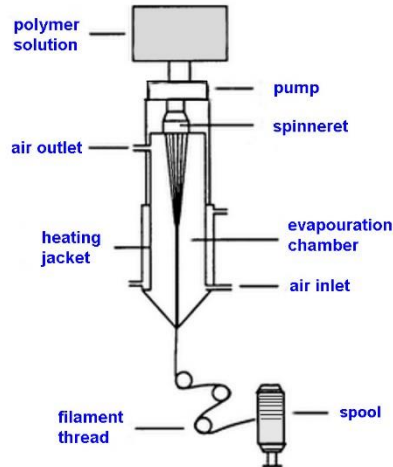


Figure 0.23. Schematic Diagram of Dry Spinning Procedure [107]

2.8.3 Melt Spinning

This technique is usually performed in polymers that can be melted. The melted polymer is extruded through the spinneret where a quench air cools the fibers as they emerge. For this particular technique, the winding speed is an important factor for the product performance as it influences the strength of the fibers. Figure 2.24 Schematic diagram of melt spinning procedure. Some advantages of melt spinning process are the following: (1) it is cost effective, (2) no washing is required as no solvent is used; and (3) it is high speed, usually the winding speed is around 8000 m/minute. Melt spinning is usually performed with polymers that will not get thermal degradation at high-temperatures required to form the melt solution. Some examples of fibers produced with this technique are nylon, polyethylene, polypropylene, and polyester.

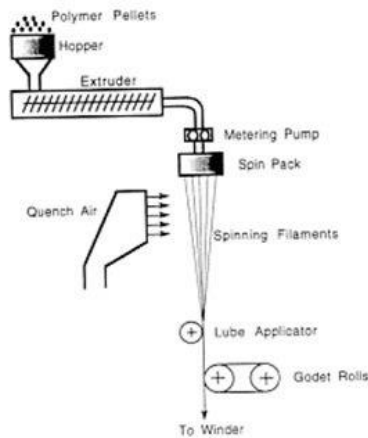


Figure 0.24. Schematic Diagram of Melt Spinning Procedure [107]

2.9 References

- [1] Asphalt Institute, "Performance graded asphalt binder specification and testing," Asphalt Institute, Lexington, 1994.
- [2] M. Sahin, "Pavement Management for Airports, Roads and Parking Lot.," Springer Science, 2005.
- [3] D. Geoffroy, "Cost-effective Preventive Maintenance," National Cooperative Highway Research Program, 1996.
- [4] L. Galehouse, J. Moulthrop and R. Hicks, "Principles of pavement preservation: definitios, benefits, issues and barriers," 2003.
- [5] E. J. Barth, "Asphalt Science and Technology," Gordon and Breach Science Publishers, New York, NY, 1962.
- [6] H. A. Wallace and J. R. Martin, "Asphalt Pavement Engineering," McGraw-Hill Book Co., New York, NY, 1961.
- [7] R. N. Traxler, "Asphalt: Its Composition, Properties and Uses," Reinhold Publishing Corp., New York, NY, 1961.
- [8] L. W. Corbett, "Refining Processing of Asphalt Cement," Transportation Research Record 999, 1984.
- [9] L. W. Corbett, "Asphalt and Bitumen," Wiley-VCH Verlag GmbH % Co. , KGaA, Weinheim, 2005.

- [10] ASTM D2397, "Standard Specification for Cationic Emulsified Asphalt," ASTM International, West Conshohocken, PA, 2003.
- [11] ASTM D977, "Standard Specifications for Anionic Emulsified Asphalt," ASTM International, West Conshohocken, PA, 2003.
- [12] E. R. Brown, P. S. Kandhal, Y. R. Kim, D.-Y. Lee and T. W. Kennedy, Hot-Mix Asphalt Materials, Mixture Design, and Construction, vol. 3, Lanham, Maryland: NAPA Research and Educational Foundation, 2009.
- [13] Z. Liao, J. Zhao, P. Creux and C. P. Yang, "Discussion on the Structural Features of Asphaltene Molecules," vol. 23, Energy & Fuels, 2009, pp. 6272-6274.
- [14] F. S. Rostler and R. M. White, Compounding Rubber with Petroleum Products, vol. 41, Industrial and Engineering Chemistry, 1949.
- [15] R. Boyer, "Asphalt Rejuvenators "Fact or Fable", " Asphalt Institute, San Antonio, TX, 2000.
- [16] C. Lau, K. Lunsford, C. Glover, R. Davison and J. Bullin, "Reaction Rates and Hardening Susceptibilities as determined from Pressure Oxygen Vessel aging of asphalts," vol. 1342, no. 50, 1992.
- [17] M. Liu, M. A. Ferry, R. R. Davison, C. J. Glover and J. A. Bullin, "Oxygen Uptake as Correlated to Carbonyl Growth in Aged Asphalts and Asphalt Corbett Fractions," Ind. & Eng. Chem. Res. , 1998.
- [18] C. H. Domke, R. R. Davison and C. J. Glover, Effect of Oxygen Pressure on Asphalt Oxidation Kinetics, vol. 39, Ind. Eng. Chem. Res, 2000, p. 592.
- [19] Y. B. Ruan, R. R. Davison and C. J. Glover, An Investigation of Asphalt Durability: Relationships between Ductility and Rheological Properties of Unmodified Asphalts, vol. 21, Pet. Sci. & Tech. , 2003, p. 231.
- [20] ASTM D3497, Standard Test Method for Dynamic Modulus of Asphalt Concrete Mixtures, West Conshohocken, PA: ASTM International, 1979.
- [21] M. W. Witczak, K. Kaloush, T. Pellinen and M. El-Basyouny, "Appendix A-Test Method for Dynamic Modulus of Asphalt Concrete Mixtures for Permanent Deformation," Transportation Research Board, National Research Council, Washington, D.C., 2002.
- [22] AASHTO T324, American Association of State Highways and Transportation Officials, Standard Method of Test for Hamburg Wheel Track Testing of Compacted Hot Mix Asphalt (HMA), Washigton, D.C., 2008.

- [23] Z. Wu, L. Mohammad, L. Wang and M. A. Mull, "Fracture Resistance Characterization of Superpave Mixture using the Semi-Circular Bending Test," *Journal of ASTM International (JAI)*, vol. 2, no. 3, March 2005.
- [24] AASHTO PP 2, American Association of State Highways and Transportation Officials, Practice for Short and Long Term Aging of Hot Mix Asphalt, Washington, D.C.: AASHTO Designation PP 2, 1994.
- [25] AASHTO TP 10-93, Standard Test Method for Thermal Stress Restrained Specimen Tensile Strength (TSRST), Washington, D.C.: AASHTO Designation: TP 10, 1993.
- [26] Rock Products New, "Asphalt Demand to Reach 26.8 Millions Tons in 2019," 2015. [Online]. Available: http://www.rockproducts.com/news-late/14601-u-s-asphalt-demand-to-reach-26-8-million-tons-in-2019.html#.V1caZ_krK00.
- [27] A. Copeland, C. Jones and J. Bukowski, Federal Highway Administration, March/April 2010. [Online]. Available: <http://www.fhwa.dot.gov/publications/publicroads/10mar/06/cfm>.
- [28] Federal Highway Association, "A Study of the Use of Recycled Paving Materials: A Report to Congress," Federal Highway Administration, Washington, DC, 1993.
- [29] J. R. Willis and P. Turner, "Characterization of Asphalt Binder Extracted from Reclaimed Asphalt Shingles," NCAT Report 16-01, 2016.
- [30] L. Flynn, "Roofing Materials Hold Promise for Pavements," *Roads and Bridges*, 1993.
- [31] Owens Corning Forms, "Owens corning forms alliance with earth911 to expand footprint of nation's leading shingle recycling program," 2012. [Online]. Available: <http://owenscorning.mediaroom.com/index.php?s=2370&item=66527>.
- [32] W. S. Mogawe, A. Boosherian, S. Vahidi and A. J. Austerman, Evaluating the Effect of Rejuvenators on the Degree of Bleeding and Performance of High RAP, RAS and RAP/RAS Mixtures, vol. 14, *Road Materials and Pavement Design*, 2013, pp. 193-213.
- [33] D. Swiertz, E. Mahmoud and H. Bahia, "Estimating the Effect of Recycled Asphalt Pavements and Asphalt Shingles on Fresh Binder, Low-Temperature Properties without Extraction and Recovery," *Journal of the Transportation Research Record*, no. 2208, pp. 48-55, 2011.
- [34] G. C. Hurley and B. D. Prowell, "Evaluation of Aspha-Min Zeolite for Use in Warm Mix Asphalt," NCAT Report 05-04, Auburn, Alabama, 2005.

- [35] B. Neitzke and B. Wasill, "Placement of Warm Mix Asphalt on the East Entrance Road of Yellowstone National Park," FHWA-WFL/TD-09-002, 2009.
- [36] J. W. Button, C. Estakhri and A. Wimsatt, "A Synthesis of Warm-Mix Asphalt," FHWA A/TX-07/0-5597-1, 2007.
- [37] C. G. Hurley and B. D. Prowell, "Evaluation of Potential Processes for Use in Warm Mix Asphalt," Journal of the Association of Asphalt Paving Technologies, Savannah, Georgia, 2006.
- [38] W. D. Hodo, A. Kvasnak and E. B. R., "Investigation of Foamed Asphalt (Warm Mix Asphalt) with High Reclaimed Asphalt Pavement (RAP) Content for Sustainment and Rehabilitation of Asphalt Content," Transportation Research Board , Washington, D.C, 2009.
- [39] J. S. Daniel and A. Iachance, "Mechanistic and Volumetric Properties of Asphalt Mixtures with RAP," Journal of Transportation Research Board, 2005.
- [40] A. Shah, R. S. McDaniel, G. A. Huber and V. Gallivan, "Investigation of Properties of Plant-Produced Reclaimed Asphalt Pavement Mixtures," Journal of the Transportation Research Board, 2007.
- [41] X. Li, M. O. Marasteanu, R. C. Williams and T. R. Clyne, "Effect of Reclaimed Asphalt Pavement (Proportion and Type) and Binder Grade on Asphalt Mixtures," Journal of the Transportation Research Board 2051, 2008.
- [42] K. K. Tam, P. Joseph and D. F. Lych, "Five Year Experience of Low-Temperature Performance of Recycled Hot Mix," Journal of the Transportation research Board 1362, 1992.
- [43] M. S. Gardiner and C. Wagner, "Use of Reclaimed Asphalt Pavement in Superpave Hot-Mix Asphalt Applications," Journal of the Transportation Research Board 1681, 1999.
- [44] I. Widyatmoko, "Mechanistic-Empirical Mixture Design for Hot Mix Asphalt Pavement Recycling," Journal of Construction and Building Materials , no. 22, pp. 77-87, 2008.
- [45] R. S. McDaniel, H. Soleymani, R. Anderson, P. Turner and R. Peterson, "Recommended Use of Reclaimed Asphalt Pavement in the SuperPave Mixture Design Method," Transportation Research Board, Washington, DC, 2000.
- [46] X. Shu, B. Huang and D. Vukosavljevic, "Laboratory Evaluation of Fatigue Characteristics of Recycled Asphalt Mixture," Journal of Construction and Building Materials, no. 22, pp. 1323-1330, 2008.

- [47] G. W. Maupin Jr, "Investigation of the Use of Tear-off Shingles in Asphalt Concrete," Virginia Transportation Research Council, 2010.
- [48] D. E. Watson, A. Johnson and H. R. Sharma, "Georgia's Experience with Recycled Roofing Shingles in Asphaltic Concrete," Transportation Research Record 1638, Washington, DC, 1998.
- [49] B. Sengoz and A. Topal, "Use of Asphalt Roofing Shingle Waste in HMA," Construction and Building Materials, no. 19, pp. 337-346, 2005.
- [50] K. Y. Foo, D. I. Hanson and T. A. Lynn, "Evaluation of Roofing Shingles in Hot Mix Asphalt," Journal of Materials in Civil Engineering, pp. 15-20, February 1999.
- [51] J. Schroer, "Missouri's Use of Recycled Asphalt Shingles (RAS) in Hot Mix Asphalt," Proceedings of the 2009 Mid-Continent Transportation Research Symposium, 2009.
- [52] S. M. Shenghua Wu, K. Zhang, H. Wen, J. DeVol and K. Kelsey, "Performance Evaluation of Hot Mix Asphalt Containing Recycled Asphalt Shingles in Washington State," American Society of Civil Engineers, 2011.
- [53] C. G. Hurley and B. D. Prowell, "Evaluation of Sasobit for Use in Warm Mix Asphalt," National Center for Asphalt Technology, Auburn, Alabama, 2005.
- [54] C. Hurley and B. D. Prowell, "Evaluation of Evotherm for Use in Warm Asphalt Mixes," National Center for Asphalt Technology, Auburn, Alabama, 2006.
- [55] J. Wielinski, A. Hand and D. M. Rausch, "Laboratory and Field Evaluations of Foamed Warm Mix Asphalt Projects," Transportation Research Record No. 2126, pp. 125-131, 2009.
- [56] B. Middleton and B. W. Forfylyow, "An Evaluation of Warm Mix Asphalt Produced with the Double Barrel Green Process," Transportation Research Record, no. No. 2126, pp. 19-26, 2009.
- [57] A. Ongel and M. Hugener, "Impact of rejuvenators on aging properties of bitumen," Construction and Building Materials, no. 94, pp. 467-474, 2015.
- [58] E. Yaghoubi, M. R. Ahadi, M. Alijanpour and H. Jahanian Pahlevanloo, "Evaluating the Performance of Hot Mix Asphalt with Reclaimed Asphalt Pavement and Heavy Vacuum Slops as Rejuvenator," International Journal of Transportation Engineering, vol. 1, no. 2, 2013.
- [59] J. Brownride, "The Role of an Asphalt Rejuvenator in Pavement Preservation: Use and Need for Asphalt Rejuvenation," Tricor Refininf, LLC..

- [60] J. Shen, S. Amirkhanian and J. A. Miller, "Effects of Rejuvenating Agents on Superpave Mixtures Containing Reclaimed Asphalt Pavement," *Journal of Materials in Civil Engineering* , vol. 19, 2007.
- [61] E. R. Brown, "Preventive Maintenance of Asphalt Concrete Pavements," NCAT Report No.88-1 , 1988.
- [62] ASTM, "Recommended Practice for Classifying Hot-Mix Recycling Agents," American Society for Testing and Material, 1980.
- [63] R. Karlsson and U. Isacsson, "Material-related Aspects of Asphalt Recycling-State of the Art," *Journal of Materials in Civil Engineer*, vol. 18, 2006.
- [64] D. I. Anderson, D. E. Peterson, M. L. Wiley and W. B. Betenson, "Evaluation of Selected Softening Agents Used in Flexible Pavement Recycling," FHWA-TS-79-204, 1978.
- [65] J. Shen, S. Amirkhanian and B. Tang, "Effects of Rejuvenator on Performance-Based Properties of Rejuvenated Asphalt Binder and Mixtures," *Construction and Building Materials* , vol. 21, 2006.
- [66] S. Van der Zwaag, "Self-Healing Materials: An Alternative Approach to 20 Centuries of Materials Science," Dordrecht: Springer Verlag, 2007.
- [67] L. Francken, "Fatigue Performance of a Bituminous Road Mix under Realistic Best Conditions," *Transportation Research Record*, 1979.
- [68] S. R. White, N. R. Sottos, P. H. Geubelle, J. S. Moore, M. R. Kessler and S. R. Sriram, "Autonomic Healing of Polymer Composites," *Nature*, pp. 794-797, 2001.
- [69] R. S. Trask, H. R. Williams and I. P. Bond, "Self-Healing polymer Composites: Mimicking Nature to Enhance Performance," *Bioinspiration & Biomimetics*, vol. 2, pp. 1-9, 2007.
- [70] K. P. Chong, "Nanotechnology and Information Technology in Civil Engineering," ASCE, pp. 1-9, 2003.
- [71] S. G. Jahromi and A. Khodaii, "Effects of Nanoclay on Rheological Properties of Bitumen Binder," *Construction and Building Materials*, vol. 23, no. 8, pp. 2894-2904, 2009.
- [72] F. Xiao, A. N. Amirkhanian and S. N. Amirkhanian, "Influence of Carbon Nanoparticles on the Rheological Characteristics of Short-Term Aged Asphalt Binders," *Materials in Civil Engineering*, vol. 23, no. 4, 2011.

- [73] H. Wang, J. Zhong, D. Feng, J. Meng and N. xie, "Nanoparticles-modified Polymer-based Solar-reflective Coating as a Cooling Overlay for Asphalt Pavement," *International Journal of Smart and Nano Materials*, vol. 4, no. 2, pp. 102-111, 2012.
- [74] F. P. Bonnaure, A. H. Huibers and A. Boonders, "A laboratory Investigation of the Influence of Rest Periods on the Fatigue Characteristics of Bituminous Mixes," *Journal of Association of Asphalt Paving Technology*, vol. 51, pp. 104-128, 1982.
- [75] T. P. Grant , "DEtermination of Asphalt Mixture Healing Rate Using Superpave Indirect Tensile Test," *Master Thesis*, 2001.
- [76] A. Garcia, E. Schlangen, M. Van de Ven and Q. Liu, "Electrical Conductivity of Asphalt Mortar Containing Conductive Fibers and Fillers," *Construction Building Materials*, vol. 23, pp. 3175-3181, 2009.
- [77] Q. Liu, E. Schalngen , M. Van de Ven and A. Garcia , "Induction Heating of Eletrically Conductive Porous Asphalt Concrete," *Construction Building Materials*, vol. 24, pp. 1207-1213, 2010.
- [78] Q. Liu, E. Schalngen, M. Van de Ven, G. Van Bochove and J. Van Montfort, "Evaluation of the Induction Healing Effect of Porous Asphalt Concrete Through Four Point Bending Fatigue Test," *Construction Building Materials*, vol. 29, pp. 403-409, 2012.
- [79] Q. Liu, S. Wu and E. Schlangen , "Induction Heating of Asphalt Mastic for Crack control," *Construction and Building Materials*, vol. 41, pp. 345-351, April 2013.
- [80] C. Chiu and M. Lee, "Effectiveness of Seal Rejuvenators for Bituminous Pavement Surfaces," *J. Test. Eval.* , vol. 34, pp. 390-394, 2006.
- [81] M. Samadzadeh, S. Hatami, M. Peikari and A. Ashrafi, "A review of Self-Healing Coatings based on Micro/Nanocapsules," *Progress in Organic Coatings*.
- [82] B. Boh and B. Sumiga, "Microencapsulation Technology and Its Applications in Building Construction Materials," *Materials and Geoenvironment* , vol. 55, 2008.
- [83] S. Shirzad, M. M. Hassan, M. A. Aguirre and L. Mohammad, "Evaluation of Sunflower Oil as a Rejuvenator and Its Microencapsulation as a Healing Agent," *Journal of Materials in Civil Engineering*, May 2016.
- [84] M. A. Aguirre, M. M. Hassan, S. Shirzad, w. H. Daly and L. Mohammad, "Micro-encapsulation of Asphalt Rejuvenator using Melamine-Formaldehyde," *Construction and Building Materials* , vol. 114, pp. 29-39, 2016.
- [85] J. Su, Y. Y. Wang, N. X. Han, P. Yang and S. Han, "Experimental Investigation and Mechanism Analysis of Novel Multi-self-healing Behaviors of Bitumen using

- Microcapsules containing Rejuvenator," *Construction and Building Materials*, vol. 106, pp. 317-329, 2016.
- [86] D. Sun, J. Hu and X. Zhu, "Size Optimization and Self-Healing Evaluation of Microcapsules in Asphalt Binder," *Colloid Polymer Science*, vol. 293, no. 12, 2015.
 - [87] A. Gibney, "Analysis of permanent deformation of hot rolled asphalt in Civil Engineering," 2002.
 - [88] A. Tabakovic, W. Post, D. Cantero, O. Copuroglu, S. J. Garcia and E. Schlangen, "The reinforcement and healing of asphalt mastic mixtures by rejuvenator encapsulation in alginate compartmented fibres," *Smart Materials and Structural*, 2016.
 - [89] S. K. Ghosh, *Functional Coatings and Microencapsulation: A General Perspective*, in *Functional Coatings: by Polymer Microencapsulation*, Wiley-VCH Verlag GmbH & Co. KGaA, 2006.
 - [90] B. Boh and B. Sumiga, "In-situ polymerization microcapsules," *Bioencapsulation Innovations*, pp. 4-6, 2013.
 - [91] M. Rodson and H. B. Scher, *Water-in-oil microencapsulation process and microcapsules produced thereby*, US 6113935, 2000.
 - [92] F. Salaun, "Microencapsulation by interfacial polymerization," in *Encapsulation Nanotechnologies*, Wiley-Scrivener, 2013, pp. 137-173.
 - [93] K. Dietrich, H. Herma, R. Nastke, E. Bonatz and W. Teige, "Amino resin microcapsules," *Acta Polymerica*, 1980, pp. 243-251.
 - [94] Z. Zhen, "Effects of protective colloid on the Mf-UF double wall micro-encapsulation containing essence oil," *Advanced Materials Research*, pp. 236-238, 2011.
 - [95] L. L. Williams, "Amino resin and plastics," in *Encyclopedia of Chemical Technology*, 4 ed., John Wiley and Sons., 1992, pp. 604-637.
 - [96] J. Smets, J. O. Dihora, A. Pintens, S. J. Guinebretiere, A. K. Druckrey, P. D. Sands and N. Yan, "Benefit agent containing delivery particle," US 8551935, 2013.
 - [97] E. H. Donald, "Capsule manufacture," US 4444699, 1984.
 - [98] Y. Yan, J. Liu and H. Zhang, "Effects of NaCl and sipersants on preparation of microencapsulated phase change paraffin," *Xinxing Cailiao*, vol. 37, no. 1, pp. 56-59, 2009.

- [99] H. Wang, "Microencapsulation of styrene/epoxydiacrylate via in-situ polymerization of melamine-formaldehyde," *Advanced Materials Research*, Vols. 393-395, pp. 1279-1282, 2012.
- [100] S. Cosco, V. Ambroggi, P. Musto and C. Carfagna, "Urea-formaldehyde microcapsules containing an epoxy resin: Influence of reaction parameters on the encapsulation yield," *Macromolecular Symposia*, vol. 234, pp. 184-192, 2006.
- [101] A. M. Bakry, S. Abbas, B. Ali, H. Majeed, M. Y. Abouelwafa, A. Mousa and L. Liang, "Microencapsulation of oils: A comprehensive review of benefits, techniques, and applications," *Comprehensive Reviews in Food Science and Food Safety*, vol. 00, 2015.
- [102] C. Perignon, G. Ongmayeb, R. Neufeld, Y. Frere and D. Poncelet, "Microencapsulation by interfacial polymerization: membrane formation and structure," *Journal of Microencapsulation*, 2014.
- [103] Poncelet, C. Perignon and G. Ongmayeb, "Interfacial polymerization versus cross-linking microencapsulation," *Bioencapsulation Innovations*, 2013.
- [104] D. Saihi, I. Vroman, S. Giraud and S. Bourbigot, "Microencapsulation of ammonium phosphate with a polyurethane shell. PartII".
- [105] G. Nelson, "Microencapsulation Innovations," [Online]. Available: <http://www.microencapsulationinnovations.com/Chemical.html#Coacervation>. [Accessed 12 April 2017].
- [106] R. Dubey, T. C. Shami and K. U. Bhasker Rao, "Microencapsulation Technology and Applications," *Defence Science Journal*, vol. 59, no. 1, pp. 82-95, 2009.
- [107] Teonline, "Textile Exchange," [Online]. Available: <http://www.teonline.com/knowledge-centre/polymer-processing.html>. [Accessed 14 April 2017].
- [108] S. H. Lee, "The mechanism and characteristics of dry-jet wet spinning of chitosan fibers," *Journal of The Korean Fiber Society*, vol. 37, pp. 374-381, 2000.
- [109] J. Knaul, M. Hooper, C. Chanyi and K. A. M. Creber, "Improved mechanical properties of chitosan fibers," *Journal of Applied Polymer Science*, vol. 69, pp. 1435-1443, 1998.
- [110] S. H. Lee, S. M. Park and Y. Kim, "Effect of the concentration of sodium acetate (SA) on crosslinking of chitosan fiber by epichlorohydrin (ECH) in a wet spinning system," *Carbohydrate Polymers*, vol. 70, no. 1, pp. 53-60, 2007.
- [111] Y. Qin, C. Agboh, X. Wang and D. K. Gilding, *Chem Fibers Int* , vol. 46, 1996.

[112] Y. Qin, Chem Fibers Int, vol. 55, p. 98, 2005.

[113] Y. Qin, "Review Alginate fibres: an overview of the production processes and applications in wound management," Polymer International, vol. 57, no. 2, pp. 171-180, 2008.

CHAPTER 3. PERFORMANCE OF ASPHALT REJUVENATORS IN HOT MIX ASPHALT CONTAINING RECYCLED ASPHALT SHINGLES

3.1 Introduction

Asphalt pavement, as the most commonly used pavement surface material around the world, draws a yearly demand of more than 110 million metric tons [1]. Furthermore, estimates predict that asphalt demand in the United States (us) will approach 28.6 million tons by 2019 [2]. This extensive demand for asphalt products, together with the continuous increase in the price of asphalt cement, motivates researchers to seek out innovative and tenable approaches.

The use of Recycled Asphalt Shingle (RAS) in asphalt paving construction represents a sustainable approach to reduce virgin materials consumption and negative environmental effects, as well as the cost of asphalt pavement. Asphalt shingles, commonly used in the roofing industry, consists of asphalt binder, mineral filler, organic paper felt, and glass fiber matting [3]. Every year, 11 million tons of waste shingles are produced, which leads to 22 million cubic yards of waste materials that in the past would be landfilled [4]. Annually, waste asphalt shingles represents 8 to 10% of building-related waste in the US; thereby, becoming the third largest source of world-wide waste from the construction industry [5]. Research found that a partial replacement of asphalt binder with RAS can reduce the need for landfill space; a previous study predicted that one barrel of asphalt binder could be replaced by one ton of recycled shingles [6].

This chapter, previously published as M. A. Aguirre, M. M. Hassan, S. Shirzad, L. N. Mohammad and S. B. Cooper, "Performance of asphalt rejuvenators in hot-mix asphalt containin recycled asphalt shingles," *Transportation Research Record*, vol. 2633, pp. 108-116, 2017, is reprinted here by permission of Transportation Research Record

Utilizing RAS in asphalt mixtures as a partial replacement of virgin binder started in the 1980's [7]. Maupin [8] used laboratory tests to study the effects of using 5% RAS in an asphalt mixture; he found that RAS did not adversely affect pavement performance compared to conventional mixtures. Anurag et al. [9] studied the effect of roofing waste fibers with different lengths and fiber contents by measuring the indirect tensile strength of asphalt mixtures. The researchers found that polyester fibers improved both the wet tensile strength and tensile strength ratios [9]. Malik and Mogawer tested three different RAS percentages (3, 5, and 7%), which showed no significant change in the volumetric and low-temperatures performance; furthermore, asphalt mixes with 5 and 7% RAS showed better rutting performance [10].

In spite of these numerous advantages, many challenges are yet to be addressed with the use of RAS in paving applications. The main challenge with using RAS is the aged binder. Properties of the binder become highly-dependent on the aging process during the service life of shingles. Due to aging and oxidation processes, the asphaltene to maltene ratio of the asphalt binder in RAS increases [11]. Having become stiff and brittle, the binder exhibits low deformation characteristics, thus causing various distresses such as fatigue and thermal cracking [12]. Furthermore, the aged binder in RAS tends to limit high percentages of recycled shingles being utilized in asphalt pavements. As a result, the use of RAS is not permitted in all states of the US; in most of the states where allowed, RAS is limited up to 5% by weight of the asphalt mixture [13]. Another issue related to the use of RAS involves the variability and inconsistency of the resources [14]. In addition, the level of blending between virgin and RAS binder, together with the RAS binder's contribution to the total asphalt content of the mixture, is largely unknown and has resulted in concerns of state transportation agencies to use RAS.

In order to address the issues related to aging of the recycled material such as RAS, the use of rejuvenators was suggested. Rejuvenators are usually composed of organic oils with high maltene constituents [15] with the ability to recover an asphalt binder's properties; thereby, changing the chemical composition of the hardened binder [16]. Rejuvenator's application has been used as a maintenance activity on the top layer of the pavement in order to revive the oxidized top portion [13]. These rejuvenators may also be used with various recycled materials to further increase the blending of the aged and virgin binders, increase deformation capability, and ultimately reduce the stiffness of the aged binder. In this study, the effects of different rejuvenators on the performance of asphalt mixtures containing RAS were evaluated and were compared to a conventional asphalt mixture without RAS.

3.2 Objectives

The objective of this study was to examine the effects of four rejuvenators on the performance of asphalt mixtures containing RAS using two approaches; 1) measuring the mechanistic engineering properties of the mixtures containing RAS and rejuvenators at high and intermediate temperatures using the dynamic complex modulus, the Semi-Circular Bending (SCB) test, and the Hamburg Wheel Tracking Device (HWTB) test; and 2) studying the molecular compositions and rheological properties of extracted asphalt binders with and without RAS, together with different rejuvenators using High-Pressure Gel Permeation Chromatography (HP-GPC) and Superpave Performance Grade (PG) grading, respectively.

3.3 Background

3.3.1 Recycled Asphalt Pavement

Over the last decade, several studies were performed in order to examine the effects of RAS on asphalt pavement performance [17-20]. Cooper et al. conducted a comprehensive laboratory

study to evaluate the performance of asphalt mixtures containing RAS. Results suggested that mixtures containing 5% RAS with no recycling agents (rejuvenating agents and/or softening agents) had the same performance as mixtures with no RAS at high, intermediate, and low temperatures. Additionally, the RAS caused an improvement in the rutting resistance of the mixtures [21]. Robinette and Epps performed a life-cycle assessment for HMA mixtures containing recycled materials, in order to study energy consumption, natural resource consumption, and emission generation. The results showed that the utilization of recycled materials in asphalt pavement will decrease emissions generation, energy consumption, and virgin material consumption, while reducing the overall cost of asphalt paving construction [22].

3.3.2 Rejuvenators

In the short-term, a rejuvenator should be able to diffuse within a RAS binder, then mobilize the stiff binder, providing enough workability to uniformly coat the mixture. In the long-term, a rejuvenator should have the ability to change the physical and chemical properties of an aged binder to prevent fatigue and low temperature cracking. However, an over-softening of the binder should be avoided [23]. Cooper et al. studied the effect of rejuvenators on the performance of asphalt mixtures containing RAS. The inclusion of a rejuvenator increased the recycled binder ratio but also showed an adverse effect on the intermediate and low-temperature performances of the mixture [21]. Shirzad et al. utilized fundamental rheological tests to evaluate the effect of two different rejuvenators, a bio-oil (sunflower oil) and a synthetic oil on the reversal of the aging process of reclaimed asphalt pavement. The results showed that sunflower oil partially restored the original properties of the aged binder, while the synthetic oil did not perform well [24].

3.4 Experimental Program

3.4.1 Materials

A polymer-modified asphalt binder (PG 70-22M) and aggregates (5/8" gravel, 3/4" gravel, coarse sand and fine sand) were selected to satisfy the mix design for a 12.5 Nominal Maximum Aggregate Size (NAMS) asphalt mixture. The aggregate's consensus properties in HMA were satisfied for all aggregates. The RAS utilized for this study were post-consumer waste shingles (PCWS) and were incorporated into the evaluated mixtures at 5% by the total weight of mix. In addition, four asphalt rejuvenators were included in the selected asphalt mixtures at 5% by the total weight of RAS.

3.4.2 Asphalt Rejuvenators

Four asphalt rejuvenators were evaluated in this study, one bio-oil and three synthetic-oils. Sunflower seed oil was selected as a bio-oil, based on availability and economic advantages. The synthetic rejuvenators, ReJUVN8, provided from SRIPATH TECHNOLOGIES, as well as Cargill1252 and Cargill1253, provided by Cargill Industries, were selected based on suggested properties, such as compatibility with asphalt binder, a high rejuvenation ability, and improved low temperature properties of the aged binder.

3.4.3 HMA Mixture Design

This study was performed by designing and preparing six Superpave asphalt mixtures with a NMAS of 12.5 mm. The Superpave asphalt mixtures were prepared in accordance with AASHTO R35-09, Standard Practice for Superpave Volumetric Design for Hot Mix Asphalt; AASHTO M 323-07, Standard Specification for Superpave Volumetric Mix Design; and Section 502 of the 2006 Louisiana Standard Specifications for Roads and Bridges. A Level 2 design ($N_{\text{initial}} = 8$, $N_{\text{design}} = 100$, $N_{\text{final}} = 160$ gyrations) was utilized. The optimum asphalt content for

each Superpave mixture was determined according to volumetrics (air voids = 3-5%, voids in mineral aggregates $\geq 13\%$, voids filled with asphalt = 68%-78%), and densification requirements ($\%G_{mm}$ at $N_{initial} \leq 89\%$, and $\%G_{mm}$ at $N_{final} \leq 98\%$).

The six HMA mixtures utilized in this study are presented in Table 3.1. The first mixture was a conventional mixture containing no RAS (70CO). The second mixture was an HMA containing 5% PCWS by weight of the total mix, 70PG5P. The third asphalt mixture, 70PG5SUN, was an HMA containing 5% PCWS by weight of the total mix, and 5% sunflower oil by weight of RAS. The fourth mixture, 70PG5REJ8, included 5% PCWS by weight of the total mix and 5% Rejuvn8 by weight of RAS. The rejuvenator product, Cargill-1252, was used at 5% by weight of RAS, combined with 5% PCWS by weight of the total mix, to design the fifth mixture, 70PG1252. Lastly, the study designed and evaluated a HMA mixture containing 5% PCWS by weight of the total mix and 5% Cargill-1253 by weight of RAS (70PG1253).

Table 0.1. HMA Mixture Description

Mixture Type	RAS Content (%)	Rejuvenator Content (%)
70CO	0.0	0.0
70PG5P	5% PCWS	0.0
70PG5SUN	5% PCWS	5% Sunflower Oil
70PG5REJ8	5% PCWS	5% Rejuvn8
70PG1252	5% PCWS	5% Cargill1252
70PG1253	5% PCWS	5% Cargill1253

Varying virgin asphalt binder contents were evaluated for each of the mixtures to determine the optimum asphalt content that satisfies both volumetrics and densification criteria. For the mixtures containing RAS, it was possible to determine the asphalt content contributed by the

recycled material after identifying the optimum virgin asphalt content. Table 3.2 presents the job-mix formula for the six Superpave asphalt mixtures evaluated in this study. As seen in Table 3.2, the amount of asphalt content contributed from the RAS in mixtures 70PG5P, 70PG5SUN, 70PG5REJ8, 70PG1252, and 70PG1253, were 0.5, 0.8, 0.8, 1.0, and 1.0%, respectively. The composite aggregate gradation blends for mixtures 70PG5P, 70PG5SUN, 70PG5REJ8, 70PG1252 and 70PG1253 were similar to the aggregate gradation blend of mixture 70CO.

Table 0.2. Job-Mix Formula

Property	70CO	70PG5P	70PG5SUN	70PG5REJ8	70PG1252	70PG1253
%Gmm at Ninitial	88.5	89	88.4	88.4	88.7	89.1
%Gmm at Nfinal	96.3	97.2	96.3	96.3	95.9	96.7
Air Voids (%)	4.2	3.8	4.0	4.2	4.5	3.8
VMA (%)	13.4	13.5	13.6	14.4	13.4	13.8
VFA (%)	68.4	72.2	70.7	70.6	66.2	72.5
Total AC (%)	5.3	5.3	5.3	5.3	5.3	5.3
Virgin AC (%)	5.3	4.8	4.5	4.5	4.3	4.3
AC from RAS (%)	0.0	0.5	0.8	0.8	1.0	1.0
Recycled Binder Ratio (%)	0 %	9.4%	15.1%	15.1%	18.9%	18.9%

3.4.4 Experimental Test Matrix

Three mechanistic tests were conducted on the six mixtures as shown in Table 3.3. The experimental matrix included two mechanistic tests (SCB and dynamic complex modulus), as well as the HWTD to evaluate the rutting performance of each mixture. Cylindrical samples were prepared using a Superpave Gyratory Compactor. Tested samples were all compacted to an air voids of $7.0 \pm 0.5\%$.

3.4.5 Description of HMA Mixtures Tests

3.4.5.1 Semi-Circular Bending Test. Mix susceptibility to cracking at intermediate temperature was characterized using the Semi-circular Bending (SCB) test. Previous studies have found a relationship between the fracture resistance of asphalt mixtures and the Critical Strain Energy, or the critical value of J-integral, J_c . The SCB test was conducted according to ASTM D 8044 “Standard Test Method for Evaluation of Asphalt Mixture Cracking Resistance using the Semi-Circular Bend Test (SCB) at Intermediate Temperatures” using semicircular specimens with three different notch depths (25.4 mm, 31.8 mm, and 38mm) at a temperature of 25°C [25]. The SCB test consists of applying a monotonical load under a constant displacement rate of 0.5 mm/min until fracture failure. The critical strain energy release rate (J_c) is defined by the following equation [26]:

$$J_c = -\left(\frac{1}{b}\right) \frac{dU}{da} \quad (3.1)$$

where

J_c = critical strain energy release rate (kJ/m²);

b = sample thickness (m);

a = notch depth (m);

U = strain energy to failure (kJ); and

dU/da = change of strain energy with notch depth (kJ/m).

Table 0.3. Mixture Performance Tests

Test	Protocol	Failure Mechanisms	Specimen Details
Dynamic Modulus, $ E^* $	AASHTO T 342	Permanent deformation and fatigue cracking resistance	Ø150mm x 100mm
HWTD	AASHTO T 324-14	Rutting and moisture susceptibility	Ø150mm x 60mm
SCB	ASTM D 8044	Fatigue cracking	Ø150mm x 57mm

The strain energy to failure (U) was determined by measuring the area under the loading portion of the load deflection curves up to the maximum load for each notch depth. Then, a regression line slope is computed by plotting the average values of U versus the different notch depths. The regression line is used to determine dU/da in Equation (1). Finally, the critical strain energy is calculated by dividing the dU/da value by the specimen thickness, b .

3.4.5.2 Hamburg Wheel Tracking Device (HWTD). The study evaluated the resistance to permanent deformation of the mixtures by using the HWTD, where cylindrical specimens were submerged in a water bath maintained at 50°C, and a 703-N steel wheel is passed across the specimen until attainment of 20,000 cycles at a rate of 56 passes per minute. The failure criteria utilized in this study consisted of a maximum rut depth of 6 mm or completing 20,000 passes at 50°C. Previous studies have shown that it is possible to assess the moisture susceptibility in the HWTD test by measuring the stripping inflection point, where the intersection of the inverse creep slope and stripping slope occurs between the secondary and tertiary regions as shown in Figure 3.1 [21].

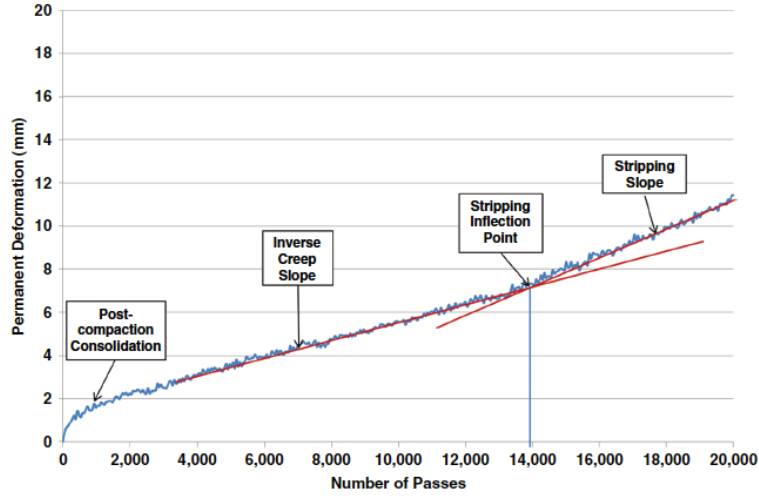


Figure 0.1. Schematic of a Typical HWT D Test Data Analysis Showing The Different Regions [21]

3.4.5.3 Dynamic Complex Modulus $|E^*|$ Test. The dynamic complex modulus, $|E^*|$, is defined as the absolute value of the complex modulus; that value is mathematically defined by the following equation:

$$|E^*| = \frac{\sigma_0}{\varepsilon_0} \quad (3.2)$$

where

σ_0 = maximum dynamic stress; and

ε_0 = maximum recoverable strain.

The dynamic modulus test was conducted at 4.4°C, 25°C, 37.8°C, and 54.4°C at loading frequencies of 0.1, 0.5, 1.0, 5.0, 10.0 and 25.0 Hz at each temperature [27].

3.4.6 Extracted Binder Tests

A PG grading, performed on the binder extracted from aged samples of the evaluated mixtures, assessed the effect of rejuvenators on the rheological properties of the recovered binder. The study conducted an extraction of the binder in accordance with AASHTO T 164, “Standard

Method of Test for Quantitative Extraction of Asphalt Binder from Hot Mix Asphalt HMA – Method A.” The AASHTO R 59, “Standard Practice for Recovery of Asphalt Binder from Solution by Abson Method,” which guided the process of distilling the solvent, was conducted as well. Finally, by use of rheological tests such as dynamic shear rheometry, rotational viscosity, and bending beam rheometer, and in accordance with AASHTO M 320-09 (Standard Specification for Performance-Graded Asphalt Binder), the study evaluated the rheological properties of the prepared blends [28]. Furthermore, the percentage of asphaltenes and maltenes in the extracted binders from the evaluated mixtures was determined to assess the effectiveness of the asphalt rejuvenators. The study measured the asphalt molecular weight distribution, utilizing a High-Pressure Gel Permeation Chromatography (HP-GPC).

3.5 Results and Analysis

3.5.1 Effects of Rejuvenator on HMA Mixture

3.5.1.1 Dynamic Modulus, $|E^*|$. A comparison of the master curves constructed for each mixture is presented in Figure 3.2. It is noted that the 70PG1253 mixture had the highest $|E^*|$ values and the 70CO mixture had the lowest $|E^*|$ values. The high stiffness of 70PG1253 was due to the high binder contribution from RAS when the Cargill-1253 recycling agent was used, as indicated in Table 3.2.

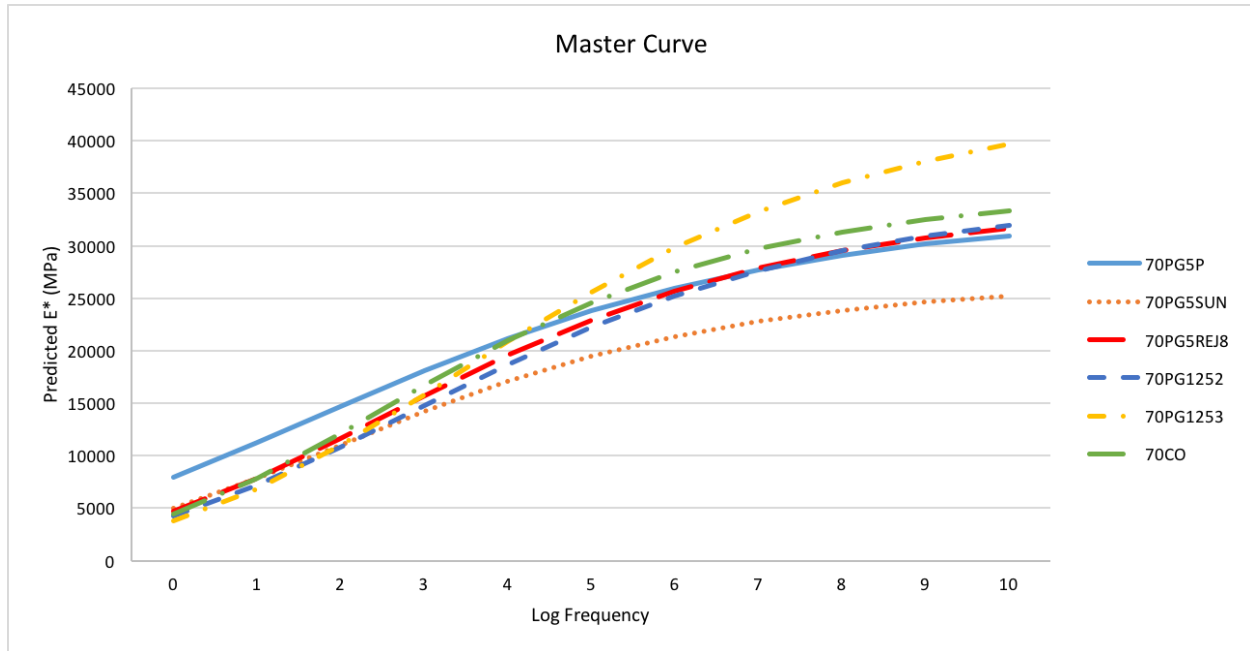
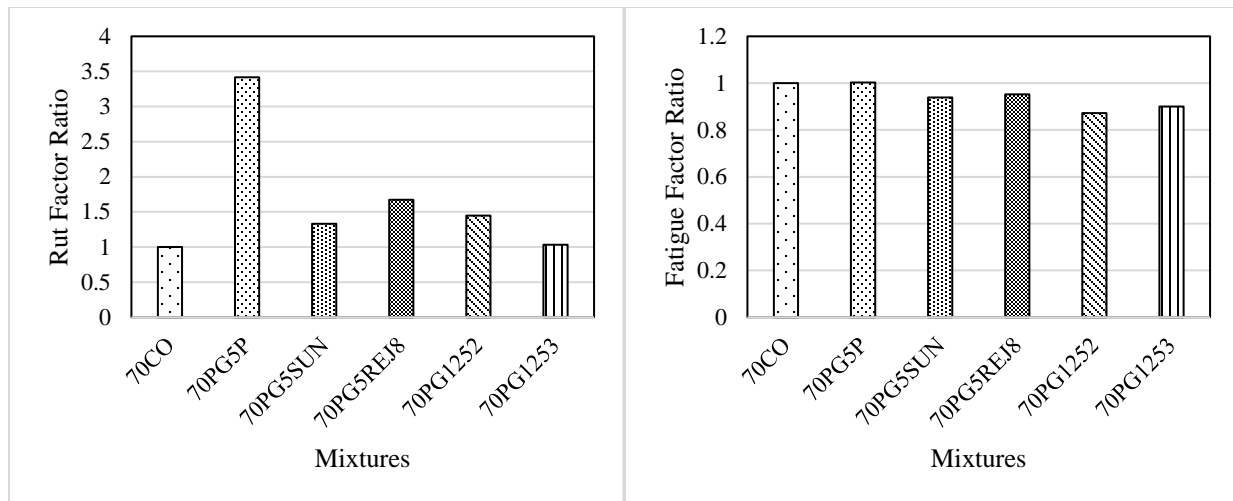


Figure 0.2. Master Curve of Asphalt Mixtures

Based on a previous study, a rut factor, $|E^*|/\sin(\delta)$ at 54°C , 5Hz, was computed to evaluate the rutting susceptibility and a fatigue factor, $|E^*|/\sin(\delta)$ at 25°C , 5Hz, was calculated to assess the fatigue susceptibility of the evaluated mixtures. Witczak et al. suggested that a lower fatigue factor indicates an enhanced performance against fatigue cracking; whereas a greater rut factor is desirable to indicate less susceptibility against rutting [27]. The mean normalized rut factor and fatigue factor, computed by dividing the rut factor/fatigue factor of each mixture by the rut factor/fatigue factor of mixture 70CO is shown in Figure 3.3. Figure 3.3(a) shows that all mixtures with the exception of 70PG1253 had a rut factor ratio greater than 1.0, which indicates a superior rutting performance of the mixtures as compared to the control mix. Furthermore, Figure 3.3(b) shows that the mixtures containing a rejuvenator product had a better performance against fatigue cracking as these mixtures had a fatigue factor ratio less than 1.0. The mixture with RAS and no rejuvenator (70PG5P) was predicted to have a similar performance against fatigue cracking as the control mixture (70CO) as the computed fatigue factor ratio was 1.0.



(a)

(b)

Figure 0.3. Dynamic Complex Modulus Test Results (a) Rut Factor Ratio, and (b) Fatigue Factor Ratio

3.5.1.2 Rutting Performance. Figure 3.4 displays the terminal permanent deformation depths for the evaluated mixtures from the HWTD test. It is shown in Figure 3.3 that the maximum allowable rut depth threshold in Louisiana (6 mm) was satisfied for all mixes. The addition of RAS decreased the terminal rut depth in mix 70PG5P, when compared to mix 70CO, which contained no RAS. However, the study observed that the addition of rejuvenator products slightly decreased the performance against rutting but it was still acceptable based on Louisiana specifications.

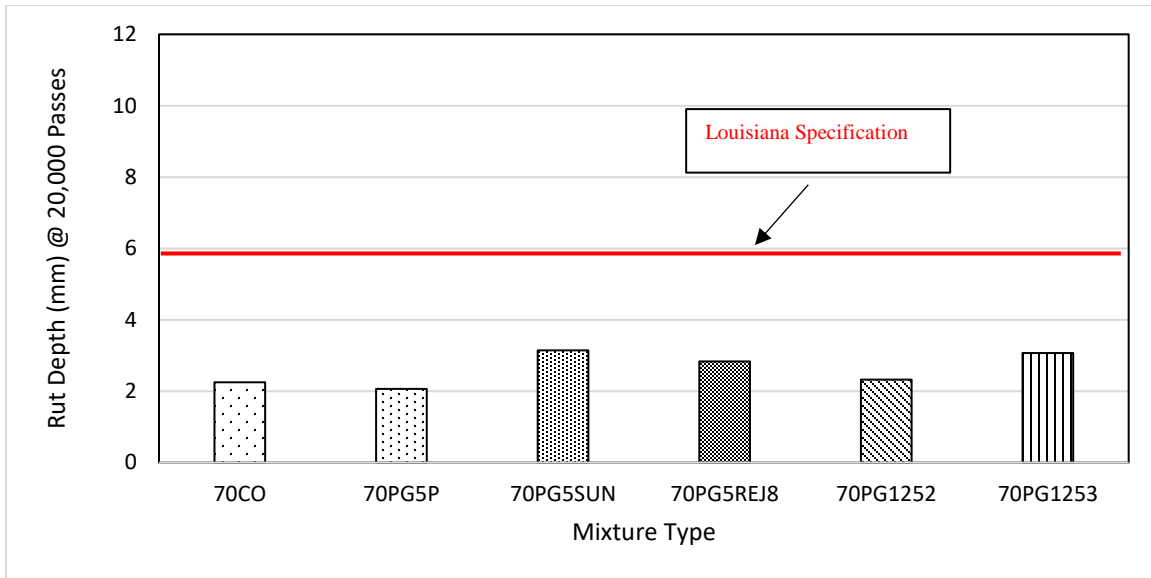


Figure 0.4. Rutting Depth for Evaluated Superpave Asphalt Mixtures

3.5.1.3 Moisture susceptibility. As previously discussed, HWTD test results can also assess the moisture susceptibility of asphalt mixtures by measuring the stripping inflection point. Figure 3.5 shows that no tertiary creep was detected in any of the evaluated mixtures. Therefore, no stripping inflection points were detected, and, therefore, the studied mixtures are not expected to be susceptible to moisture damage, as measured by the HWTD test.

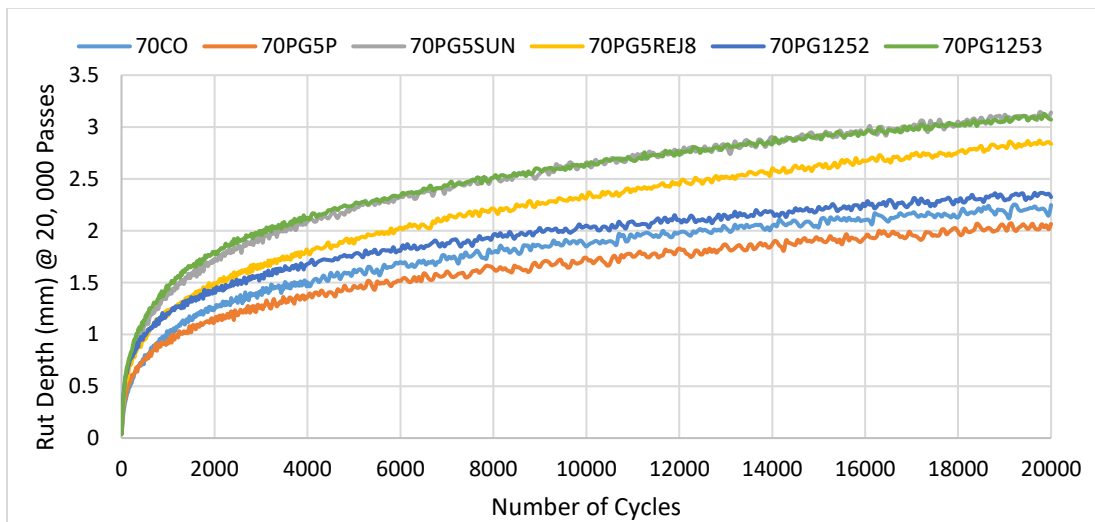


Figure 0.5. Rutting Depth versus Number of Cycles

3.5.1.4 Intermediate-Temperature Cracking. Previous studies have recommended a minimum threshold J_c value of 0.5 to 0.65 kJ/m² to measure intermediate-temperature cracking susceptibility [25]. Figure 3.6 shows the critical strain energy release rate for the evaluated mixtures. The result shows a slightly greater J_c for the control mixture (70CO) as compared to the mixture containing RAS without rejuvenator (70PG5P). Furthermore, Figure 6 indicates that the mixes with rejuvenators had a slightly lower J_c as compared to the mixture with RAS and no rejuvenator (70PG5P). This can be explained by the RBR of these mixes; 70PG5P had a RBR of 9.4%, which indicates that the remaining RAS acted as a black rock. On the other hand, the RBR of the other mixes was increased as a result of the rejuvenator application, which reversely affected cracking susceptibility of the mixtures.

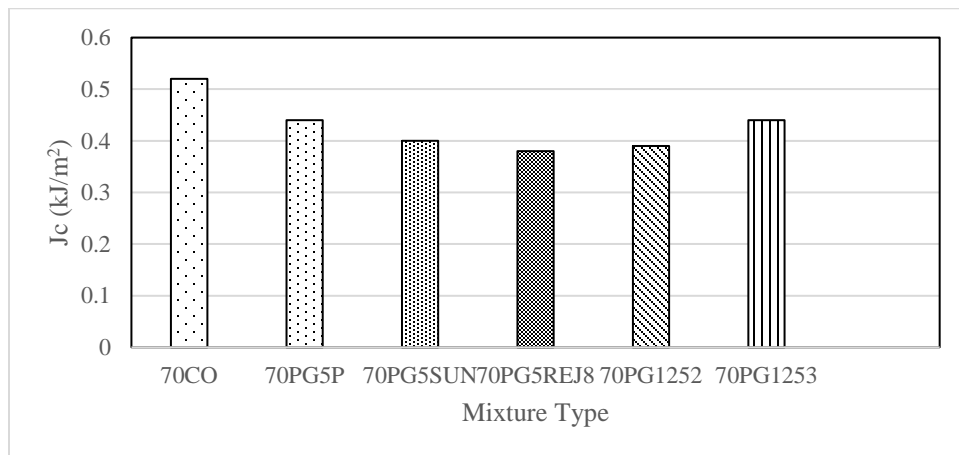


Figure 0.6. Critical Strain Energy Release Rate

3.5.1.5 Statistical Analysis. A statistical analysis was conducted to determine whether the differences in performance observed in both HWTD and SCB results were significant. The study conducted an Analysis of Variance (ANOVA) for each test to determine whether there were any statistical differences in mixture performance. Results of the ANOVA showed that there were significant differences between the mixture performances at a confidence level of 0.05 in HWTD

and SCB results. Therefore, a t-test was performed at a confidence level of 0.05 on all the possible combinations (i.e., 70CO vs. 70PG5P or 70PG1252 vs. 70PG5SUN) to identify the mixes that were statistically different. Table 3.4 shows the statistical ranking of the mixtures for the HWTD and SCB test results. The statistical results for each grouping are ranked by using letters A, B, C, and so forth. The letter A is assigned to the mix with the highest mean, followed by the letter B and so forth. Double letters (e.g., A/B, B/C) indicate that the mixture may be categorized in both groups. The statistical analysis showed differences and similarities between the mixtures in the performance against cracking and rutting but it did not show a significant difference between the mixtures with highest and lowest rut depths (i.e., 70PG5SUN vs. 70PG5P). It is noted, however, that all mixtures were below the 6.0-mm maximum rut depth specified by Louisiana.

Table 0.4. Statistical Ranking of Mixtures

Mixture Type	HWTD		SCB	
	Mean	Rank	Mean	Rank
70CO	2.250	A/B	0.525	A
70PG5P	2.065	B	0.440	A/B
70PG5Sun	3.145	A/B	0.437	A/B
70PG5REJ8	2.835	A/B	0.390	B
70PG51252	2.325	A	0.417	A/B
70PG51253	3.070	A/B	0.460	A/B

3.5.2 Rheological Properties of Extracted Binders

3.5.2.1 PG Grading from Extracted Binder. The rheological properties of the extracted aged binders from the evaluated mixtures were characterized, according to AASHTO M 320-09. Table 3.5 shows the PG grading of the extracted binder blends, based on Superpave laboratory binder

testing. Table 3.5 reveals that there exists a short-term aging effect during mix/compaction heating and extraction heating, since the extracted binder from the control mixture (70CO) was stiffer than the original virgin binder (PG 70-22). Furthermore, the results indicate that the use of Rejuvn8 and Cargill-1253 as asphalt rejuvenators did not positively affect the PG of the extracted binder from mixtures 70PG5REJ8 and 70PG1253 (i.e., PG 88-10), when compared to 70CO (i.e., PG 76-16) and 70PG5P (i.e., PG 82-16). In addition, the PG grading of extracted binders from mixtures 70PG5SUN and 70PG1252 (i.e., PG 82-16) showed a better performance compared to the extracted binders from mixtures 70PG5REJ8 and 70PG1253 (i.e., PG 88-10).

Table 0.5. Rheological Test Results of Extracted Asphalt Binder Blends

Mixture	PG Grading	Continuous Grading	UTI
70CO	PG 76-16	77.7-16.8	95
70PG5P	PG 82-16	87.9-16.1	104
70PG5SUN	PG 82-16	87.1-16.8	104
70PG5REJ8	PG 88-10	93.9-11.1	105
70PG1252	PG 82-16	83.6-21.3	105
70PG1253	PG 88-10	89.3-14.8	104

Evaluation of these results shows that the PG grading of the extracted binders with RAS and rejuvenators were due to the different percentages of virgin binder in the corresponding mixture; for example, the %AC of virgin binder in mixture 70PG5P was 4.8%, whereas the %AC of virgin binder in mixtures 70PG5REJ8 and 70PG5SUN was 4.5%. Besides the PG grading of the extracted binder blends, the Useful Temperature Interval (UTI) is shown in Table 3.5. UTI can be defined as the range between the minimum and maximum temperature where the binder is

expected to perform satisfactorily. Table 3.5 shows that mixture 70CO has the lowest UTI and that the use of rejuvenators did not improve the UTI compared to mixture 70PG5P.

3.5.2.2 High-Pressure Gel Permeation Chromatography (HP-GPC). The present study evaluated the asphalt molecular weight distributions of the extracted binder blends by performing a HP-GPC. The effectiveness of the asphalt rejuvenators to restore the asphaltenes/maltenes ratio may be measured by analyzing the percentage of asphaltenes and maltenes on the different extracted binder blends. The HP-GPC results are shown in Table 3.6. As shown in this table, the addition of the commercial product Cargill1253 was the most effective in restoring the asphaltene/maltene ratio, since the percentages of asphaltenes and maltenes from the extracted binder of mixture 70PG1253 were 26.4% and 66.6 %, respectively; reflecting a similar percentage to the asphaltenes and maltenes in the extracted binder in the control mixture, i.e., 27.4% and 66.1%, respectively.

Table 0.6. HP-GPC Calculations for Extracted Binders

Mixture	High molecular weight (%)	Asphaltene (%)	Maltene (%)	Asphaltene /Maltene Ratio
70CO	6.46	27.44	66.1	0.42
70PG5P	9.23	28.29	62.48	0.45
70PG5SUN	10.4	28.58	61.02	0.47
70PG5REJ8	10.38	29.84	59.78	0.50
70PG1252	11.24	28.54	60.22	0.47
70PG1253	6.93	26.42	66.65	0.40

3.6 Conclusions

The present study evaluated the effects of incorporating recycled asphalt shingle and rejuvenator products on the performance of HMA mixtures. A set of laboratory tests was performed to

characterize the performance of asphalt mixtures against distresses such as permanent deformation and fatigue cracking. The characterization was conducted in conventional HMA mixtures, mixtures containing 5% RAS, and asphalt mixtures containing 5% RAS with 5% of asphalt rejuvenator products. In addition, the asphalt binders were extracted from the mixtures and rheological and chemical analyses were conducted and evaluated. Based on the results from the experimental program, the following conclusions may be drawn:

The addition of 5% RAS showed an improvement in permanent deformation when compared to a conventional mixture with no RAS. Yet, the use of asphalt rejuvenators slightly decreased the performance against permanent deformation.

The addition of RAS did not adversely affect moisture susceptibility, and no moisture susceptibility was predicted by the HWTD.

SCB test results showed that the asphalt mixtures containing RAS and asphalt rejuvenators had a lower J_c value than the minimum threshold value (0.5 kJ/m^2), which indicated a greater susceptibility to intermediate-temperature cracking.

The addition of the commercial product Cargill 1253 restored the asphaltenes/maltenes ratio, when compared with mixture 70CO. Yet, the fracture resistance of the mix was still affected by the use of RAS.

3.7 References

- [1] García, A., Schlangen, E., van de Ven, M., Sierra-Beltrán, G. (2010). Preparation of capsules containing rejuvenators for their use in asphalt concrete. *Journal of Hazardous Materials* 184 603–611.
- [2] Rock Products News, (2015). U.S. Asphalt Demand to Reach 26.8 Million Tons in 2019. http://www.rockproducts.com/news-late/14601-u-s-asphalt-demand-to-reach-26-8-million-tons-in-2019.html#.V1caZ_krK00

- [3] Willis, J.R., Turner, P. (2016). Characterization of Asphalt Binder Extracted From Reclaimed Asphalt Shingles. NCAT Report 16-01.
- [4] Flynn, L. (1993). Roofing Materials Hold Promise for Pavements. Roads and Bridges.
- [5] BioCycle. (2003). Analyzing What's Recyclable in C & D Debris. p. 53.
- [6] Owens Corning Forms. (2012). Owens corning forms alliance with earth911 to expand footprint of nation's leading shingle recycling program. Retrieved July 2012, from <http://owenscorning.mediaroom.com/index.php?s=2370&item=66527>.
- [7] Davis, J. (2012). Roofing the Road – Using Asphalt Shingles as Binder.” Asphalt Magazine, <http://www.asphaltmagazine.com> – October 2009, Accessed March 13, 2012.
- [8] Maupin W. (2010). Investigation of the use of tear-off shingles in asphalt concrete. Virginia Transportation Research Council. Report no. FHWA/VTRC 10–R23.
- [9] Anurag, K., Xiao, F., Amirkhanian, S.N. (2009). Laboratory investigation of indirect tensile strength using roofing polyester waste fibers in hot mix asphalt. Construction and Building Materials 23.
- [10] Mallick, R. B., and W. S. Mogawer. (2000). Evaluation of Use of Manufactured Waste Asphalt Shingles in Hot Mix Asphalt. Technical Report No. 26.Chelsea Center for Recycling and Economic Development, University of Massachusetts, Lowell.
- [11] Ongel, A., Hugener, M. Impact of rejuvenators on aging properties of bitumen. Construction and Building Materials 94 (2015) 467–474.
- [12] Yaghoubi, E., Ahadi, M.R., Alijanpour Sheshpoli, M., Jahanian Pahlevanloo, H. (2013).Evaluating the Performance of Hot Mix Asphalt with Reclaimed Asphalt Pavement and Heavy Vacuum Slops as Rejuvenator. International Journal of Transportation Engineering, Vol.1/ No.2.
- [13] Mogawer, W.S., Booshehrian, A., Vahidi, S., Austerman, A.J. (2013). Evaluating the effect of rejuvenators on the degree of blending and performance of high RAP, RAS, and RAP/RAS mixtures. Road Materials and Pavement Design. Vol. 14, No. S2, 193–213.
- [14] Swiertz, D., Mahmoud, E., & Bahia, H. (2011). Estimating the effect of recycled asphalt pavements and asphalt shingles on fresh binder, low-temperature properties without extraction and recovery. Journal of the Transportation Research Board, 2208, 48–55.

- [15] Petersen, J.C. (2009). A Review of the Fundamentals of Asphalt Oxidation: Chemical, Physicochemical, Physical Property, and Durability Relationships. Transportation Research Circular E-C140, Washington, DC.
- [16] Shen, J., Amirkhanian, S., Aune Miller, J. (2007). Effects of Rejuvenating Agents on Superpave Mixtures Containing Reclaimed Asphalt Pavement. *Journal of Materials in Civil Engineering*, Vol. 19, No. 5, pp. 376–384.
- [17] Grzybowski K.F. (1993). Recycled asphalt roofing materials - A multifunctional low cost hot – mix asphalt pavement additive. Use of waste materials in hot-mix asphalt, ASTM STP-1193;. p. 159–79.
- [18] Button J.W, Williams D, Scherocman J A. (1995). Roofing shingles and toner in asphalt pavements. Texas Department of Transportation. Report No. FHWA/TX-96/1344-2F.
- [19] Foo K, Hanson D, Lynn T. (1999). Evaluation of roofing shingles in hot mix asphalt. *Journal of Materials in Civil Engineering*; 11(1):15–20.
- [20] Sengoz, B., Topal, A. (2005). Use of asphalt roofing shingle waste in HMA. *Construction and Building Materials* 19, pages 337-346.
- [21] Cooper, S, B., Mohammad, L, N., Elseifi, M, A. (2014). Laboratory Performance of Asphalt Mixtures Containing Recycled Asphalt Shingles. *Journal of the Transportation Research Board*, No. 2445, Washington, D.C, pp. 94–102.
- [22] Robinette, C., Epps, J. (2010). Energy, Emissions, Material Conservation and Prices Associated with Construction, Rehabilitation and Material Alternatives for Flexible Pavement. 89th Annual Meeting of the Transportation Research Board, Transportation Research Board, National Research Council, Washington, D.C., TRB 2010 CD-ROM.
- [23] Zaumanis, M., Mallick², R.B., Frank, R. (2013). Use of Rejuvenators for Production of Sustainable High Content RAP Hot Mix Asphalt. *Baltic Road Conference 2013*, At Vilnius, Lithuania.
- [24] Shirzad, S., Hassan, M. Aguirre, M.A., Mohammad, L.N., Daly, W.H. (2016). Evaluation of Sunflower Oil as a Rejuvenator and its Microencapsulation as a Healing Agent. *J. Mater. Civ. Eng.* , 10.1061/(ASCE)MT.1943-5533.0001625 , 04016116.
- [25] Wu, Z., L. Mohammad, L.B. Wang, and M.A. Mull. (2005). Fracture Resistance Characterization of Superpave Mixture Using the Semi-Circular Bending Test. *Journal of ASTM International*, Vol. 2, No. 3.

- [26] Rice, J.R. (1968). A Path Independent Integral and the Approximate Analysis of Strain Concentration by Notches and Crack. *Journal of Applied Mechanics*, Vol. 35, , pp. 379-386.
- [27] Witczak, M. W., Kaloush, T. Pellinen, M. El-Basyouny, and H. Von Quintus. (2002). NCHRP Report 465: Simple Performance Test for Superpave Mix Design. Transportation Research Board of the National Academies, Washington, D.C.
- [28] Aguirre, M., M.M. Hassan, S. Shirzad, W.H. Daly, L.N. Mohammad, Micro-encapsulation of asphalt rejuvenators using melamine-formaldehyde, *Construction and Building Materials*, Volume 114, 1 July 2016, Pages 29-39, ISSN 0950-0618.
- [29] Cooper, Samuel B. Jr. (2015). Sustainable Materials for Pavement Infrastructure: Design and Performance of Asphalt Mixtures Containing Recycled Asphalt Shingles. PhD Dissertation, Department of Civil and Environmental Engineering, Louisiana State University.

CHAPTER 4. LABORATORY TESTING OF SELF-HEALING MICROCAPSULES IN ASPHALT MIXTURES PREPARED WITH RECYCLED ASPHALT SHINGLES

4.1 Introduction

In the United States, roads and highways extend for more than 2.6 million miles through the nation; at present, 93% of these roads, considered to be transportation necessities, display an asphalt surface. In the last 40 years, the rising cost of petroleum-based products, inclusive of asphalt cement, has prompted a search for innovative methods to reduce the amount of virgin binder in Hot Mix Asphalt (HMA). Furthermore, the environmental impacts from carbon emissions, associated with the production of asphalt binder, motivates research on sustainable pavement technologies, such as the utilization of recycled materials. In response to this need, state agencies are considering the use of Recycled Asphalt Shingles (RAS) in pavement applications.

Studies indicate that the use of RAS in HMA could result in savings between \$1.00 and \$2.80 per ton of HMA by using 5% shingles [1]. In addition to the reduction in costs, studies show that recycled materials reduce related negative environmental impacts, such as extraction, transportation, and processing of virgin materials [2]. Recycled agents may be utilized in HMA containing RAS, not only to avoid any negative effect on pavement performance, but also to restore the properties of the aged binder [3].

This chapter, previously published as M. A. Aguirre, M. M. Hassan, S. Shirzad, L. N. Mohammad, S. Cooper and I. I. Negulescu, "Laboratory Testing of Self-Healing Microcapsules in Asphalt Mixtures Prepared with Recycled Asphalt Shingles," *Journal of Materials in Civil Engineering*, 2017, is reprinted here by permission of American Society of Civil Engineers

The implementation of rejuvenators as a recycling agent has the potential to restore the properties of aged asphalt binders [3]. Rejuvenators display an ability to restore the asphaltenes/maltenes ratio; thereby allowing for recovery of the relaxation capacity of an asphalt binder [4]. Yet, one concern for a rejuvenator application is that the agent must penetrate into the asphalt layer in order to reverse the aging process of the binder [5]. Therefore, research seeks an innovative approach in order to disperse the rejuvenator into the asphalt mix, such as the microencapsulation method [6].

Self-healing concept may be applied to asphalt concrete by utilizing microcapsules, which contain a rejuvenator product. Microcapsules containing rejuvenator demonstrate a capacity to seal micro-cracks produced by traffic and environmental loads in the asphalt pavement, as well as to permeate the surrounding binder. In addition to the healing of micro-cracks, the restoration of aged binder properties may also be achieved, thus enhancing pavement performance. Self-healing mechanisms would also enhance the use of recycled materials such as RAS by restoring the properties of the aged binder.

4.2 Objectives

This study had two main objectives: (1) Characterization of microcapsules containing an asphalt rejuvenator product as core material in order to test thermal stability; and (2) Evaluation of self-healing efficiency of double-walled microcapsules through crack healing and stiffness recovery of damaged mixture specimens under two different healing conditions.

4.3 Background

4.3.1 Recycled Materials in HMA

In the last few years, due to increased costs in asphalt cement, recyclable materials such as Reclaimed Asphalt Pavement (RAP) and Recycle Asphalt Shingles (RAS) were evaluated to

determine the subsequent effects on pavement performance. In this process, not only recycled materials were evaluated, but new processes such as Warm Mix Asphalt (WMA) were developed as well, in an attempt to lower the amount of energy required to construct asphalt pavements.

Watson et al. conducted a study to evaluate the effects of adding waste roofing shingles on asphalt mixtures [7]. The study evaluated asphalt mixtures containing 5% of manufactured waste shingles (MWS) by total weight. The research concluded that the performance of mixtures modified with RAS were similar to the control mix. In addition, the study observed that the extracted binder from the mixture containing RAS was stiffer than the one extracted from the control, thus the addition of RAS to asphalt mixture could positively enhance pavement performance against rutting.

Another study conducted by Maupin evaluated the addition of 5% post-consumer waste shingles (PCWS) in asphalt mixtures [8]. The purpose of the study was to evaluate whether the addition of RAS may negatively affect the mixture performance against major distresses. A conclusion from the study was that the addition of 5% PCWS made no difference on the fatigue performance of the mixtures. Additionally, although the results from the permanent deformation test differed, the rut depths satisfied the specification criteria from the Virginia Department of Transportation (VDOT).

4.3.2 Asphalt Rejuvenators

One of the most common methods presented to preserve asphalt pavement is the use of an asphalt rejuvenator to extend pavement service life, thus decreasing maintenance costs. Asphalt rejuvenators include cationic emulsions containing maltenes, which serve to restore the asphaltenes/maltenes ratio by softening the oxidized asphalt concrete pavement surface [9] [10]. Studies showed that the application of rejuvenator products in asphalt concrete reduced

hardening and temperature susceptibility of the pavement [11]. Yet, many studies determined that asphalt rejuvenators do not penetrate the asphalt pavement deeply enough to effectively restore the properties of the aged binder [5].

4.3.3 Microencapsulation of Asphalt Rejuvenators

The poor penetration of rejuvenator products may be addressed by developing microcapsules containing a core material product to be utilized during asphalt mixture production.

Microencapsulation may be defined as a process to encapsulate a solid, liquid, or gas as a core material, which is surrounded by a coating layer or shell [12]. The concept in using microcapsules containing a rejuvenator product is to release the product when the microcapsules break, due to the presence of a certain stress value.

Aguirre et al. [13] successfully microencapsulated a recycling agent by in-situ polymerization, using melamine-formaldehyde. The research utilized a double polymerization technique to enhance the rigidity and toughness of shell. Selection of the encapsulated product was based on an evaluation of the restoring capabilities of the rejuvenator in an aged binder. Results showed that the product would positively influence both high and low grade temperatures of the tested binders.

A study evaluated a common vegetable oil to determine its efficiency in reversal of the aging processes of asphalt binder [14]. The study conducted a PG grading of aged PG 70-22, PG 76-22, and RAP binder mixed with 5% of vegetable oil by weight of the binder. The study showed that the vegetable oil had a positive influence on both high and low temperature grades of the aged binder. In addition, the research developed a double-walled microcapsule (urea-formaldehyde/polyurethane) specifically designed for vegetable oil using an in-situ polymerization process [14].

4.4 Experimental Program

4.4.1 Microencapsulation Synthesis and Properties

4.4.1.1 Chemicals. The core material of the microcapsules consisted of a green bio-oil product, Rejuvn8, from Sripath Technologies (density 0.919 g/cm³). The experimental program used urea, ammonium chloride (NH₄Cl), resorcinol, formaldehyde solution, and a commercial polyurethane prepolymer (Desmodur L 75) as shell materials for the developed microcapsules. In addition, Ethyl Phenylacetate (EPA) represented the solvent used to dissolve the rejuvenator product with polyurethane prepolymer and with ethylene-maleic anhydride (EMA) copolymer (Zemac-400) powder applied in a 2.5 wt. % aqueous solution as a dispersant.

4.4.1.2 Microencapsulation Procedure. Shirzad et al. optimized a microencapsulation procedure for double-walled microcapsules [14]. The double-walled microcapsules were synthesized via in-situ polymerization, using polyurethane and urea-formaldehyde. The purpose of incorporating polyurethane into urea-formaldehyde microencapsulation was to increase thermal stability at high temperature, while maintaining the interfacial bonding by means of urea-formaldehyde microcapsules [15]. Moreover, studies showed that the combination of polyurethane/urea-formaldehyde improves long-term stability at room temperature and thus increases the ability to contain liquids [16].

Having mixed 100 ml of de-ionized (DI) water and 25 ml of 2.5% by wt. aqueous EMA copolymer solution in a 500 ml beaker, the microencapsulation procedure consisted of agitating the solution by means of an overhead stirrer and placing the resulting solution atop a ceramic hot plate. An agitation at 1000 rpm dissolved 2.5g of urea, 0.25 g of resorcinol, and 0.25 g of ammonium chloride. The procedure then adjusted the pH drop-wise to 3.50 by using sodium hydroxide and/or hydrochloric acid solutions. In another beaker, the researcher added 10 g of

rejuvenator with 5 g of polyurethane, and mixed the emulsion with 30 mL of ethyl phenylacetate. The process then added the thoroughly mixed emulsion to the main solution slowly, in order to maintain the pH between 3.0 and 3.5. After a 15-minute stabilization, the process added 6.33 g of 37% formaldehyde solution and heated the solution for four hours at the desired temperature at a rate of 1°C per minute, adding deionized water throughout the heating time to maintain the desired water level. Once the four hours of heating were complete, the solution was cooled under a fume hood and was vacuum-filtered to arrive at the final product.

4.4.1.3 Microcapsules Morphology. The study employed a Scanning Electron Microscope (SEM-FEI Quanta 3D FEG Dual Beam SEM/FIB) to evaluate the morphology of the produced microcapsules. Having sprinkled microcapsules on top of a double-sided tape attached to a pin stub specimen mount, the researcher sputter-coated the microcapsules with platinum for four minutes before imaging the specimens under a secondary electron mode at an accelerated voltage of 5 kV.

4.4.1.4 Thermogravimetric Analysis. Asphalt binder is typically added to the aggregate blend at around 163°C in a Superpave Hot-Mix Asphalt (HMA). Therefore, the study conducted a Thermogravimetric Analysis (TGA) on the prepared microcapsules as a means to study their degradation at high temperatures.

4.4.2 Self-Healing Mixture Testing

4.4.2.1 Materials. The selected materials in the mixture preparation consisted of a styrene-butadiene-styrene (SBS) polymer-modified binder, which was selected based on the Louisiana specifications for PG 70-22M; 16mm gravel, 6.35mm gravel, coarse sand, and fine sand, thus satisfying the mix design requirements of a 12.5mm Nominal Maximum Aggregate Size (NMAS). Post-consumer waste shingles (PCWS) were incorporated into the evaluated mixtures

at 5% by total weight of mix. In addition, the experimental program considered the use of an asphalt rejuvenator and the microcapsules in selected mixtures at 5% by total weight of RAS, see Table 4.1.

4.4.2.2 Specimen Preparation. Table 4.1 presents the prepared asphalt mixtures for the study. The mixture 70CO is a conventional mixture containing no RAS. Mixture 70PG5P used 5% PCWS by weight of the total mix. The experimental program considered the use of 5% PCWS by weight of the total mix and 5% Rejuvn8 by weight of RAS for the mixture 70PG5Rej8. Lastly, the MCrej8 mixture contained 5% PCWS by weight of the total mix and 5% microcapsules by weight of RAS.

Table 0.1. Job-Mix Formula

Mixture Type	RAS	Rejuvenator (%)	Microcapsules Content (%)
70CO	-	-	-
70PG5P	5% PCWS	-	-
70PG5Rej8	5% PCWS	5% Rejuvn8	-
MCrej8	5% PCWS	-	5%

Six specimens were prepared for each asphalt mixture type, with three to be exposed to room-temperature healing conditions and three to be exposed to high-temperature healing conditions after cracking. Cylindrical samples were prepared using a Superpave Gyratory Compactor (SGC) and rectangular specimens with dimensions 40mm x 40mm x 160mm (as shown in Figure 4.1) were obtained by sawing the cylindrical samples. All specimens were prepared to an air voids of $7.0 \pm 0.5\%$.

4.4.2.3 Self-Healing Test Description. A three-point bending setup was used to induce cracks at room-temperature in the prepared rectangular specimens with span length of 100mm without any prior conditioning through a strain-controlled load applied at a rate of 0.25 mm/min, which allowed stopping the test before any sudden failure. The three-point bending setup is shown in Figure 4.1(b).



(a)



(b)

Figure 0.1. (a) Rectangular Specimen Obtained by Sawing Cylindrical Samples and (b) Three-Point Bending Test Setup

The three-point bending test results were used to calculate the stiffness for three different conditions (undamaged, damaged, and healed). The test was stopped 100 seconds after reaching the peak load in each condition. As shown in Figures 2(a and b), the undamaged stiffness was defined as the slope of the linear equation from the steepest part of the load-deformation plot. A box in Figure 4.2(a) identifies the part of the curve analyzed in Figure 4.2(b). The same procedure was repeated for a second three-point bending test before healing in order to calculate the damaged stiffness and to increase the severity of the cracks before healing. Following healing, a third three-point bending test was conducted in order to estimate the healed stiffness.

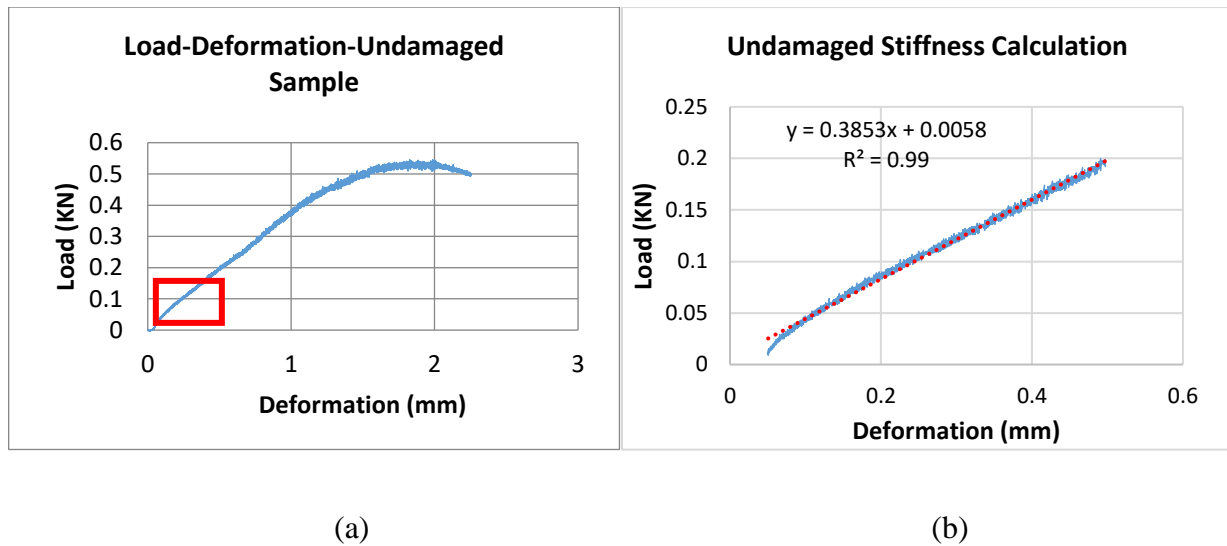


Figure 0.2. Calculation of Undamaged Stiffness (a) Load-Deformation Plot from First Bending Test (b) and Stiffness Calculation

Utilizing an optical light microscope, the study quantified the healing process of cracked specimens as a function of time, by adopting a magnification rate of 12x in order to measure the different cracks in the specimens. Immediately after crack characterization, specimens were then subjected to a 6-day healing period under controlled environmental conditions. Specimens were placed horizontally over a flat surface during the healing period. Cracks were observed at healing

periods of 0, 1, 2, 3 and 6 days. The study also performed a digital image analysis to measure the crack width over time.

4.4.2.4 Environmental Conditions for Self-Healing. Three specimens for each of the evaluated asphalt mixtures were exposed to two different dry temperature conditioning. The first temperature conditioning was applied at room temperature ($26 \pm 2^\circ\text{C}$). The second conditioning was conducted at a temperature of $50 \pm 2^\circ\text{C}$, which was maintained for 6 days using a conventional oven.

4.4.2.5 Quantification of self-healing. Healing of specimens as a function of time was quantified by digital image analysis using light microscopy. The light microscope utilized for data acquisition was a Zeiss SteREO Lumar.V12. The crack width was measured before healing (day 0), and at day 1, day 2, day 3 and day 6 of the healing period to quantify the healing efficiency of the specimens. The healing efficiency of the specimens at the different healing periods was calculated as follows:

$$H_e = \left(1 - \frac{Cw_t}{Cw_0}\right) * 100 \quad (4.1)$$

where H_e = Healing efficiency (%); Cw_0 = Initial Crack width, mm; and Cw_t = Crack width at the time of analysis, mm. Furthermore, a relationship between damaged and healed stiffness was evaluated to determine the stiffness recovery at the end of the healing period. The undamaged and healed stiffness values were compared by the ratio between the healed stiffness and the undamaged stiffness.

4.5 Results and Analysis

4.5.1 Microencapsulation of Rejuvn8

4.5.1.1 Characterization of Microcapsules. Microcapsules containing a commercial bio-oil product as the core material were prepared. Size is an important property of the produced microcapsules as the microcapsules should be smaller than the spaces between the aggregates but not too small to be broken during asphalt mixture production. The yield rate was calculated using Equation (4.2) to determine how much of the core material is being encapsulated. The diameter measurements and yield rates for the prepared microcapsules are shown in Table 4.2.

$$\% \text{Yield Rate} = \frac{\text{Weight of microcapsules}}{\text{Weight of ingredients}} \times 100 \quad (4.2)$$

Table 0.2. Diameter Measurements and Yield Rates for Double-Walled Microcapsules

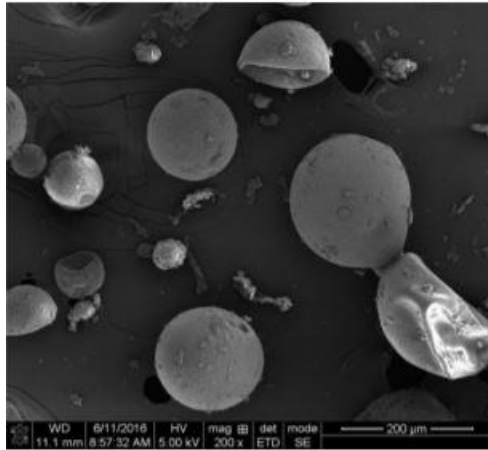
DIAMETER STATS	VALUE
Mean	152.91 μm
Std. Deviation	84.34 μm
Max	342.97 μm
Min	35.03 μm
Yield Rate	63.2%

*For the following production parameters: (a) agitation rate of 1000 rpm, (b) heating temperature of 55°C, and (c) reaction time of 4 hr.

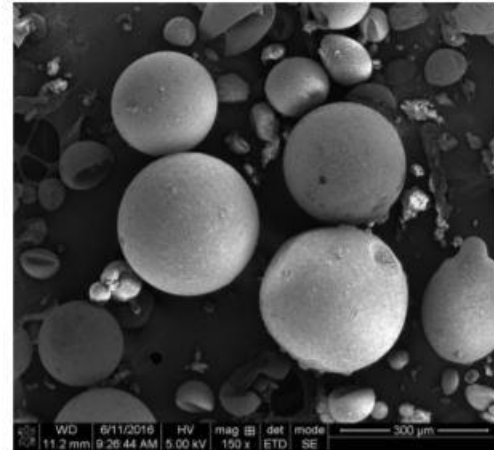
Figure 4.3(a) shows the double-walled microcapsules containing the asphalt rejuvenator as core material. The produced microcapsules were maintained at a temperature of 163°C for two hours to assess the behavior of the microcapsules during HMA mixture production. Figure 4.3(b) shows the microcapsules after two hours of thermal degradation at a temperature of 163°C. As

shown in Figure 4.3(b), the microcapsules showed little to no damage due to high temperatures, since the majority of the microcapsules did not break during the experiment. Furthermore, the behavior of the developed microcapsules to resist the HMA mixing process was evaluated by performing a small experiment consisting of mixing the microcapsules and 9.5mm aggregates in a mixing bowl for five minutes. Figure 4.3(c) shows the microcapsules after five minutes of mixing with 9.5mm aggregates. As shown in Figure 4.3(c), microcapsules did not break during the mixture process experiment. These results indicate that the produced microcapsules have demonstrated encouraging thermal and mixing resistance. Nevertheless, further evaluation in the field and at the plant of the microcapsules is needed.

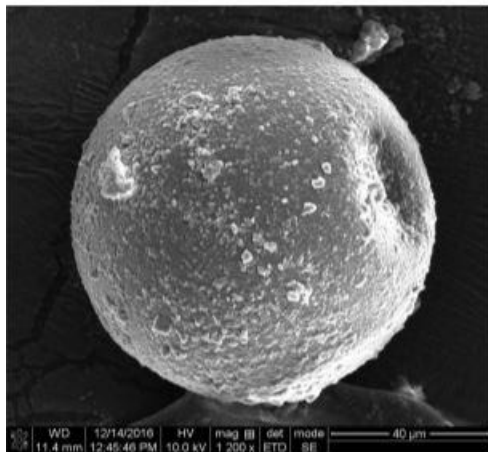
4.5.1.2 Thermogravimetric Analysis. The thermal stability of the produced microcapsules was analyzed using TGA. Figure 4.3(d) shows the change, both in weight (%) and the derivation weight (%/°C), as the temperature increased. Figure 4.3(d) supports the results presented earlier in Figure 3(b), where the microcapsules show little to no damage at a temperature of 163°C, presenting a decrease of less than 8% of the sample's weight. Based on these results, it is concluded that the produced microcapsules are suitable for use during asphalt mixture production, in view of the fact that the sample's weight decreased by 50% at a temperature (308°C), a temperature higher than the one used in an asphalt mixture production. The 50% reduction in microcapsule's weight at 308°C is attributable to the disintegration of the microcapsules due to the exposure to extreme high-temperature condition. Furthermore, the derivation weight (%/°C) in Figure 4.3(d) shows that highest weight variation (i.e. loss in microcapsule's weight) occurs at a temperature around 260°C, which can be seen as the turning point where microcapsules starts to disintegrate. A second turning point in weight derivation is observed around 410°C where microcapsules suffered another high % weight loss.



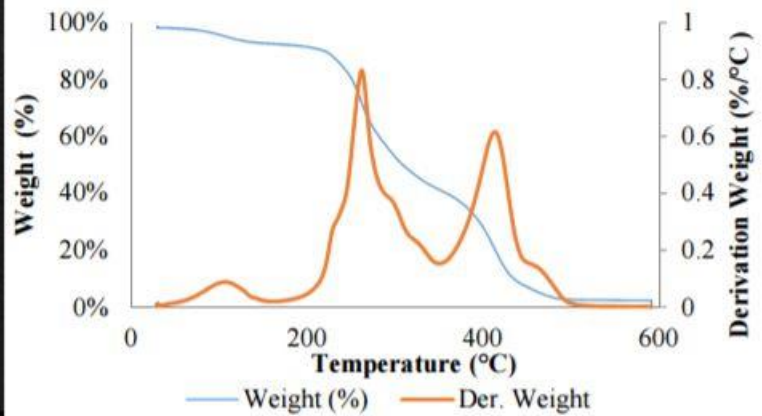
(a)



(b)



(c)



(d)

Figure 0.3. Double-Walled Microcapsules Containing an Asphalt Rejuvenator: (a) Undamaged Microcapsules; (b) Microcapsules After 2 H at 136°C; (c) Microcapsules After Mixing Experiment; and (d) Thermogravimetric Analysis Results

4.5.2 Self-Healing Experiment

4.5.2.1 Initial Crack Width. Light microscope images were obtained after inducing the cracks on the rectangular specimens before the healing period. The six specimens for each mixture were divided into two groups, Group I was defined as the specimens subjected to room-temperature healing conditions and Group II was defined as the specimens maintained at a temperature of 50°C utilizing a conventional oven. Digital image analysis was utilized to calculate the initial average crack width. The initial average crack widths were divided into two categories, series 1

was defined as the initial cracks with average width less than 0.4 mm and series 2 was defined for those initial cracks with average widths larger than 0.4 mm. The self-healing experiment was focused on cracks larger than 0.4 mm to simulate real field conditions. Table 4.3 and Table 4.4 present the details of the initial crack width measurements for room-temperature and high-temperature healing conditions for series 2, respectively. It is observed that there is no difference between the average crack widths in the specimens used for both healing conditions; thus, a comparison of the healing efficiencies of the mixtures can be performed between the two healing conditions.

Table 0.3. Room-Temperature Healing Condition

Mixture	Crack Width (mm)			
	n*	Mean	Std. Deviation	CV
70COO	50	0.5377	0.1233	22.9%
70PG5P	50	0.5789	0.1524	26.3%
70PG5Rej8	50	0.5139	0.0797	15.5%
MCRcj8	50	0.5928	0.0166	2.8%

*Number of measurements across the cracks

Table 0.4. High-Temperature Healing Condition

Mixture	Crack Width (mm)			
	n*	Mean	Std. Deviation	CV
70COO	50	0.5500	0.0983	17.9%
70PG5P	50	0.5469	0.1165	21.3%
70PG5Rej8	50	0.4779	0.0865	18.1%
MCRcj8	50	0.4299	0.0249	5.8%

* Number of measurements across the cracks

4.5.2.2 Healing Quantification. After inducing the cracks and taking the initial cracks measurements, samples were conditioned into their corresponding environmental condition. Light microscope was utilized to capture images from the specimens at 1, 2, 3 and 6 days during the healing period. The analysis of the images revealed that the cracks in the specimens started to heal as early as one day into the healing period. Furthermore, the analysis showed a daily improvement in the cracks width in both environmental conditions. Figure 4.4 shows a comparison between cracks from series 2 from the different mixtures from day 0 to day 6 at a healing temperature of $26 \pm 2^{\circ}\text{C}$ (room-temperature). A similar comparison for high-temperature healing condition is presented in Figure 4.5.

The study performed a healing quantification before and after healing by comparing the initial crack widths with the crack widths at 1, 2, 3 and 6 days into the healing period. As previously discussed, the study calculated the healing efficiency for each mixture using Equation (1). Figure 4.6(a) shows that the mixture with 5% Rejuvn8 showed the best recovery with 82.3% healing efficiency, thus it was similar to the 70CO at room temperature. The mix with microcapsule (MCRej8) had a 71.4% healing efficiency, which was lower than the 70PG5Rej8 and 70CO mixes. This is because that not all microcapsules have broken during the test since microcapsules are expected to break over time and not all at once. When a new crack occurs, more rejuvenator product will be released to initiate a new healing process. The reason that mix 70CO performed well is possibly due to the virgin polymer-modified binder used in this mix without aged binder contribution from RAS.

The study performed a similar analysis for the high-temperature healing condition in order to assess the healing efficiency of the studied mixtures. Figure 4.6(b) shows the healing efficiency

of the evaluated mixtures at a temperature of $50 \pm 2^\circ\text{C}$ for crack widths larger than 0.4 mm. As shown in this figure, the mixture prepared virgin binder (70CO) had the best healing efficiency with close to 70% as compared to the mixture with microcapsules (MCRej8), which had a 53.1% healing efficiency. Interestingly, the mix with RAS performed similarly to the mix with rejuvenator at high-temperature (70PG5P vs. Rejuvn8).

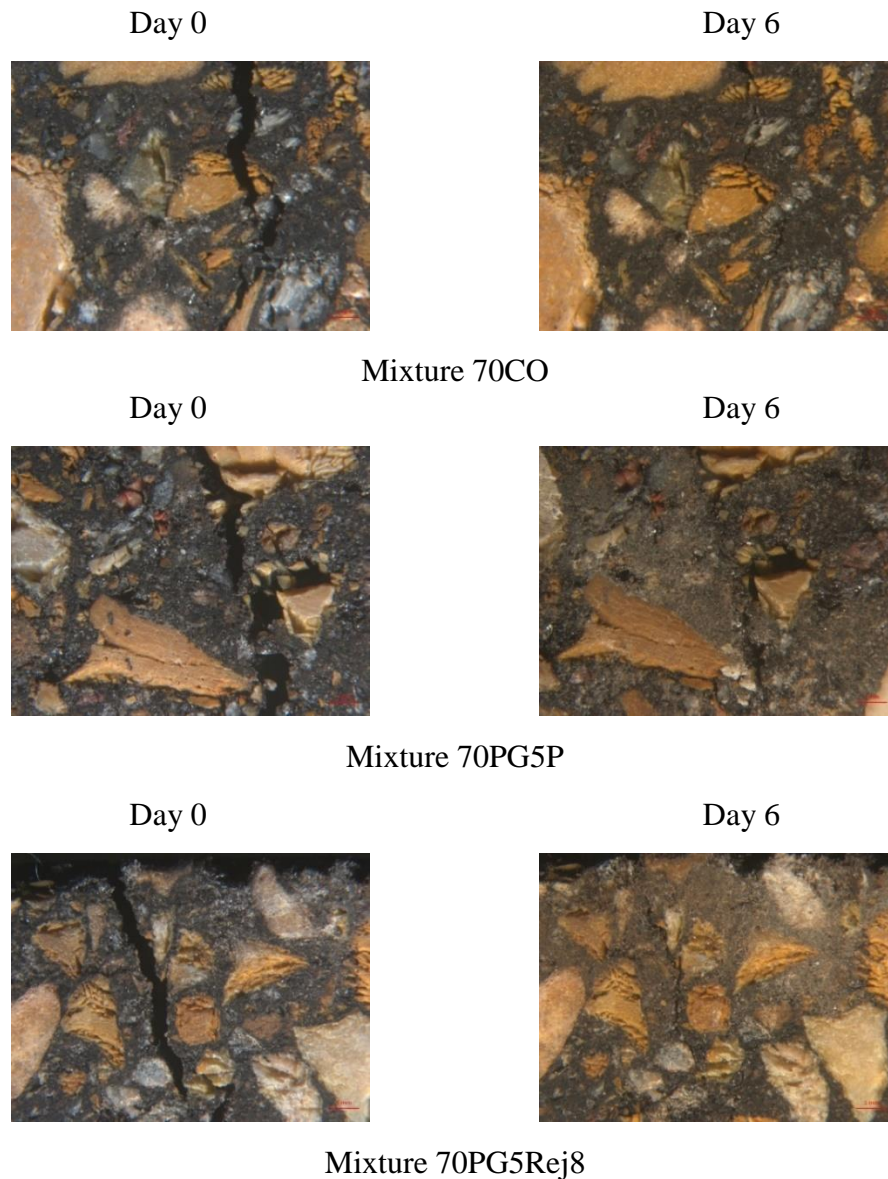
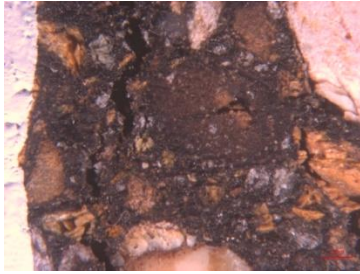


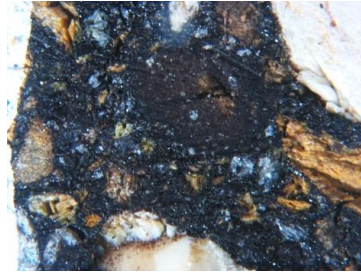
Figure 0.4. Cracks Before and After Healing at Room-temperature

Figure 4.4. cont'd

Day 0

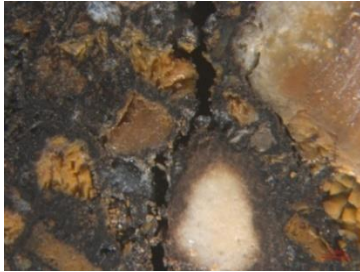


Day 6



Mixture MCRej8

Day 0

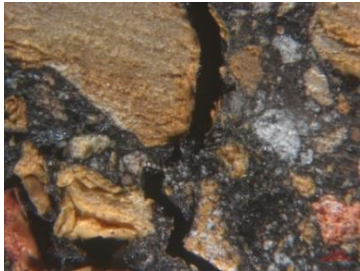


Day 6

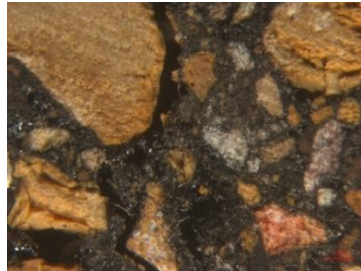


Mixture 70CO

Day 0



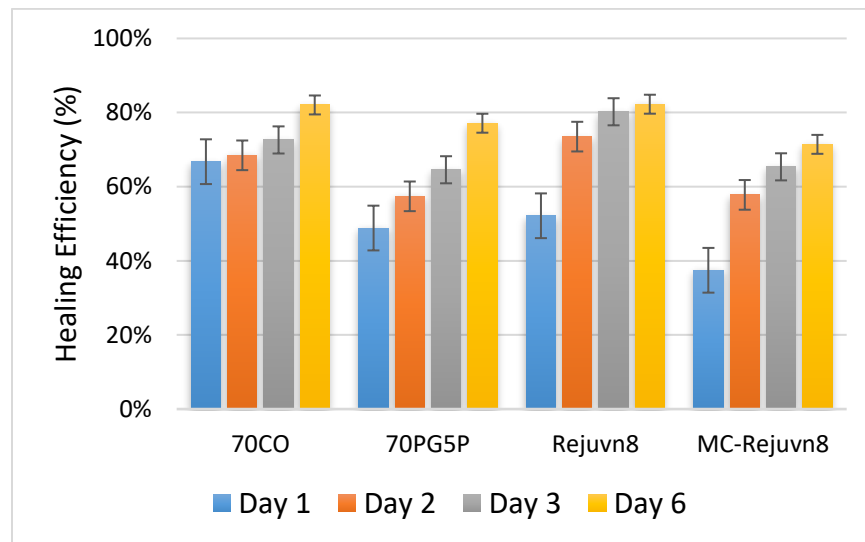
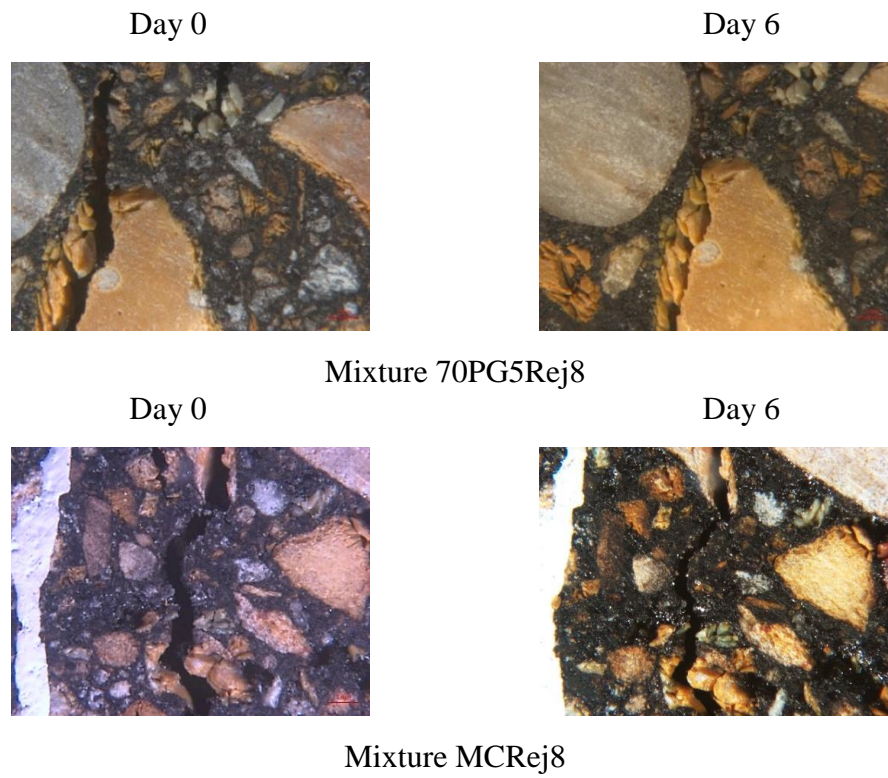
Day 6



Mixture 70PG5P

Figure 0.5. Cracks Before and After Healing at High-Temperature

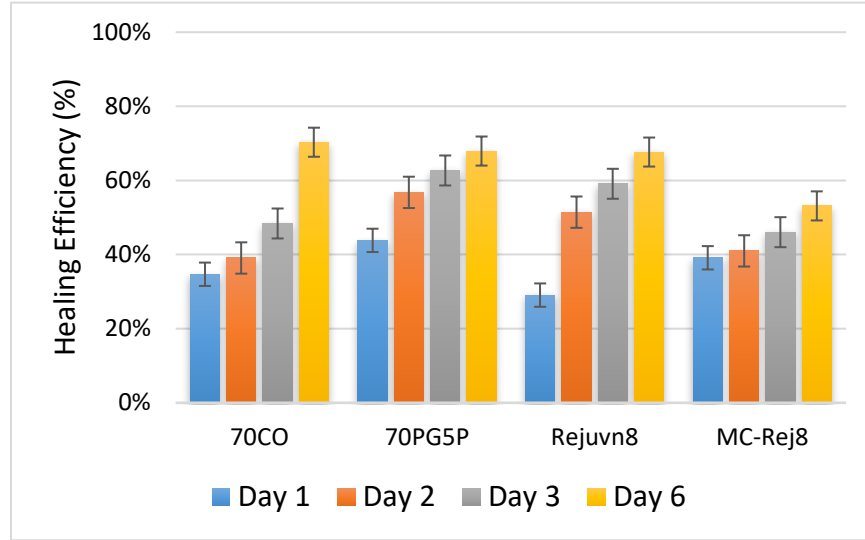
Figure 4.5. cont'd



(a)

Figure 0.6. Healing Efficiency at (a) Room-Temperature; and (b) High-Temperature

Figure 4.6. cont'd



(b)

When comparing both healing conditions, it is possible to observe that the control mixture (70CO) had the best healing performance with an average of 76% healing efficiency. The mixture containing 5% asphalt rejuvenator (Rejuvn8) showed a better performance at room-temperature (82.3% healing efficiency) than at high-temperature healing condition (67.7% healing efficiency). Similarly, the mixture containing 5% microcapsules showed a better performance at room-temperature (71.4% healing efficiency) than at high-temperature (53.1% healing efficiency). The mixture containing 5% RAS without rejuvenator also showed a better performance at room-temperature (77.1% healing efficiency) than at high-temperature (67.9% healing efficiency).

4.5.2.3 Statistical Analysis. A statistical analysis was conducted to determine whether the differences in healing efficiencies observed at both healing conditions were significant. This analysis focused on cracks larger than 0.4 mm in order to simulate real field conditions for both healing conditions. By performing an Analysis of Variance (ANOVA) for each healing

condition, the analysis assessed whether there was a statistical difference in the mixture performance at a confidence level of 0.05. Furthermore, the analysis included a t-test was at a confidence level of 0.05 on all the possible combinations (i.e., 70CO vs. 70PG5P or 70PG5Rej8 vs. MCrej8) to identify those mixes that were statistically different.

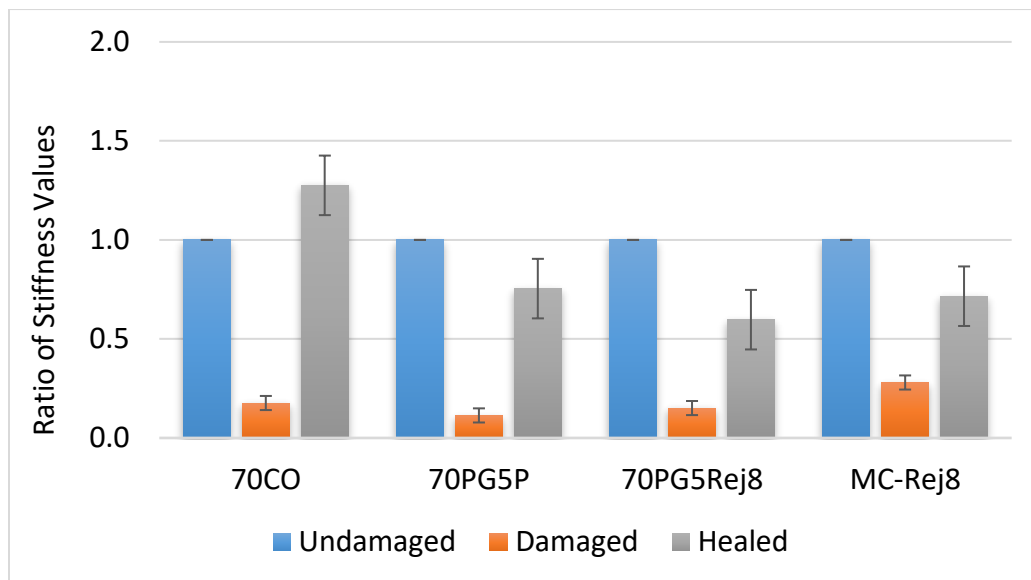
Table 4.5 shows the statistical ranking of the mixtures at the two healing conditions. The statistical results for each grouping are ranked by using letters A, B, C, and so forth. The letter A is assigned to the mix with the highest mean, followed by the letter B, and so forth. Double letters (e.g., A/B, B/C) indicate that the mixture can be categorized in both groups. Table 4.5 shows that the mixture with the highest healing efficiency at room temperature (70PG5Rej8) was not significantly different than the mixture with the lowest healing-efficiency (MCrej8). However, the statistical analysis shown that there was a difference between the mixture MCrej8 and the other mixtures for high-temperature healing condition.

Table 0.5. Statistical Analysis of Test Results

Mixture Type	Room-Temperature		High-Temperature	
	Mean	Rank	Mean	Rank
70CO	82.1%	A/B	70.3%	A
70PG5P	77.1%	B	67.9%	A
70PG5Rej8	82.3%	A	67.7%	A
MCrej8	71.4%	A/B	53.1%	B

4.5.2.4 Stiffness Recovery. Besides evaluating the healing efficiency of the mixtures, a comparison between the undamaged, damaged and healed stiffness was performed. Figure 4.7(a) shows the undamaged and healed stiffness ratios in reference to the undamaged stiffness for

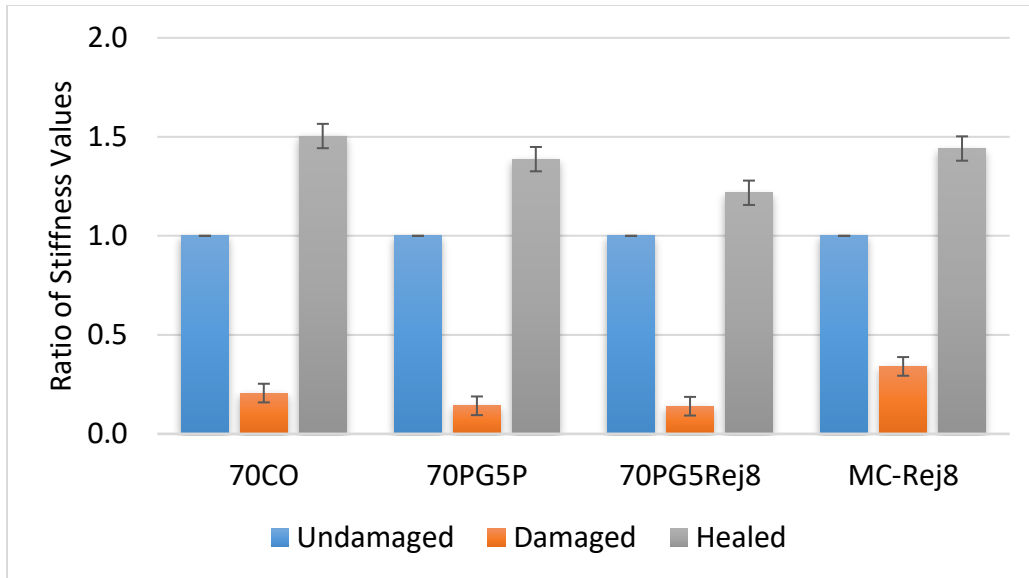
room-temperature healing condition. As shown in this figure, there was a recovery in the stiffness of the mixtures as the healed stiffness was greater than the damaged stiffness but less than the undamaged stiffness, an exception is with mixture 70CO where the healed stiffness was greater than the undamaged stiffness. A greater stiffness recovery was observed at high-temperature as shown in Figure 4.7(b). Figure 4.7(b) shows that the healed stiffness values from all mixtures were higher than the undamaged and damaged stiffness. This behavior could be explained by the aging process of the binder during the five-days conditioning period in the oven at a temperature of $50 \pm 2^\circ\text{C}$.



(a)

Figure 0.7. Stiffness Ratio Recovery at (a) Room-temperature; and at (b) High-Temperature

Figure 4.7. Cont'd



(b)

4.6 Summary and Conclusions

The objectives of this study were to characterize microcapsules containing an asphalt rejuvenator product as core material in order to test thermal and mixing stability and to evaluate self-healing efficiency of double-walled microcapsules through crack healing and stiffness recovery of damaged mixture specimens under two different healing conditions. Scanning electron microscopy was utilized to characterize the produced microcapsules and to evaluate thermal and mixing stability. Furthermore, an evaluation of self-healing efficiency was conducted using cracks induced through a strain-controlled three-point bending test at two healing conditions: room-temperature and high-temperature. Based on the results of the experimental program, the following conclusions may be drawn:

SEM images showed that the developed microcapsules maintained their shape and did not break due to the exposure to high temperatures. In addition, TGA results showed that there is a small reduction in the weight of the produced microcapsules at the temperature encountered during

mix production. SEM images also showed that the developed microcapsules did not break during mixing with the aggregates.

An analysis of light microscope images revealed a reduction in the size of the cracks at both healing conditions for a period that spanned from day 0 to day 6.

The healing efficiencies of the evaluated mixtures at room-temperatures reflected higher healing efficiency than at high-temperature for all mixtures. The lower healing efficiency of the specimens at high-temperature can be attributed to the aging process occurred in the binder due to the prolonged exposure to a high-temperature.

The mix with microcapsule (MCRej8) had a lower healing efficiency than the mix with no RAS or the one with the rejuvenator blended directly with the mix ingredients. This is because that not all microcapsules have broken during the test since microcapsules are expected to break over time and not all at once.

There was a recovery in the stiffness of the mixtures as the healed stiffness was greater than the damaged stiffness but less than the undamaged stiffness. A greater stiffness recovery was observed at high-temperature, which could be explained by the aging process during the five-days conditioning period.

Further laboratory evaluation of the prepared microcapsules is recommended. Furthermore, future research study should evaluate the self-healing efficiency of the developed microcapsules in a full-scale asphalt pavement subjected to real traffic and environmental loadings.

4.7 References

- [1] Construction Materials Recycling Association, "Economics of Shingle Recycling," 2013. [Online]. Available: <http://www.shinglerecycling.org/content/economics-shingle-recycling>. [Accessed 22 May 2016].
- [2] N. H. Tran, A. Taylor and R. Willis, "Effect of Rejuvenator on Performance Properties of HMA Mixtures with High RAP and RAS Contents," Auburn, ala, 2012.
- [3] R. Karlsson and U. Isacsson, "Material-related aspects of asphalt recycling-state of the art," J. Master. Civil Eng. , vol. 18, 2006.
- [4] J. Shen, S. Amirkhanian and J. A. Miller, "Effects of rejuvenating agents on superpave mixtures containing reclaimed asphalt pavement," J. Master Civil Eng., vol. 19, no. 5, 2007.
- [5] C. Chiu and M. Lee, "Effectiveness of seal rejuvenators for bituminous pavement surfaces," J. Test. Eval. , vol. 34, pp. 390-394, 2006.
- [6] A. Garcia, E. Schlangen, M. van de Ven and G. Sierra-Beltran, "Preparation of capsules containing rejuvenator for their use in asphalt concrete," J. Hazard. Mater. , vol. 184, pp. 603-611, 2010.
- [7] D. E. Watson, A. Johnson and H. R. Sharma, "Georgia's Experience with Recycled Roofing Shingles in Asphaltic concrete," In Transportation Research Record 1638, pp. 15-20, 1998.
- [8] G. W. Maupin Jr, "Investigation of the Use of Tear-Off Shingles in Asphalt concrete," Charlottesville, 2010.
- [9] J. Brownridge, "The Role of an Asphalt Rejuvenator in Pavement Preservation: Use and Need for Asphalt Rejuvenation," Bakersfield, California, 2010.
- [10] ASTM D4552/D4552M-10, "Standard Practice for Classifying Hot-Mix Recycling Agents," ASTM International, 2010.
- [11] G. Peterson, R. Davison, C. Glover and J. Bullin, "Effect of Composition on Asphalt Recycling Agent Performance," Transportation Research Record, 1994.
- [12] M. Samadzadeh, S. Hatami, M. Peikari and A. Ashrafi, "A Review on Self-Healing Coatings Based on Micro/Nanocapsules," Progress in Organic Coatings, vol. 68, no. 3, pp. 159-164, July 2010.

- [13] M. A. Aguirre, M. M. Hassan, S. Shirzad, W. H. Daly and L. N. Mohammad , "Micro-encapsulation of Asphalt Rejuvenators using Melamine-Formaldehyde," Construction and Building Materials, vol. 114, pp. 29-39, 1 July 2016.
- [14] S. Shirzad, M. M. Hassan, M. A. Aguirre, L. N. Mohammad and W. H. Daly, "Evaluation of sunflower Oil as a Rejuvenator and Its Microencapsulation as a Healing Agent," J. Mater. Civil. Eng., 2016.
- [15] E. N. Brown, M. R. Kessler, N. R. Sottos and S. R. White, "In situ poly (urea-formaldehyde) microencapsulation of dicyclopentadiene," microencapsulation 20, 2003.
- [16] G. Sun and Z. Zhang, "Mechanical Strength of Microcapsules Made of Different Wall Materials," 2002.

CHAPTER 5. EVALUATION OF HOLLOW-FIBERS ENCAPSULATING A REJUVENATOR IN ASPHALT BINDERS WITH RECYCLED ASPHALT SHINGLES

5.1 Introduction

Asphalt pavements are the most common road types in the United States extending for more than 2.6 million miles through the nation. In the last 40 years, researchers have investigated innovative methods to reduce the virgin asphalt binder content in hot mix asphalt (HMA) due to the rising cost of petroleum-based products. In addition, a reduction of virgin asphalt binder in asphalt pavements would promote more sustainable construction operations by reducing the negative environmental impacts from carbon emissions during the refinery processes. Utilizing recycled materials such as recycled asphalt shingles (RAS) in HMA has emerged as a promising approach to promote more sustainable road construction in the nation.

The use of 5% RAS per ton of HMA could result in savings between \$1.00-2.80/ton as reported in a previous study [1]. In addition, studies have shown that using RAS could decrease the negative environmental impacts related to the extraction, transportation, and processing of virgin materials [2]. In spite of these benefits, the aged binder is the main challenge with using RAS in asphalt pavements as the performance against fatigue and thermal cracking may be negatively impacted [3]. The use of rejuvenator products has been suggested as a potential solution to address the negative effects of utilizing RAS in HMA.

Asphalt rejuvenators have a high maltene content with the ability to recover the properties of the aged binder, and thus supporting the use of recycled materials [4, 5]. The effectiveness of a rejuvenating product is linked to the depth of penetration into the asphalt pavement layer, which has been shown to be about 20 mm [6]. Encapsulating a rejuvenating product has been suggested as a possible solution to uniformly dispersing the asphalt rejuvenator into a new asphalt mixture.

Self-healing concepts may be applied to an asphalt mixture by utilizing polymer fibers containing a rejuvenator. The proposed self-healing mechanism is promising, as it would allow an asphalt pavement to resist the initiation and propagation of cracks caused by vehicular and environmental loading. Furthermore, the restoration of aged binder properties may be achieved resulting in an enhancement in pavement performance. The development of polymer fibers containing a rejuvenator type product would promote the use of recycled materials by restoring the properties of the aged binder and improving the properties of HMA.

5.2 Objectives

The main objectives of this study were as follows: (1) Develop a synthesis procedure for the production of hollow-fibers containing a rejuvenator type product; (2) Identify the optimum production parameters that would enhance the thermal stability and the tensile strength of the developed fibers; and (3) Evaluate the rheological properties of asphalt binder blends with and without sodium-alginate fibers and with and without RAS extracted binder.

5.3 Background

5.3.1 Asphalt Rejuvenation

The asphaltene to maltene ratio is an asphalt binder's property that is affected by the aging and oxidation processes; the increase in this ratio negatively influences HMA performance against fatigue and thermal cracking [3, 7]. A promising solution to address the issues related to aging process is the use of a rejuvenating product. Asphalt rejuvenator products are used to restore the rheological properties of oxidized asphalt binder by diffusing into it and restore its colloidal structure and reconstitute its chemical components [8]. A rejuvenating product may also be used in a combination with a recycled material in order to increase the blending of aged and virgin binders and to enhance deformation capability; thereby, ultimately reducing the stiffness of the

aged binder. Previous studies have concluded that asphalt rejuvenators are the most effective treatment to restore the properties of an aged binder [9]. In addition, asphalt rejuvenator products are recommended to be added to the asphalt binder during asphalt mixture production and not be used as a seal coat to avoid negative effects such as reduction in friction on the pavement and poor rejuvenation efficiency [6].

5.3.2 Self-Healing Mechanisms in Asphalt Pavements

The encapsulation of asphalt rejuvenators has emerged as an innovative idea to address the poor penetration of rejuvenator products. The concept of encapsulating a rejuvenator product is to release the product when the microcapsule breaks at a predefined stress.

5.3.2.1 Microcapsules Containing Asphalt Rejuvenators. Aguirre et al. [10] developed single-walled microcapsules containing a rejuvenator type product using melamine-formaldehyde as a shell material. The rejuvenator was selected based on Performance Grade (PG) test results of asphalt binder blends, which showed a positive influence at both high- and low-grade temperatures of the asphalt binder. The authors also developed double-walled microcapsules containing sunflower oil as the rejuvenator using urea-formaldehyde/polyurethane as a shell material [11]. The study found that the addition of polyurethane improved the microcapsules stability at high-temperature and the ability to encapsulate liquids in the long-term. A study evaluated the healing efficiency of HMA containing microcapsules with a rejuvenator product by performing a three-point bending test under two healing conditions: room temperature and high-temperature [12]. An optical microscope was used to quantify the healing progress of cracked specimens as a function of time. The study reported a lower healing efficiency for the mixtures containing microcapsules compared to the control. Researchers concluded that a lower healing

efficiency of the mixtures containing microcapsules was observed as not all microcapsules broke during the test since they were designed to break over time and not all at once.

5.3.2.2 Hollow-Fibers with Asphalt Rejuvenators. Hollow fibers containing an asphalt rejuvenator can be used to address the poor penetration of rejuvenator products into the asphalt mixture. Studies have shown that the addition of fibers into HMA would avoid undesirable decrease in binder stiffness, which may result from the addition of sand-like particles such as microcapsules containing a rejuvenating product [13, 14]. In addition, chemical compounds such as melamine-formaldehyde (i.e., microcapsules shell materials) are an environmental threat when used in large quantities, which can be avoided in the production of fibers.

Alginate is a natural derived polysaccharide, which is extracted from brown sea algae. Utilizing alginate, as shell material in fibers, is promising as the materials provide properties such as (1) water-solubility, (2) fast coagulation in the presence of divalent ions; and (3) adequate mechanical properties [15]. Alginate has been investigated as a shell material for the production of hollow-fibers containing liquid filled vacuoles [16]. The study successfully synthesized sodium-alginate fibers containing o-dichlorobenzene (DCB) via wet-spinning process.

Furthermore, the results showed good thermal stability and high tensile strength of the developed fibers, which may offer the possibility to incorporate sodium-alginate fibers as self-healing products in asphalt pavement applications.

5.4 Experimental Program

5.4.1 Fiber's Synthesis and Properties

5.4.1.1 Chemicals. The core material of the fibers consisted of a green bio-oil product, from Sripath Technologies (density 0.919 g/cm^3). The experimental program used sodium alginate as a shell material in the developed fibers. In addition, PEMA (ethylene-alt-maleic-anhydride) was

added as a surfactant in a 2.5 wt % aqueous solution. Furthermore, ethylene glycol was incorporated in the present study as a plasticizer material. Lastly, the coagulation bath contained a 0.6 Molarity (M) solution of calcium chloride hexahydrate ($\text{CaCl}_2 \cdot 6\text{H}_2\text{O}$).

5.4.1.2 Production of Fibers. Mookhoek et al. presented a procedure to prepare hollow fibers containing o-dichlorobenzene (DCB) [16]. The hollow fibers were synthesized via wet-spinning process from an oil-in-water emulsion containing the shell material and the core material. Sodium alginate was selected as the shell material because it provides suitable properties such as water solubility, fast coagulation in the presence of divalent ions, and adequate mechanical properties [15].

For the production of the fibers, 5 g of sodium alginate was dissolved in 100 ml of de-ionized (DI) water using a high shear impeller at room temperature for 30 min. In addition, a 2.5 wt % polymeric surfactant solution, PEMA, was prepared by dissolving the copolymer in water at 70°C and mixing it for 60 min. The PEMA solution was allowed to cool down to room temperature. A healing solution of PEMA/rejuvenator was prepared by mixing different percentages of PEMA by weight of rejuvenator. PEMA was used to stabilize the healing solution. The healing solution was then mixed with the sodium alginate solution at different rejuvenator-to sodium alginate ratios at 40 rpm for 20 sec. Previous studies have identified that the size of the rejuvenator compartments can be controlled by modifying the stirring rate and stirring time of the final prepared solution [17]. The spinning of the fibers was conducted via a small-scale wet spinning pilot line. The pilot-size spinning line consisted of a motor controlled plunger-extruder and a motor controlled filament winder. A 100-ml syringe with an 18-gauge straight-cut needle was utilized to extrude the emulsion into the coagulation bath. The syringe was submerged into a coagulation bath containing a 0.6 M solution of calcium chloride

hexahydrate ($\text{CaCl}_2 \cdot 6\text{H}_2\text{O}$) in water at room temperature. The coagulated fiber was leaded out of the coagulation bath and it was coiled on a plastic bobbin under slight tension at a constant rate matching that of the extrusion (i.e., draw ratio = 1). Afterwards, the bobbin with the fibers was placed inside a fume-cabinet at room temperature with air convection to dry slowly over at least a period of 48 hours before further testing.

5.4.1.3 Fibers Characterization. The study employed a Scanning Electron Microscope (SEM-FEI Quanta 3D FEG Dual Beam SEM/FIB) to evaluate the morphology of the produced fibers.

Fibers were sprinkled on top of a double-sided tape attached to a pin stub specimen mount and sputter-coated with platinum for four minutes before imaging. The specimens were examined under a secondary electron mode at an accelerated voltage of 5 kV.

5.4.2 Optimization of Production Parameters for Fiber Synthesis

The objective of the optimization process was to evaluate the thermal stability and tensile strength of the fibers prepared according to Table 5.1 in order to assess their resistance to HMA production processes. Different fiber samples were prepared using different production parameters, which varied the percentage of emulsifier (i.e., PEMA), percentage of plasticizer (i.e., ethylene glycol), and the amount of rejuvenator used. The different percentages of emulsifier were expected to affect the stability of the solution between the rejuvenator product and the encapsulating material. Furthermore, the study assessed the effects of adding a plasticizer into the healing solution to study its influence on the thermal stability of the developed fibers. In addition, different ratios of rejuvenator to encapsulating material were evaluated in the experimental matrix to determine its effects on both thermal stability and tensile strength of the fibers. Table 5.1 summarizes the experimental test factorial for the optimization process.

Table 0.1. Test Matrix for Fiber's Optimization

Sample ID	Rejuvenator to Shell Material Ratio	Emulsifier Content (%)	Plasticizer Content (%)
Fiber1	1:1.5	30	-
Fiber2	1:1.5	40	-
Fiber3	1:1.5	50	-
Fiber4	1:1.5	30	10
Fiber5	1:1.5	30	20
Fiber6	1:1.5	30	30
Fiber7	1:1.5	30	40
Fiber8	2:1	30	10
Fiber9	2:1	30	40
Fiber 10	3:1	30	10
Fiber 11	3:1	30	40

5.4.2.1 Thermogravimetric Analysis (TGA). Adequate thermal stability is needed for the fibers to resist high-temperature during asphalt mixture production. Thermal stability was evaluated by performing a Thermogravimetric Analysis (TGA) with a rate of 10.00°C/min from room temperature (i.e., 25°C) to 600°C for the developed fibers to determine their high-temperature degradation rate.

5.4.2.2 Tensile Strength. Tensile strength was assessed to evaluate the fibers resistance to breakage during the mixing processes. Based on the literature, the fibers should have an Ultimate Tensile Strength (UTS) higher than 12 MPa to resist typical pressure during asphalt mixture production processes [18, 19]. The UTS of the developed fibers was tested in tension using a force testing system with a 50 N load cell. Based on a previous study, the selected crosshead speed was 5.0 mm/s [20]. Prior to testing, the developed fibers were aligned within a custom paper window with a window gauge length of 66 mm. Super glue was used to fix the fibers in the paper window to avoid any undesirable deformation outside of the window gauge. Furthermore, the paper window was clamped in the tensile machine using two fixed grips. Finally, the paper window was cut and without any preload in the fibers, the tensile test was performed in a constant rate.

5.4.3 Evaluation of the Rheological Properties of Asphalt Binder Blends with Fibers

The objective of this phase of the study was to assess the effects of adding sodium-alginate fibers on asphalt binder blends containing RAS. An unmodified and SBS-polymer modified asphalt binder classified as PG 64-22 and PG 70-22 were blended with 5% RAS, post-consumer waste shingles (PCWS), by weight of the binder and different contents of fibers as shown in Table 5.2.

5.4.3.1 Performance Grading (PG Grading). The asphalt binder from the recycled material (i.e., PCWS) was added to selected asphalt blends at 5% by total weight of asphalt binder and was extracted in accordance with AASHTO T 164 [21]. Afterward, the solution obtained from AASHTO T 164 —Method A [21] was distilled to a point where most of the solvent was removed and then carbon dioxide gas was introduced to remove all traces of trichloroethylene. This procedure was conducted in accordance with AASHTO R 59 [22]. The recovered asphalt binder was then blended with virgin binder at a 5% dosage rate. The asphalt binder blends

shown in Table 5.2 were prepared by mixing virgin binder with the produced fibers and extracted binder at a mixing temperature of 163°C. The different asphalt blends were prepared by using a Silverson high-shear blender at 3,600 rpm for 30 minutes at a mixing temperature of 163°C to achieve good mixing and dispersion of the fibers and extracted binder in the different asphalt binder blends.

The rheological properties of the different asphalt binder blends in Table 5.2 were characterized using fundamental rheological tests (i.e., dynamic shear rheometer and bending beam rheometer) and by comparing the PG of the modified blends to the unmodified asphalt binder (Blend1) and modified asphalt binder (Blend6) in accordance to AASHTO M 320 [23].

Table 0.2. Test-Matrix for Optimization of Content of Fibers in Asphalt Binder

Blend ID	Asphalt Binder	RAS Content	Fiber Content (%)
Blend1	PG 64-22	-	-
Blend2	PG 64-22	5% PCWS	-
Blend3	PG 64-22	5% PCWS	1%
Blend4	PG 64-22	5% PCWS	3%
Blend5	PG 64-22	5% PCWS	5%
Blend6	PG 70-22	-	-
Blend7	PG 70-22	5% PCWS	-
Blend8	PG 70-22	5% PCWS	1%
Blend9	PG 70-22	5% PCWS	3%
Blend10	PG 70-22	5% PCWS	5%

5.4.3.2 Multiple Stress Creep Recovery (MSCR). The rutting resistance of the asphalt blends was characterized by conducting the MSCR test. The MSCR tests consisted of applying creep and recovery periods to measure the percentage of recovery and non-recoverable creep compliance (J_{nr}). The MSCR was performed in accordance to AASHTO TP 70 [24] at a testing temperature of 67°C. The test consists of applying low stress (0.1 kPa) for 10 creep/recovery cycles with a subsequent stress increase to 3.2 kPa for 10 additional cycles.

5.4.3.3 Linear Amplitude Sweep (LAS). The fatigue resistance of the asphalt blends was characterized by conducting the LAS test. The LAS tests consisted of applying cyclic loading employing systematic, linearly increasing load amplitudes. The LAS was performed in accordance to AASHTO TP 101 [25] in samples aged using RTFO and PAV to simulate the aging for in-service asphalt pavements. LAS test was conducted to determine two fatigue parameters (“a” and “b”) based on the asphalt binder fatigue law ($N_f = a \times \gamma_{max}^b$). The LAS test consisted in two steps: (1) a frequency sweep test at a low strain amplitude of 0.1% is used to obtain undamaged material properties (parameter “b” of fatigue law); and (2) an amplitude sweep test with a series of cyclic loading at systematically linearly increasing strain amplitudes at a constant frequency of 10 Hz is used to determine the parameter “a” of the fatigue law through the viscoelastic continuum damage (VECD) mechanics analysis.

5.4.3.4 Complex Shear Modulus, $|G^*|$. Frequency sweeps were performed at temperatures ranging between 4.4°C to 54.4°C and frequencies between 0.1 to 100 radians/second to evaluate the complex shear modulus ($|G^*|$) of the prepared asphalt binder blends presented in Table 5.2. This dynamic test consists of applying a sinusoidal strain to the specimen and the resulting stress is measured as a function of frequency in the dynamic mechanical analysis. A previous study has

found that the dynamic mechanical properties are directly related to the creep properties of the asphalt binders [26].

5.4.4 Chemical Analysis of Asphalt Binder Blends with Fibers

5.4.4.1 Fourier Transform Infrared Spectroscopy (FTIR). A Bruker Alpha FT-IR spectrometer (alpha) was utilized to obtain the FTIR spectra for the evaluated binder blends. An OPUS 7.2 data collection programme was used for the data analysis. The following settings were used for data collection: 32 scans per sample, spectral resolution 4 cm^{-1} and a wave number range $4000\text{--}500\text{ cm}^{-1}$. Approximately 1% solution of mix samples was made in carbon disulphide (CS_2) solvent and filtered using a $0.2\text{ }\mu$ filter. A few drops of the solution were kept on the diamond crystal and allowed to evaporate the solvent. Spectrum was collected after the complete evaporation of the solvent. The effects of adding fibers in the blends was analyzed by estimating the carbonyl index suggested from previous studies [27]. Eq. (5.1) was used to determine the carbonyl index for the evaluated binder blends.

$$\text{Carbonyl Index (ICO)} = \frac{\text{Area around } 1700\text{ cm}^{-1}}{\text{Area around } 1460\text{ cm}^{-1} \text{ and Area around } 1375\text{ cm}^{-1}} \quad (5.1)$$

5.5 Results and Analysis

5.5.1 Sodium-Alginate Fibers with Rejuvenator

Sodium-alginate fibers containing a commercial bio-oil product as the core material were prepared. The first part of the study consisted of the optimization process of sodium-alginate fibers by varying the production parameters and determining the effects of each parameter on the thermal stability and tensile strength of the developed fibers. The following production parameters were varied: percentage of emulsifier (i.e. PEMA), percentage of plasticizer (i.e. Ethylene glycol), and amount of rejuvenators used.

5.5.1.1 Thermogravimetric Analysis (TGA). The thermal stability of the produced fibers was analyzed using TGA. The evaluated parameter in TGA was the percentage weight retained at 163°C. Table 5.3 summarizes the TGA analysis for the different sodium-alginate fibers. As shown in Table 5.3, sodium alginate fibers with no additives (Control) were prepared and tested, which retained 68.6% of the initial weight at elevated temperature (i.e., 163°C). The increase in the emulsifier content from 30 to 50% (i.e., Fiber 1, Fiber 2, and Fiber 3) had a negative impact on the percentage weight retained as Fiber 3 had a lower weight retained (i.e., 67.3%) compared to Fiber 1 and Fiber 2 (76.2% and 77.3%, respectively). It was also observed that the addition of Ethylene glycol as plasticizer at a dosage rate of 10% and 40% had a positive effect in the percentage weight retained (i.e., 82.1 and 81.5%, respectively) compared to adding the plasticizer material at a dosage rate of 20 and 30% (i.e., 77.1 and 76.9%, respectively). Increasing the rejuvenator to shell material ratio from 1:1.5 to 2:1 and 3:1 resulted in the highest percentage weight retained in Fiber 11 with 88.1% weight retained of the initial weight.

Table 0.3. Optimization Test Results of Sodium-Alginate Fibers

Sample ID	TGA Test Results		UTS Test Analysis					
			Peak Stress (MPa)		Failure Strain (%)		Stiffness (N/m)	
	Temperature (°C)	Weight Retained (%)	Mean	STDEV	Mean	STDEV	Mean	STDEV
Fiber 1	163	76.2	3.5	1.3	16.0%	11.5%	91.1	63.0
Fiber 2	163	77.3	1.3	0.3	8.4%	4.1%	22.6	7.3
Fiber 3	163	67.3	1.9	0.6	8.8%	4.6%	35.9	19.8
Fiber 4	163	82.1	11.4	6.1	24.1%	13.3%	457.9	434.7
Fiber 5	163	77.1	12.1	2.9	23.4%	14.0%	404.7	69.5

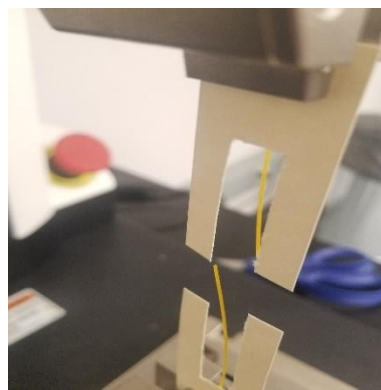
Table 5.3. Cont'd

Sample ID	Temperature (°C)	Weight Retained (%)	Mean	STDEV	Mean	STDEV	Mean	STDEV
Fiber 6	163	76.9	23.0	8.1	11.1%	10.8%	1844.3	847.6
Fiber 7	163	81.5	28.4	3.7	4.2%	1.5%	2456.4	240.0
Fiber 8	163	86.2	22.7	4.1	4.8%	1.9%	1914.2	275.2
Fiber 9	163	87.6	9.9	1.6	12.3%	4.1%	687.1	200.4
Fiber 10	163	87.5	7.3	0.9	21.9%	9.8%	516.2	75.7
Fiber 11	163	88.1	14.7	4.2	5.2%	3.0%	1165.1	433.5
Control	163	68.6	N/A					

5.5.1.2 Tensile Strength. Tensile strength was measured to evaluate the fibers resistance to breakage during the mixing process. The tensile test setup is shown in Figure 5.1(a). Figure 5.1(b) shows a broken sodium alginate fiber after a tensile test was performed.



(a)



(b)

Figure 0.1. (a) Tensile Test Setup for Sodium-Alginate Fibers and (b) Broken Sodium-Alginate Fiber

The results from the UTS test are presented in Table 5.3. Ten fibers from three different batches for each prepared fiber type were tested. As discussed earlier, a UTS higher than 12 MPa is desirable, as it has been reported to be the tensile strength needed to resist typical stresses during asphalt mix production processes [18, 19]. It is noted from the results presented in Table 5.3 that Fiber 6, Fiber 7, Fiber 8, and Fiber 11 successfully satisfied the 12 MPa UTS requirement at a range of Mean \pm STDEV. In addition, a relationship was noticed between UTS and ductility as higher UTS was measured at lower failure strain percentages as shown when comparing Fiber 4 vs. Fiber 7 (i.e., 24.1% and 4.2%, respectively). Furthermore, the stiffness of the fibers was calculated from the slope of the linear equation from the steepest part of the load-deformation curve. The stiffness analysis showed that there is relation between the UTS and stiffness as stiffness increased with the increase in UTS.

5.5.1.3 Optimum Preparation Procedure for Sodium-alginate Fibers Containing Rejuvenator.

Different rejuvenator to shell material ratios, emulsifier content percentages, and plasticizer content percentages were evaluated to select the optimum parameters to produce sodium-alginate fibers containing a rejuvenator product. Based on the aforementioned results, a rejuvenator to shell material ratio of 1:1.5, a 30% emulsifier content, and 40% plasticizer content were selected as the optimum production parameters for the fiber synthesis (i.e., Fibers 7), Table 5.1. These production parameters were selected based on the results from TGA and UTS. Figure 5.2(a) shows a SEM picture of the selected fibers. It is noticed in Figure 5.2(a) that the developed fibers had a rough morphology, which may improve the bonding of the fibers with the asphalt binder. In addition, the strain-hardening property of the developed fibers is shown in the load-deformation plot obtained from the UTS test in Figure 5.2(b). Lastly, the TGA results for Fibers 7 are shown in Figure 5.2(c).

5.5.2 Effects of Fibers on the Binder Rheological Properties

Ten asphalt binder blends were prepared and evaluated in this study to assess the effects of the addition of sodium-alginate fibers containing a rejuvenating product on the rheological properties of the binder blends as compared to the unmodified and SBS-polymer modified asphalt binders. In addition, an extracted binder from a recycled material (i.e., PCWS) was added at 5% by weight of the virgin binder as shown in Table 5.2. A Silverson mechanical stirrer was used at 3,600 rpm for 30 minutes and at a mixing temperature of 163°C to achieve good mixing and dispersion of the fibers and extracted binder in the asphalt binder blends. It is noted that the length of the fibers was less than 1 mm, which should not affect the rheological testing procedure for the prepared asphalt binder blends. Table 5.4 and Table 5.5 present the measured rheological properties of the asphalt binder blends based on laboratory testing conducted using a Dynamic Shear rheometer (DSR) and Bending Beam Rheometer (BBR).

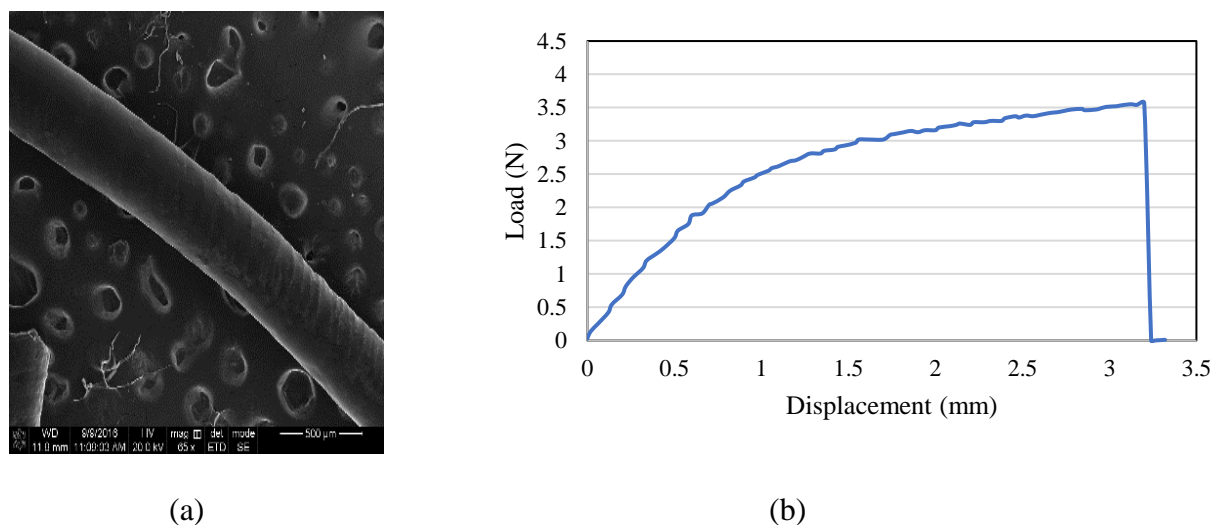
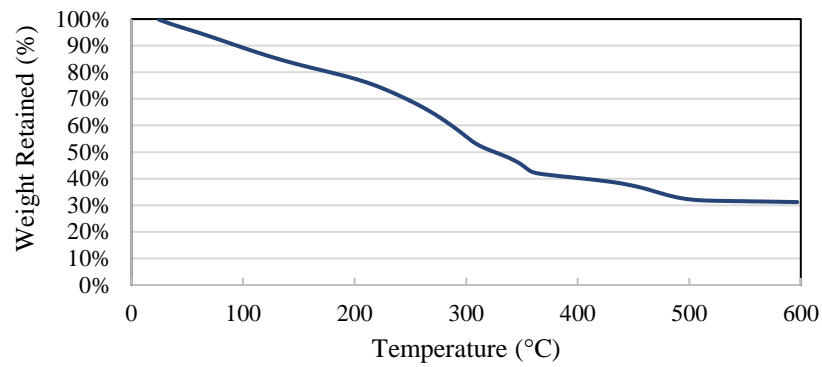


Figure 0.2. Fibers with Optimum Parameters (a) SEM Picture with 65x Magnification, (b) UTS Test Results, and (c) TGA Test Results

Figure 5.2. Cont'd



(c)

Table 0.4. Rheological Test Results of Asphalt Binder Blends Prepared with PG 64-22

Test	Specification	Temperature	Blend1	Blend2	Blend3	Blend4	Blend5
Test on Original Binder							
DSR ($G^*/\sin\delta$), 10 rad/s, AASHTO T315	>1.0 kPa	64 °C	1.92	2.73	2.68	2.42	2.19
DSR ($G^*/\sin\delta$), 10 rad/s, AASHTO T315	>1.0 kPa	70 °C	0.88	1.24	1.24	1.13	1.02
DSR ($G^*/\sin\delta$), 10 rad/s, AASHTO T315	>1.0 kPa	76 °C	-	0.61	0.62	0.56	0.509
Test on RTFO							
DSR ($G^*/\sin\delta$), 10 rad/s, AASHTO T315	>2.2 kPa	64 °C	3.75	-	-	-	-
DSR ($G^*/\sin\delta$), 10 rad/s, AASHTO T315	>2.2 kPa	70 °C	1.68	2.55	2.53	2.38	2.35
DSR ($G^*/\sin\delta$), 10 rad/s, AASHTO T315	>2.2 kPa	76 °C	-	1.2	1.19	1.14	1.12
Test on RTFO+PAV							
DSR ($G^*, \sin\delta$), 10 rad/s, AASHTO T315	<5000 kPa	25 °C	3920	4885	4110	4460	2405
DSR ($G^*, \sin\delta$), 10 rad/s, AASHTO T315	<5000 kPa	22 °C	5795	6925	5910	6465	3515
DSR ($G^*, \sin\delta$), 10 rad/s, AASHTO T315	<5000 kPa	19 °C	-	-	-	-	5015
BBR (Stiffness) AASHTO T313	<300 MPa	-12	197	189.5	196	196	151

Table 5.4. Cont'd

Test	Specification	Temperature	Blend1	Blend2	Blend3	Blend4	Blend5
BBR (Stiffness) AASHTO T313	<300 MPa	-18	351	360	414	356	281
BBR (m-value) AASHTO T313	>0.3	-12	0.312	0.302	0.3	0.3	0.306
BBR (m-value) AASHTO T313	>0.3	-18	0.268	0.264	0.263	0.274	0.28
PG- Grading	-----	-----	64-22	70-22	70-22	70-22	70-22
Continuous PG- Grading	-----	-----	68-23.6	71.8-22.3	71.4-22	70.9-22	70.3-23.4

Table 0.5. Rheological Test Results of Asphalt Binder Blends Prepared with PG 70-22

Test	Specification	Temperature	Blend6	Blend7	Blend8	Blend9	Blend10
Test on Original Binder							
DSR ($G^*/\sin\delta$), 10 rad/s, AASHTO T315	>1.0 kPa	70 °C	1.77	2.65	2.91	2.35	2.58
DSR ($G^*/\sin\delta$), 10 rad/s, AASHTO T315	>1.0 kPa	76 °C	0.97	1.44	1.56	1.29	1.42
Test on RTFO							
DSR ($G^*/\sin\delta$), 10 rad/s, AASHTO T315	>2.2 kPa	70 °C	3.23	4.39	4.43	3.59	4.48
DSR ($G^*/\sin\delta$), 10 rad/s, AASHTO T315	>2.2 kPa	76 °C	1.73	2.36	2.34	1.93	2.38
Test on RTFO+PAV							
DSR ($G^*.\sin\delta$), 10 rad/s, AASHTO T315	<5000 kPa	25 °C	3180	3030	3715	3320	2690
DSR ($G^*.\sin\delta$), 10 rad/s, AASHTO T315	<5000 kPa	22 °C	4660	4525	5340	4840	3900
DSR ($G^*.\sin\delta$), 10 rad/s, AASHTO T315	<5000 kPa	19 °C	6620	6505	-	6860	5550
BBR (Stiffness) AASHTO T313	<300 MPa	-12	178	161	180	156.5	145
BBR (Stiffness) AASHTO T313	<300 MPa	-18	317	323	384	328.5	281

Table 5.5. Cont'd

Test	Specification	Temperature	Blend6	Blend7	Blend8	Blend9	Blend10
BBR (m-value) AASHTO T313	>0.3	-12	0.336	0.330	0.309	0.329	0.314
BBR (m-value) AASHTO T313	>0.3	-18	0.290	0.275	0.26	0.272	0.273
PG- Grading	-----	-----	70-22	76-22	76-22	76-22	76-22
Continuous PG- Grading	-----	-----	74.7-26.7	78.2-25.3	80.6-23.1	78.6-25.1	79.7-25.1

5.5.2.1 High-Temperature Performance Grade. Results presented in Table 5.4 indicate that the addition of 5% PCWS caused stiffening of the virgin binder at high-temperature from PG 64-22 to PG 70-22 (i.e., Blend1 and Blend2, respectively). In addition, results in Table 5.4 indicate that the addition of fibers did not affect the high-temperature grade compared to Blend2. However, the continuous PG grading exhibited a decrease in the high-temperature performance grade (HTPG) with the addition of the fibers from 71.8°C for Blend2 to 70.3°C for Blend5. The reduction in the HTPG is possibly due to the release of some rejuvenator materials from the fibers while preparing the asphalt binder blends and during testing.

A similar increase in the high-temperature grade was observed with the addition of 5% PCWS between Blend6 and Blend7 as the PG grading increased from PG 70-22 to PG 76-22, respectively as shown in Table 5.5. However, it is shown that the addition of fibers did not decrease the HTPG of the binder blends prepared with PG 70-22 as it was observed for the blends prepared with PG 64-22.

Overall, the results presented in Table 5.4 and Table 5.5 indicate that the addition of fibers did not considerably affect the final temperature at both high and low temperature grades compared to the asphalt binders containing 5% PCWS extracted binder by weight of the total binder, (i.e., Blend2 and Blend7).

5.5.2.2 Rut Factor, $G^*/\sin\delta$. Results presented in Table 5.4 show an improvement in $G^*/\sin\delta$ for the unaged binder (PG 64-22) at 70°C with the addition of the fibers as $G^*/\sin\delta$ decreased from 1.24 kPa (i.e., Blend2) to 1.13 kPa (i.e., Blend4) and 1.02 kPa (i.e., Blend5). A similar trend was observed with the Rolling-Thin Film Oven (RTFO) samples where $G^*/\sin\delta$ at 70°C decreased from 2.55 kPa (i.e., Blend2) to 2.53 kPa (i.e., Blend3), 2.38 kPa (i.e., Blend4), and 2.35 kPa (i.e., Blend5). The decrease in $G^*/\sin\delta$ with the addition of the fibers indicates that the fibers are counteracting the negative effects of adding aged binder from the recycled shingles.

Similarly, results presented in Table 5.5 show a decrease in $G^*/\sin\delta$ for the unaged binder (PG 70-22) at 70°C with the addition of the fibers as $G^*/\sin\delta$ decreased from 1.56 kPa (i.e., Blend7) to 1.29 kPa (i.e., Blend9). However, the addition of 5% fibers in Blend10 resulted in an increase in $G^*/\sin\delta$ compared to Blend9 from 1.29 kPa to 1.42 kPa. A similar trend was observed for the short-term aged binder where $G^*/\sin\delta$ at 70°C decreased from 4.39 kPa (i.e., Blend7) to 3.59 kPa (i.e., Blend9), but the addition of 5% fibers resulted in an increase in $G^*/\sin\delta$ to 4.48 kPa (i.e., Blend10).

5.5.2.3 Fatigue Factor, $G^*\sin\delta$. The softening effect due to the addition of fibers was also observed in the fatigue factor ($G^*\sin\delta$ at 25°C) for the long-term aged asphalt binder blends as it decreased from 4,885 kPa (i.e., Blend2) to 2,405 kPa (i.e., Blend5) as shown in Table 5.4. The addition of 5% fibers in the asphalt binder blends prepared with PG 64-22 resulted in the lowest fatigue factor at 25°C (i.e., 2,405 kPa) suggesting a decrease in the fatigue cracking susceptibility of the virgin binder (PG 64-22).

A similar trend was observed in Table 5.5 where the fatigue factor ($G^*\sin\delta$ at 25°C) for the long-term aged asphalt binder blends prepared with PG 70-22 decreased from 3,030 kPa (i.e., Blend7) to 2,690 kPa (i.e., Blend10). In addition, a lower fatigue factor was observed for the asphalt

binder blend with 5% fibers (i.e., Blend10) as compared to the virgin binder PG 70-22 (i.e., Blend6) suggesting a more resistance asphalt binder against fatigue cracking.

5.5.2.4 Low-Temperature Performance Grade. The addition of 5% of fibers by weight of virgin binder (i.e., Blend5) resulted in an improved performance in the BBR test at -18°C where the stiffness decreased from 351 MPa (i.e., Blend1) to 281MPa and the m-value increased from 0.264 (i.e., Blend1) to 0.280 as shown in Table 5.4. Furthermore, the addition of 5% fibers in Blend5 improved the low-temperature grade compared to Blend2 decreasing it from -22.3°C to -23.4°C , which was close to the low-temperature grade for the control asphalt blend for PG 64-22 (i.e., -23.6°C).

Table 5.5 shows a similar trend for the asphalt binder blends prepared with PG 70-22 where the addition of 5% of fibers decreased the stiffness at -18°C from 317 MPa (i.e., Blend6) to 281 MPa (i.e., Blend10). However, the m-value of Blend10 (i.e., 0.273) did not improve compared to the virgin binder PG 70-22 (i.e., 0.290) at -18°C in the BBR test. The addition of the fibers did also not improve the continuous low-temperature grade of the binder blends prepared with PG 70-22 in contrast to the improvement observed in the binder blends prepared with PG 64-22.

5.5.2.5 Multiple Stress Creep Recovery (MSCR). Table 5.6 indicates that the addition of 5% extracted binder from RAS positively improved the rutting resistance of the asphalt binder blend, Blend2, compared to Blend1 as the non-recoverable creep compliance (J_{nr}) decreased from 3.47 kPa^{-1} to 2.32 kPa^{-1} at a stress level of 0.1 kPa and from 3.77 kPa^{-1} to 2.6 kPa^{-1} at a stress level of 3.2 kPa. A similar reduction in the J_{nr} values was observed with the asphalt binder blend prepared with 1% fibers, Blend3. The addition of 3 and 5% fibers reduced the rutting resistance of the asphalt binder blends as the J_{nr} values for both 0.1 kPa and 3.2 kPa stress levels increased compared to the Blend2; however, both blends (i.e., Blend4 and Blend5) had better rutting

resistance compared to the virgin binder PG 64-22 (i.e., Blend1) based on the J_{nr} values. It was also noticed that the addition of 5% fibers increased the elasticity of the binder as the percentage of recovery at a stress level of 0.1 kPa was the greatest (i.e., 4.99%) compared to the other asphalt binder blends presented in Table 5.6.

The improved rutting resistance with the addition of extracted binder from RAS was also observed in the asphalt binder blends prepared with PG 70-22 where the J_{nr} decreased from 0.803 kPa^{-1} to 0.636 kPa^{-1} at a stress level of 0.1 kPa and from 1.195 kPa^{-1} to 0.899 kPa^{-1} at a stress level of 3.2 kPa as shown in Table 5.7 for Blend6 and Blend7. An improvement against permanent deformation was observed with the addition of 5% fibers as the J_{nr} decreased at both stress levels compared to the virgin binder PG 70-22 as shown in Table 5.7. The addition of 5% fibers in Blend10 also resulted in the highest percentage of recovery at both 0.1 Pa and 3.2 kPa stress levels with 59.5% and 48.8% compared to the remaining asphalt binder blends shown in Table 5.7. The increase in percentage of recovery in Blend10 suggests an asphalt binder blend with a better performance against permanent deformation.

Table 0.6. MSCR Test Results of Asphalt Binder Blends Prepared with PG 64-22

Blend ID	MSCR				
	$J_{nr0.1}$ @ 67 °C, kPa^{-1}	$J_{nr3.2}$ @ 67 °C, kPa^{-1}	% J_{nr} diff	% Recovery	
				Stress, 0.1 kPa	Stress, 3.2 kPa
Blend1	3.47	3.77	8.65	1.62	-0.50
Blend2	2.32	2.60	12.31	4.86	0.58

Table 5.6. Cont'd

Blend ID	$J_{nr0.1}$ @ 67 °C, kPa ⁻¹	$J_{nr3.2}$ @ 67 °C, kPa ⁻¹	% J_{nr} diff	Stress, 0.1 kPa	Stress, 3.2 kPa
Blend3	2.34	2.62	11.98	4.82	0.56
Blend4	2.59	2.93	12.35	4.00	0.28
Blend5	2.54	2.89	13.90	4.99	0.42

Table 0.7. MSCR Test Results of Asphalt Binder Blends Prepared with PG 70-22

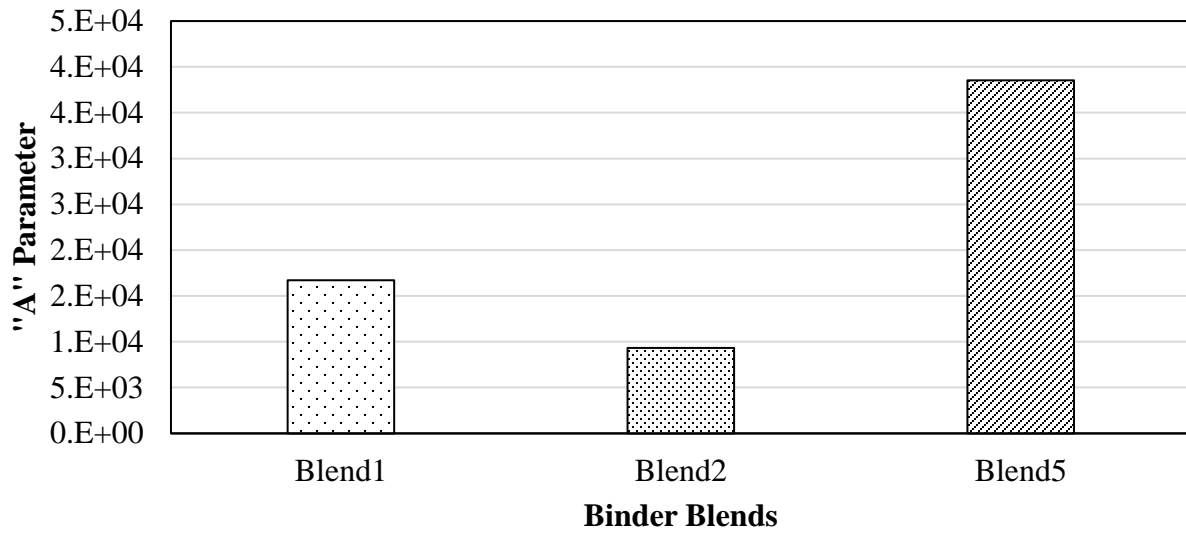
Blend ID	MSCR				
	$J_{nr0.1}$ @ 67 °C, kPa ⁻¹	$J_{nr3.2}$ @ 67 °C, kPa ⁻¹	% J_{nr} diff	% Recovery	
				Stress, 0.1 kPa	Stress, 3.2 kPa
Blend6	0.803	1.195	48.82	49.10	30.17
Blend7	0.636	0.899	41.52	45.47	28.36
Blend8	0.667	0.901	35.08	40.85	25.12
Blend9	0.736	1.035	41.06	42.28	24.86
Blend10	0.662	0.952	43.69	59.54	48.75

5.5.2.6 Linear Amplitude Sweep (LAS). Figure 5.3 shows the A parameter of the fatigue law of the evaluated binder blends. The A parameter is related to the storage modulus of the binder blends, which indicates the ability of the binder to keep its integrity during loading cycles and due to accumulated damage. Figure 5.3(a) shows that the addition of RAS to virgin binder PG 64-22 resulted in a decreased in the A parameter which indicates a decrease in the ability of the binder to resist damage. However, it can be observed in Figure 5.3(a) that the addition of

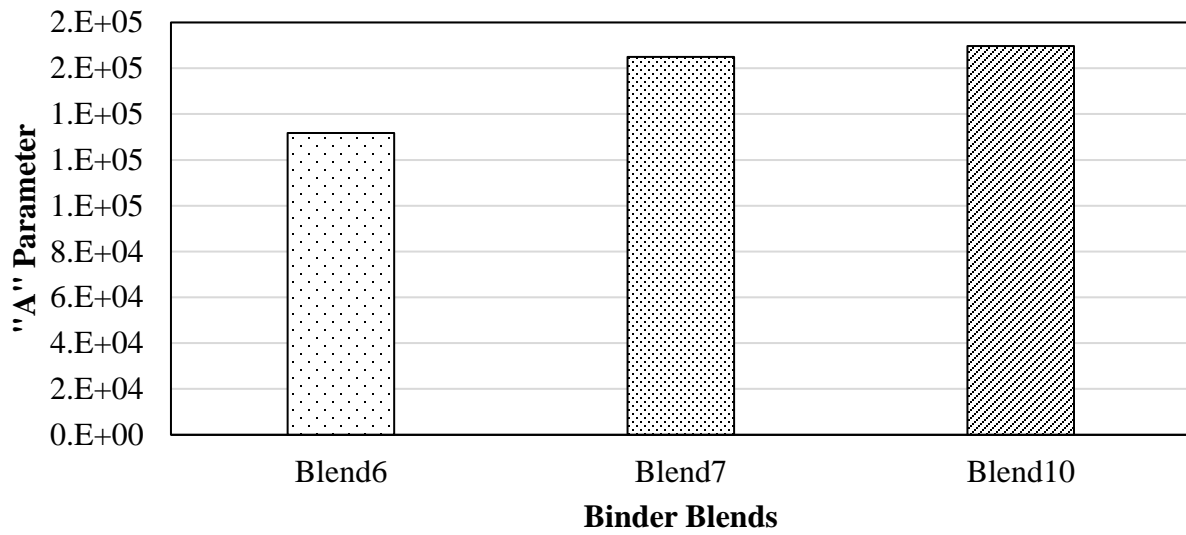
sodium-alginate fibers enhanced the ability of Blend5 to resist damage as an increased in the A parameter was observed. Figure 5.3(b) shows that the addition of RAS in virgin binder PG 70-22 did not have a negative effect in the ability of the blend to resist damage as an increased in the A parameter was observed compared to Blend6.

Figure 5.4 shows the B parameter of the fatigue law of the evaluated binder blends. The B parameter is related to the sensitivity of the binder to the change in strain level. Figure 5.4(a) shows that the evaluated binder blends prepared with binder PG 64-22 have a similar B parameter, which indicates that the addition of RAS and fibers did not have any effect in the rate of deterioration of the virgin binder as strain levels increases. A similar behavior is observed in Figure 5.4(b) for the binder blends prepare with binder PG 70-22. However, it is possible to observe in Figure 5.4 that the addition of SBS polymer in binder PG 70-22 resulted in a decrease in the absolute value of B parameter, which indicates that binder PG 70-22 would have a lower deterioration rate than binder PG 64-22.

Figure 5.5 shows the number of cycles to failure (N_f) at 2.5% and 5% strain levels of the evaluated binder blends. Figure 5.5(a) shows a decrease in the number of cycles to failure at both strain levels with the addition of RAS in Blend2 compared to virgin binder PG 64-22. However, it is shown in Figure 5.5(a) that the addition of fibers resulted in an enhancement in the fatigue resistance of Blend5 as the N_f increased for both strain levels compared to Blend1 and Blend2. Figure 5.5(b) shows that the addition of RAS and fibers did not have any effect in the N_f of blends prepared with binder PG 70-22. The presence of SBS polymer in binder PG 70-22 could have neglected the negative effect of adding RAS in the fatigue resistance of Blend7 and Blend10.

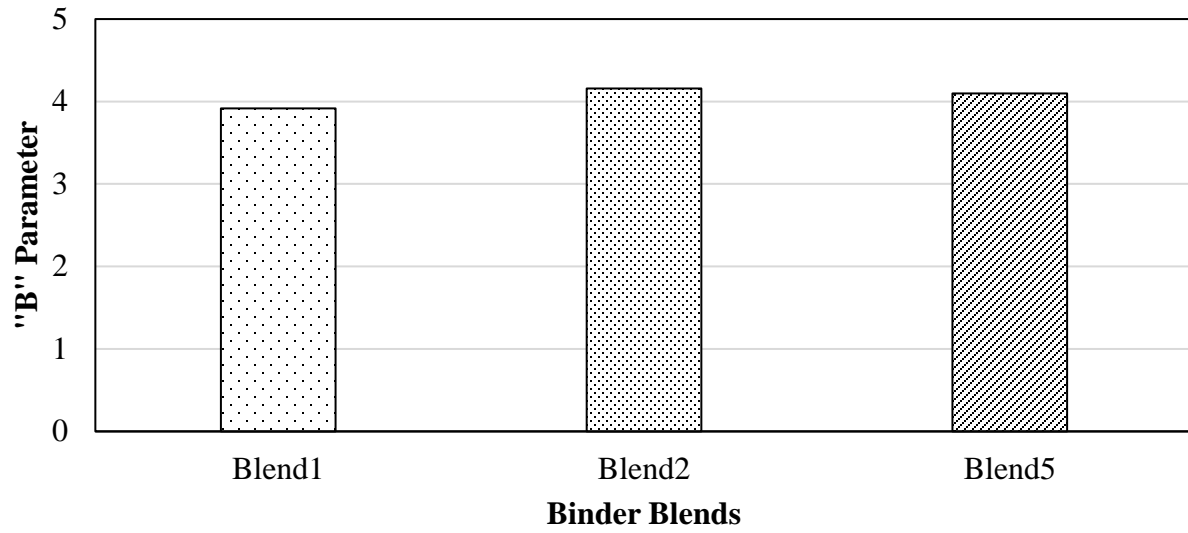


(a)

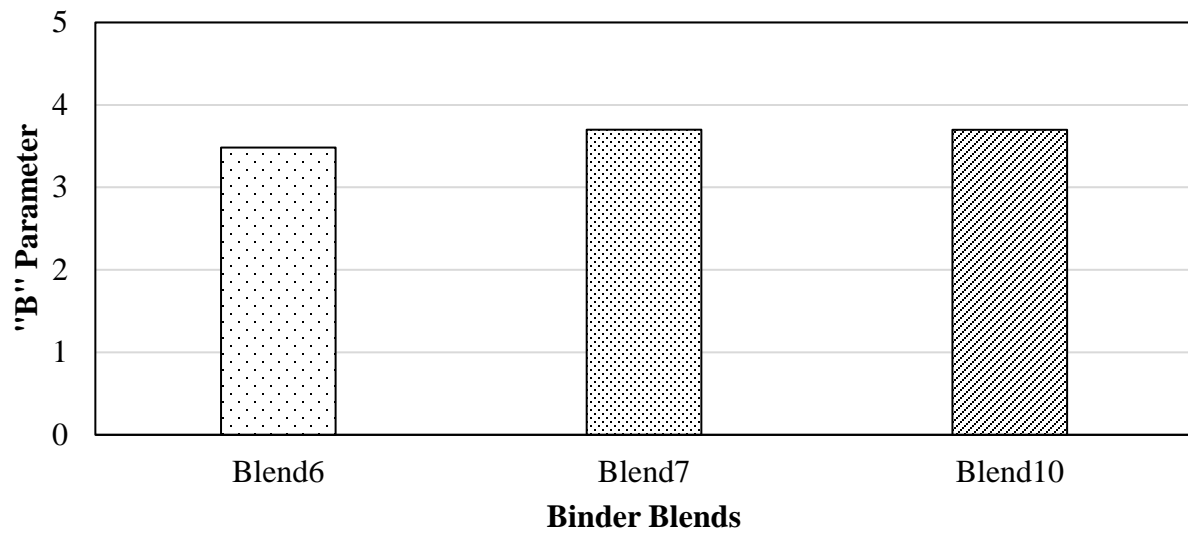


(b)

Figure 0.3. "A" Parameter of Fatigue Law: (a) Asphalt Blends Prepared with PG 64-22, and (b) Asphalt Blends Prepared with PG 70-22

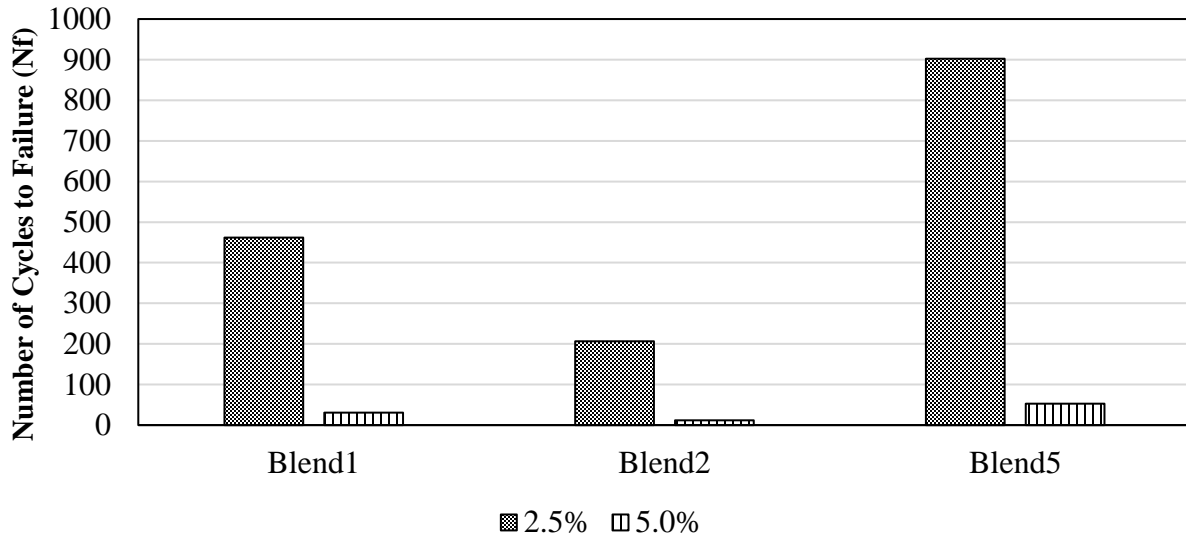


(a)

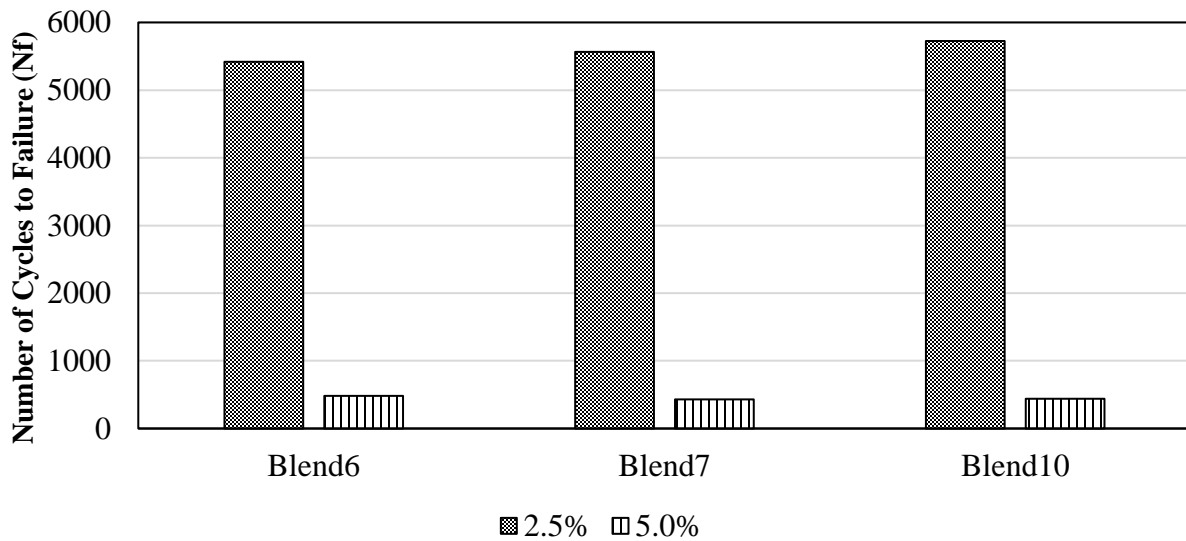


(b)

Figure 0.4. Absolute "B" Parameter of Fatigue Law: (a) Asphalt Blends Prepared with PG 64-22, and (b) Asphalt Blends Prepared with PG 70-22



(a)



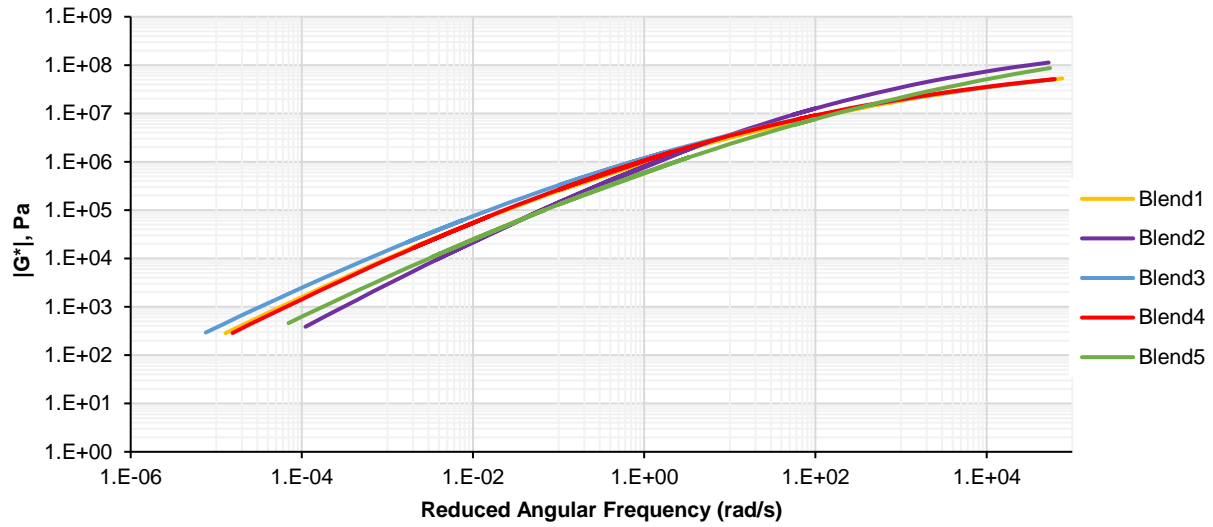
(b)

Figure 0.5. Number of Cycles to Failure (Nf): (a) Asphalt Blends Prepared with PG 64-22, and (b) Asphalt Blends Prepared with PG 70-22

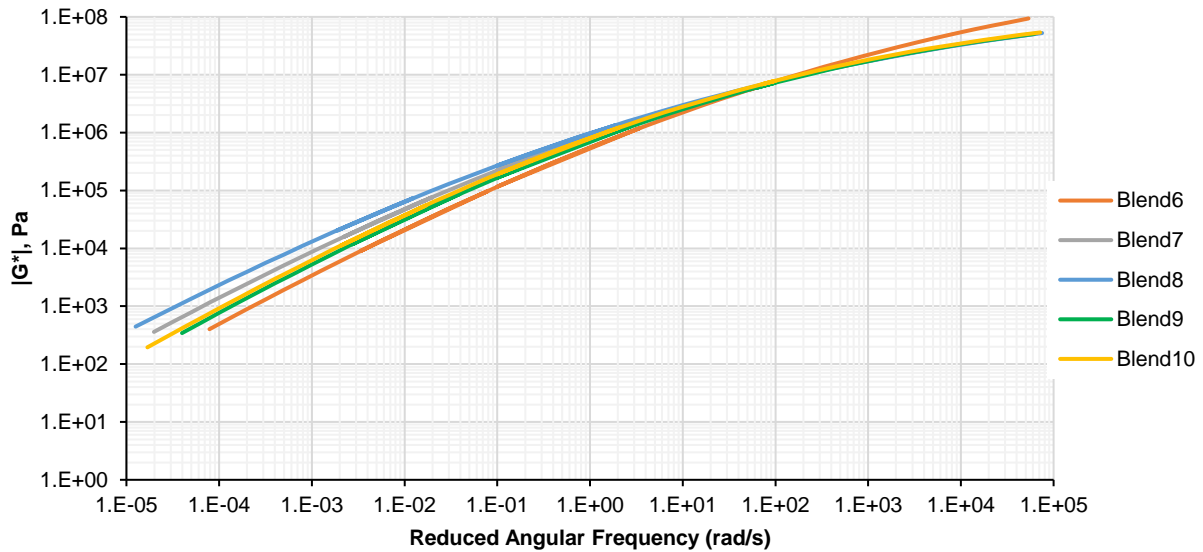
5.5.2.7 Complex Shear Modulus, $|G^*|$. The purpose of the complex shear modulus $|G^*|$ is to evaluate the visco-elastic response characteristics of the evaluated binder blends over a given range of temperatures and frequencies. Figure 5.6 presents the complex shear modulus $|G^*|$ at 4

test temperatures (5.4, 25, 37.8, and 54.4 °C) and 16 frequencies (0.02, 0.03, 0.04, 0.06, 0.10, 0.16, 0.25, 0.40, 0.63, 1, 1.59, 2.52, 4, 6.34, 10, and 15.90 Hz) for binder blends prepared with binder PG 64-22 and PG 70-22. The reference temperature was 25 °C. Figure 5.6(a) shows the complex shear modulus ($|G^*|$) for the asphalt binder blends prepared with PG 64-22. Results indicate that Blend2 would be the asphalt binder blend that is the most susceptible to low-temperature cracking as it had the highest $|G^*|$ values at high frequencies. The addition of 1% and 3% of fibers showed a reduction in $|G^*|$ values at high frequencies compared to Blend2, which suggests a better performance at low-temperatures. The addition of 5% fibers in Blend5 resulted in the asphalt binder blend with the lowest $|G^*|$ values at intermediate temperature suggesting a reduction in fatigue cracking susceptibility. Furthermore, Figure 5.6(a) suggests that the addition of 1% fibers in Blend3 would provide a better rutting performance as it had the highest $|G^*|$ values at low frequencies compared to the other asphalt binder blends prepared with PG 64-22.

Figure 5.6(b) suggests that Blend6 would be the binder blend that is the most susceptible to low-temperature cracking as it had the highest $|G^*|$ values at high frequencies compared to the rest of blends prepared with PG 70-22. However, it was observed that the addition of fibers and RAS resulted in lower $|G^*|$ values at high frequencies suggesting a better performance at low-temperature than Blend6. Furthermore, it is shown in Figure 5.6(b) that the addition of 3% fibers reduced the negative effect of adding extracted binder from RAS as the $|G^*|$ values at intermediate temperature from Blend9 were lower than for Blend7. In addition, it is shown that the addition of 1% fibers in Blend8 resulted in the highest $|G^*|$ values at low frequencies similar to Figure 5.6(a), which implies a better rutting performance as compared to the other asphalt binder blends.



(a)



(b)

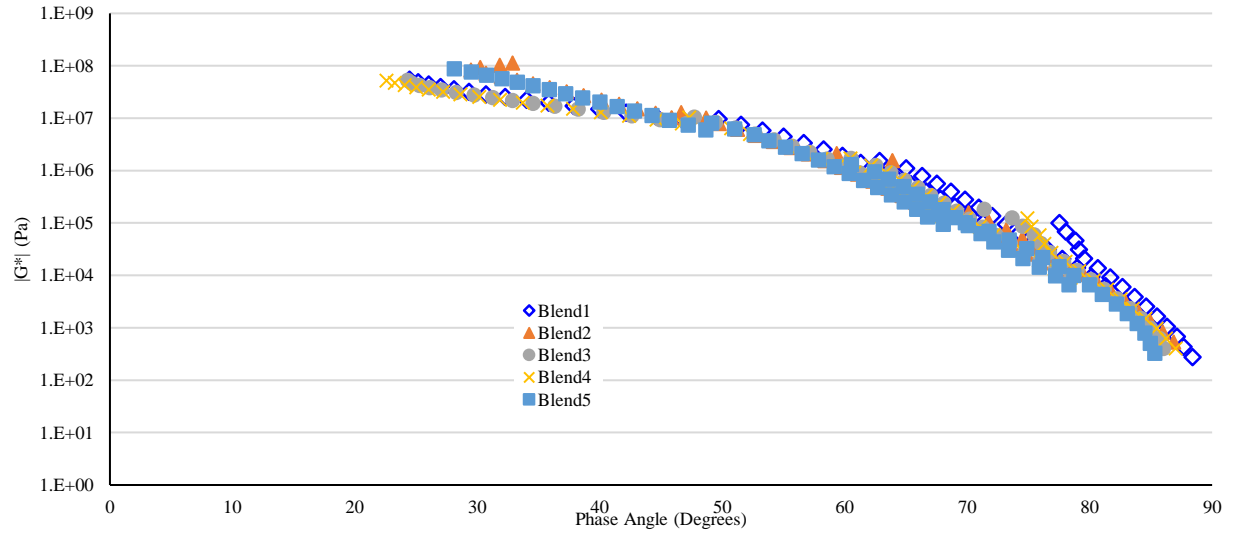
Figure 0.6. Complex Shear Modulus ($|G^*|$) (a) Asphalt Blends Prepared with PG 64-22, and (b) Asphalt Blends Prepared with PG 70-22

Figure 5.7 shows the black diagrams for the evaluated binder blends. Black diagrams shows the relationship between the complex modulus $|G^*|$ and the phase angle containing no reference to

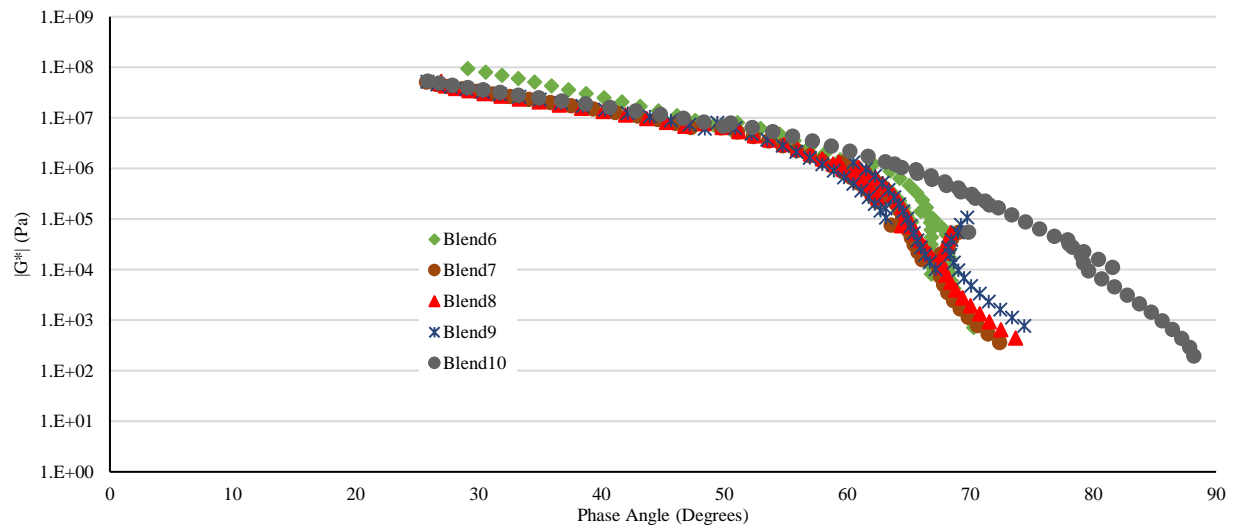
temperature or frequency. Figure 5.7(a) shows that the black diagrams for binder blends prepared with binder PG 64-22 have a similar behavior except for Blend2 and Blend 5 at low phase angles values. An increased in $|G^*|$ values at lower phase angles are observed for Blend2 and Blend5, which could explain the higher $|G^*|$ values observed for these blends in Figure 5.6(a) at high-frequencies levels. The black diagrams for binder blends prepared with binder PG 70-22 are shown in Figure 5.7(b). Figure 5.7(b) shows that the addition of 5% fiber resulted in a change in the behavior compared to the other evaluated binders. The modification is pronounced at high phase angles when Blend10 starts to have a viscous behavior. Also, the change of shape in the black diagram for Blend10 may be due a chemical reaction between the SBS polymer in the binder PG 70-22 and the shell material of the developed fibers.

5.5.2.8 Optimum Content of Sodium-Alginate Fibers Containing Rejuvenator. Different sodium-alginate fibers percentages were tested to select the optimum amount of fibers that would enhance the properties of the binder and reduce the negative effects of adding recycled materials (e.g., brittleness of aged binder). Based on the test results, a 5% content by weight of the binder was identified as the optimum fiber content. Blend10 showed an improvement in the rutting performance as the addition of 5% fibers increased the rut factor compared to the virgin binder (PG 70-22) indicating less susceptibility to permanent deformation. In addition, the improvement in rutting performance was observed in MSCR tests results where the addition of 5% fibers in Blend5 and Blend10 decreased the J_{nr} values at both stress levels compared to Blend1 and Blend6. Furthermore, performance improvement is expected at intermediate temperature for Blend5 and Blend10 compared to the virgin binders (PG 64-22 and PG 70-22) as the addition of 5% fibers resulted in a lower fatigue factor based on DSR test results. Lastly, the low-temperature performance of Blend5 and Blend10 was improved with the addition of 5% fibers as

a reduction in the stiffness was observed at -12°C and -18°C compared to the virgin binders (PG 64-22 and PG 70-22).



(a)



(b)

Figure 0.7. Black Diagrams (a) Asphalt Blends Prepared with PG 64-22, and (b) Asphalt Blends Prepared with PG 70-22

5.5.3 Chemical Composition of Binder Blends with Fibers

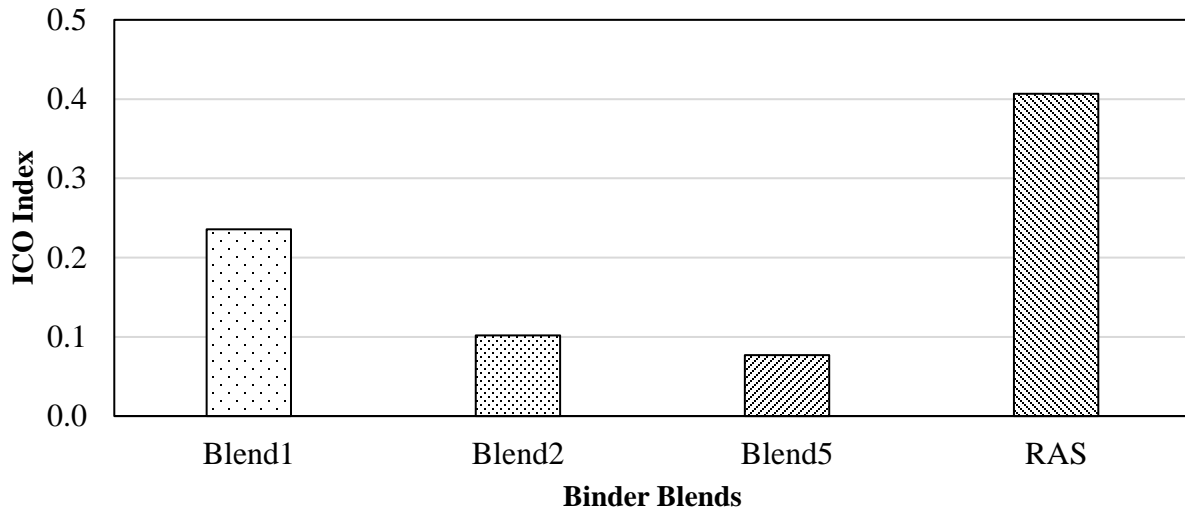
A FTIR test was performed in the binder blends containing 5% sodium-alginate fibers. The 5% fiber content was selected based on the improvement against permanent deformation, the decreased in the fatigue factor, and the reduction in stiffness at low-temperature observed in the binder tests results.

5.5.3.1 Characterization of Oxidative Asphalt Aging. A FTIR spectrum was obtained from the evaluated binder blends to evaluate the formation of carbonyl molecules, which is related to the oxidation process in the aging process of asphalt binders. The Carbonyl Index (ICO) was calculated using eq. (5.1) to determine the effect of adding extracted binder from RAS and the addition of fibers in virgin binders. The ICO for the evaluated binder blends are shown in Figure 5.8.

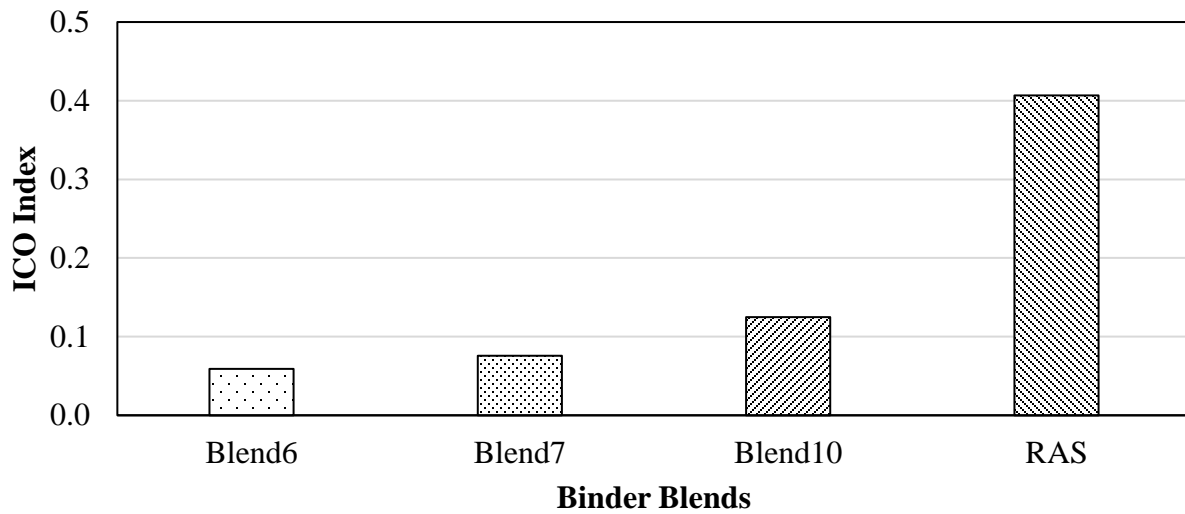
Figure 5.8(a) suggests that that the addition of RAS in Blend2 resulted in an increased in the ICO compared to the virgin binder PG 64-22. The higher ICO index explained the increased in the HTPG observed in the PG grading results with the addition of 5% RAS. However, it is shown in Figure 5.8(a) that the addition of 5% fibers resulted in a decreased in the ICO index compared to Blend2. The softening effect observed in Blend5 could be explained by the release of the rejuvenator product during the blending preparation which resulted in the reduction in the ICO index and in the HTPG.

Figure 5.8(b) shows the ICO index for the evaluated binder blends prepared with binder PG 70-22. Similarly, as observed in bends with binder PG 64-22, the addition of RAS resulted in an increased in the ICO index in Blend7. Therefore, the addition of RAS resulted in an increased in the aging susceptibility of the blend due the addition of oxidized binder which explained the increased in the HTPG observed in the PG grading results. Also, it is seen in Figure 5.8(b) that

the addition of developed fibers did not decreased the ICO index as observed with binder PG 64-22. It was possible fibers did not break during the blending process, which may explain the reduction in the softening effect in Blend10.



(a)



(b)

Figure 0.8. Carbonyl Index (ICO) (a) Asphalt Blends Prepared with PG 64-22, and (b) Asphalt Blends Prepared with PG 70-22

5.6 Summary and Conclusions

The objectives of this study were to develop a synthesis procedure for the production of hollow-fibers containing a rejuvenator product; identify the optimum production parameters that would enhance the thermal stability and the tensile strength of the fibers; and to evaluate the rheological properties of the asphalt binder blends containing PCWS and sodium alginate fibers. The optimization procedure was conducted by performing UTS and TGA tests on fibers with different production parameters. Furthermore, an evaluation of the effect of the fibers on the rheological properties of asphalt binder was conducted by performing PG grading, MSCR test, LAS test and frequency sweep test. Lastly, chemical analyses were conducted to evaluate the effect of RAS and fibers in the chemical composition of the binder blends. Based on the results of the experimental program, the following conclusions may be drawn:

The fibers prepared with a rejuvenator to shell material of 1:1.5, an emulsifier content of 30%, and a plasticizer content of 40% were selected as the optimum fibers as the TGA test results showed a good thermal stability at the mixing temperature (i.e., 163°C) with a weight retained percentage of 81.5%. In addition, these fibers had sufficient tensile strength (28.4 MPa) to resist the mixing and compaction processes of a HMA mixture.

PG grading results showed an improvement at both high and low temperature performance with the addition of fibers compared to the asphalt binder blends with PCWS and no fibers. In addition, the BBR test results showed a reduction in the stiffness of the blends with fibers compared to the virgin binders (i.e., PG 64-22 and PG 70-22).

The addition of sodium-alginate fibers resulted in an enhancement in the fatigue performance in binder blends prepared with PG 64-22 as an increased in the number of cycles to failure (N_f) was

observed. Binder blends prepared with PG 70-22 did not have any positive nor negative effect with the addition of RAS and developed fibers.

An improvement in the viscoelastic behavior of asphalt blends with fibers was also observed in the MSCR test results with an increase in the percentage of recovery.

An enhancement in dynamic shear moduli was observed at both high and low frequencies with the addition of fibers.

A decrease in the ICO index was observed with the addition of fibers in binder PG 64-22, which could be explained with the rejuvenating efficiency of the core material of the fibers. However, an increased in the ICO index was observed in blends prepared with binder PG 70-22.

Future studies will evaluate the effects of hollow-fibers with rejuvenator on laboratory asphalt mixture performance. The effect in the volumetric and compaction requirements in asphalt mixtures containing the fibers will be evaluated in future studies. The mechanical properties of asphalt mixtures containing sodium-alginate fibers will be evaluated to assess the performance against common distresses such as rutting, fatigue cracking and low-temperature cracking. In addition, a self-healing experiment must be performed to evaluate the healing ability and strength recovery ability of the developed fibers in asphalt mixtures. A benefit-cost analysis should also be conducted for hollow fibers with rejuvenator.

5.7 References

- [1] Construction Materials Recycling Association, "Economics of Shingle Recycling," 2013. [Online]. Available: <http://www.shinglerecycling.org/content/economics-shingle-recycling>. [Accessed 22 May 2016].
- [2] N. H. Tran, A. Taylor and R. Willis, "Effect of Rejuvenator on Performance Properties of HMA Mixtures with High RAP and RAS Contents," Auburn, ala, 2012.
- [3] E. Yaghoubi, M. R. Ahadi, M. Alijanpour and H. Jahanian Pahlevanloo, "Evaluating the Performance of Hot Mix Asphalt with Reclaimed Asphalt Pavement and Heavy Vacuum

- Slops as Rejuvenator," International Journal of Transportation Engineering, vol. 1, no. 2, 2013.
- [4] J. C. Petersen, "A review of the fundamentals of asphalt oxidation: chemical, physicochemical, physical property, and durability relationships.," Transportation Research Circular E-C140, 2009.
- [5] J. Shen, S. Amirkhanian and J. A. Miller, "Effects of rejuvenating agents on superpave mixtures containing reclaimed asphalt pavement," J. Master Civil Eng., vol. 19, no. 5, 2007.
- [6] E. R. Brown, "Preventative Maintenance Of Asphalt Concrete Pavements," 1988.
- [7] A. Ongel and M. Hugener, "Impact of rejuvenators on aging properties of bitumen," Construction and Building Materials, no. 94, pp. 467-474, 2015.
- [8] J. Brownridge, "The Role of an Asphalt Rejuvenator in Pavement Preservation: Use and Need for Asphalt Rejuvenation," Bakersfield, California, 2010.
- [9] R. Karlsson and U. Isacsson, "Material-related aspects of asphalt recycling-state of the art," J. Master. Civil Eng. , vol. 18, 2006.
- [10] M. A. Aguirre, M. M. Hassan, S. Shirzad, W. H. Daly and L. N. Mohammad , "Micro-encapsulation of Asphalt Rejuvenators using Melamine-Formaldehyde," Construction and Building Materials, vol. 114, pp. 29-39, 1 July 2016.
- [11] S. Shirzad, M. M. Hassan, M. A. Aguirre, L. N. Mohammad and W. H. Daly, "Evaluation of sunflower Oil as a Rejuvenator and Its Microencapsulation as a Healing Agent," J. Mater. Civil. Eng., 2016.
- [12] M. A. Aguirre, M. M. Hassan, S. Shirzad, L. N. Mohammad, S. Cooper and I. I. Negulescu, "Laboratory Testing of Self-Healing Microcapsules in Asphalt Mixtures Prepared with Recycled Asphalt Shingles," Journal of Materials in Civil Engineering, 2017.
- [13] D. Sun, J. Hu and X. Zhu, "Size Optimization and Self-Healing Evaluation of Microcapsules in Asphalt Binder," Colloid Polymer Science, vol. 293, no. 12, 2015.
- [14] A. Gibney, "Analysis of permanent deformation of hot rolled asphalt in Civil Engineering," 2002.
- [15] R. H. McDowell, Properties of alginates, London (UK): Alginate Industries, 1977.

- [16] S. D. Mookhoek, H. R. Fischer and S. van der Zwaag, "Alginate fibres containing discrete liquid filled vacuoles for controlled delivery," *Composites Part A: Applied Science and Manufacturing*, vol. 43, no. 12, pp. 2176-2182, 2012.
- [17] M. Prajer, "Direct and indirect observation of multiple local healing events in successively loaded fibre reinforced polymer model composites using healing agent-filled compartmented fibres," *Compos. Sci. Technol.*, vol. 106, pp. 127-133, 2015.
- [18] A. M. Hartman, M. D. Gilchrist and G. Walsh, "Effect of mixture compaction on indirect tensile stiffness and fatigue," *J. Transp. Eng.*, vol. 127, no. 5, 2001.
- [19] J. Bonnot, "Selection and use of the procedure for laboratory compaction of bitumen mixtures," *Performance Related Test Procedures for Bitumen Mixtures*, 1997.
- [20] A. Tabakovic, W. Post, D. Cantero, O. Copuroglu, S. J. Garcia and E. Schlangen, "The reinforcement and healing of asphalt mastic mixtures by rejuvenator encapsulation in alginate compartmented fibers," *Smart Mater. Struct.*, 2016.
- [21] AASHTO, "Standard method of test for quantitative extraction of asphalt binder from hot mix asphalt HMA," AASHTO T164, Washington, DC, 2014.
- [22] AASHTO, "Standard practice for recovery of asphalt binder from solution by Abson method," AASHTO R59, Washington, DC, 2011.
- [23] AASHTO, "Standard specification for performance-graded for asphalt binder," AASHTO M320, Washington, DC, 2015.
- [24] AASHTO, "Standard Method of Test for Multiple Stress Creep Recovery (MSCR) Test of Asphalt Binder Using a Dynamic Shear Rheometer (DSR)," AASHTO TP 70, Washington, DC, 2013.
- [25] AASHTO, "Standard Method of Test for Estimating Fatigue Resistance of Asphalt Binders Using the Linear Amplitude Sweep," 2016.
- [26] D. W. Christensen and D. A. Anderson, "Interpretation of Dynamic Mechanical test data for Paving Grade Asphalt Cements," *Association of Asphalt Paving Technologies, Proceedings of the Technical Sessions*, vol. 61, pp. 67-116, 1992.
- [27] G. Liu, E. Nielsen, J. Komacka, G. Leegwater and M. Ven, "Influence of the soft bitumen on the chemical and rheological properties of reclaimed polymer-modified binders from the "old" surface-layer asphalt," *Construction Building Material*, vol. 79, pp. 129-135, 2015.

- [28] C. Chiu and M. Lee, "Effectiveness of seal rejuvenators for bituminous pavement surfaces," *J. Test. Eval.* , vol. 34, pp. 390-394, 2006.
- [29] A. Garcia, E. Schlangen, M. van de Ven and G. Sierra-Beltran, "Preparation of capsules containing rejuvenator for their use in asphalt concrete," *J. Hazard. Mater.* , vol. 184, pp. 603-611, 2010.
- [30] D. E. Watson, A. Johnson and H. R. Sharma, "Georgia's Experience with Recycled Roofing Shingles in Asphaltic concrete," In *Transportation Research Record* 1638, pp. 15-20, 1998.
- [31] G. W. Maupin Jr, "Investigation of the Use of Tear-Off Shingles in Asphalt concrete," Charlottesville, 2010.
- [32] ASTM D4552/D4552M-10, "Standard Practice for Classifying Hot-Mix Recycling Agents," ASTM International, 2010.
- [33] G. Peterson, R. Davison, C. Glover and J. Bullin, "Effect of Composition on Asphalt Recycling Agent Performance," *Transportation Research Record*, 1994.
- [34] M. Samadzadeh, S. Hatami, M. Peikari and A. Ashrafi, "A Review on Self-Healing Coatings Based on Micro/Nanocapsules," *Progress in Organic Coatings*, vol. 68, no. 3, pp. 159-164, July 2010.
- [35] E. N. Brown, M. R. Kessler, N. R. Sottos and S. R. White, "In situ poly (urea-formaldehyde) microencapsulation of dicyclopentadiene," *microencapsulation* 20, 2003.
- [36] G. Sun and Z. Zhang, "Mechanical Strength of Microcapsules Made of Different Wall Materials," 2002.

CHAPTER 6. LABORATORY TESTING OF SELF-HEALING FIBERS IN ASPHALT MIXTURES PREPARED WITH RECYCLED MATERIALS

6.1 Introduction

The increasing need to construct new roads and to rehabilitate existing ones has increased the demand on petroleum and petroleum by-products, such as asphalt binder, which led to an increase in material costs and the environmental impacts associated with these products. The use of recycled materials has emerged as a sustainable solution to reduce cost by replacing virgin aggregate and binder and to reduce the impacts on ecological systems. However, the main challenge of incorporating recycled materials in asphalt mixtures is the level of blending between aged and virgin asphalt binders. The blending of both aged and virgin binders increases the susceptibility of an asphalt mixture to fatigue and thermal cracking due to the increase of the mixture's stiffness and brittleness.

Recycling agents, such as asphalt rejuvenators, have been evaluated to increase the blending between aged and virgin asphalt binders and to reverse the aging process in the recycled binder [1, 2]. Although rejuvenators can be directly applied on the pavement surface, spreading these products on the pavement surface has negative side effects such as the loss of skid resistance and poor penetration into the Asphalt Concrete (AC) layer [3]. Self-healing and encapsulation mechanisms have emerged as an innovative approach to disperse the rejuvenator product into the AC mix.

Researchers have proposed the encapsulation of asphalt rejuvenators as a self-healing agent for asphalt pavement to restore the original properties of the aged binder and to improve the mechanical properties of asphalt mixtures. The encapsulation of asphalt rejuvenators in asphalt mixtures is a promising approach as it would enhance pavement performance by releasing the

rejuvenator product when a crack starts to propagate and break the shell material and thus, reducing the viscosity of the binder to improve the self-healing ability of asphalt binders [4].

6.2 Objectives

The objectives of this study were the following: (1) Evaluate the self-healing efficiency of hollow-fibers, through the study of stiffness recovery of damaged mixture specimens under two different healing conditions; and (2) Evaluate the performance against fatigue cracking, low temperature cracking, and rutting susceptibility of AC with fibers through laboratory tests

6.3 Background

6.3.1 Asphalt Rejuvenation

Asphalt rejuvenators products can be defined as a low viscosity oil with high maltenes content, which has been shown to be the most effective treatment to partially restore asphalt properties [5]. Studies have shown that rejuvenating products can increase the recycled binder ratio in asphalt mixture but may also cause an adverse effect on the intermediate and low-temperature performances of asphalt mixtures [6]. In addition, studies have shown a softening effect in asphalt mixtures with the addition of rejuvenator products, which resulted in an increase in the rut depth at high-temperature [7]. Researchers have also found a limited penetration of asphalt rejuvenators when they are applied on the pavement surface reducing the effectiveness in reversing the aging process in asphalt binders [3].

6.3.2 Self-Healing Mechanisms in Asphalt Pavements

In recent years, researchers have adapted the biology's concept of self-healing into asphalt pavements by encapsulating a rejuvenator product in microcapsules or fibers with a polymer as a shell material. The concept of encapsulating a rejuvenator product is to release the product when the microcapsules or fibers break at a predefined stress.

6.3.2.1 Double-Walled Microcapsules with Asphalt Rejuvenators. Shirzad et al. conducted an optimization process in the production parameters of double-walled microcapsules containing sunflower oil as a core material [8]. The study successfully produced microcapsules with adequate thermal and mechanical properties to resist an asphalt mixing process. Aguirre et al. evaluated the healing efficiency of microcapsules containing a bio-oil as a core material by monitoring the crack size of damaged specimens during a 5-day healing period at two environmental curing conditions [9]. The study concluded that the healing efficiency of microcapsules was dependent on the breakage of the capsules, and thus, the release of the core material to soften the binder around the crack.

6.3.2.2 Compartment-Fibers with Asphalt Rejuvenators. A previous study conducted an optimization process to determine the optimum production parameters for the synthesis of compartment alginate fibers containing a rejuvenator product [10]. The study determined that the optimum shell/core material ratio was 70:30, which resulted in fibers with sufficient thermal stability and mechanical strength for asphalt mixture applications. In addition, Tabakovic et al. conducted a study to evaluate the efficiency of compartment alginate fibers as an asphalt pavement healing system by performing an indirect tensile strength (IDS) test, 4-point bending fatigue test, and a semi-circular bending (SCB) test [11]. Researchers reported that SCB and IDT tests were unsuitable for the evaluation of hollow fibers due to the large deformation that occurred in the specimens after performing the test. However, the study determined that the 4-point bending test was the most suitable test to evaluate the healing efficiency as micro-cracks can be induced as the test is strain-controlled. The 4-point bending test showed that the asphalt mixtures with compartment fibers had a better stiffness recovery ability than a conventional AC mixture.

6.4 Experimental Program

6.4.1 Fiber's Synthesis and Properties

6.4.1.1 Chemicals. The core material of the fibers consisted of a green bio-oil product, from Sripath Technologies (density of 0.919 g/cm^3). The experimental program used sodium alginate as a shell material in the prepared fibers. In addition, PEMA (ethylene-alt-maleic-anhydride) was added as a surfactant in a 2.5 wt % aqueous solution. Furthermore, ethylene glycol was incorporated in the present study as a plasticizer material. Lastly, the coagulation bath contained a 0.6 Molarity (M) solution of calcium chloride hexahydrate ($\text{CaCl}_2 \cdot 6\text{H}_2\text{O}$).

6.4.1.2 Production of Fibers. Aguirre et al. optimized the synthesis procedure for sodium-alginate hollow fibers containing a rejuvenating product [12]. The sodium-alginate hollow fibers were synthesized from an oil-in-water emulsion containing the shell material and the core material. More details on the synthesis procedure and spinning process can be found elsewhere [12].

6.4.2 Self-Healing Mixture Testing

6.4.2.1 Materials. An unmodified binder (i.e., PG 64-22), a SBS-polymer-modified asphalt binder (i.e., PG 70-22M) and aggregate blend (i.e., 16-mm gravel, 6.35-mm gravel, coarse sand, and fine sand) were selected to satisfy the mix design criteria for a 12.5 nominal maximum aggregate size (NMAS) asphalt mixture. Post-consumer waste shingles (PCWS) and reclaimed asphalt pavement (RAP) were incorporated into the evaluated mixtures at 5% and 20% by total weight of mix, respectively. In addition, the experimental program added the hollow-fibers in selected mixtures at a 5% fiber content, see Table 0.1. Test Matrix for the Study.

6.4.2.2 Specimen Preparation. Table 6.1 presents the prepared asphalt mixtures for the healing experiment. Six specimens were prepared for each asphalt mixture type, with three to be exposed

to room-temperature healing curing conditions and three to be exposed to high-temperature healing curing conditions after cracking. The rectangular beam specimens with dimensions 40 x 40 x 160 mm were prepared by sawing a rectangular slab (i.e., 260.8 x 320.3 x 50 mm) to the required dimensions. All specimens were prepared to an air void of $7.0 \pm 0.5\%$.

Table 0.1. Test Matrix for the Study

Mixture	Asphalt Binder	RAS Content	RAP Content	Fiber Content	Self-Healing Experiment	Mixture testing		
					Strength Recovery	SCB	LWT	TSRST
70CO	PG 70-22	-	-	-	X	X	X	X
70PG5F	PG 70-22	-	-	5%	X	-	-	-
70PG5P	PG 70-22	5%	-	-	X	X	X	X
70PG5P1F	PG 70-22	5%	-	1%	X	-	-	-
70PG5P3F	PG 70-22	5%	-	3%	X	-	-	-
70PG5P5F	PG 70-22	5%	-	5%	X	X	X	X
70PG20RAP	PG 70-22	-	20%	-	X	X	X	X
70PG20RAP5F	PG 70-22	-	20%	5%	X	X	X	X
70PG5P20RAP	PG 70-22	5%	20%	-	-	X	X	X
70PG5P20RAP5F	PG 70-22	5%	20%	5%	-	X	X	X
64CO	PG 64-22	-	-	-	X	X	X	X
64PG5F	PG 64-22	-	-	5%	X	-	-	-
64PG5P	PG 64-22	5%	-	-	X	X	X	X
64PG5P5F	PG 64-22	5%	-	5%	X	X	X	X

Table 6.1. Cont'd

Mixture	Asphalt Binder	RAS Content	RAP Content	Fiber Content	Strength Recovery	SCB	LWT	TSRST
64PG20RAP	PG 64-22	-	20%	-	X	X	X	X
64PG20RAP5F	PG 64-22	-	20%	5%	X	X	X	X
64PG5P20RAP	PG 64-22	5%	20%	-	-	X	X	X
64PG5P20RAP5F	PG 64-22	5%	20%	5%	-	X	X	X

*X = test performed

6.4.2.3 Self-Healing Test Description. The self-healing experiment consisted of inducing micro-cracks in rectangular beam specimens at room-temperature with a three-point bending setup with a span length of 100 mm through a strain-controlled load applied at a rate of 0.5 mm/min, which allowed stopping the test before sudden failure. Figure 6.1(a) shows the three-point bending setup adopted in the self-healing experiment. The three-point bending test results were used to calculate the strength for three main conditions (undamaged, damaged, and healed states). The undamaged strength of the specimens was defined as the first three-point bending test performed to induce damage in the rectangular specimens. The same procedure was repeated for a second three-point bending test before healing in order to calculate the damaged strength and to increase the severity of the cracks before healing. Following healing, a third three-point bending test was conducted in order to estimate the healed strength. Immediately after the second three-point bending test, specimens were subjected to a 6-day healing period under controlled environmental conditions (i.e., room temperature or high-temperature). The strength recovery efficiency (SRE) for the different conditions was calculated as follows:

$$S_e = \left(1 - \frac{S_0 - S_t}{S_0}\right) * 100 \quad (6.1)$$

S_e = Strength Recovery efficiency (%);

S_0 = Strength in undamaged condition, kN; and

S_t = Strength in damaged or healed condition, kN.



(a)

Figure 0.1. (a) Three-Point Bending Test Setup

6.4.3 Effects of Sodium-Alginate Fibers on Asphalt Mixture Performance

The objective of this phase of the study was to evaluate the effects of sodium-alginate hollow fibers on the laboratory performance of a Superpave asphalt mixture with a NMAS of 12.5 mm. Superpave asphalt mixtures were prepared in accordance with AASHTO R 35-09, AASHTO M 323-07, and Section 502 of the 2006 Louisiana Standard Specifications for Roads and Bridges [13]. The evaluated asphalt mixtures are shown in Table 6.1.

6.4.3.1 Laboratory Performance Tests. Asphalt mixtures presented in Table 6.1 were evaluated through laboratory tests to predict the performance of each mixture against intermediate-temperature cracking, permanent deformation, and low-temperature cracking. Asphalt mixture performance tests were conducted based on the test factorial shown in Table 6.2. Two mechanical tests and a simulative test (Loaded-Wheel Test [LWT]) were conducted to

characterize the performance of asphalt mixtures. The target air voids for all specimens prepared in this phase were $7.0 \pm 0.5\%$.

Table 0.2. Asphalt Mixture Performance Tests

Tests	Test Standard	Performance Characteristics	Specimen Details
SCB	ASTM D 8044	Intermediate Temperature: fatigue and fracture cracking resistance	$\phi 150 \text{ mm} \times 57 \text{ mm}$
LWT at 50°C	AASHTO T 324	Rutting susceptibility and moisture resistance	$\phi 150 \text{ mm} \times 60 \text{ mm}$
TSRST	AASHTO TP 10	Low temperature: thermal cracking resistance	$50 \text{ mm} \times 50 \text{ mm} \times 250 \text{ mm}$

6.4.4 Statistical Analysis

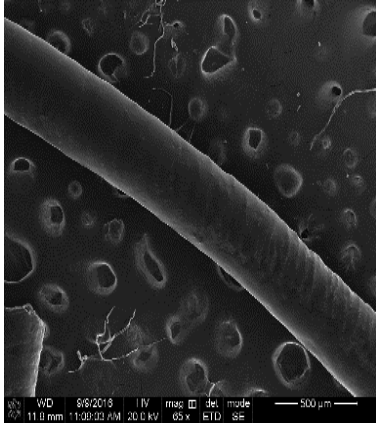
A statistical analysis was performed to evaluate whether the differences in performance observed in the self-healing experiment and mixture testing results were significant. An Analysis of Variance (ANOVA) at a 5% confidence level was performed for each self-healing and mixture test to identify statistically significant differences in the test results. A Tukey's HSD test was also performed on all possible combinations to identify the mixes that were statistically different based on the previous results from ANOVA. The statistical results for each grouping were ranked by using letters A, B, C, and so forth. The letter A was assigned to the mix with the best performance, followed by the letter B and so forth. Double letters (e.g., A/B, B/C) indicate that the mixture may be categorized in both groups.

6.5 Results and Analysis

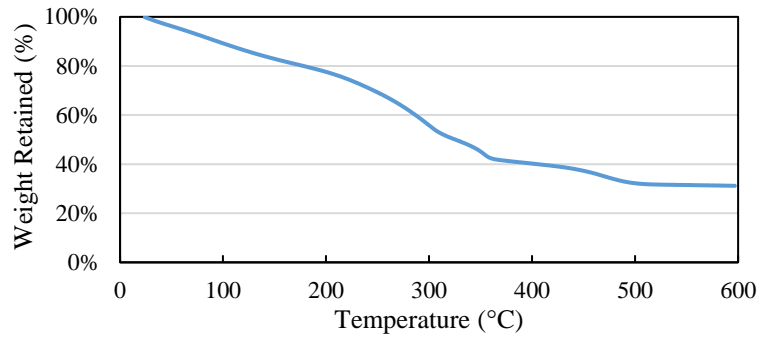
6.5.1 Hollow-Fibers with Rejuvn8 as Core Material

Sodium-alginate fibers containing a commercial rejuvenator product were prepared as shown in Figure 6.2(a). The thermal stability of the produced fibers was analyzed using thermogravimetric analysis (TGA). Figure 6.2(b) shows the change in weight (%) as the temperature was increased. A reference temperature of 163°C was selected to analyze TGA results based on the upper range of temperature typically used to prepare asphalt mixtures. Figure 6.2(b) shows an 18.5% decrease in weight at the reference temperature, which may be explained by the evaporation of the water absorbed by the fibers during the synthesis procedure. Based on these results, it was deemed that the prepared fibers were suitable for use during asphalt mixture production in view of the fact that the sample's weight decreased by 50% at a temperature (above 300°C) higher than the one used in an asphalt mixture production.

The tensile strength of the produced fibers was also measured to evaluate the resistance of the fiber to breakage during the mixing process. The tensile test setup is shown in Figure 6.2(c). Based on the results of past studies, asphalt additives need to have an ultimate tensile strength (UTS) higher than 12 MPa to resist typical pressure during asphalt mixing processes [14, 15]. The tensile strength of the produced fibers was measured to be 28.4 MPa with a standard deviation of ± 3.7 MPa. Figure 6.2(d) shows a load-deformation plot obtained from the UTS test.



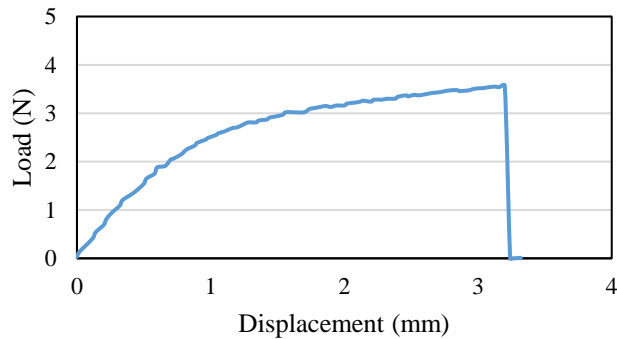
(a)



(b)



(c)



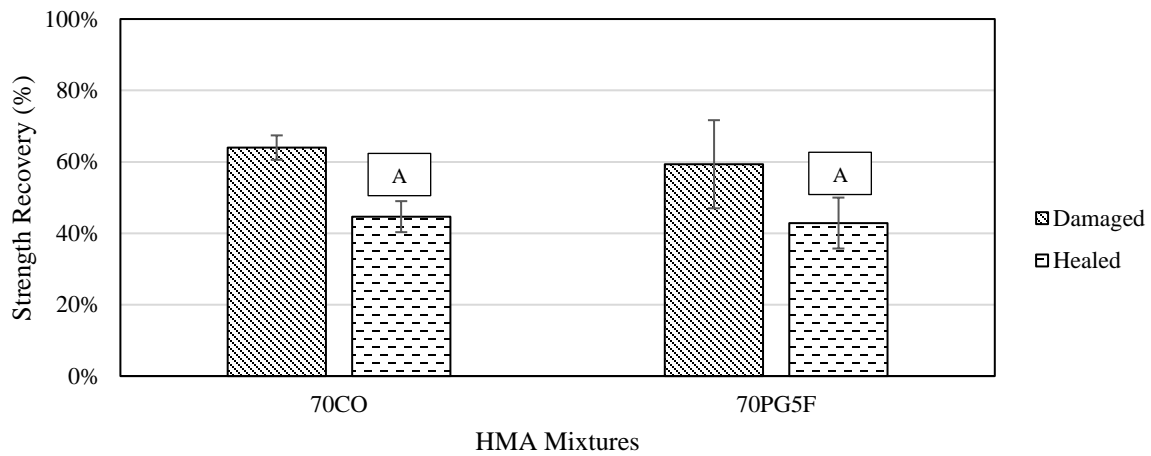
(d)

Figure 0.2. Fibers with Optimum Parameters (a) SEM Picture with 65x Magnification, (b) TGA Test Results, (c) Tensile Test Setup, and (d) UTS Test Results

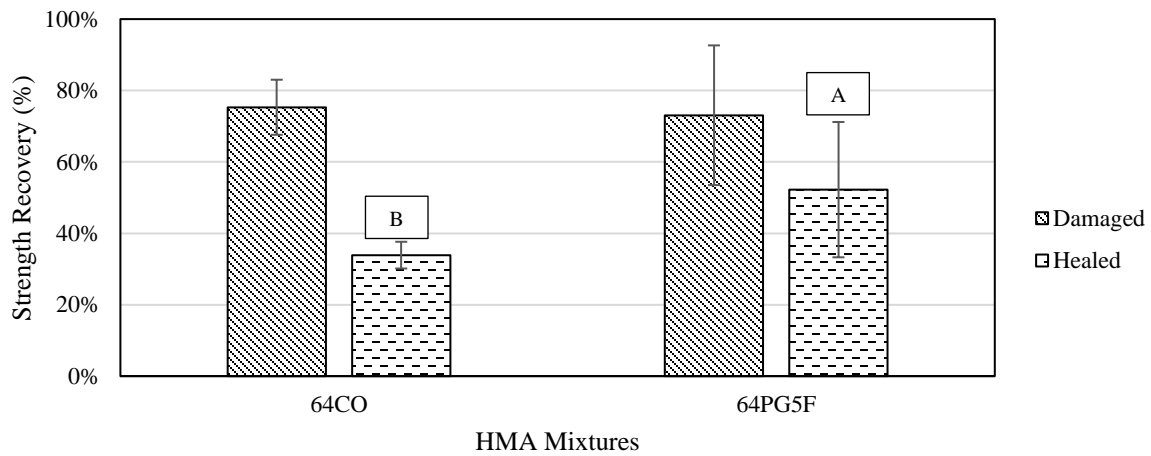
6.5.2 Strength Recovery Properties of Sodium-Alginate Fibers in Asphalt Mixtures

6.5.2.1 Effect of Binder PG on the Strength Recovery Properties of Sodium-Alginate Fibers. The strength recovery of the prepared asphalt mixtures was calculated based on Equation (1). For asphalt mixtures prepared with PG 70-22, Figure 6.3(a) shows that the strength recovery of the conventional asphalt mixture (70CO) was statistically equivalent to the mixture prepared with the hollow fibers (70PG5F). In contrast, Figure 6.3(b) shows that the addition of sodium-alginate fibers enhanced the strength recovery for the asphalt mixture prepared with the unmodified

binder PG 64-22 after the 6-day healing period as compared to the conventional mixture 64CO. In this case, differences were statistically significant. The difference between the two binders may be due to chemical interaction between the polymer in the PG 70-22 binder and the sodium-alginate hollow fibers.



(a)



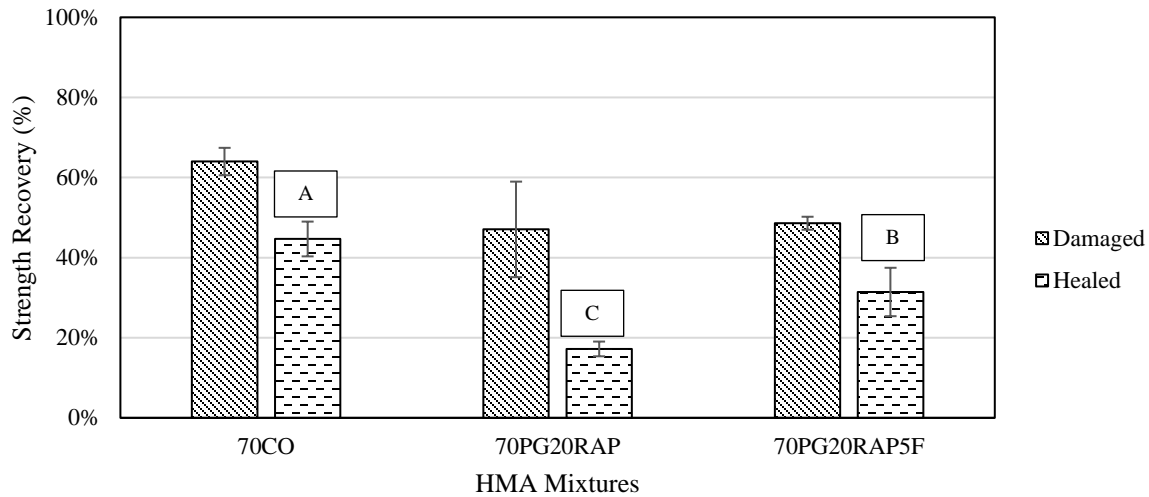
(b)

Figure 0.3. Strength Recovery at Room-Temperature for: (a) Mixtures Prepared with Binder PG 70-22 Containing Fibers, and (b) Mixtures Prepared with Binder PG 64-22 Containing Fibers

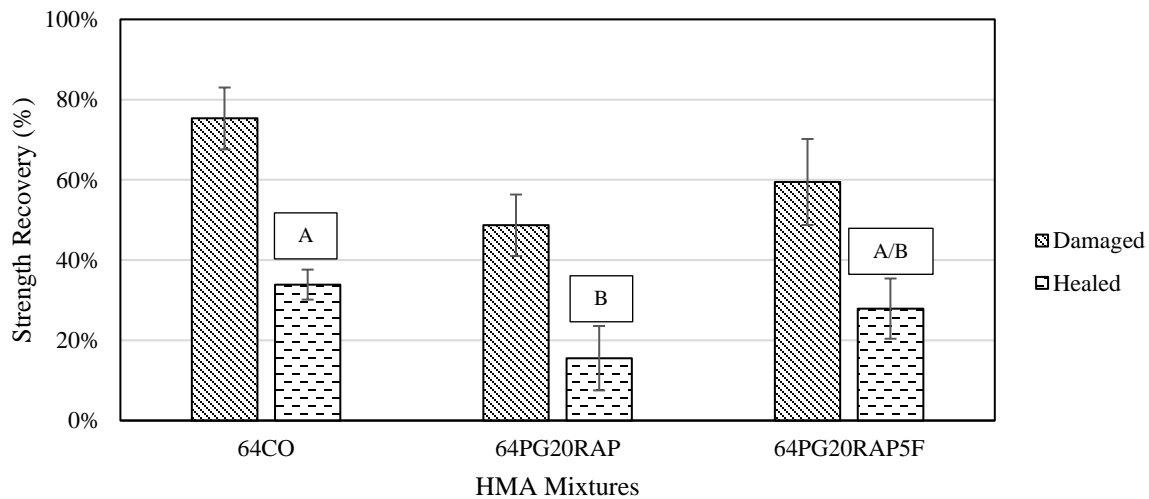
6.5.2.2 Effect of Recycled Materials on the Strength Recovery Properties of Sodium-Alginate Fibers. Figure 6.4(a) shows the effect of RAP on the strength recovery of mixtures prepared with binder PG 70-22. The addition of RAP resulted in a more brittle mixture compared to the conventional mixture as mixes 70PG20RAP and 70PG20RAP5F were more susceptible to fracture as interpreted from the decrease in strength recoveries in comparison to mixture 70CO. However, Figure 6.4(a) shows that the addition of the fibers (70PG20RAP5F) had a positive effect as a higher strength recovery was observed after the healing period in comparison to mix 70PG20RAP.

The effect of adding RAP in the strength recovery of mixtures prepared with binder PG 64-22 is shown in Figure 6.4(b). The reduction in strength recovery in the damaged and healed states with the addition of RAP was also observed for the mixtures prepared with binder PG 64-22. A similar trend was also observed in Figure 6.4(b), which shows that the hollow fibers enhanced the healing efficiency in comparison to mix 64PG20RAP.

Figure 6.5(a) shows the effect of RAS in the strength recovery of mixtures prepared with binder PG 70-22. Figure 6.5(a) shows that the strength recovery of the mixture with 5% RAS (70PG5P) was lower than the conventional mixture 70CO after the healing period. The brittle behavior of the binder in the RAS material could explain the difference in strength recoveries after the healing period. Figure 6.5(a) also shows that the mixture containing fibers (70PG5P5F) had a lower strength recovery in both the damaged and healed conditions than the conventional mixture containing RAS; yet, differences were not statistically significant.



(a)

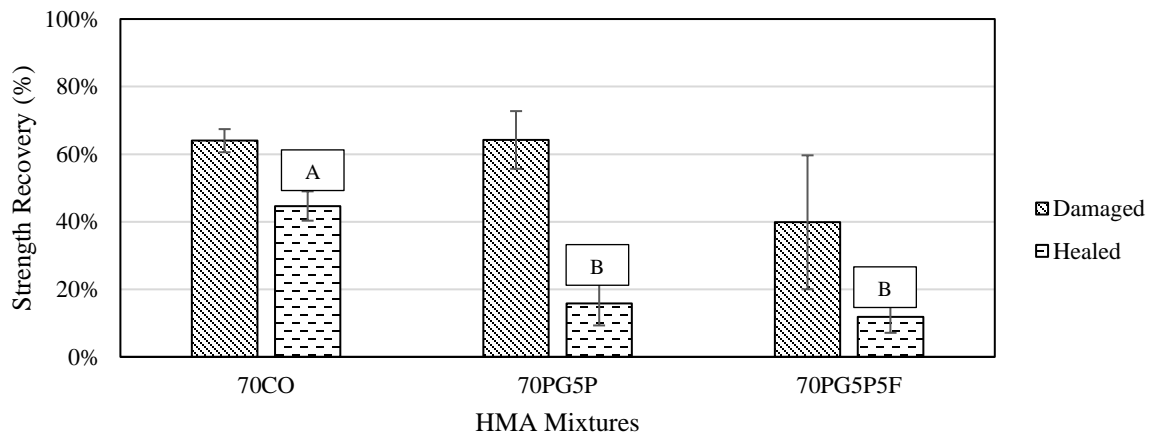


(b)

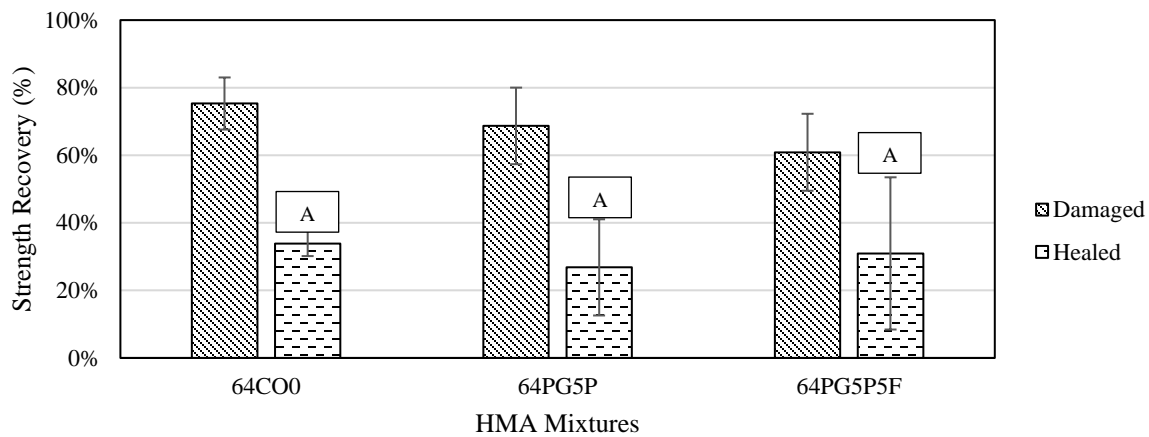
Figure 0.4. Strength Recovery at Room-Temperature for (a) Mixtures Prepared with Binder PG 70-22 And Containing RAP and (b) Mixtures Prepared with Binder PG 64-22 and Containing RAP

The effect of adding RAS in the strength recovery of mixtures prepared with binder PG 64-22 is shown in Figure 6.5(b). Figure 6.5(b) shows the same negative effect of adding RAS on mixtures

prepared with binder PG 64-22 as the conventional mixture 64CO had a higher strength recovery after the 6-days healing period; yet differences were not statistically significant. Figure 5(b) also shows that the mixture containing fibers (64PG5P5F) had a similar strength recovery in both the damaged and healed conditions than the mixture containing RAS.



(a)

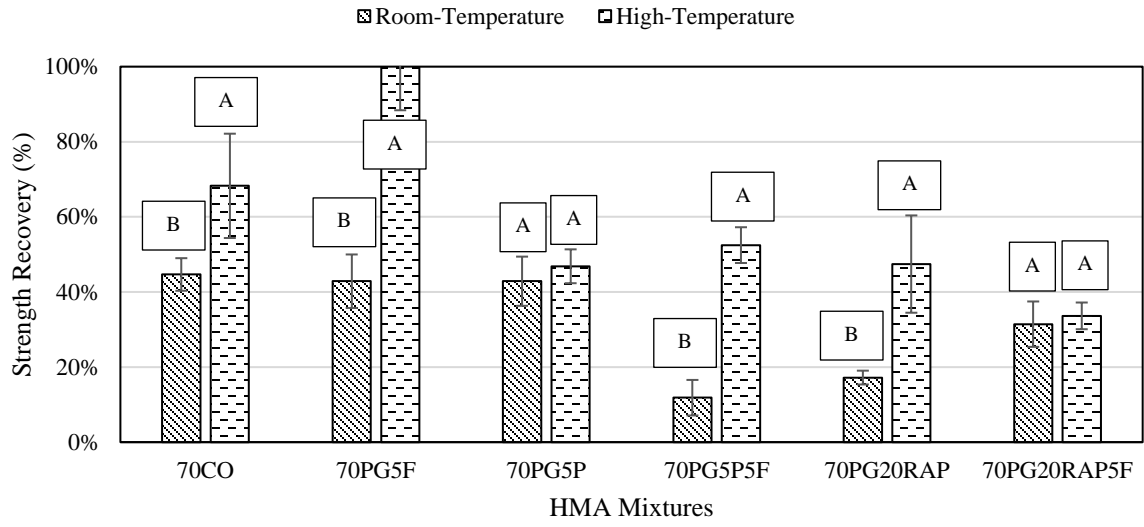


(b)

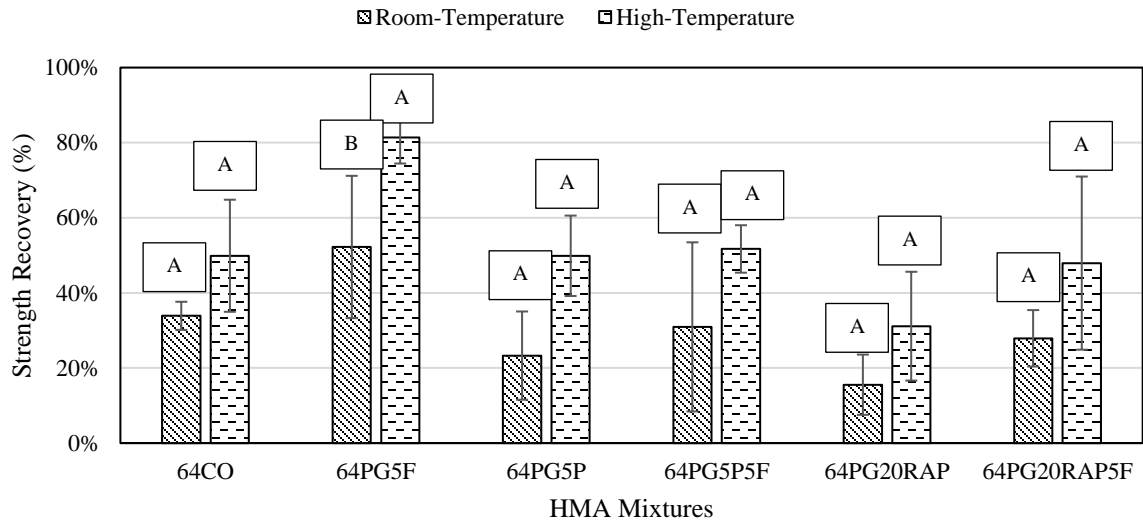
Figure 0.5. Strength Recovery at Room-Temperature for (a) Mixtures Prepared with Binder PG 70-22 and Containing RAS and (b) Mixtures Prepared with Binder PG 64-22 and Containing RAS

6.5.2.3 Effect of Curing Conditions on the Strength Recovery Properties of Sodium-Alginate Fibers. Figure 6.6(a) shows that the increase in temperature enhanced the strength recovery of the evaluated asphalt mixtures. It is shown that the conventional mixture containing sodium-alginate fibers (70PG5F) exhibited a 100% strength recovery at high-temperature curing condition. The higher strength ratios for the beam specimens is due to the high temperature curing condition, which enhanced the flow of the binder and the healing of the cracks. Figure 6.6(b) shows the same trends for the mixtures prepared with the unmodified PG 64-22 binder. Similar to the trends observed for the PG 70-22 binder, the conventional mixture with fibers, 64PG5F, had the highest strength recovery at high-temperature curing condition after 6-day of healing period. In addition, it is shown that the mixture containing sodium-alginate fibers had the best strength recovery at the high-temperature curing condition.

A t-test analysis was performed for each type of mixture to evaluate the effect of curing conditions on the strength recovery ability of the evaluated asphalt mixtures. Figure 6.6(a) shows that the increase in temperature during the healing period had a significant effect on the strength recovery of the mixtures containing recycled materials with the exception of mixture 70PG20RAP5F. Yet, Figure 6.6(b) shows that the enhancement in the strength recovery of the mixtures was not significantly different. The variability observed in the strength recovery analysis test results could have contributed to neglect the effect of increasing the temperature from 25°C to 50°C during the healing period.



(a)



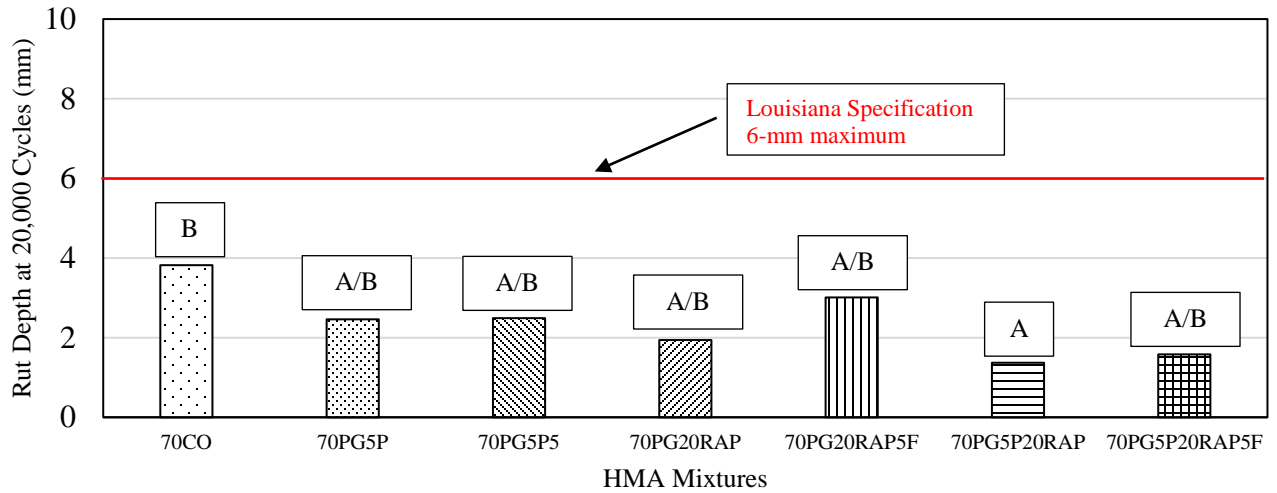
(b)

Figure 0.6. Effect of Curing Conditions in The Strength Recovery of: (a) Mixtures with Binder PG 70-22 and (b) Mixtures with Binder PG 64-22

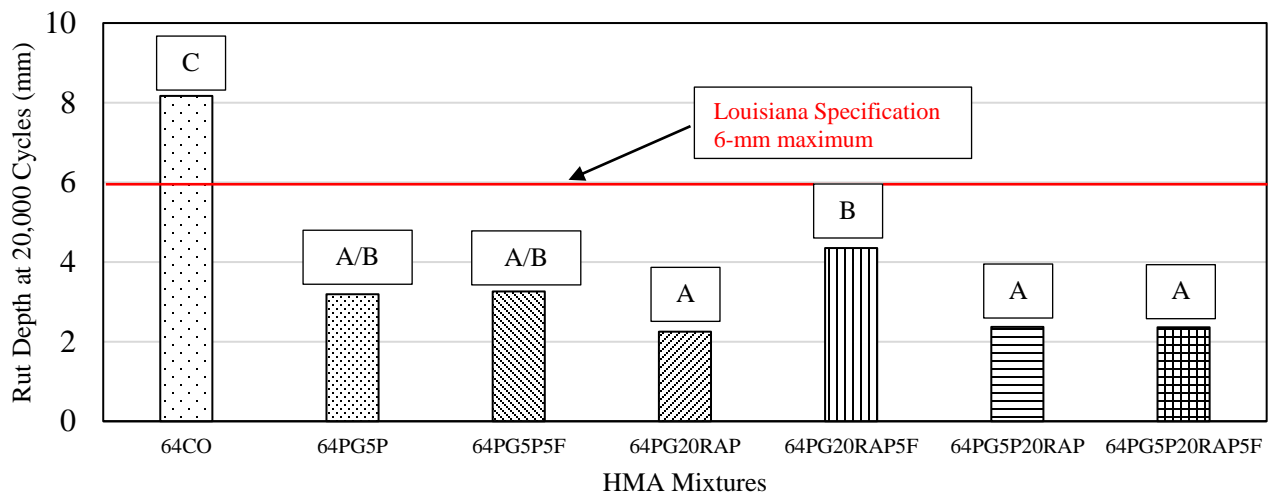
6.5.3 Performance of HMA Mixtures with Sodium-Alginate Fibers

6.5.3.1 Rutting Performance. Figure 6.7 presents the terminal permanent deformation depths for the evaluated mixtures from the LWT test. It is shown in Figure 6.7(a) that the maximum allowable rut depth threshold in Louisiana (6 mm) was satisfied for all the mixes. The addition of recycled materials decreased the terminal rut depth as compared to the conventional mixture (70CO). However, results show that the addition of the hollow fibers slightly increased the rut depth as compared to the mixtures containing recycled materials with no fibers. The small increase in the rut depth may be caused by the breakage of fibers during the LWT test, which released the rejuvenating product and caused a softening effect. In addition, the statistical analysis results indicated that the performance of mixture containing RAS/RAP, 70PG5P20RAP, was significantly different from the conventional mixture against permanent deformation. Furthermore, the rest of the evaluated mixtures showed a similar performance compared to 70PG5P20RAP based on the pairwise comparison shown in Figure 6.7(a).

Figure 6.7(b) shows that the conventional asphalt mixture (64CO) had a rut depth greater than the maximum allowable rut depth threshold in Louisiana (6 mm). Furthermore, Figure 6.7(b) shows that the addition of recycled materials improved the rutting susceptibility of the mixtures by reducing the rut depth after 20,000 cycles. Similarly, as observed in Figure 6.7(a), a small increase in the rut depth was observed in the mixtures containing recycled materials with the addition of hollow fibers. The statistical analysis results showed that the asphalt mixtures containing recycled materials with/without fibers had a statistically significant improvement against rutting susceptibility as compared to the conventional mixture (64CO).



(a)



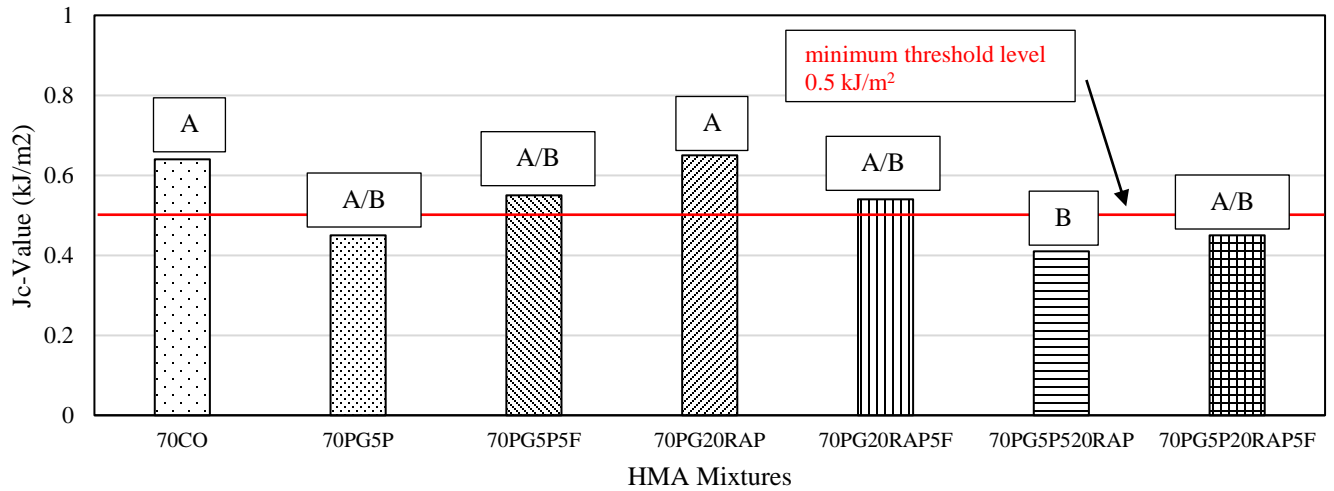
(b)

Figure 0.7. Rutting Susceptibility: (a) HMA Mixtures with PG 70-22 and (b) HMA Mixtures with PG 64-22

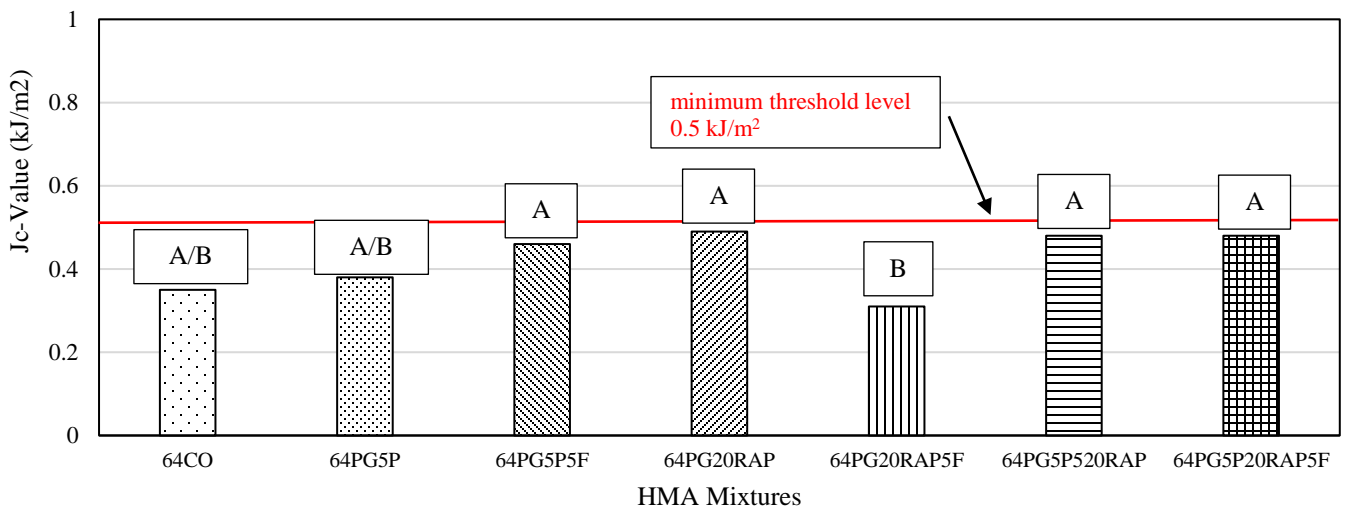
6.5.3.2 Fracture Resistance at Intermediate Temperature. Earlier studies recommended a minimum threshold J_c value of 0.5 to 0.65 kJ/m² to identify intermediate-temperature cracking susceptibility [16]. Figure 6.8 shows the critical strain energy release rate for the evaluated asphalt mixtures. Figure 6.8(a) shows a decrease in the J_c value when RAS and RAS/RAP were

added in mixes 70PG5P and 70PG5P20RAP as compared to the conventional mixture (70CO). The addition of RAP resulted in a similar fracture resistance at intermediate temperature as the conventional mixture (70CO). Figure 6.8(a) also shows that the addition of fibers in the mix containing RAS (70PG5P5F) had a positive effect as an increase in the J_c value was noted from 0.45 to 0.55 kJ/m². The same positive effect due to the addition of fibers was observed in mix 70PG5P20RAP5F as an increase in the J_c value was observed as shown in Figure 6.8(a). The rejuvenating properties of the hollow fibers may explain the enhancement of the fracture properties of mixes 70PG5P5F and 70PG5P20RAP5F. The statistical analysis results show that the inferior performance of mixture containing RAS/RAP, 70PG5P20RAP, was significantly different from the conventional mixture. However, it is observed in Figure 6.8(a) that adding the hollow fibers in the mixtures containing recycled materials showed a statistically-equivalent performance against fracture at intermediate temperature as the conventional mixture.

Figure 6.8(b) shows that the asphalt mixtures prepared with PG 64-22 did not satisfy the minimum threshold level of 0.5 kJ/m². However, similar to the trends observed with PG 70-22, the addition of hollow fibers enhanced the fracture properties of mixtures containing RAS (64PG5P5F) and RAS/RAP (64PG5P20RAP5F). Yet, the addition of hollow fibers decreased the fracture resistance of the mixture prepared with 20% RAP (64PG20RAP compared to 64PG20RAP5F).



(a)



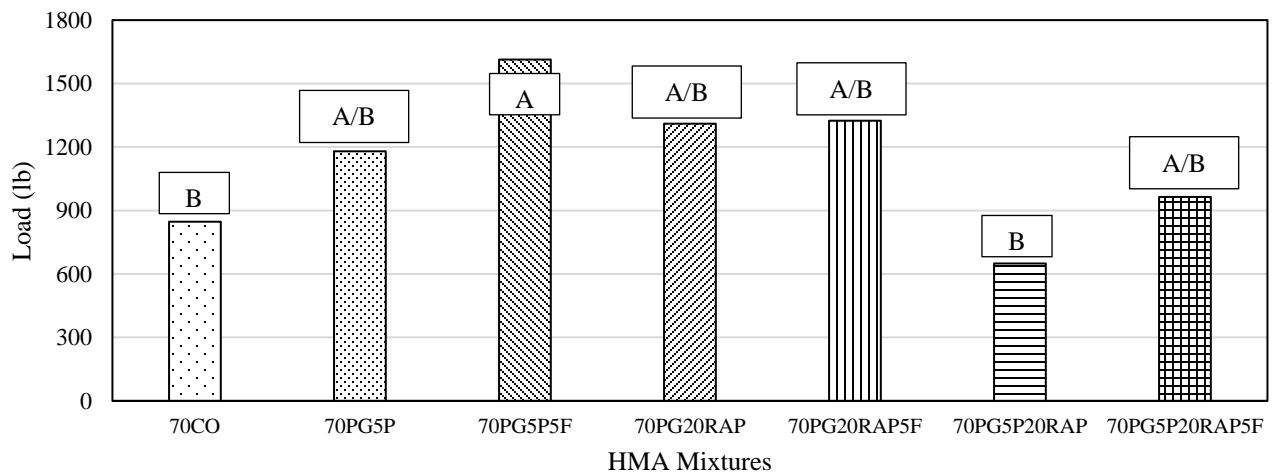
(b)

Figure 0.8. Fracture Resistance: (a) HMA Mixtures with PG 70-22 and (b) HMA Mixtures with PG 64-22

6.5.3.3 Low-Temperature Cracking Resistance. Figure 9 shows the fracture load for the evaluated asphalt mixtures. Mixture aging was performed according to AASHTO R30-02. Figure 6.9(a) shows that the addition of RAS or RAP resulted in higher fracture load compared to the conventional mixture. Furthermore, it is shown in Figure 6.9(a) that the addition of the hollow

fibers enhanced the fracture load of mixtures containing recycled materials (70PG5P vs. 70PG5P5F; 70PG20RAP vs. 70PG20RAP5F; and 70PG5P20RAP vs. 70PG5P20RAP5F). Therefore, the addition of RAS or RAP with the hollow fibers resulted in asphalt mixtures with higher load capacity at low-temperature. The statistical analysis results showed that the mixtures containing recycled materials with sodium-alginate fibers had a similar fracture resistance at low-temperature than the conventional mixture 70CO.

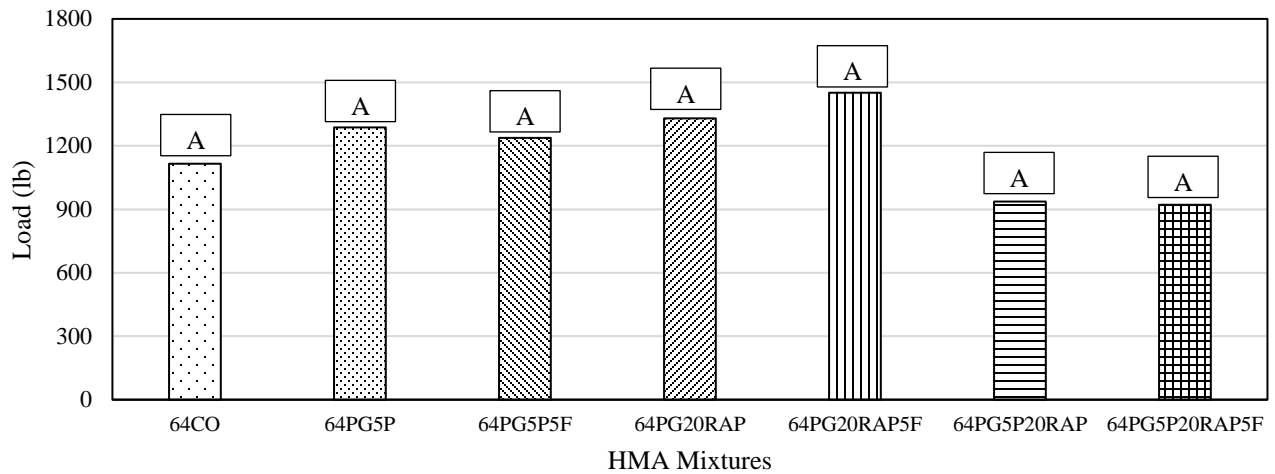
Figure 6.9(b) shows a similar improvement in the fracture resistance of mixtures with the addition of RAS and/or RAP. The fracture load also improved with the addition of hollow fibers in mixtures containing recycled materials. As a result, the addition of RAS or RAP with the hollow fibers resulted in asphalt mixtures with higher load capacity at low-temperature. However, observed differences were within the test variability and were not statistically significant.



(a)

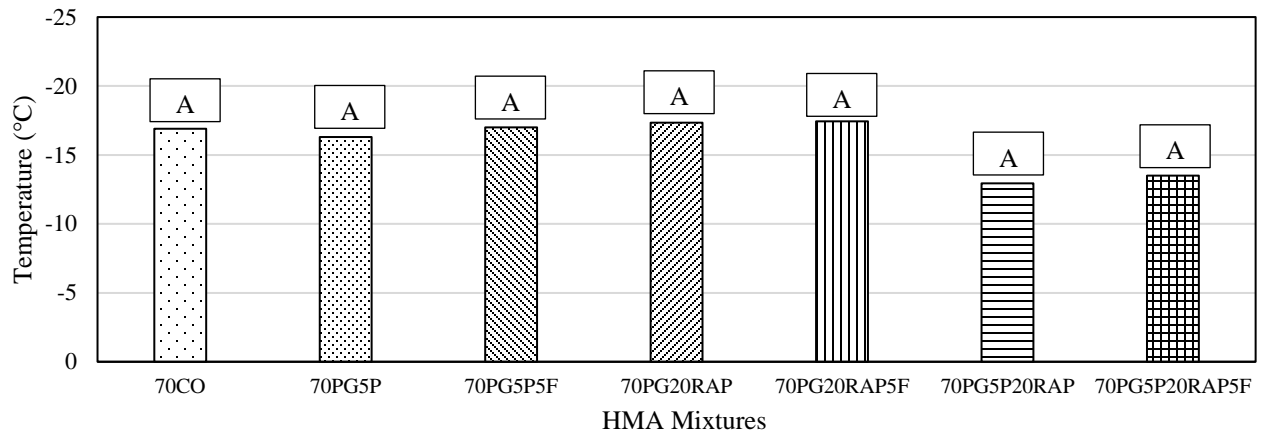
Figure 0.9. Failure Load: (a) HMA Mixtures with PG 70-22 and (b) HMA Mixtures with PG 64-22

Figure 6.9. cont'd

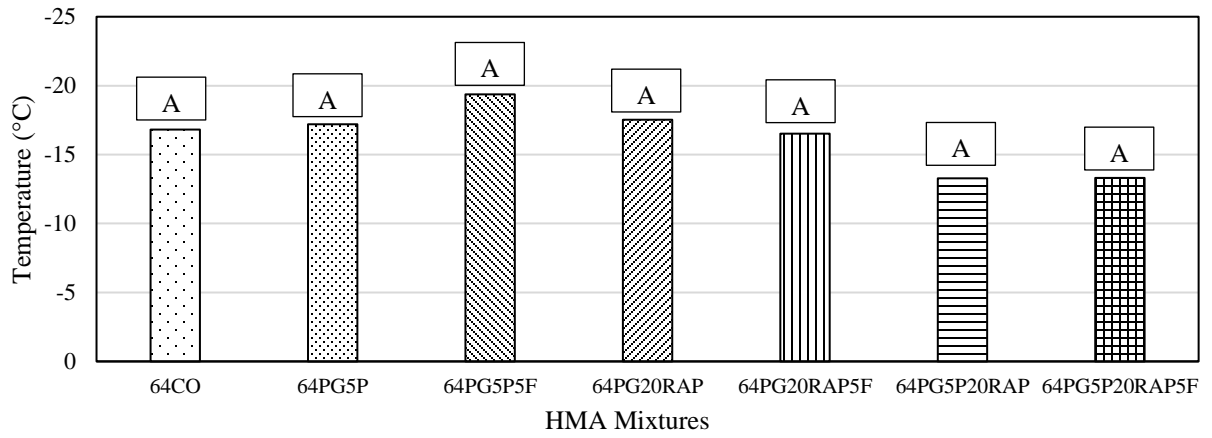


(b)

The failure temperature of the evaluated mixtures from the TSRST test results are shown in Figure 6.10. Figure 6.10(a) shows that the addition of RAS or RAP resulted in a similar failure temperature as the conventional mixture 70CO. Also, it is shown in Figure 6.10(a) that the addition of the hollow fibers did not enhance the fracture temperature of mixtures containing recycled materials; thus, they had a similar failure temperature than the conventional mixture. A drop in the failure temperature was observed in the mixtures containing RAS and RAP, which in conjunction with results from Figure 6.9, shows that the evaluated mixtures containing both recycled materials would be more susceptible to fracture at low-temperatures. However, observed differences were within the test variability and were not statistically significant. Similar trends were observed with the mixtures prepared with binder PG 64-22, see Figure 6.10(b).



(a)



(b)

Figure 0.10. Failure Temperature for: (a) Mixtures with PG 70-22 and (b) Mixtures with PG 64-22

6.6 Summary and Conclusions

The objectives of this study were to evaluate of self-healing efficiency of hollow-fibers through the study of strength recovery of damaged mixture specimens under two different healing conditions; and to evaluate the performance against fatigue cracking, low temperature cracking, and rutting susceptibility of asphalt mixtures with fibers through laboratory tests. The following findings and conclusions are drawn based on the results of the experimental program.

With respect to strength recovery:

The self-healing experiment test results showed that the addition of sodium-alginate fibers improved the strength recovery of mixtures prepared with unmodified binder. For mixtures prepared with polymer-modified binder, the strength recovery of the conventional asphalt mixture was statistically equivalent to the mixture prepared with the hollow fibers.

The increase in temperature from 25°C to 50°C during the healing period resulted in higher strength recovery percentages in all the evaluated mixtures. Furthermore, the conventional mixture containing sodium-alginate fibers exhibited a 100% strength recovery at high-temperature curing condition.

With respect to the effects of the fibers on the laboratory performance of asphalt mixtures:

LWT test results showed that the addition of sodium-alginate fibers in the mixtures containing recycled materials resulted in an increase in the rut depth; yet, the mixtures performed better than the conventional mixture and satisfied the Louisiana specifications.

SCB test results suggested that the conventional mixture would have the best performance against fracture as it had the highest Jc-value. However, SCB test results showed that the

addition of fibers enhanced the mechanical properties against fracture at intermediate temperature of mixtures containing RAS and RAS/RAP.

TSRST test results showed that the addition of fibers improved the loading capacity of mixtures containing recycled materials compared to the conventional mixtures. Yet, the failure temperature of mixtures containing recycled materials with fibers did not show significance differences from the conventional mixtures.

This study is a first step towards the evaluation of sodium-alginate hollow fibers in asphalt pavement applications. Based on the outcomes of this study, the authors recommend conducting further research prior to implementing the developed fibers in practice. It is recommended to test the developed fibers with other binder types and other RAP and RAS sources to evaluate their effects on the rheological properties of the binders and their enhancement of the mechanical and healing properties of the mixtures.

6.7 References

- [1] F. S. Zhou, D. Morton, R. Lee, S. Hu and T. Scullion, "Rejuvenator characterization, blend characteristics, and proposed mix design method," Association of Asphalt Paving Technologies, no. Proc. Technical Sessions, 2015.
- [2] G. Holleran, T. Wieringa and T. Tailby, "Rejuvenation treatments for aged pavements," Transit New Zealand and New Zealand Institute Technology (NZIHT), 2006.
- [3] C. Chiu and M. Lee, "Effectiveness of seal rejuvenators for bituminous pavement surfaces," J. Test. Eval., vol. 34, pp. 390-394, 2006.
- [4] A. Garcia, E. Schlangen, M. Van de Ven and G. Sierra-Beltran, "Preparation of capsules containing rejuvenators for their use in asphalt concrete," J. Hazardous MAter., vol. 184, no. 1, 2010.
- [5] R. Karlsson and U. Isacson, "Material-related aspects of asphalt recycling-state of the art," Journal of Materials in Civil Engineer, vol. 18, 2006.

- [6] S. Cooper, L. N. Mohammad and M. A. Elseifi, "Laboratory Performance of Asphalt Mixtures Containing Recycled Asphalt Shingles," *Journal of the Transportation Research Board*, vol. 2445, pp. 94-102, 2014.
- [7] M. A. Aguirre, M. M. Hassan, S. Shirzad, L. N. Mohammad and S. B. Cooper, "Performance of asphalt rejuvenators in hot-mix asphalt containin recycled asphalt shingles," *Transportation Research Record*, vol. 2633, pp. 108-116, 2017.
- [8] S. Shirzad, M. M. Hassan, M. A. Aguirre, L. N. Mohammad and W. H. Daly, "Evaluation of sunflower Oil as a Rejuvenator and Its Microencapsulation as a Healing Agent," *J. Mater. Civil. Eng.*, 2016.
- [9] M. A. Aguirre, M. M. Hassan, S. Shirzad, L. N. Mohammad, S. Cooper and I. I. Negulescu, "Laboratory Testing of Self-Healing Microcapsules in Asphalt Mixtures Prepared with Recycled Asphalt Shingles," *Journal of Materials in Civil Engineering*, 2017.
- [10] A. Tabakovic, D. Braak, M. Van Gerwen, O. Copuroglu, W. Post, S. J. Garcia and E. Schlangen, "The compartment alginate fibres optimization for bitumen rejuvenator encapsulation," *Journal of Traffic and Transportation (English Edition)*, 2017.
- [11] A. Tabakovic, L. Schuyffel, A. Karac and E. Schlangen, "An evaluation of the efficiency of compartmented alginate fibers encapsulating a rejuvenator as an asphalt pavement healing system," *Applied Science*, vol. 7, no. 647, 2017.
- [12] M. A. Aguirre, M. M. Hassan, S. Shirzad, S. B. Cooper, I. I. Negulescu and L. N. Mohammad, "Evaluation of hollow-fibers encapsulating a rejvuenator in asphalt binders with recycled asphalt shingles," *Under Review*, 2017.
- [13] LDOTD (Louisiana Department of Transportation and Development), "Louisiana standard specifications for roads and bridges," Baton Rouge, LA, 2006.
- [14] A. M. Hartman, M. D. Gilchrist and G. Walsh, "Effect of mixture compaction on indirect tensile stiffness and fatigue," *J. Transp. Eng.*, vol. 127, no. 5, 2001.
- [15] J. Bonnot, "Selection and use of the procedure for laboratory compaction of bitumen mixtures," *Performance Related Test Procedures for Bitumen Mixtures*, 1997.
- [16] Z. Wu, L. Mohammad, L. B. Wang and M. A. Mull, "Fracture Resistance Characterization of Superpave Mixture Using the Semi-Circular Bending Test," *Journal of ASTM International*, vol. 2, no. 3, 2005.

CHAPTER 7. EVALUATION OF SODIUM-ALGINATE HOLLOW FIBERS AS A REJUVENATING MECHANISM FOR ASPHALT BINDERS WITH RECYCLED MATERIALS

7.1 Introduction

The incorporation of recycled materials such as recycled asphalt shingles (RAS) and reclaimed asphalt pavement (RAP) into asphalt mixtures has emerged as a sustainable solution to reduce the negative impacts on the environment associated with the extraction, transportation, and construction of new pavement roads. In addition, the use of recycled materials could potentially preserve valuable landfill space and reduce the costs of new roads construction caused by the increase in aggregate and petroleum prices. However, the durability of asphalt mixtures containing recycled materials, which is related to the level of blending between aged and virgin asphalt binders, is the main concern of the pavement community and highway agencies.

Asphalt rejuvenating agents have emerged as a solution to improve the life expectancy of asphalt mixtures containing recycled materials by increasing the blending between aged and virgin asphalt binders. Asphalt rejuvenators include cationic emulsions containing maltenes, which are used to deposit the blend of maltene fractions on the films of aged binder [1]. Thus, the addition of maltene fractions might reverse the aging process of asphalt binder by restoring the maltene-to-asphaltene ratio [2]. However, spreading rejuvenator on the surface has negative effects such as loss of the skid resistance and poor penetration into the pavement [3].

The encapsulation of a rejuvenator product has emerged as an innovative approach to disperse the rejuvenator product into the asphalt mix. An encapsulation mechanism is used in sodium-alginate hollow fibers filled with a rejuvenator, which consists of a polymer shell and a rejuvenating product as the core material. It is a promising approach as it would enhance the

distribution of the rejuvenating product, and thus restoring the original properties of the aged binder in the recycled materials. Furthermore, the elastic property of polymer shell could potentially improve the performance of asphalt binder and asphalt mixtures against common distresses such as permanent deformation and cracking at low and intermediate temperature.

7.2 Objectives

The objectives of this study were the following: (1) Evaluate the rheological properties of asphalt binder blends with sodium-alginate hollow fibers filled with a rejuvenator through laboratory tests; and (2) Assess the molecular/fractional compositions of binder blends with hollow fibers through a series of chemical analysis. The effects of the hollow fibers on asphalt mixture healing and mechanical behaviors are presented in a separate paper [4].

7.3 Background

7.3.1 Recycled Materials in Asphalt Pavement

The manufacturing process of asphalt shingles includes air-blown asphalt, which results in a binder with greater viscosity than regular asphalt binder used in hot-mix asphalt (HMA) [5]. Previous studies have evaluated the effect of adding 5 to 10% recycled asphalt shingles (RAS) on the mechanical properties of asphalt mixtures compared to conventional mixtures without recycled materials [6, 7]. The results showed that the addition of RAS resulted in a decrease in the tensile strength and creep stiffness of the evaluated mixtures, but an improvement in the resistance to moisture damage. Yet, other studies have showed that RAS may negatively impact low temperature performance and the cracking resistance of asphalt mixtures [2].

Reclaimed asphalt pavement (RAP) is a processed asphalt pavement at the end of the service life. The addition of RAP in asphalt mixtures results in a decrease of virgin materials consumption such as aggregate and binder. Previous studies have shown that the addition of high percentages

of RAP, more than 20% by weight of the total mixture, resulted in an increase in the dynamic complex modulus compared to a conventional mixture, which may increase the cracking susceptibility of an asphalt mixture [8, 9]. In addition, Li et al. reported that the addition of RAP resulted in an increase in the low-temperature cracking susceptibility of asphalt mixtures compared to a virgin asphalt mixture [10].

7.3.2 Asphalt Rejuvenation

Asphalt rejuvenators products include low viscosity oil with high maltenes content, which has been shown to be the most effective treatment to partially restore asphalt properties [11]. A study evaluated the effect of asphalt rejuvenators on a binder classified as PG 58-22 by conducting a series of laboratory tests [12]. The study observed a softening effect with the addition of the evaluated rejuvenators, which resulted in a decrease in viscosity, increase in rutting susceptibility and enhancement against cracking. Similarly, another study concluded that the addition of rejuvenator products in asphalt mixtures containing recycled materials resulted in an improvement in the fatigue cracking resistance compared to conventional mixtures [13]. The softening effect of asphalt rejuvenators was also reported in a study conducted by Aguirre et al. where the addition of asphalt rejuvenators resulted in an increase in the rut depth of asphalt mixtures at high-temperature [14].

7.3.3 Encapsulation of Asphalt Rejuvenator Products

The idea of encapsulating a rejuvenator product is to control the release of the core material by controlling the permeability of the shell material. Sunflower oil, as a rejuvenator product, was encapsulated in double-walled microcapsules via in situ polymerization technique using polyurethane and urea-formaldehyde as shell materials [15]. Another study conducted an optimization process of the production parameters of microcapsules containing a bio-oil

rejuvenator product as core materials, which resulted in microcapsules with adequate thermal stability to resist high-temperatures in asphalt mixing processes [16].

Another technique to encapsulate an asphalt rejuvenator is the synthesis of hollow-fibers containing a rejuvenator product as core material. Tabakovic et al. developed compartment alginate fibers containing a rejuvenator as a healing agent delivery, as well as a healing triggering mechanism for asphalt pavements [17]. Furthermore, Aguirre et al. conducted an optimization process on the production parameters of sodium-alginate fibers containing a bio-oil product as core material as self-healing and rejuvenating agents for aged asphalt binder [18]. In addition, the study found that 5% fiber content by weight of virgin binder was the optimum fiber content to enhance rheological properties of binder blends containing extracted binder from recycled materials.

7.4 Experimental Program

7.4.1 Fiber's Synthesis and Properties

7.4.1.1 Chemicals. The core material of the fibers consisted of a green bio-oil product, from Sripath Technologies (density 0.919 g/cm³). The experimental program used sodium alginate as a shell material in the developed fibers. In addition, PEMA (ethylene-alt-maleic-anhydride) was added as a surfactant in a 2.5 wt % aqueous solution. Furthermore, ethylene glycol was incorporated in the present study as a plasticizer material. Lastly, the coagulation bath contained a 0.6 Molarity (M) solution of calcium chloride hexahydrate (CaCl₂·6H₂O).

7.4.1.2 Production of Fibers. Aguirre et al. optimized a synthesis procedure for sodium-alginate fibers containing a rejuvenator product [18]. The sodium-alginate fibers were synthesized from an oil-in-water emulsion containing the shell material and the core material. To this aim, a 5% wt% solution of sodium-alginate in de-ionized water was prepared. At the same time 2.5 wt%

polymeric surfactant solution, PEMA, was prepared by dissolving the copolymer in water at 70°C and mixing it for 60 min. A healing solution was prepared by mixing the rejuvenator product with 30% by weight of rejuvenator of PEMA solution. In addition, ethylene glycol was added to the healing solution in a proportion of 40% by weight of rejuvenator. The healing solution was mixed thoroughly. Then, the healing solution was mixed with the sodium alginate solution in 1/1.5 rejuvenator/sodium alginate proportion at 40 rpm for 20 sec. The emulsions were spun with a plunger-based lab scale wet spinning line in a conventional wet spinning process to form the rejuvenator-filled compartment fibers. More details on the synthesis procedure and spinning process can be found elsewhere [18].

7.4.2 Evaluation of the Rheological Properties of Asphalt Binder Blends with Fibers

The objective of the binder experiment was to evaluate the effects of adding sodium-alginate fibers on asphalt binder blends containing recycled materials. The experimental test matrix is shown in Table 7.1. Two binder types were selected to evaluate the effect of adding the synthesized fibers: unmodified and SBS-polymer modified binders (i.e., PG 64-22 and PG 70-22, respectively). In addition, extracted binder from recycled materials (RAS and RAP) were incorporated in the selected binder blends at 5 and 20% by weight of the virgin binder, respectively. Asphalt binder was extracted from the recycled materials in accordance with AASHTO T 164 [19]. Afterward, the solution obtained from AASHTO T 164 —Method A was distilled to a point where most of the solvent was removed and then carbon dioxide gas was introduced to remove all traces of trichloroethylene. This procedure was conducted in accordance with AASHTO R 59 [20]. The recovered asphalt binder was then blended with a virgin binder. The asphalt binder blends shown in Table 7.1 were prepared by mixing virgin binder with the prepared fibers and extracted binder at a temperature of 163°C. The different

asphalt blends were prepared by using a high-shear mixer rotating at a speed of 3,600 rpm for 30 minutes to achieve good mixing and dispersion of the fibers and extracted binder in the different asphalt binder blends.

7.4.2.1 Performance Grading (PG Grading). Rheological tests such as Dynamic Shear Rheometer (DSR) and Bending Beam Rheometer (BBR) were used to assess the rheological properties of the asphalt binder blends shown in Table 7.1. PG grading was performed in accordance with AASHTO M 320 [21].

7.4.2.2 Multiple Stress Creep Recovery (MSCR). The MSCR test was conducted to characterize the rutting susceptibility of the different asphalt binder blends. MSCR test consists of applying creep and recovery periods and to measure the percentage of recovery and non-recoverable creep compliance (J_{nr}). The MSCR was performed in accordance to AASHTO TP 70 at a testing temperature of 67°C [22].

7.4.2.3 Linear Amplitude Sweep (LAS). The fatigue resistance of the asphalt blends was characterized by conducting the LAS test. The LAS tests consisted of applying cyclic loading employing systematic, linearly increasing load amplitudes. The LAS was performed in accordance with AASHTO TP 101 [23] in samples aged using RTFO and PAV to simulate the aging for in-service asphalt pavements. LAS test was conducted to determine two fatigue parameters (“A” and “b”) based on the asphalt binder fatigue law ($N_f = A \times \gamma_{max}^b$). The LAS test consisted of two steps: (1) a frequency sweep test at a low strain amplitude of 0.1% is used to obtain undamaged material properties (parameter “b” of fatigue law); and (2) an amplitude sweep test with a series of cyclic loading at systematically linearly increasing strain amplitudes at a constant frequency of 10 Hz is used to determine the parameter “A” of the fatigue law through viscoelastic continuum damage (VECD) mechanics analysis.

Table 0.1. Test Matrix for Evaluation of the Effects of Adding Sodium-Alginate Fibers in Asphalt Binder Blends

Blend ID	Asphalt Binder	RAS Content	RAP Content	Fiber Content (%)
70CO	PG 70-22	-	-	-
70PG3F	PG 70-22	-	-	3%
70PG5F	PG 70-22	-	-	5%
70PG10F	PG 70-22	-	-	10%
70PG5P	PG 70-22	5% PCWS	-	-
70PG5P5F	PG 70-22	5% PCWS	-	5%
70PG20RAP	PG 70-22	-	20%	-
70PG20RAP5F	PG 70-22	-	20%	5%
70PG5P20RAP	PG 70-22	5% PCWS	20%	-
70PG5P20RAP5F	PG 70-22	5% PCWS	20%	5%
64CO	PG 64-22	-	-	-
64PG3F	PG 64-22	-	-	3%
64PG5F	PG 64-22	-	-	5%
64PG10F	PG 64-22	-	-	10%
64PG5P	PG 64-22	5% PCWS	-	-
64PG5P5F	PG 64-22	5% PCWS	-	5%
64PG20RAP	PG 64-22	-	20%	-
64PG20RAP5F	PG 64-22	-	20%	5%
64PG5P20RAP	PG 64-22	5% PCWS	20%	-
64PG5P20RAP5F	PG 64-22	5% PCWS	20%	5%

7.4.3 Chemical Analysis of Asphalt Binder Blends with Fibers

7.4.3.1 High-Pressure Gel Permeation Chromatography. High Pressure Gel Permeation

Chromatography (HP-GPC) was performed using an EcoSEC system (HLC-8320GPC) of Tosoh Corporation, equipped with a differential refractive index detector (RI) and UV detector. A set of four micro-styragel columns of pore sizes 200 Å, 75 Å (2 columns) and 30 Å from Tosoh Bioscience was used for the analysis. Tetrahydrofuran (THF) at a flow rate of 0.35 mL/ min. was used as the solvent. Columns were calibrated using polystyrene standard mixtures PStQuick B (MW= 5480000, 706000, 96400, 10200, and 1000 daltons), PStQuick E (MW= 355000, 37900, 5970, and 1000 daltons), and PStQuick F (MW= 190000, 18100, 2500, and 500 daltons) from

Tosoh Bioscience. Filtered solutions prepared with the binder blends and THF solvent were prepared using a 0.45-micron Teflon filters prior to running the HP-GPC test analysis. The concentration of asphalt solution was 0.5%.

7.4.3.2 Fourier Transform Infrared Spectroscopy (FTIR). FTIR spectra were obtained using a diamond single reflection attenuated total reflectance (ATR) instrument (Bruker Optics alpha) with the following settings for data collection: 32 scans/sample, spectral resolution 4 cm⁻¹, wave number range 4000-500 cm⁻¹. A few drops of the GPC asphalt solution (0.5% in THF) was placed on the ATR crystal plate and the solvent allowed evaporating. The spectrum was collected after the complete evaporation of the solvent. FTIR spectra of the aged samples show a peak around 1700 cm⁻¹, which is the characteristic of C=O species. The carbonyl index was calculated from the band areas measured from valley to valley [24] according to Equation (7.1). This was accomplished using the OPUS spectroscopy software provided with the Bruker FTIR instrument.

$$\text{Carbonyl Index (ICO)} = \frac{\text{Area around } 1700 \text{ cm}^{-1}}{\text{Area around } 1460 \text{ cm}^{-1} \text{ and Area around } 1375 \text{ cm}^{-1}} \quad (7.1)$$

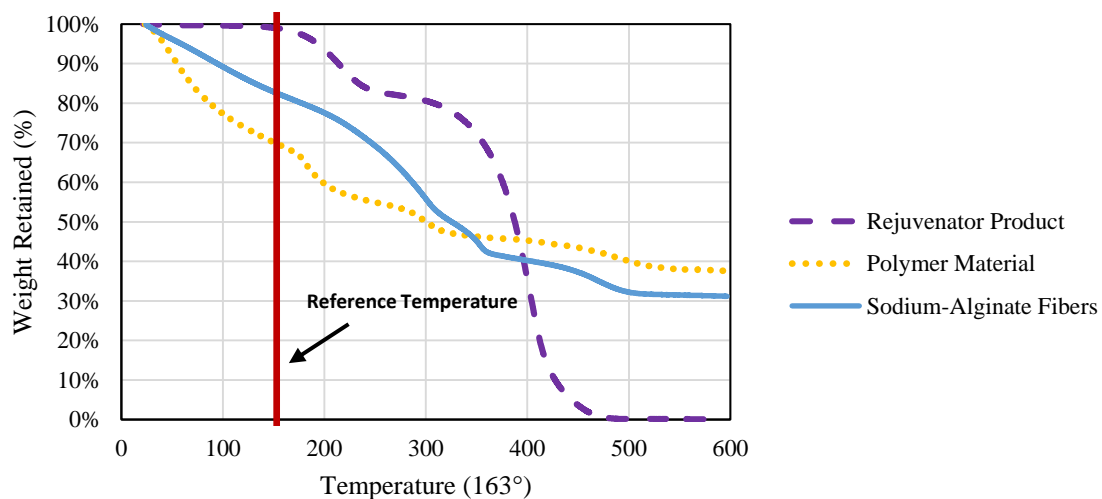
7.5 Results and Analysis

7.5.1 Hollow-Fibers with Rejuvn8 as Core Material

A Thermogravimetric analysis (TGA) was conducted on the prepared fibers to evaluate the resistance to high-temperatures during asphalt mixing processes. Figure 7.1(a) shows the change in weight (%) as temperature was increased for the core material, shell material, and the produced sodium-alginate fibers. A reference temperature of 163°C was selected to analyze TGA results based on the temperature typically used to prepare asphalt binder blends and HMA mixtures. Figure 7.1(a) shows that the prepared fibers absorbed water during the synthesis

procedure as an 18.5% decrease in weight at the reference temperature is observed. Furthermore, it is shown in Figure 7.1(a) that the produced fibers degraded at a temperature (above 300°C) higher than the one used in an asphalt mixture production based on a 50% reduction in the sample's weight.

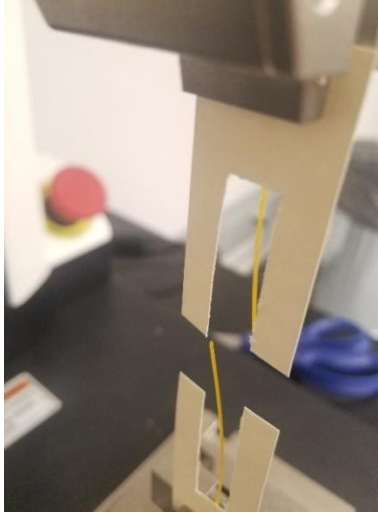
The resistance of breakage of the produced fibers during asphalt mixing process was evaluated by conducting a pull test. Figure 7.1(b) shows a broken sodium-alginate fiber after conducting a tensile test for strength evaluation. Based on the literature, asphalt additives should have an ultimate tensile strength (UTS) higher than 12 MPa to resist typical pressure during asphalt mixing processes [25, 26]. The tensile strength of the produced fibers was determined to be 28.4 MPa with a standard deviation of ± 3.7 MPa. Thus, the produced hollow-fibers should be suitable to resist the blending process for the preparation of the evaluated binder blends in this study.



(a)

Figure 0.1. Fibers with Optimum Parameters (a) TGA Test Results of Fiber's Material Composition, and (b) Broken Fiber after Tensile Test

Figure 7.1. Cont'd



(b)

7.5.2 Chemical Composition of Binder Blends with Fibers

7.5.2.1 Molecular Weight Distribution. HP-GPC was used to measure asphalt blends molecular weight distributions, i.e., the percentage of asphaltenes to maltenes that are present in the binder blends. Determining the percentage of asphaltenes and maltenes before and after blending the virgin binders with recycled materials and fibers provided information about the efficiency of the fibers to act as a rejuvenator. The HP-GPC results are shown in Table 7.2. The maltenes, Low-Molecular Weight (LMW), were defined as the molecules with a weight less than 3k Daltons; asphaltenes, High-Molecular Weight (HMW), were defined as the molecules between 3k and 19k Daltons; polymer and other components, were defined as the molecules with weight greater than 19k Daltons [27]. Table 7.2 shows that the extracted binders from RAS and RAP had the highest high-molecular weight/ low-molecular weight ratio (HMW/LMW) among the evaluated binder blends. Furthermore, it is shown in Table 7.2 that the addition of sodium-alginate fibers resulted in an increase in the HMW/LMW ratio. Asphalt rejuvenators are known to facilitate the extraction of the asphaltenes from the recycled materials and to improve the blending between

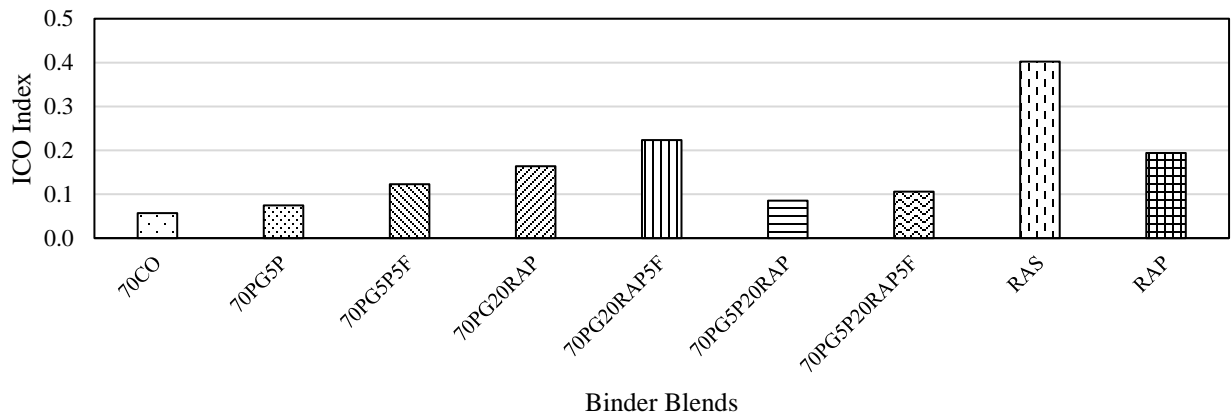
aged and virgin binder [2]. Thus, the increase in the HMW/LMW ratio suggests the release of the rejuvenating product from the hollow fibers in the evaluated binder blends.

Table 0.2. Chemical Composition of Evaluated Binder Blends

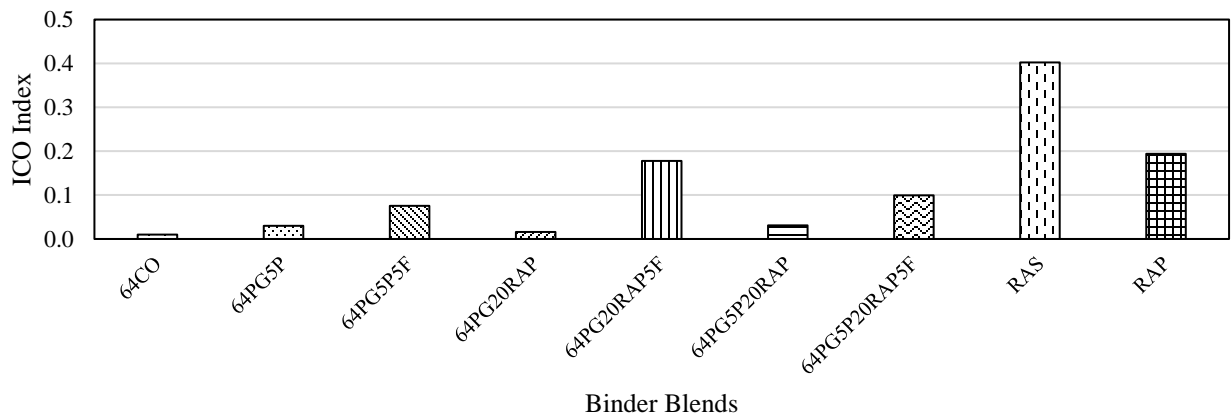
Sample	Others (%)	HMW (%)	LMW (%)	HMW/LMW Ratio
70CO	4.92	21.73	73.35	0.30
70PG5P	6.42	22.82	70.76	0.32
70PG5P5F	6.71	23.33	69.59	0.34
70P20RAP	6.28	23.73	70.26	0.34
70PG20RAP5F	5.38	26.19	70.89	0.37
70PG5P20RAP	6.81	22.31	70.89	0.31
70PG5P20RAP5F	6.7	21.96	71.34	0.31
64CO	0.52	17.35	82.13	0.21
64PG5P	1.82	23.63	74.55	0.32
64PG6P5F	1.9	24.8	73.3	0.34
64PG20RAP	3.44	25.35	71.21	0.36
64PG20RP5F	3.33	23.46	70.89	0.33
64PG5P0RAP	3.83	23.94	72.23	0.33
64PG5P20RAP5F	4.14	24.61	71.2	0.35
RAS	8.1	26.69	65.21	0.41
RAP	13.31	30.31	56.38	0.54

7.5.2.2 Characterization of Oxidative Asphalt Aging. The carbonyl Index (ICO) was calculated to evaluate the formation of carbonyl molecules in the binder blends, which is related to the oxidation process in the aging process of asphalt binders. Figure 7.2(a) shows that the addition of extracted binder from either RAS and/or RAP resulted in an increase in the ICO index. Also, it is shown that the addition of fibers in blends containing recycled material resulted in an increase in the ICO, which suggests that the rejuvenating product facilitates the extraction of aged binder from the recycled materials and thus, increased the asphaltene content resulting in stiffer blends. Figure 7.2(b) shows that the overall ICO indices for blends prepared with binder PG 70-22 were higher than the ICO index for blends prepared with binder PG 64-22. The higher ICO indices

suggest that binder PG 70-22 would be more susceptible to aging compared to a softer binder such as PG 64-22. In addition, a similar trend was observed with the addition of fibers as the ICO index increased compared to the blends containing recycled materials, which is related to the increase in the HMW/LMW ratios observed in the HP-GPC test results.



(a)



(b)

Figure 0.2. ICO Aging Index for (a) Binder PG 70-22 and (b) Binder PG 64-22

7.5.3 Rejuvenation of Asphalt Binders with Sodium-Alginate Fibers

7.5.3.1 PG Grading of Binder Blends. Table 7.3(a) presents the measured PG Grading of the asphalt binder blends prepared with binder PG 70-22 based on laboratory testing conducted using a Dynamic Shear Rheometer (DSR) and Bending Beam Rheometer (BBR). Table 7.3(a) shows that the addition of the hollow fibers did not change the PG grading of the virgin binder, 70CO; yet, a decrease in the low-temperature performance grade (LTPG) was observed with the addition of 3, 5 and 10% fiber contents compared to the virgin binder. The same decrease in the LTPG was observed in the binder blends 70PG5P5F and 70PG20RAP5F with the addition of hollow fibers.

Table 7.3(a) also shows that the addition of the extracted binder from PCWS and/or RAP resulted in an increase in the PG grading compared to the virgin binder from PG 70-22 to PG 76-22 (70PG5P); PG 82-16 (70PG20RAP); and PG 88-16 (70PG5P20RAP). The increase in the high temperature grade of the binder blends containing recycled materials may be due to the increase in asphaltene contents from the recycled materials as observed in the HP-GPC test results. Based on the PG grading results, the addition of the developed fibers did not seem to enhance the final PG of the binder blends except for blend 70PG5P20RAP5F. Yet, the marginal effect of the hollow fibers on the PG grading of the binder blends was expected based on the increase in HMW/LMW ratios and ICO Index on the chemical analysis test results. However, the continuous PG showed a reduction in the HTPG in the binder blends containing the hollow fibers, which may indicate a softening effect of the aged binders from recycled materials except for 70PG5P5F.

The results of the PG grade for the binder blends prepared with binder PG 64-22 are presented in Table 7.3(b). Similar to the results of PG 70-22, the addition of the hollow fibers did not change

the PG grade of the binder blends prepared with PG 64-22 except for 64PG5P20RAP5F, which was the stiffest binder blend. The PG grading of blend 64PG5P20RAP5F could be correlated with the HP-GPC test results as this blend had the second highest HMW/LMW ratio for blends prepared with PG 64-22 shown on Table 7.2. However, similar to binder PG 70-22, the continuous PG showed a reduction in the HTPG for the binder blends containing the hollow fibers, which may indicate softening of the aged binders. Also, it was noted in the continuous PG grading that the LTPG improved in the binder blends with sodium-alginate fibers, which may indicate an improvement in the low-temperature performance of the binder blends containing only extracted binder from recycled materials.

Table 0.3. Summary of PG Grading Results for: (a) Binder PG 70-22 and (b) Binder PG 64-22

(a) Binder PG 70-22

Binder Blend	PG-Grading	Continuous PG-Grading	UTI
70CO	70-22	73.8-27.4	101
70PG3F	70-22	73.3-24.4	98
70PG5F	70-22	73.7-23.2	98
70PG10F	70-22	73.3-24.5	98
70PG5P	76-22	78.2-25.3	104
70PG5P5F	76-22	79.7-24.1	104
70PG20RAP	82-16	87.3-21.9	109
70PG20RAP5F	82-16	85.4-20.4	106
70PG5P20RAP	88-16	88.8-18.2	107
70PG5P20RAP	82-16	85.9-20.6	107

Table 7.3. Cont'd

(b) Binder PG 64-22

Binder Blend	PG-Grading	Continuous PG-Grading	UTI
64CO	64-22	68-23.6	92

64PG3F	64-22	68-24.4	92
64PG5F	64-22	69.5-23.8	93
64PG10F	64-22	67-23.7	91
64PG5P	70-22	71.8-22.3	94
64PG5P5F	70-22	70.3-22.6	93
64PG20RAP	76-16	81.8-16.8	99
64PG20RAP5F	76-16	80.8-19.4	100
64PG5P20RAP	76-16	81.8-18.0	100
64PG5P20RAP5F	82-16	82.4-18.0	100

7.5.3.2 Multiple Stress Creep Recovery. The MSCR test results for binder PG 70-22 are shown in Table 7.4(a). It is shown in Table 7.4(a) that the addition of 3 and 5% fiber content increased the rutting susceptibility as the non-recoverable creep compliance increased and the percentage of recovery decreased compared to the virgin binder 70CO. However, it can be observed that the addition of 10% fiber content enhanced the rutting performance as the non-recoverable creep compliance decreased compared to the virgin binder. In addition, Table 7.4(a) shows that the addition of extracted binder from recycled materials improved the rutting resistance of the virgin binder (70CO) as the non-recoverable creep compliance values decreased at both stress levels and an improvement in the percentage of recovery was also observed. The increase in the non-recoverable creep compliance of the binder blends containing recycled materials with the addition of the hollow-fibers suggests a release of the rejuvenator product from the fibers during the blending process, which is supported by the increase in the HMW/LMW ratios and ICO Index observed in the chemical analysis test results shown in Table 7.2 and Figure 7.2.

The MSCR test results for binder PG 64-22 are shown in Table 7.4(b). Similar to binder PG 70-22, the binder blends containing extracted binder from recycled materials showed a decrease in the non-recoverable creep compliance and an increase in the percentage recovery, which indicate an improved rutting resistance compared to the virgin binder PG 64-22. Also, a softening effect

from the release of the rejuvenating product from the hollow fibers was observed in Table 7.4(b) as noted from the increase in the non-recoverable creep compliance. The reduction in the percentage recovery of the blends containing sodium-alginate fibers could be related to the lack of time to fully recover due to the time-dependent behavior of asphalt binders.

Overall, MSCR test results suggest that the addition of sodium-alginate fibers and extracted binder from recycled materials resulted in an improved performance against permanent deformation compared to the conventional virgin binder.

Table 0.4. MSCR Test Results for: (a) Binder PG 70-22 and (b) Binder PG 64-22

(a) Binder PG 70-22

Asphalt Binder Blends	MSCR				
	$J_{nr0.1}$ @ 67 °C, kPa ⁻¹	$J_{nr3.2}$ @ 67 °C, kPa ⁻¹	%J _{nr} diff	% Recovery	
				Stress, 0.1 kPa	Stress, 3.2 kPa
70CO	0.80	1.20	48.82	49.10	30.17
70PG3F	1.15	1.59	55.15	32.95	14.78
70PG5F	1.02	1.42	38.38	35.20	16.82
70PG10F	0.66	0.88	32.67	38.60	22.40
70PG5P	0.64	0.90	41.52	45.47	28.36
70PG5P5F	0.66	0.95	43.69	42.40	24.10
70PG20RAP	0.20	0.26	31.58	59.54	48.75
70PG20RAP5F	0.24	0.32	31.97	53.55	41.65
70PG5P20RAP	0.13	0.18	31.38	63.57	53.78
70PG5P20RAP	0.26	0.36	34.89	55.13	42.34

(b) Binder PG 64-22

Asphalt Binder Blends	MSCR				
	$J_{nr0.1}$ @ 67 °C, kPa ⁻¹	$J_{nr3.2}$ @ 67 °C, kPa ⁻¹	%J _{nr} diff	% Recovery	
				Stress, 0.1 kPa	Stress, 3.2 kPa
64CO	3.47	3.77	8.65	1.62	-0.50

Table 7.4. Cont'd

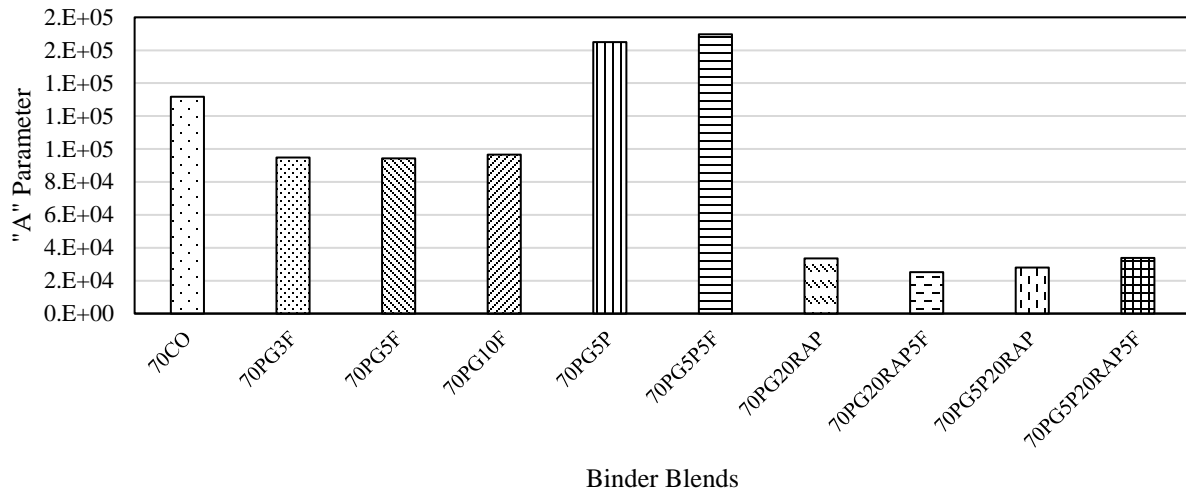
Asphalt Binder Blends	$J_{nr0.1}$ @ 67 °C, kPa ⁻¹	$J_{nr3.2}$ @ 67 °C, kPa ⁻¹	%J _{nr} diff	Stress, 0.1 kPa	Stress, 3.2 kPa
-----------------------	--	--	-----------------------	-----------------	-----------------

	kPa ⁻¹				
64PG3F	3.76	4.11	9.15	1.26	-0.72
64PG5F	3.63	4.00	10.49	1.85	-0.65
64PG10F	4.36	4.85	11.25	1.44	-1.04
64PG5P	2.32	2.60	12.31	4.86	0.58
64PG5P5F	2.54	2.89	13.90	4.99	0.42
64PG20RAP	0.43	0.49	15.00	21.80	13.59
64PG20RAP5F	0.51	0.59	43.12	20.85	11.86
64PG5P20RAP	0.45	0.51	15.93	22.36	13.17
64PG5P20RAP5F	0.38	0.45	16.18	24.41	14.82

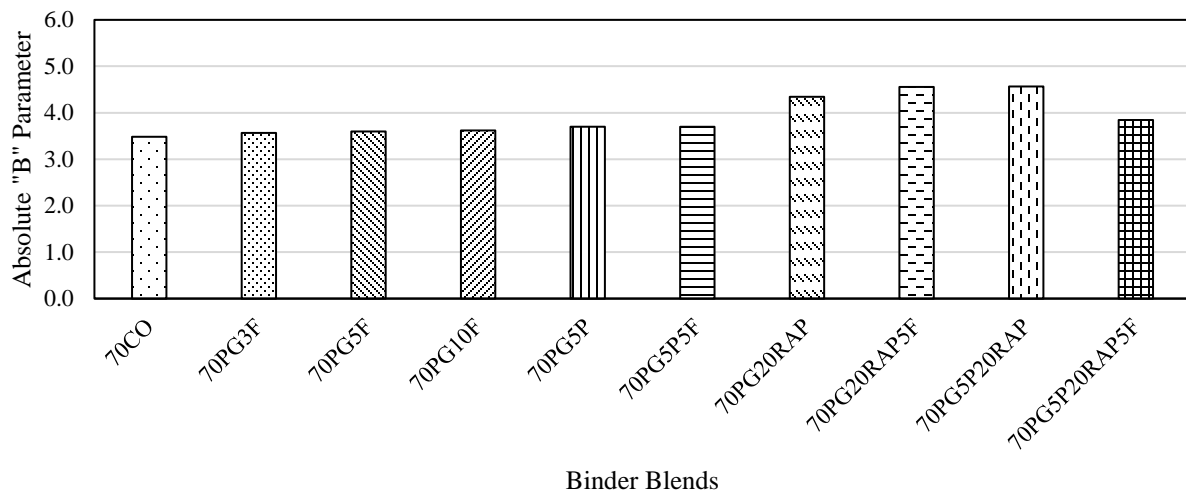
7.5.3.3 Linear Amplitude Sweep. Figure 7.3 shows the LAS test results for binder blends prepared with PG 70-22. Figure 7.3(a) shows that the addition of hollow fibers to the virgin binder resulted in a decrease in the “A” parameter, which indicates a reduction in the elastic behavior of the binder. Interestingly, it is shown that the addition of extracted binder from RAS enhanced the resistance to damage in blend 70PG5P compared to the virgin binder. The enhancement in the A parameter with the addition of RAS could be due to the presence of polymer in the RAS source as shown in Table 7.2. The opposite behavior was observed with the addition of RAP as the “A” parameter decreased compared to the virgin binder. The used RAP in this study presented the highest HMW/LMW ratio, which could have affected the elastic property of the virgin binder in blends 70PG20RAP and 70PG20RAP5F. The addition of hollow fibers in blends 70PG5P5F and 70PG5P20RAP5F resulted in binder blends with better elastic properties during the loading cycles compared to the virgin binder as an increase in the “b” parameter was observed. Figure 7.3(b) shows that the addition of RAP in blends 70PG20RAP and 70PG5P20RAP increased the sensitivity of the virgin binder to the change in strain level. Results from Figure 7.3(b) also shows that binder blends containing sodium-alginate fibers would have a similar deterioration rate as the strain level was increased compared to the virgin binder PG 70-22.

The opposite trend was observed with binder blends prepared with PG 64-22. Figure 7.4(a) shows that the addition of 5 and 10% fiber content in virgin binder enhanced the elastic properties of virgin binder PG 64-22 as the “A” parameter increased. Also, it is shown that the addition of aged binder from either RAS or RAP would result in a binder blend more susceptible to cracking as a decrease in the “A” parameter was observed for blends 64PG5P, 64PG20RAP and 64PG5P20RAP compared to the virgin binder. However, the addition of the hollow fibers partially reversed the negative impact of adding an aged binder and the ability of binder blends 64PG5P5F and 64PG20RAP5F to resist fatigue damage. Yet, Figure 7.4(b) shows that the addition of fibers did not have a pronounced effect on improving the susceptibility of blends to a change in strain levels as the calculated “b” parameter was equal to or higher than the virgin binder PG 64-22.

Overall, Figure 7.3(b) and Figure 7.4(b) shows that addition of SBS polymer in binder PG 70-22 resulted in a decrease in the absolute value of b parameter, which indicates that binder PG 70-22 would have a lower deterioration rate than binder PG 64-22. In addition, Figure 7.3 and Figure 7.4 shows that the high HMW/LMW ratios and high percentage content of RAP utilized in the study may explain the increase in fracture susceptibility of blends containing RAP as observed in the “A” parameter and absolute “b” parameter values in the LAS test results. Also, the polymer content in RAS (i.e. based on HP-GPC test results) and low percentage content of RAS (i.e. 5%) utilized in the blends could have reduced the negative impact in the fracture susceptibility of blends containing RAS compared to blends containing RAP.

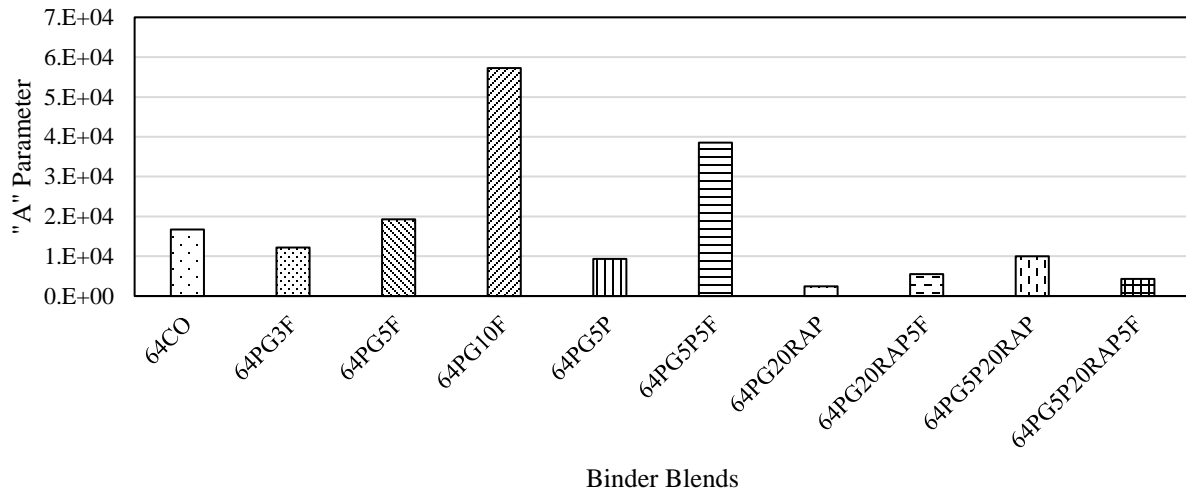


(a)

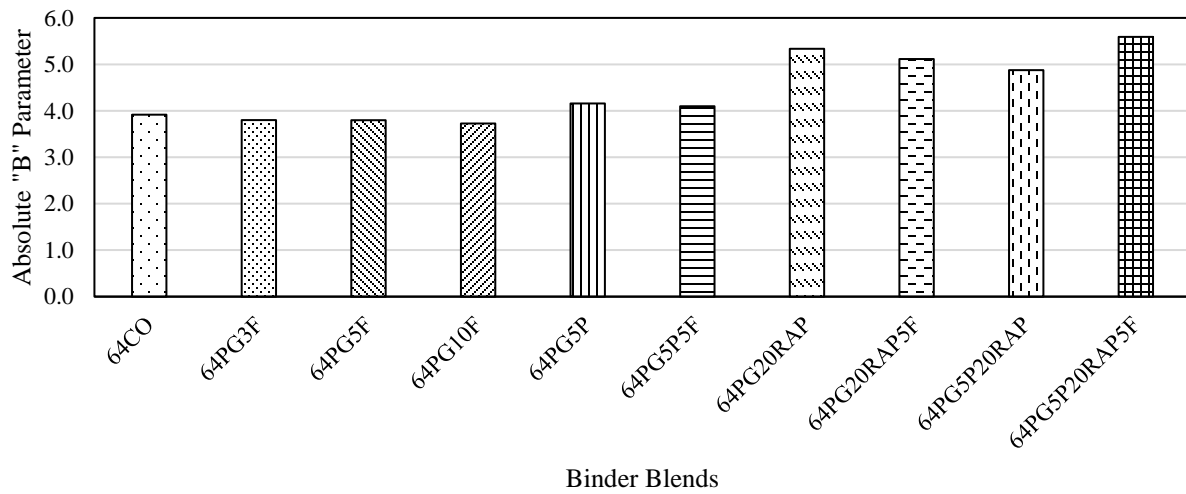


(b)

Figure 0.3. LAS Test Results for Binder PG 70-22: (a) "A" Parameter Fatigue Law and (b) Absolute "B" Parameter Fatigue Law



(a)



(b)

Figure 0.4. LAS Test Results for Binder PG 64-22: (a) "A" Parameter Fatigue Law and (b) Absolute "B" Parameter Fatigue Law

7.6 Summary and Conclusions

The objectives of this study were to evaluate the rheological properties of asphalt binder blends prepared with hollow fibers through laboratory tests, and to assess the chemical compositions of binder blends with fibers through a series of chemical analysis. The following findings and conclusions are drawn based on the results of the experimental program:

With respect to the effects of the fibers on the chemical composition of asphalt binder:

HP-GPC test results showed that the addition of fibers in blends containing recycled materials resulted in an increase in the HMW/LMW ratio. The increase of the asphaltene fraction suggests that some fibers were broken during the blending process, which released the core material and facilitate the blending between aged and virgin binder in the blends.

FTIR results showed that the addition of extracted binder from either RAS and/or RAP resulted in an increase in the ICO index. The addition of fibers in blends containing recycled material also resulted in an increase in the ICO, which suggests that the rejuvenating product facilitates the extraction of aged binder from the recycled materials and thus, increased the asphaltene content resulting in stiffer blends.

With respect to the effects of the fibers on the rheological properties of asphalt binder:

Rheological properties of the binder blends containing recycled materials and sodium-alginate fibers suggested that the fibers did not have a noticeable effect on the final PG grade.

MSCR test results showed that a binder blend with extracted binder from recycled materials and sodium-alginate fibers would have less rutting susceptibility than a conventional virgin binder would.

LAS test results showed that the hollow fibers recovered some of the elastic behavior lost due to the addition of aged binder from RAS and/or RAP. However, the addition of fibers in virgin binders resulted in a decrease in the “A” parameter of the fatigue law except with 10% fiber content in binder PG 64-22.

7.7 References

- [1] J. Brownride, "The role of an asphalt rejuvenator in pavement preservation: use and need for asphalt rejuvenation," Tricor Refining, LLC.
- [2] G. Holleran, T. Wieringa and T. Tailby, "Rejuvenation treatments for aged pavements," Transit New Zealand and New Zealand Institute Technology (NZIHT), 2006.
- [3] C. Chiu and M. Lee, "Effectiveness of seal rejuvenators for bituminous pavement surfaces," J. Test. Eval., vol. 34, pp. 390-394, 2006.
- [4] M. A. Aguirre, M. Hassan, s. SHIRZAD, S. B. Cooper and L. Mohammad, "Testing of Self-Healing Fibers in Asphalt Mixutres Prepared with Recycled Materials," Under Review, 2018.
- [5] K. Y. Foo, D. I. Hanson and T. A. Lynn, "Evaluation of roofing shingles in hot mix asphalt," Journal of Materials in Civil Engineering, vol. 11, pp. 15-20, 1999.
- [6] J. W. Button, D. Williams and J. A. Scherocman, "Shingles and toner in asphalt pavements," Federal Highway Administration (FHWA) (Rep. No. FHWA/TX-96/1344-2F), College Station, TX, 1996.
- [7] M. A. Elseifi, S. Salari, L. N. Mohammad, M. Hassan, W. Daly and S. Dessouky, "A new approach to recycle asphalt shingles in hot mix asphalts," Journal of Materials in Civil Engineering, vol. 24, no. 11, pp. 1403-1411, 2012.
- [8] J. S. Daniel and A. Iachance, "Mechanistic and Volumetric Propertoes of Asphalt Mixtures with RAP," Journal of Transportation Research Board, 2005.
- [9] A. Shah, R. S. McDaniel, G. A. Huber and V. Gallivan, "Investigation of Properties of Plant-Produced Reclaimed Asphalt Pavement Mixtures," Journal of the Transportation Research Board, 2007.
- [10] X. Li, M. O. Marasteanu, R. C. Williams and T. R. Clyne, "Effect of Reclaimed Asphalt Pavement (Proportion and Type) and Binder Grade on Asphalt Mixtures," Journal of the Transportation Research Board 2051, 2008.

- [11] R. Karlsson and U. Isacson, "Material-related aspects of asphalt recycling-state of the art," *Journal of Materials in Civil Engineering*, vol. 18, 2006.
- [12] A. Booshehrian, W. S. Mogawer and S. Vahidi, "Evaluating the Effect of Rejuvenators on the Degree of Blending and Performance of High RAP, RAS, RAP/RAS Mixtures," *Road Materials and Pavement Design*, 2013.
- [13] J. Shen, S. Amirkhanian and J. Aune Miller, "Effects of rejuvenating agents on Superpave mixtures containing reclaimed asphalt pavement," *Journal of Materials in Civil Engineering*, vol. 19, no. 5, pp. 376-384, 2007.
- [14] M. A. Aguirre, M. M. Hassan, S. Shirzad, L. N. Mohammad and S. B. Cooper, "Performance of asphalt rejuvenators in hot-mix asphalt containing recycled asphalt shingles," *Transportation Research Record*, vol. 2633, pp. 108-116, 2017.
- [15] S. Shirzad, M. M. Hassan, M. A. Aguirre, L. N. Mohammad and W. H. Daly, "Evaluation of sunflower Oil as a Rejuvenator and Its Microencapsulation as a Healing Agent," *J. Mater. Civil. Eng.*, 2016.
- [16] M. A. Aguirre, M. M. Hassan, S. Shirzad, W. H. Daly and L. N. Mohammad, "Micro-encapsulation of asphalt rejuvenators using melamine-formaldehyde," *Construction and Building Materials*, vol. 114, pp. 29-39, 2016.
- [17] A. Tabakovic, L. Schuyffel, A. Karac and E. Schlangen, "An evaluation of the efficiency of compartmented alginate fibers encapsulating a rejuvenator as an asphalt pavement healing system," *Applied Science*, vol. 7, no. 647, 2017.
- [18] M. A. Aguirre, M. M. Hassan, S. Shirzad, S. B. Cooper, I. I. Negulescu and L. N. Mohammad, "Evaluation of hollow-fibers encapsulating a rejuvenator in asphalt binders with recycled asphalt shingles," *Under Review*, 2017.
- [19] AASHTO, "Standard method of test for quantitative extraction of asphalt binder from hot mix asphalt HMA," AASHTO T164, Washington, DC, 2014.
- [20] AASHTO, "Standard practice for recovery of asphalt binder from solution by Abson method," AASHTO R59, Washington, DC, 2011.
- [21] AASHTO, "Standard specification for performance-graded for asphalt binder," AASHTO M320, Washington, DC, 2015.
- [22] AASHTO, "Standard Method of Test for Multiple Stress Creep Recovery (MSCR) Test of Asphalt Binder Using a Dynamic Shear Rheometer (DSR)," AASHTO TP 70, Washington, DC, 2013.

- [23] AASHTO, "Standard Method of Test for Estimating Fatigue Resistance of Asphalt Binders Using the Linear Amplitude Sweep," 2016.
- [24] G. Liu, E. Nielsen, J. Komacka, G. Leegwater and M. Ven, "Influence of the soft bitumen on the chemical and rheological properties of reclaimed polymer-modified binders from the "old" surface-layer asphalt," *Construction Building Material*, vol. 79, pp. 129-135, 2015.
- [25] A. M. Hartman, M. D. Gilchrist and G. Walsh, "Effect of mixture compaction on indirect tensile stiffness and fatigue," *J. Transp. Eng.*, vol. 127, no. 5, 2001.
- [26] J. Bonnot, "Selection and use of the procedure for laboratory compaction of bitumen mixtures," *Performance Related Test Procedures for Bitumen Mixtures*, 1997.
- [27] W. H. Daly, I. I. Negulescu and S. Balamurugan, "Implementation of GPC characterization of asphalt binders at Louisiana Materials Laboratory," *Project Capsule 10-6B*, 2013.

CHAPTER 8. SUMMARY AND CONCLUSIONS

Self-healing asphalt concrete through encapsulation of asphalt rejuvenator products in microcapsules and hollow-fibers is a promising technology that could potentially address the infrastructure deterioration problem by adding durability and reducing the costly maintenance and repairs needed for asphalt pavement structures. Before this technology is to be applied on asphalt pavement infrastructure, there are several questions that needed to be answered, such as the identification of the core material for the microcapsules and hollow-fibers that could potentially reverse the aging process in asphalt binders, and the effect of the addition of microcapsules and hollow-fibers on the intrinsic asphalt concrete material properties and self-healing potential.

To address these questions, the objectives of this study were to: (a) Evaluate the effects of asphalt rejuvenators on hot-mix asphalt mixtures in order to test its effects in the fundamental engineering properties of the mixtures; (b) Develop a synthesis procedure for production of microcapsules and hollow-fibers containing an asphalt rejuvenator; and (c) Evaluate the short-term healing efficiency of such microcapsules and hollow-fibers in asphalt mixtures under two different curing conditions.

8.1 Evaluation of Asphalt Rejuvenators on HMA Mixtures

The first part of the study was dedicated to evaluate different asphalt rejuvenator products on HMA mixtures in order to test its effects on the fundamental properties of the mixtures. The asphalt rejuvenators evaluated included one bio-oil and three synthetic-oils. Sunflower seed oil was selected as a bio-oil, based on availability and economic advantages. The synthetic rejuvenators, Rejuvn8, Cargill1252 and Cargill1253, were selected based on suggested properties, such as compatibility with asphalt binder, a high rejuvenation ability, and improved

low temperature properties of the aged binder. The mechanical engineering properties of HMA mixtures were measured by conducting a series of laboratory tests such as dynamic complex modulus, Semi-Circular Bending test, and the Hamburg Wheel Tracking Device test. In addition, the molecular composition and rheological properties of extracted binder from evaluated mixtures were studied using High-Pressure Gel Permeation Chromatography and Superpave Performance Grade grading, respectively.

Results indicated that the use of recycled material, RAS, improved the permanent deformation susceptibility compared to a conventional asphalt mixture. Although, the combination of adding recycled materials and rejuvenator products slightly decreased the performance against rutting. Also, the results showed that the addition of recycled materials and rejuvenator products did not adversely affect moisture susceptibility of the evaluated asphalt mixtures. The susceptibility of the evaluated asphalt mixtures to fracture at intermediate temperature increased with the addition of RAS and asphalt rejuvenators as SCB test results showed lower J_c values than the minimum threshold value (0.5 kJ/m^2). The chemical analysis test results showed that the synthetic oil, Cargill 1253, restored the asphaltenes/maltenes ratio compared to the virgin binder indicating a reverse in the aging process from the addition of a recycled material.

8.2 Development of Self-Healing Mechanisms for Asphalt Pavement

8.2.1 Synthesis of Double-Walled Microcapsules containing a Rejuvenator Product

This part of the study was dedicated to modify a synthesis procedure for the production of double-walled microcapsules containing a rejuvenator product. The double-walled microcapsules were synthesized via in-situ polymerization, using polyurethane and urea-formaldehyde as shell materials. In-situ polymerization technique was selected given its low cost and simple

encapsulation procedure. Microcapsule properties such as size, encapsulation efficiency and thermal resistance of the produced microcapsules were characterized.

The production parameters for the synthesis procedure of double-walled microcapsules were an agitation rate of 1000 rpm, a heating temperature of 55°C, and a reaction time of 4 hr. The modified synthesis procedure produced microcapsules with an average diameter of 152.91 µm and an encapsulation efficiency of 63.2%. In addition, the produced double-walled microcapsules showed good thermal properties at mixing temperature (i.e. 163°C) where the thermal gravimetric analysis showed a decrease of less than 8% of microcapsule's weight. The thermal gravimetric analysis showed that the produced microcapsules would start deterioration at a temperature higher than 300°C as the weight started to decrease by 50%.

8.2.2 Synthesis of Hollow-Fibers containing a Rejuvenator Product

An optimization process of the production parameters for the synthesis procedure to produce hollow-fibers containing a rejuvenator product was conducted. In addition, a characterization of hollow-fibers properties such as thermal stability and tensile strength were evaluated with the variation of the production parameters. The production parameters investigated in the optimization process included the percentage of emulsifier, percentage of plasticizer and the amount of rejuvenator used. The hollow-fibers were synthesized via wet-spinning process from an oil-in-water emulsion containing the shell material and the core material. Sodium alginate was selected as the shell material because it provides suitable properties such as water solubility, fast coagulation in the presence of divalent ions, and adequate mechanical properties.

The results of the optimization of the production parameters for the synthesis of fibers indicated that fibers prepared with a rejuvenator to shell material of 1:1.5, an emulsifier content of 30%, and a plasticizer content of 40% produced hollow-fibers containing a rejuvenator product with

optimum thermal and mechanical properties as the TGA test results showed a good thermal stability at the mixing temperature (i.e., 163°C) with a weight retained percentage of 81.5%. In addition, these produced fibers had sufficient tensile strength (28.4 MPa) to resist the mixing and compaction processes of a HMA mixture.

8.3 Evaluation of Self-Healing Properties of the Developed Self-Healing Mechanisms

8.3.1 Self-Healing Efficiency of Double-Walled Microcapsules containing a Rejuvenator Product

Self-Healing asphalt concrete was investigated through microencapsulated asphalt rejuvenator. The experimental matrix investigated the effect of 5% microcapsules content added in asphalt mixtures containing recycled asphalt shingles. The healing efficiency of produced microcapsules was quantified as a function of time by measuring the width of an induced crack in beam specimens before healing (day 0), and at day 1, day 2, day 3 and day 6 of the healing period. Furthermore, a relationship between damaged and healed stiffness was evaluated to determine the stiffness recovery at the end of the healing period. The healing efficiencies and stiffness recoveries were evaluated in mixtures containing recycled asphalt shingles with and without microcapsules. In addition, the effect of environmental conditions in the healing efficiency and strength recovery was evaluated by exposing three specimens for each of the evaluated asphalt mixtures to two different dry temperature curing conditions: room-temperature ($26 \pm 2^\circ\text{C}$) and high-temperature condition ($50 \pm 2^\circ\text{C}$).

The digital image analysis of light microscope images revealed a reduction in the size of the cracks for all evaluated beam specimens at both healing conditions for a period that spanned from day 0 to day 6. The addition of 5% microcapsules content in asphalt mixtures containing recycled asphalt shingles showed a lower healing efficiency than the mix with no RAS or the one

with the rejuvenator blended directly with the mix ingredients. The lower healing efficiency with microcapsules was due to not all microcapsules having broken during the test since microcapsules are expected to break over time and not all at once. Also, the study results revealed that the healing efficiencies of the evaluated mixtures at room-temperature reflected higher healing efficiency than at high-temperature for all mixtures. The prolonged exposure to high-temperature could have accelerated the aging process in the binder, decreasing the healing efficiency observed at room-temperature curing condition.

With respect to the stiffness recovery, the study results showed that there was a recovery in the stiffness of the mixtures as the healed stiffness was greater than the damaged stiffness but less than the undamaged stiffness. A greater stiffness recovery was observed at high-temperature, which could be explained by the aging process during the five-day conditioning period.

8.3.2 Self-Healing Efficiency of Hollow-Fibers containing a Rejuvenator Product

A similar self-healing experiment was performed in an experimental matrix to investigate the effect of 5% fiber content added in asphalt mixtures containing recycled materials. A series of three-point bending tests were conducted to calculate the strength for three main conditions (undamaged, damaged, and healed states). The undamaged strength of the specimens was defined as the first three-point bending test performed to induce damage in the rectangular specimens. The same procedure was repeated for a second three-point bending test before healing in order to calculate the damaged strength and to increase the severity of the cracks before healing. Following healing, a third three-point bending test was conducted in order to estimate the healed strength. Immediately after the second three-point bending test, specimens were subjected to a 6-day healing period under controlled environmental conditions.

The self-healing experiment test results showed that the addition of sodium-alginate fibers improved the strength recovery of mixtures prepared with unmodified binder. For mixtures prepared with polymer-modified binder, the strength recovery of the conventional asphalt mixture was statistically equivalent to the mixture prepared with the hollow fibers. Furthermore, the increase in temperature from 25°C to 50°C during the healing period resulted in higher strength recovery percentages in all the evaluated mixtures. Lastly, the conventional mixture containing sodium-alginate fibers exhibited a 100% strength recovery at high-temperature curing condition.

8.3.2.1 Effects of Sodium-Alginate Fibers on Asphalt Mixture Laboratory Performance. The objective of this phase of the study was to evaluate the effects of sodium-alginate hollow fibers on the laboratory performance of a Superpave asphalt mixtures. Two mechanical tests and a simulative test were conducted to characterize the performance of asphalt mixtures with and without fibers against intermediate-temperature cracking, permanent deformation, and low-temperature cracking.

The simulative test to characterize the rutting susceptibility of the evaluated mixtures showed that the addition of sodium-alginate fibers in the mixtures containing recycled materials resulted in an increase in the rut depth; yet, the mixtures performed better than the conventional mixture and satisfied the Louisiana specifications. Furthermore, the study showed that the mechanical properties against fracture at intermediate temperature of mixtures containing recycled materials were improved with the addition of the produced fibers; yet, conventional mixtures had a better fracture performance. The low-temperature cracking test results showed that the addition of fibers improved the loading capacity of mixtures containing recycled materials compared to the

conventional mixtures. Yet, the failure temperature of mixtures containing recycled materials with fibers did not show significant differences from the conventional mixtures.

8.3.2.2 Effects of Sodium-Alginate Fibers on Rheological Properties of Asphalt Binders. The objective of the binder experiment was to evaluate the effects of adding sodium-alginate fibers to asphalt binder blends containing recycled materials. The rheological properties of the asphalt binder blends were evaluated by conducting a Performance grading, multiple stress creep recovery test and linear amplitude sweep test. In addition, the chemical composition of the prepared binder blends containing recycled materials and produced fibers were evaluated by conducting a high-pressure gel permeation chromatography and determining an aging index via Fourier transform infrared spectroscopy.

The HP-GPC test results showed that the addition of fibers in blends containing recycled materials resulted in an increase in the HMW/LMW ratio. An improvement in the blending between aged and virgin binder in the blends were expected due to the release of the core material furring the blending process. Furthermore, the FTIR results showed that the addition of extracted binder from either RAS and/or RAP resulted in an increase in the ICO index. The addition of fibers in blends containing recycled material also resulted in an increase in the ICO, which suggests that the rejuvenating product facilitates the extraction of aged binder from the recycled materials and thus, increased the asphaltene content resulting in stiffer blends.

With respect to the effects of the fibers on the rheological properties of asphalt binder, the rheological properties of the binder blends containing recycled materials and sodium-alginate fibers suggested that the fibers did not have a noticeable effect on the final PG grade. Also, MSCR test results showed that a binder blend with extracted binder from recycled materials and sodium-alginate fibers would have less rutting susceptibility than a conventional virgin binder

would. Lastly, LAS test results showed that the hollow fibers recovered some of the elastic behavior lost due to the addition of aged binder from RAS and/or RAP.

8.4 Future Work

The results of this project lead to future research opportunities, including:

- Different rejuvenator products must be tested to determine the effect of each one on the rheological properties of aged binders.
- Test different dosage rates to define an optimum ratio between weight of rejuvenator and weight of a binder.
- Determine if the developed microcapsules and hollow-fibers are a cost-effective technique to use to increase the serviceability of asphalt pavement roads.
- The overall environmental impact from cradle-to-grave of self-healing asphalt by encapsulated asphalt rejuvenator.
- The use of a different core material to compare healing efficiencies.
- It is recommended to test the developed fibers with other binder types and other RAP and RAS sources to evaluate their effects on the rheological properties of the binders and their enhancement of the mechanical and healing properties of the mixtures.
- Future research study should evaluate the self-healing efficiency of the developed microcapsules and hollow-fibers in a full-scale asphalt pavement subjected to real traffic and environmental loadings.

8.5 General Limitations

Self-healing mechanisms, such as microcapsules or hollow-fibers, filled with an asphalt rejuvenator present an emerging technology that would enhance an asphalt mixture's resistance

to cracking damage caused by vehicular and environmental loading. However, the study results showed some limitations in order to incorporate the developed mechanisms in the asphalt industry. The enhancement in the mechanical properties, healing recovery and strength recovery observed in the asphalt mixtures with the addition of the developed self-healing mechanism are attached to the type of asphalt binders used in Louisiana based on the climatic conditions. It is recommended to evaluate the effect of adding the developed self-healing mechanisms in softer and stiffer binders to assess their effects in the rheological properties.

In addition, it is expected that the effects in the mechanical properties, healing recovery and strength recovery observed in the asphalt mixtures with the addition of the developed self-healing mechanism might varied by incorporating recycled materials (RAS, RAP or RAS/RAP) from other sources as the one utilized in the presented study. Also, additional mixture tests should be conducted in order to evaluate the performance of asphalt mixtures containing the developed self-healing mechanisms in climatic conditions different from Louisiana.

Finally, it is recommended to determine the optimum fiber content based on a performance-based characterization against common distresses such as rutting, fatigue cracking and low-temperature cracking.

APPENDIX A. COPYRIGHT

Dear Max,

Thank you for your inquiry. For your first request, as an original author of an ASCE journal article or proceedings paper, you are permitted to reuse your own content (including figures and tables) for another ASCE or non-ASCE publication, provided it does not account for more than 25% of the new work. This email serves as permission to reuse your works in your dissertation:

"Laboratory Testing of Self-healing Microcapsules in Asphalt Mixtures Prepared with Recycled Asphalt Shingles" coauthored with M.M. Hassan, S. Shirzad, L. N. Mohammad, S. B. Cooper and I. I. Negulescu (Published in 2017), [https://doi.org/10.1061/\(ASCE\)MT.1943-5533.0001942](https://doi.org/10.1061/(ASCE)MT.1943-5533.0001942)

Sincerely,

Leslie Connelly

Senior Marketing Coordinator

American Society of Civil Engineers

Dear Max Aguirre:

The Transportation Research Board grants you permission to use your paper, “Performance of Asphalt Rejuvenators in Hot-Mix Asphalt Containing Recycled Asphalt Shingles,” coauthored with M.M. Hassan, S. Shirzad, L. N. Mohammad and S. B. Cooper, in your dissertation, as identified in your request dated August 13, subject to the following conditions:

1. Please cite the publication as *Transportation Research Record: Journal of the Transportation Research Board*, 2017. 2633: 108–116. DOI: <http://dx.doi.org/10.3141/2633-13>.
2. Please acknowledge that the material from your paper is reproduced with permission of the Transportation Research Board.
3. None of this material may be presented to imply endorsement by TRB of a product, method, practice, or policy.

Every success with your dissertation. Please let me know if you have any questions.

Sincerely,

Jennifer J. Weeks

Publishing Projects Manager, Transportation Research Record

VITA

Max Aguirre was born in 1992 in San Salvador, El Salvador. In 2013, he finished his Bachelor of Science in Civil Engineering from Louisiana State University. He always was interested to have knowledge in both in engineering design and construction practices, so he decided to enter the Department of Construction Management at Louisiana State University in 2014. He graduated from his Master of Science in Construction Management in 2016. He continued with his studies at Louisiana State University to pursue a Doctor of Philosophy in Engineering Science degree. His research interests include infrastructure condition assessments, innovative construction materials, and sustainability in engineering.